Engineering Transmission Lines with High Capacity Low Sag ACCC Conductors

CTC GLOBAL

First Edition

Purpose of Document

The purpose of this document is to offer engineering and design guidelines specific to the use of ACCC conductors on electrical transmission lines so their electrical, mechanical, and cost attributes and benefits can be fully realized. While some of the discussion contained in this manual may be considered academic or basic to experienced transmission engineers, much of the material is included so the ACCC conductor's substantial differences and attributes can be discovered, understood, and put into appropriate context as it relates to a number of performance and design criteria. It is intended that the material presented is useful for both the experienced transmission community as well as for those who may not be engaged in projects on a regular basis, or for those who might be relatively new to the task. As a number of topics discussed in this document are highly complex, certain aspects may be beyond its scope, however an extensive number of references are provided for additional review.

Disclaimer

The information provided in this document is offered to increase the knowledge base of transmission personnel engaged in the planning, analysis, design and construction of transmission and distribution lines. While great care has been taken to ensure that all of the data and formulas provided herein are free of errors and reflect current and best design, engineering, and installation practices, no warrantees are expressed or implied regarding the accuracy or completeness of the data, or for the suitability of ACCC conductor in any specific application. For additional support, please contact CTC Global Engineering Department at +1 (949) 428-8500 or e-mail: support@ctcglobal.com

Acknowledgements

The primary authors and editor of this document would like to thank their colleagues at CTC Global, EA Technology, Power Engineers and a number of Utility, University, and Test Lab personnel for their assistance and support. Gratitude is also expressed to several members of the IEEE Tower, Pole, and Conductor Subcommittee, the Power Energy Society, EPRI, CIGRE and other individuals and organizations who continue to study and invest in transmission line efficiency and new technology.

CTC Global

CTC Global (formerly CTC Cable Corporation) was founded in 2002 to develop unique solutions for the electric utility industry. CTC Global currently manufactures ACCC conductor core at its Irvine, California manufacturing plant. ACCC conductor core is subsequently shipped to one of more than a dozen ACCC conductor stranding partners, worldwide. The core is wrapped with conductive strands, placed on reels and shipped to project sites. All core production and conductor stranding operations are certified to current ISO 9001-2008 standards.

Executive Summary

For over one hundred years steel core strands have been used to increase the tensile strength and reduce thermal sag of bare overhead conductors to accommodate longer spans between fewer or shorter structures. As demand for electricity continues to grow and approvals for new projects remain challenging to secure, increasing the capacity and efficiency of existing or proposed transmission lines is becoming increasingly important. While several new conductor types have been introduced over the last several decades that offer increased electrical capacity at higher operating temperatures, higher operating temperatures are generally associated with increased line losses.

In 2002, CTC Global pioneered the development of the 'High-Capacity Low-Sag' ACCC ("Aluminum Conductor Composite Core") conductor. After substantial testing, ACCC conductor was commercially deployed in 2005. The new conductor achieved its high capacity objective while offering a substantial reduction in thermal sag compared to any other commercially available conductor, due to its very low coefficient of thermal expansion. More importantly, due to the composite core's decreased weight compared to steel, an ACCC Drake size conductor, for instance, could incorporate 28% more aluminum using compact trapezoidal shaped strands, with a slight overall reduction in weight. The added aluminum content and improved conductivity of the annealed Typed 1350-O aluminum used in ACCC conductors (63% IACS) allow them to operate more efficiently compared to any other commercially available conductor of the same diameter and comparable weight. The ACCC conductor achieves the highest ampacity at the coolest operating temperature compared to the other high temperature capable conductors, as shown in Figure 1.
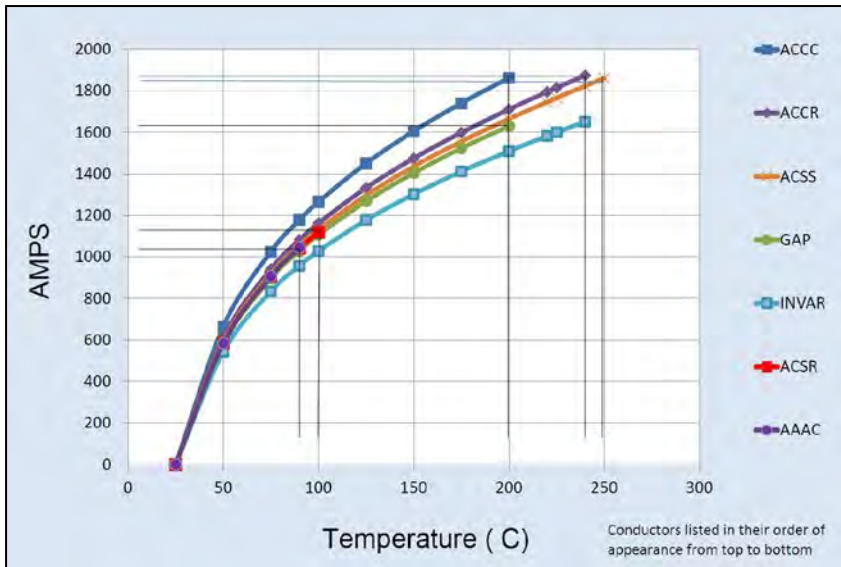
Figure 1 - Conductor comparison showing ampacity capabilities, attainable at recommended thermal limits of several conductor types. The ACCC conductor delivers greater emergency current at 200°C than other conductors operated at temperatures as high as 250°C.

Cooler operating temperatures under high load conditions reflect substantial reductions in line losses that can decrease generation requirements, reduce fuel consumption (and associated emissions), and decrease lifecycle costs. These and several other attributes described in this document have led to the successful deployment of over 50,000 km of ACCC conductor at over 500 project sites worldwide.

A conductor thermal sag comparison (shown in Figure 2) was based on testing performed at Kinectrics Lab by Hydro One, wherein 1600 amps of current was run through each conductor type on a 65 meter (215 ft) indoor test span[1]. Note that the ACCC conductor operated at 60° to 80°C cooler than the other conductors tested under equal load conditions.

---

[1] Goel, A., Kamarudin, A., Pon, C. New High Temperature Low Sag Conductors, NATD Conference & Expo May 2005
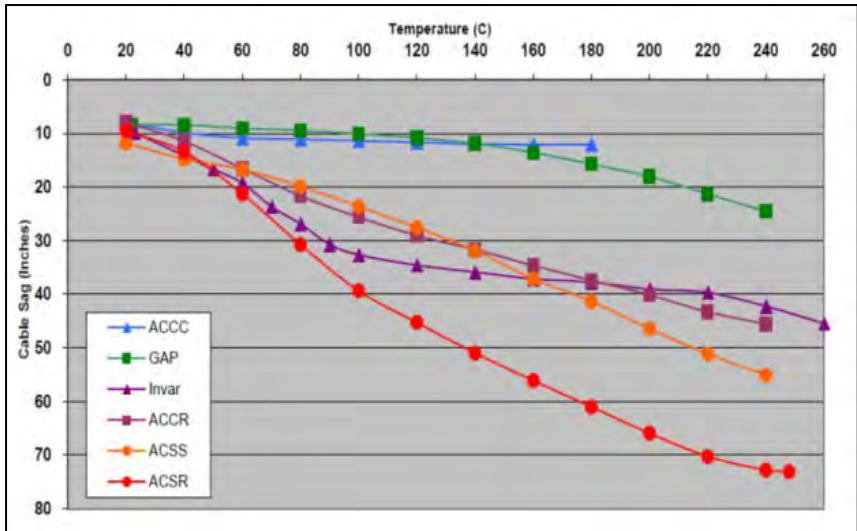
Figure 2 - Sag / temperature comparison of several conductors tested by Ontario Hydro at Kinectrics lab. The graph not only shows the substantially reduced sag, it also shows the particular ACCC conductor tested operated at 60° to 80° C cooler than the other conductors tested under an equal 1,600 amp load conditions. (The conductors are listed in the sequence in which they appear from top to bottom)

While the differences in sag are readily apparent, note also the cooler operating temperature of the ACCC conductor under equal load conditions, resulting in additional substantial reduction in I^2R line losses due to the lowered resistance at lower operating temperature. Significant power saving can be obtained by deploying ACCC conductors, as shown in Figure 3, where line losses were assessed as a function of load factor at a peak current of 1,400 amps in a 32 km (20 mile) 230 kV 3-phase circuit.
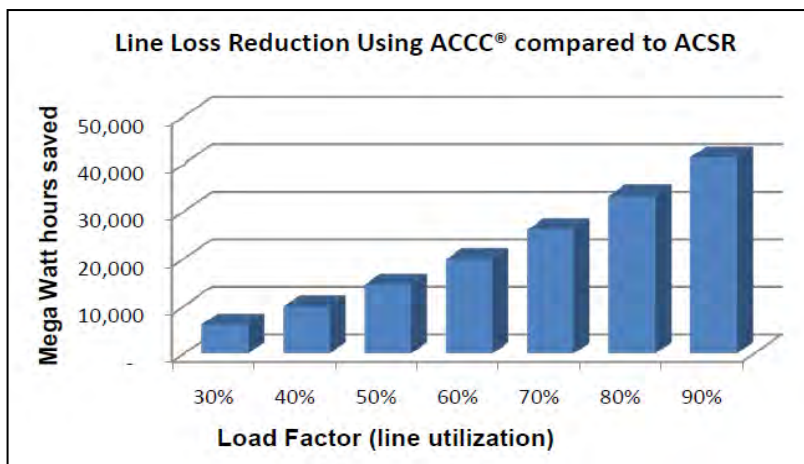
Figure 3 - ACCC line loss reduction over comparable Drake size ACSR conductor
as a function of load factor on a 32 km (20 mile) line.

- In the western United States, most transmission lines operate at a load factor of approximately 60%. The conductors compared were common Drake size conductors slightly greater than one inch (25mm) in diameter.
- Assuming a load factor of 60% in this example, *the use of ACCC conductor would save nearly 20,100 MWh per year,* or over $1 million per year at $50/MWh.
- If one considers that the three phase 20 mile / 32 km AC example would require 316,800 feet or 96,560 meters of conductor, the *annual* savings would equate to $3.30 per foot or $10.84 per meter of conductor in direct economic benefit from line loss avoidance. *Reduction in line losses compared to an equivalently sized ACSR conductor would more than pay for the ACCC conductor's potentially higher cost in a very short period of time.* If the load factor or the cost of energy was higher, this could happen even sooner. The ACCC conductor's other attributes also contribute to reduced structural costs on reconductoring and new line projects. If fully utilized, they would further decrease upfront capital costs and improve overall project economics.

CTC Global believes that utilities, consumers, and regulators all recognize that access to affordable, reliable, and renewable energy is essential for the future health of our planet, economy, and security in general. Without it, water cannot be pumped to support growing populations, products cannot be economically

manufactured to maintain viable economies, and poverty cannot be mitigated in underdeveloped countries that are economically dependent on more developed countries facing their own challenges. Considering that the world consumes over 20 Trillion kWh of electricity every year and that more than 1.4 Trillion kWh are lost in the inefficient transmission of that energy[2], CTC Global believes the time has come to consider the importance of investment, not just in more efficient clean generation, but also in improved transmission technologies. As several key industry executives have stated "It is cheaper to save a 'Negawatt' than it is to produce a Megawatt."[3]

From a fuel conservation or environmental perspective, there are an estimated 1.2 Trillion Metric Tons of CO_2 created annually as a by-product of transmission line losses. If that number could be reduced by one-third (or more) by deploying ACCC conductors *worldwide*, a reduction in CO_2 emissions of over 290 Million Metric Tons could be realized every year, based on the US average of all fuel sources including hydro, renewables, and fossil fuels. Using the average value of 1.372 lbs CO_2/kWh, this is comparable to removing 55.8 Million cars from the road. This hypothetical one-third reduction in transmission losses also reflects 466,620,000 MWh of electrical savings. This is the energy equivalent of 53,267 MW of generation,[4] or the amount of generation required to power nearly 48 million homes. From an oil-energy perspective, at a Btu conversion efficiency rate of 42%, the energy saved would equal over 1.9 billion barrels of oil annually.[5] The question that should be considered is: *"Is it cheaper to create energy or save it?"* This topic is discussed in more detail in Section 2.7.

In addition to notable reductions in thermal sag and line losses, the ACCC conductor also offers a number of other significant advantages. These advantages include increased tensile strength to enable greater spans between fewer and/or shorter structures; lower tension to existing tower structures in reconductoring projects, free of metallurgical corrosion associated with steel core; excellent self-damping characteristics; extreme ice load survivability due to the high strength and elasticity of the composite core; and improved resistance to cyclic load fatigue - all of which serve to improve the conductor's

---

[2] United States Energy Information Administration, "International Energy Outlook 2010"

[3] The term Negawatt was coined by Amory Lovins of the Rocky Mountain Institute in 1989

[4] This does not take capacity factor into account.

[5] The Union of the Electric Industry (EURELECTRIC) "Efficiency in Electricity Generation" July 2003

performance and service life. The ACCC conductor's characteristics are so unique in so many respects that transmission personnel are encouraged to explore these differences as presented in this document.

While much of the information presented is of a technical, and in some cases, a comparative nature; economics, efficiency and capacity are also discussed at length, as the ACCC conductor continues to raise the performance bar over conventional and high temperature conductors. While capable of High-Temperature Low-Sag (HTLS) operation, the ACCC conductor is actually a "High-Capacity Low-Sag" (HCLS) conductor, as it is capable of carrying approximately twice the current of conventional all-aluminum or conventional steel-reinforced ACSR conductors, at much cooler operating temperatures than other HTLS conductors. The cooler operating temperatures reflect a substantial reduction in line losses compared to any other commercially available conductor today. Figure 4 reflects an average reduction in line losses of up to 35% compared to other similarly sized conductors. This comparison is described in more detail in section 1.2.3.
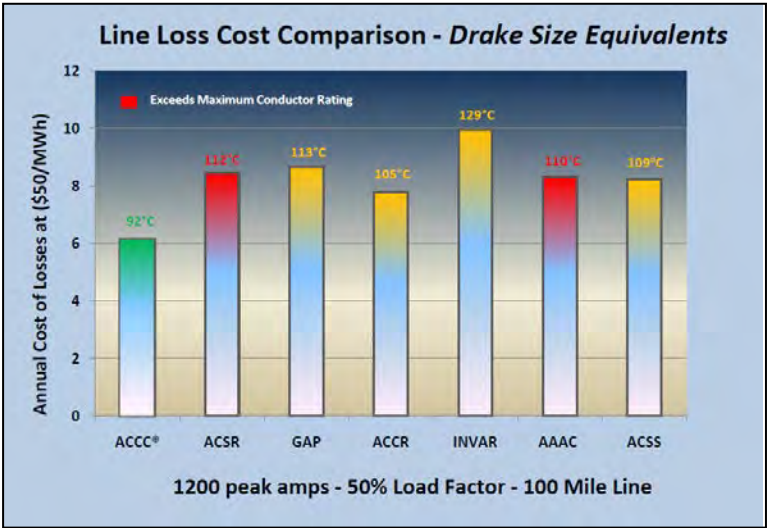

Figure 4 - Comparison of line losses (and operating temperatures) of various conductors on a 1,200 amp, 100 mile (162 km) transmission line, at a load factor of 50%. The cooler operating temperature of ACCC conductor contributes to significant reduction in line loss, as much as 35% as compared to ACSR and other conductor types.

The information presented in this document begins with an overview of the unique characteristics and advantages of the ACCC conductor. A comparison with other conductor types is offered to put various attributes and conductor properties into perspective. General project considerations are briefly discussed. A review of project economics is followed by a discussion on important structural and electrical considerations. Ampacity, line ratings and line loss considerations are discussed, as well as a continued discussion as to how the ACCC conductor can reduce the economic and environmental impact of line losses.

A detailed review of the ACCC conductor's mechanical characteristics is presented, followed by a discussion on the impact and management of heavy ice loads, conductor galloping, and Aeolian vibration mitigation. The topic of acceptable conductor tensions (prior to, during, and after load conditions) is discussed in great detail. A review of CIGRE, IEEE, and other guidelines is presented along with data specific to ACCC conductors. Several useful resources and references are listed throughout the document as well as recommendations specific to the optimized use of ACCC conductor. Calculation of sag and tension is briefly reviewed, followed by a discussion of various modeling methods used worldwide. Particular emphasis is placed on the Experimental Plastic Elongation Model (EPE) that is used in popular software programs including PLS CADD™, Sag 10®, and others.

Within the 'Modeling ACCC Conductor Sag and Tension' section, a review of the stress-strain relationship is presented along with a continued discussion of how the ACCC conductor can be correctly modeled and data interpreted. The relationship of load-sharing between the aluminum strands and composite core is also discussed at length, as the relationship is dynamic due to thermal conditions and mechanical load history. Following the Chapter on modeling ACCC conductor, several project examples are offered that review common reconductoring and new project objectives. The section goes on to discuss how the ACCC conductor can be utilized to achieve a number of objectives at the lowest overall project cost. The data presented is based on real-world experience gained through an installed base of over 50,000 km of ACCC conductor at over 500 project sites, worldwide.

As this is the first document to focus on the performance and design characteristics of the Energy-Efficient High-Capacity Low-Sag ACCC conductor, it is anticipated that the document will be updated periodically. Should you have any questions that are not addressed in this document, please

contact CTC Global for additional support at +1 (949) 428-8500 or support@ctcglobal.com). Feedback and suggestions would be greatly appreciated. Thank you for your interest in ACCC conductor.

Table of Contents

1. Overview of ACCC Conductor

Chapter 1 of this manual offers an overview of the features of ACCC conductors. Chapter 2 bears down on the various subjects in much more detail to put the nature and advantages of ACCC conductors into a clear context relative to other conductor types and engineering principles in general. Chapter 3 discusses sag and tension calculations for ACCC conductors using industry standards and modeling tools, and Chapter 4 offers case study examples. References and Appendix data are also offered to direct the reader to other important documents and considerations beyond the scope of this document.

1.1. Historical Perspective of Conductors

Historically (pre WWI), copper was used for overhead conductors due to its excellent conductivity. Due to the war effort, and the associated demand for copper, copper was replaced with much lighter, but less conductive aluminum. Over time, various aluminum alloys were introduced that offered improved strength (with some reduction in conductivity), and steel core strands were added to increase the conductors' overall strength to accommodate greater spans with reduced sag. During WWII, aluminum supply was directed toward aircraft manufacturing and some transmission lines built during that period reverted back to copper conductors (some of which manufactured with steel cores).

While the pre-1970's electric grid in the US became heavily loaded as the country's demand for electricity grew and new pathways became more difficult to secure, the existing electrical grid needed increased capacity, often on existing rights-of-way (ROW). At this point in time, new conductors were introduced to address the challenges. Trapezoidal strand (TW) aluminum conductors packed more aluminum into a diameter to minimize wind load on structures and offered added ampacity. Conductors capable of operating at higher temperatures were introduced. SSAC, now known as ACSS ("Aluminum Conductor Steel Supported") was deployed to increase line capacity; although it's relatively high thermal sag characteristics limited its deployment to some degree.[6] The ACSS conductor's high operating temperatures also reflected increased line losses which resulted to some degree in increased fuel

---

[6] US Department of Energy "National Transmission Grid Study" 2002

consumption (or depletion of hydro resource), and additional generation requirements to offset line losses.

Today there are a vast number of conductor types and sizes available, but the basic formula hasn't changed much in nearly a hundred years. All aluminum/alloy conductors are still widely utilized (such as AAC, AAAC and ACAR) in certain applications, and ACSR ("Aluminum Conductor Steel Reinforced") is generally the basic conductor of choice. In addition to ACSS, other "High Temperature, Low-Sag" (HTLS) conductor types were developed[7] to increase capacity with reduced sag.

While high temperature/low sag capabilities can be extremely important on key spans where clearance requirements are challenging, they can also be very important during N-1 or N-2 conditions when adjacent lines are out of service and the remaining line(s) are relied upon to handle additional current. However, high temperature operation has historically been reserved for special circumstances, as high temperature operation also reflects high (I^2R) losses[8] and their associated costs.

1.2. General Description of ACCC Conductors

The ACCC conductor consists of a hybrid carbon and glass fiber composite core which utilizes a high-temperature epoxy resin matrix to bind hundreds of thousands of individual fibers into a unified load-bearing tensile member. The central carbon fiber core is surrounded by high-grade boron-free glass fibers to improve flexibility and toughness while preventing galvanic corrosion between the carbon fibers and the aluminum strands. The composite core exhibits an excellent, highest-in-the-industry, strength to weight ratio, and has a lowest-in-the-industry coefficient of thermal expansion which reduces conductor sag under high electrical load / high temperature conditions. The composite core is surrounded by aluminum strands to carry electrical current (see Figure 5). The conductive strands are generally fully annealed aluminum and trapezoidal in shape to provide the greatest conductivity and lowest possible electrical resistance for any given conductor diameter.

---

[7] Transmission Line Uprating Guide, EPRI, Palo Alto, CA: 2000. 1000717.

[8] Ringer, M.B., Transmission and Distribution of Electricity: Costs, Losses and Materials National Renewable Energy Laboratory NREL/MP 510-33141 Sept 2003

Figure 5 - ACSR and ACCC Conductors

The ACCC conductor is rated for continuous operation at up to 180°C (200°C short-term emergency), and operates significantly cooler than round wire conductors of similar diameter and weight under equal load conditions due to its increased aluminum content and the higher conductivity offered by Type 1350-O aluminum. Though the ACCC conductor was initially developed as a "High-Temperature, Low-Sag" (HTLS) conductor to increase the capacity of existing transmission and distribution lines with minimal structural changes, its improved conductivity and reduced electrical resistance makes it ideally suited for reducing line losses on new transmission and distribution lines where improved efficiency and reduced upfront capital costs are primary design objectives.

The lighter weight composite core allows an increased aluminum content (using compact trapezoidal strands) without a weight penalty. ACCC conductors operating well below 200°C can provide the same capacity as other HTLS conductors operating well above 200°C. In addition to the increased losses with other HTLS conductors, continuous or cyclic operation to temperatures above

3

200°C may accelerate degradation of core strands and increase lifecycle costs.[9] Unlike ACCC conductors that use standard installation equipment and procedures, several other HTLS conductors often require specialized equipment, or difficult installation procedures that can delay project completion and increase overall project costs.

1.2.1. Design Premise & Nomenclature

ACCC conductors were developed initially as a replacement for standard ASTM conductors. CTC Global and its numerous stranding partners created several conductor sizes with names and outside diameters that match the ACCC conductor's ACSR and ACSS counterparts. For example, Drake ACCC conductor is equal in diameter to ACSR Drake or ACSS Drake. CTC Global chose this nomenclature because the conductor's size remains essentially unchanged compared to ACSR or ACSS round wire conductors. While other trapezoidal stranded conductors offer the advantages of compact design and/or increased aluminum content (e.g., ACSS/TW Suwannee has the same diameter as a Drake conductor), they come with significant weight penalties which can translate into increased conductor sag.

When ACCC conductors were subsequently introduced outside of the US, city names were selected to differentiate from other International Electrotechnical Commission (IEC) conductor sizes. In North America, additional conductor sizes have also been developed that are also referred to by city names. The current (2011) list of ASTM and IEC ACCC conductor sizes is provided in section 1.2.4.

1.2.2. Conductor Properties

There are a number of electrical and mechanical properties that are important to conductor performance, longevity, and efficiency.[10] These characteristics impact initial capital costs as well as lifecycle costs. They include current carrying capability, strength, weight, diameter, corrosion resistance, creep rate, coefficient of thermal expansion, self-damping, fatigue resistance, operating

---

[9] Increased Power Flow Through Transmission Circuits: Overhead Line Case Studies and Quasi-Dynamic Rating. EPRI, Palo Alto, CA: 2006. 1012533

[10] Thrash, R. Bare Overhead Transmission Conductors, Selection and Application, IEEE TP&C Winter Meeting, Albuquerque, NM Jan. 2006

temperature range, short-circuit capability, and thermal stability. Using equivalent diameter and overall conductor weight as a basis for conductor comparisons, the ACCC conductor offers advantages in virtually every category.

When making comparisons of conductor costs, it is important to consider the conductor's impact on the overall project cost. ACCC conductor is often viewed as being more costly on a 'per unit length basis' (given a particular diameter) over ACSR conductor, rather than on a per unit length per capacity. One must bear in mind that ACCC conductors (operated at higher temperatures) offer approximately twice the capacity of an equivalent diameter ACSR conductor which can result in significantly reduced structural loads compared to installing a larger/heavier conventional conductor. The properties of ACCC conductors offer planners and designers greater versatility than any other family of conductors on the market today.

The ACCC Conductor's mechanical properties are based on the specific properties of its composite core and aluminum strands, and the interaction between the two.

Strength, Elasticity, Creep

With conductors that use fully annealed aluminum strands, like ACSS and ACCC conductors, their core serves as their primary strength member since annealed aluminum strands readily yield under very little load. Table 1 lists the comparative properties of most conductor types' core materials. The standard ACCC conductor core offers 2,158 to 2,585 MPa (313-375 ksi) of tensile strength and a modulus of elasticity of ~112.3 to 147 GPa (16.3-21.3 msi). For comparison, a conventional steel core offers 1,275 MPa (185 ksi) of tensile strength and a modulus of elasticity of 200 GPa (29 msi), while a high strength steel core offers a tensile strength of 1,965 MPa (285 ksi) with the same 200 GPa (29 msi) modulus.

Core Materials				
Description	Weight (lbs/inch³)	Modulus of Elasticity (msi)	Tensile Strength (ksi)	Coefficient of Thermal Exp. (x 10-6/°C)
HS Steel	0.281	29	200-210	11.5
EHS Steel	0.281	29	220	11.5
EXHS Steel (Galfan coated)	0.281	29	285	11.5
Carbon Hybrid Epoxy	0.070	16-21	330-375	1.6
Alum Clad (20.3 IACS)	0.238	23.5	160-195	13.0
Galv. Invar Alloy	0.281	23.5	150-155	3.0
Mishmetal Std	0.281	29	200-210	11.5
Mishmetal HS	0.281	27	220-235	11.5
Al Oxide Metal Matrix	0.120	31.2	190	6.0

Table 1 - Characteristics of core materials used in overhead conductors. Note the low coefficient of thermal expansion and high strength of the Carbon Hybrid Epoxy core used in the ACCC conductor.

While the modulus of elasticity of the ACCC conductor's core is lower than its steel counterpart, meaning that it will stretch more easily, unlike steel, the composite core will not yield (i.e., plastically deform) or creep over time. The ACCC conductor's core is purely elastic and heavy loading will not permanently deform it. However, under ice or wind load conditions, the very pliable annealed aluminum will yield under relatively modest load conditions, which favorably reduces stress in the aluminum strands and improves resistance to Aeolian vibration fatigue (as discussed in Section 2.13). The elasticity of the core and the rapid relaxation of the aluminum strands also improve its self-damping characteristics, reduce its susceptibility to fatigue failure, and allow for very low thermal sags.

Self Damping Characteristics

All conductors are subjected to Aeolian Vibration. The frequency and amplitude of the vibration is based on wind speed, the angle at which the wind hits the conductor, conductor properties, and other variables. The impact of vibration primarily relates to fatigue failure of the aluminum strands at the interface of suspension clamps where strand deformation, high stress levels and bending constraints can accelerate fatigue failure. Metallic strands under

particularly high-tension are generally more susceptible to Aeolian vibration induced fatigue failure.[11]

Over the length of conductor in a span between suspension clamps, much vibration energy is dissipated due to interfacial rubbing of the aluminum strands. Trapezoidal shaped strands generally offer greater surface contact area between strands compared to round strands, which further improves the self-damping function and lowers the contact point stress even during cold temperature conditions when tension increases.

Heavy ice or wind loads or optional conductor pre-tensioning will stretch the conductor causing the more pliable aluminum strands to yield or 'relax.' This serves to lower the thermal knee-point and improve self damping characteristics under all but extremely cold conditions, when the loosened strands tighten back up as function of thermal contraction. The elasticity of the ACCC conductor's core, combined with its very pliable aluminum strands allows strand relaxation to occur relatively quickly. As discussed in greater detail in Section 2.15.3, a small amount of pre-tensioning can effectively cause this to happen during installation which reduces thermal sag, improves self-damping characteristics, and reduces stress in the aluminum strands that, in combination with Aeolian vibration, are associated with strand fatigue failure.

Thermal Limits & Longevity

Like any conductor, the ACCC conductor has thermal limits that should be understood. Considering that the ACCC conductor uses fully annealed aluminum that has a thermal limit well above 250°C, its thermal limits are based on the thermal limits of the composite core. After extensive testing, CTC established a maximum continuous operating temperature of 180°C for ACCC conductors. At this temperature, over prolonged periods of time, a minimal amount of surface oxidation may be observed. This oxidation reaction subsequently forms a dense layer approximately one-hundred microns thick, retarding further oxidation. The photo below depicts a core sample aged at 220°C for 52 weeks. The oxidation process, in this case, was accelerated. Figure 6 reveals a section of the composite core with integrity under the 'charred' skin

---

[11] Electric Power Research Institute, "Transmission Line Reference Book, Wind Induced Conductor Motion", Research Project 795, 1978

(removed mechanically to allow for inspection of the glass layer immediately below the oxidation).
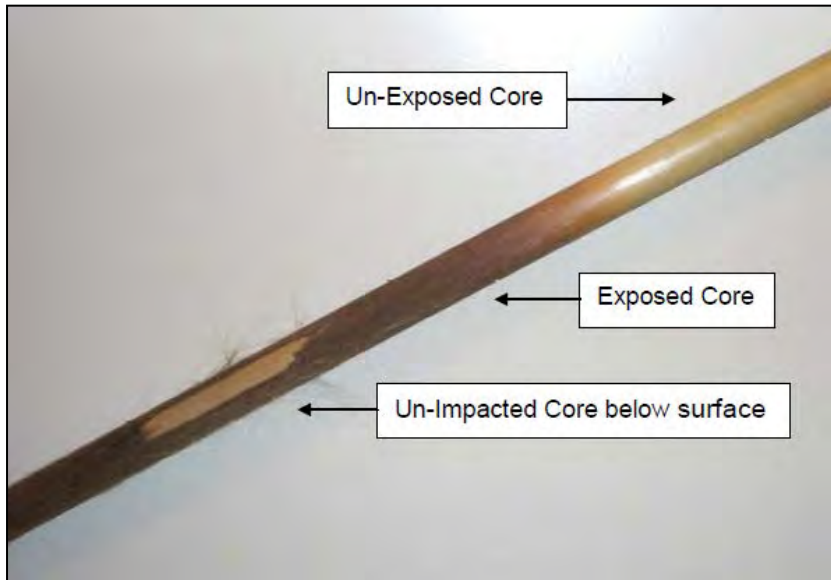
Figure 6 - ACCC core sample after 52 weeks exposure at 220°C. Oxidized layer removed mechanically to examine core below oxidized layer.

Generally speaking, the thermal limits of a carbon/glass fiber composite material can be established by the thermal limits of its resin or 'matrix.' Degree of curing of the matrix phase during composite manufacturing can be appraised via testing for 'glass transition' temperature (Tg). Tg testing offers insight relative to the consistency of resin matrix curing from batch to batch during production, and it is appropriately used for R&D and quality control purposes.[12] Tg is easily measured using Dynamic Mechanical Analysis (DMA) (see Figure 7), and is particularly useful for composite applications where matrix dominated properties (e.g., shear, compressive strength, etc.) are design critical, as in laminated composite structure comprised of numerous layers of material that are bound by a resin matrix and subject to compression or shear load, where

---

[12] Tsotsis, T.K & Shaw, M.L., Long Term Thermo-Oxidative Aging in Composite Materials: Failure Mechanisms, Composites Science and Technology 58 (1998) 355-368

delamination may result if there is insufficient matrix integrity due to excessive high temperature exposure. However, for a uni-directional composite core used in overhead conductor applications, the tensile strength, tensile modulus and axial thermal expansion are the *critical design properties which are fiber dominated (not matrix dominated) properties. T_g is a very poor indicator of fiber dominated properties in a uni-directional composite, and should not be used for durability or longevity criteria for conductors.*
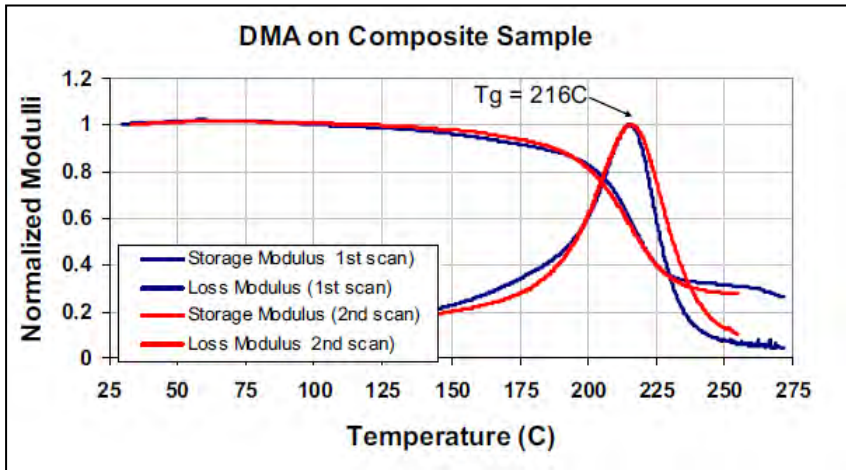
Figure 7 - Glass Transition (Tg) Test using Dynamic Mechanical Analysis. The peak in Loss Modulus curve is used to determine if the degree of cure in the matrix has been achieved.

While the oxidized layer shown in Figure 6, retards further oxidation which limits the overall impact of thermal exposure, exposure to temperatures above 200°C is not recommended for the ACCC conductor, but can be tolerated for brief periods. System testing has shown that the ACCC conductor and ancillary hardware can be subjected to at least one (1) eight hour cycle per year to 215°C over the life of the conductor, with little consequence.[13] Although the ACCC conductor core exhibits fiber-dominated mechanical properties, exposure to

---

[13] Zsolt Peter, Dmitry Ladin, Michael Kastelein, Greg Brown, Heat Cycling Test at Maximum Departure Angle on LONDON ACCC/TW Conductor Through A PLP AGS Suspension Assembly, Kinectrics North America Inc. Report No.: K-419205-RC-0002-R00 (Sept 2010)

higher temperatures for prolonged periods can reduce the ability of the polymer matrix to effectively transfer flexural and tensile loads among the load bearing fibers and may reduce its overall strength. Nevertheless, the ACCC conductor's uni-directional composite core exhibits fiber dominated properties which are far less susceptible to the aging mechanisms or fatigue of metallic materials. This is why carbon fiber composites are being broadly deployed in other highly demanding applications, including aerospace, where high-strength, light-weight, thermal stability, resistance to corrosion and cyclic load fatigue are critical.

1.2.3. Conductor Comparisons

In Section 1.2.2 above, several important conductor properties were discussed. Table 2 compares a number of conductive materials properties used in overhead conductors. As it relates to the conductive aluminum strands, various alloys can be used to improve their tensile strength and/or resistance to annealing. Type 1350-H19 aluminum; for instance, will begin to anneal at approximately 93°C. Type 1350-O is pre-annealed. Annealing reduces strength but favorably improves conductivity and fatigue resistance, as fatigue cracks will not propagate as quickly through softer, more ductile materials. Various alloys offer improved strength, but do so at a notable loss in conductivity and ductility. The conductivity values in Table 2 are presented as a percentage in comparison with annealed copper, per the International Annealed Copper Standard ("IACS"). A value of 100% refers to a conductivity of 5.80 x 10^7 Siemens per meter.

Aluminum Conducting Materials				
Description	Name	Conductivity (%IACS)	Tensile Strength (ksi)	Max Cont. Op. Temperature (degrees C)
Hard Drawn	1350-H19	61.2	23-25	90
MS Alloy	5005-H19	53.3	36	90
HS Alloy	6201-T81	52.5	46-48	90
Fully Annealed	1350-O	63	6-14	250
Thermal Resistant	TAL	60	24-27	150
HS Thermal Resistant	KTAL	55	27-36	150
Ultra Thermal Resistant	ZTAL / UTAL	60	24-27	200
Extra Thermal Resistant	XTAL	58	24-27	230

Table 2 - Properties of Aluminum used in Overhead Conductors. Type 1350-O aluminum, as used in the ACCC conductor, offers the highest conductivity of all available choices.

As compared in Table 2, a number of core material properties are important as they relate to bare overhead conductor. Higher strength, lower weight, and lower coefficients of thermal expansion offer obvious advantages, while a lower modulus of elasticity offers a less obvious advantage in terms of heavy ice response. Under extremely heavy ice load conditions, a conductor with a lower modulus (more elastic) core will stretch more than a stiffer higher modulus core, but the lower modulus composite core is highly elastic and not subject to permanent elongation, deformation, or yielding. The ACCC conductor's overall properties are compared with a number of other conductor types in Table 3. A number of ACCC conductors engineered for heavy ice load are also available. These typically utilize a larger, higher strength and higher modulus core.

Conductor Properties		Conductive Strands			Core Strands			
Code Name	Conductor Description	aluminum type	tensile strength	conductivity (%IACS)	type	tensile strength	modulus	CTE
AAC	All Aluminum Conductor	1350-H19	24- 28 ksi	61.2	1350-H19	24-28 ksi	10 msi	23.0
AAAC	All Aluminum Alloy Conductor	6201-T81	46-48 ksi	52.5	6201-T81	46-48 ksi	10 msi	23.0
ACAR	Aluminum Conductor Al Alloy Reinforced	1350-H19	24- 28 ksi	61.2	6201-T81	46-48 ksi	10 msi	23.0
ASCR	Aluminum Conductor Steel Reinforced	1350-H19	24- 28 ksi	61.2	coated steel	200-220 ksi	29 msi	11.5
AACSR	Aluminum Alloy Conductor Steel Reinforced	6201-T81	46-48 ksi	52.5	coated steel	200-220 ksi	29 msi	11.5
ACSS	Aluminum Conductor Steel Supported	1350-O	~8.5 ksi	63.0	coated steel	220-285 ksi	29 msi	11.5
ACIR	Aluminum Conductor Invar Reinforced	Al-Zr alloy	23-26 ksi	60.0	invar steel	150 - 155 ksi	22 msi	3.7
ACCR	Aluminum Conductor Composite Reinforced	Al-Zr alloy	23-26 ksi	60.0	metal matrix	190 ksi	32 msi	6
ACCC	Aluminum Conductor Composite Core	1350-O	~8.5 ksi	63.0	carbon hybrid	313-375 ksi	16-21 msi	1.6

Table 3 - Conductor type comparison showing core and conductive material properties. Notice the highlighted 'best in class' properties of ACCC Conductor (low tensile strength of the aluminum translates into reduced stress and improved fatigue resistance)

1.2.4. ACCC Conductor Types

ACCC conductors utilize a carbon and glass fiber core embedded in a toughened polymer resin matrix. The central carbon fiber core is surrounded by glass fibers of sufficient thickness to improve flexibility and create a durable barrier that prevents galvanic corrosion. Aluminum with carbon fiber composite is among the most reactive galvanic pairing possible where aluminum material is gradually corroded away. The insulation layer between aluminum strands and carbon fiber core must be of sufficient integrity to survive the constant fretting (from conductor vibration or the differential thermal expansion with temperature) between the inner aluminum strands and the composite core over its life time. Aerospace structures typically require 1 to 2 layers of fiberglass insulation (~10 mil or 0.25 mm per layer) to prevent galvanic coupling of aluminum and carbon fibers. The ACCC conductor core is designed to maintain a minimum glass layer of 0.50 mm to ensure the integrity of the galvanic corrosion barrier over the conductor's service life.

The composite core is helically-wrapped with two to five layers of aluminum strands. The outer layer typically has a right-hand lay but is subject to customer specification. The ratio and type of carbon and glass fibers used in the standard ACCC core offers 2,158 to 2,585 MPa (313-375 ksi) of tensile strength and a modulus of elasticity of ~112.3 to 147 GPa (16.3-21.3 msi). Higher strength and higher modulus cores are also available for long spans or extreme wind/ice load applications. *Standard ACCC sizes include several conductor designs wherein the core size and aluminum ratios provide optimized solutions for various applications including heavy wind and ice zones as well as long spans.*

1.2.5. Standard ACCC Conductor Sizes

Currently, there are nine standard sizes of ACCC conductor core that are incorporated into approximately 40 finished conductors ranging from 300 kcmil (150 mm^2) to 2,800 kcmil (1,400 mm^2). Table 4 shows the properties of each core size. Table 5 and Table 6 summarize the IEC and ASTM ACCC® sizes. For the most current list, please visit **www.ctcglobal.com** or contact **support@ctcglobal.com.**

ACCC® Composite Core Specifications									
METRIC									
CTC Part Number	200-003	200-004	200-005	200-006	200-007	200-008	200-009	200-010	200-011
Metric Core Name Designation (mm)	5.97	7.11	7.75	8.13	9.53	8.76	9.78	10.03	10.54
Nominal Diameter of Composite Core (mm)	5.97	7.11	7.75	8.13	9.53	8.76	9.78	10.03	10.54
Diameter Tolerance (mm)	±0.05	±0.05	±0.05	±0.05	±0.05	±0.05	±0.05	±0.05	±0.05
Nominal Cross-sectional Area of Core (mm^2)	28.0	39.7	47.1	51.9	71.3	60.3	75.1	79.1	87.3
Rated Strength of Composite Core (MPa)	2158	2158	2158	2158	2158	2158	2158	2158	2158
Rated Tensile Load at Failure (kN)***	60.4	85.7	101.7	112.0	153.8	130.2	162.1	170.6	188.3
Core Nominal Mass (kg/km)	54	76	86	98	132	113	143	147	164
Final Modulus of Elasticity (GPa)	112.3	112.3	112.3	112.3	112.3	116.0	112.3	112.3	112.3
Coefficient of Thermal Expansion (x10^{-6}/°C)	1.61	1.61	1.61	1.61	1.61	1.45	1.61	1.61	1.61
Specific Heat Capacity of Core (J/g/°C)	0.813	0.813	0.813	0.813	0.813	0.813	0.813	0.813	0.813
Heat Capacity of the Core mCp (J/m/°C)	43.5	61.7	70.2	79.8	107.7	91.9	116.1	119.8	133.1
Electrical Conductivity of the Core (% IACS)	0	0	0	0	0	0	0	0	0
Recommended Operating Temperature of Core (°C)*	180	180	180	180	180	180	180	180	180
Emergency Operating Temperature of Core (°C) **	200	200	200	200	200	200	200	200	200
IMPERIAL									
CTC Part Number	200-003	200-004	200-005	200-006	200-007	200-008	200-009	200-010	200-011
Imperial Core Name Designation (mils)	235	280	305	320	375	345	385	395	415
Nominal Diameter of Composite Core (in.)	0.235	0.280	0.305	0.320	0.375	0.345	0.385	0.395	0.415
Diameter Tolerance (in.)	±0.002	±0.002	±0.002	±0.002	±0.002	±0.002	±0.002	±0.002	±0.002
Nominal Cross-sectional Area of Core (in^2)	0.043	0.062	0.073	0.080	0.110	0.093	0.116	0.123	0.135
Rated Strength of Composite Core (ksi)	313.0	313.0	313.0	313.0	313.0	313.0	313.0	313.0	313.0
Rated Tensile Load at Failure (klbf)***	13.6	19.3	22.9	25.2	34.6	29.3	36.4	38.4	42.3
Core Nominal Mass (lb/kft)	36	51	58	66	89	76	96	99	110
Final Modulus of Elasticity (Msi)	16.29	16.29	16.29	16.29	16.29	16.82	16.29	16.29	16.29
Coefficient of Thermal Expansion (x10^{-6}/°F)	0.894	0.894	0.894	0.894	0.894	0.806	0.894	0.894	0.894
Specific Heat Capacity of Core (J/g/°F)	0.452	0.452	0.452	0.452	0.452	0.452	0.452	0.452	0.452
Heat Capacity of the Core mCp (J/m/°F)	24.2	34.3	39.0	44.4	59.8	51.1	64.5	66.5	73.9
Electrical Conductivity of the Core (% IACS)	0	0	0	0	0	0	0	0	0
Recommended Operating Temperature of Core (°F)	356	356	356	356	356	356	356	356	356
Emergency Operating Temperature of Core (°F)	392	392	392	392	392	392	392	392	392

*The recommended operating temperature of the composite core in ACCC® conductors is up to 180°C (356°F).
**The maximum recommended emergency temperature rating of the composite core in ACCC® is 200°C (392°F), which CTC defines as 10,000 hours over the conductor lifetime.
***Rate tensile loads have been rounded to the first decimal place.
All values are determined at room temperature unless otherwise indicated.

Table 4 - Specifications for ACCC conductor cores in metric and imperial units.

1.2.6. Custom ACCC Conductor Sizes

Every project has its unique requirements. Terrain, electrical current, line capacity, environmental conditions and the condition of the existing structures, or possible placement of new structures all come into play. One of CTC's

standard conductor designs (in a range of the types described above) can offer an optimal solution for most projects. Occasionally, custom (or new) sizes are developed to accommodate a particular requirement. Please contact **support@ctcglobal.com** for assistance.

ASTM SIZES							
ACCC®	Aluminum Area	Diameter	Core Diameter	Weight	Core Rated Strength	Conductor Rated Strength	Max. Resistance DC @ 20°C
ATSM Size	(kcmil)	(in)	(in)	(lb/kft)	(kips)	(kips)	(ohm/mile)
PASADENA	305	0.616	0.235	321	13.6	15.5	0.2942
LINNET	431	0.720	0.235	440	13.6	16.3	0.2096
ORIOLE	439	0.741	0.280	463	19.3	22.1	0.2059
WACO	454	0.770	0.305	485	22.9	25.8	0.1990
LAREDO	530	0.807	0.280	548	19.3	22.7	0.1704
IRVING	610	0.882	0.345	649	29.3	33.2	0.1483
HAWK	611	0.858	0.280	625	19.3	23.2	0.1477
DOVE	714	0.927	0.305	728	22.9	27.5	0.1265
GROSBEAK	821	0.990	0.320	837	25.2	30.4	0.1103
LUBBOCK	904	1.040	0.345	924	29.3	35.1	0.0999
GALVESTON	1011	1.090	0.345	1025	29.3	35.7	0.0892
DRAKE	1026	1.108	0.375	1052	34.6	41.2	0.0880
PLANO	1060	1.127	0.345	1073	29.3	36.0	0.0857
CORPUS CHRISTI	1103	1.146	0.345	1113	29.3	36.3	0.0823
ARLINGTON	1151	1.177	0.375	1173	34.6	41.9	0.0788
CARDINAL	1222	1.198	0.345	1225	29.3	37.1	0.0743
FORT WORTH	1300	1.240	0.375	1312	34.6	42.9	0.0698
EL PASO	1350	1.252	0.345	1345	29.3	37.9	0.0672
BEAUMONT	1429	1.294	0.375	1436	34.6	43.7	0.0635
SAN ANTONIO	1475	1.315	0.385	1486	36.4	45.9	0.0615
BITTERN	1582	1.345	0.345	1566	29.3	39.4	0.0577
DALLAS	1795	1.452	0.385	1795	36.4	47.9	0.0507
HOUSTON	1927	1.506	0.415	1934	42.3	54.7	0.0468
LAPWING	1949	1.504	0.385	1940	36.4	48.9	0.0467
FALCON	2045	1.545	0.415	2045	42.3	55.4	0.0445
CHUKAR	2242	1.604	0.395	2220	38.4	52.7	0.0406
BLUEBIRD	2741	1.762	0.415	2703	42.3	59.9	0.0333

Table 5 - ASTM ACCC Conductor Sizes

Note: Ampacity values based on 60 Hz, zero elevation, 90˚ sun altitude, 40˚C ambient temperature, 0.5 Solar Absorptivity, 0.5 Emissivity, 2 ft/sec (0.61 m/sec) wind and 96 Watt/ft2 (1033 W/m2), at corresponding surface temperatures.

INTERNATIONAL SIZES							
ACCC®	Aluminum Area	Conductor Diameter	Core Diameter	Weight	Core Rated Strength	Conductor Rated Strength	Max. Resistance DC @ 20°C
International Size	(mm²)	(mm)	(mm)	(kg/km)	(kN)	(kN)	(ohm/km)
HELSINKI	153.7	15.65	5.97	480	60.4	69.0	0.1860
COPENHAGEN	223.0	18.29	5.97	670	60.4	72.9	0.1279
REYKJAVIK	226.2	18.82	7.11	703	85.7	98.5	0.1263
GLASGOW	239.8	19.53	7.75	750	101.7	115.2	0.1192
CASABLANCA	276.7	20.50	7.11	843	85.7	101.3	0.1033
OSLO	317.7	22.40	8.76	992	130.2	148.0	0.0900
LISBON	318.6	21.79	7.11	957	85.7	103.7	0.0896
AMSTERDAM	371.3	23.55	7.75	1113	101.7	112.6	0.0769
BRUSSELS	425.3	25.15	8.13	1276	112.0	135.9	0.0672
STOCKHOLM	467.2	26.39	8.76	1406	130.2	156.4	0.6120
WARSAW	514.5	27.71	8.76	1539	130.2	159.1	0.0556
DUBLIN	528.8	28.14	9.53	1595	153.8	183.5	0.0541
HAMBURG	553.4	28.63	8.76	1647	130.2	161.3	0.0517
MILAN	574.7	29.11	8.76	1705	130.2	162.5	0.0498
ROME	599.5	29.90	9.53	1793	153.8	187.5	0.0477
VIENNA	636.2	30.43	8.76	1872	130.2	165.9	0.0449
BUDAPEST	675.3	31.50	9.53	2003	153.8	191.8	0.0424
PRAGUE	697.1	31.78	8.76	2050	130.2	169.4	0.0411
MUNICH	740.2	32.84	9.53	2190	153.8	195.4	0.0388
LONDON	766.0	33.40	9.78	2268	162.1	205.2	0.0373
PARIS	820.7	34.16	8.76	2386	130.2	176.3	0.0349
ANTWERP	951.9	36.86	9.78	2779	162.1	215.6	0.0301
BERLIN	1015.5	38.20	10.54	2974	188.3	245.5	0.0282
MADRID	1023.6	38.20	9.78	2977	162.1	219.7	0.0279

Table 6 - IEC ACCC Conductor Sizes

Note: Ampacity values based on 60 Hz, zero elevation, 90˚ sun altitude, 40˚C ambient temperature, 0.5 Solar Absorptivity, 0.5 Emissivity, 2 ft/sec (0.61 m/sec) wind and 96 Watt/ft2 (1033 W/m2), at corresponding surface temperatures.

1.2.7. Surface Finishes

ACCC conductors are normally delivered with a smooth and reflective surface finish typical of any new high-quality conductor that uses smooth-surfaced trapezoidal shaped strands. The end user can also request a non-specular mat-grey finish which is less reflective. The non-specular finish is achieved by a media blasting process prior to the conductor being placed on its shipping reel. The reflectivity of the non-specular surface meets ANSI Standard C7.69 (and other corresponding standards) which is typically ~0.6. The non-specular surface effectively changes the conductor's emissivity (ability to dissipate heat)

which serves to slightly improve current carrying capability. A non-specular finish will also reduce the propensity of moisture to bead on the conductor, which helps mitigate corona discharge and associated noise on wet AC lines.

1.2.8. Reel Types, Sizes, and Conductor Lengths

ACCC conductor is typically delivered on wood or steel reels depending upon the customer's preference. Metal reels usually require a deposit fee and are normally returnable. Wood reels are usually considered non-returnable, but there may be exceptions in either case. If the reels are expected to be stored outside for prolonged periods of time, steel reels should be used, as wood reels deteriorate relatively quickly.

It is important to note that there are substantial differences in handling equipment for wood reels and steel reels. Steel reels are much heavier and require a strong axle to support their weight. **Both reel types require a heavy duty (usually hydraulic) braking system to ensure and maintain adequate back tension.** Wood reel holders support the reel via a compression method. Most metal reels do not have cross bracing inside the drum section. When a wood reel holder is used to support a metal reel the compressive force can cause buckling of the arbor assembly and fail. Reel stands have to be capable of securely and safely supporting ACCC conductor.

Aluminum conductors are shipped in sturdy, carefully designed containers or reels that safeguard the conductor from damage in transit, storage, and at the point of installation. The conductor is carefully inspected during all stages of fabrication; packaging is inspected prior to shipment, and only properly packaged material is delivered to the carrier. All reels will have 91.5 cm (36 in) diameter drum (D) or larger with 13.4 cm (5.25 in) arbor holes for 228.6 cm (90 in) reels and 8.3 cm (3.25 in) arbor holes for 188 cm (74 in) reels unless otherwise specified. Reel sizes can vary with conductor size, required conductor length and other factors. Please contact **support@ctcglobal.com** for more information.

1.3. Quality Control & Strander Variations

ACCC conductor core is produced by CTC Global in Irvine, California. After the core is produced, tested, and certified to ISO 9001-2008 quality assurance standards, the core is carefully packaged and shipped to one of nine ISO certified

and CTC Global qualified international stranding partners located regionally in the US, Canada, South America, China, Europe, Middle East, India, and Indonesia. Each strander has its own production equipment and tooling that may result in minor differences in the finished product. These differences are consistent with the variations allowed in conventional conductors from manufacturer to manufacturer.

1.4. Applicable Standards, Rules, Design and Installation Guidelines

There are several national and international organizations that have developed manufacturing standards, operating rules, design guidelines and installation procedures that relate to bare overhead conductors. In addition to these standards many utilities have developed their own company policies that often provide revised margins of safety, installation tolerances, or "buffer zones" based on their unique circumstances. Standards published by any particular organization may or may not be accepted in a particular region.

ASTM International (formerly known as American Society for Testing of Materials) has a global presence, but in many cases IEC (International Electrotechnical Commission) standards may prevail in particular regions. This can also be true with Trade Associations such as IEEE and CIGRE, whose work often overlaps. The work compiled by these and other Trade Organizations' Technical Advisory Groups and Working Groups, is regularly used as a basis for new or revised standards through joint efforts with other organizations such as IEC, CSA, ASTM, NESC, RUS, ANSI, BSI (UK), CNIS (China), BIS (India) and other associated organizations in many countries around the world. While recommendations or standards may have slight differences, their common purpose serves to help improve product quality, enhance public safety, facilitate trade and uniformity, and build consumer confidence, among other things.

2. Engineering with ACCC Conductor

The primary focus of this Chapter is to discuss in detail the electrical, mechanical, and economic factors that impact or influence the performance of conductors on transmission lines and describe how the ACCC conductor's unique attributes can be used to achieve maximum performance in a variety of project conditions. In particular, the information discusses all factors that guide proper transmission line conductor selection based on electrical performance and appropriate sag and tension calculations. The intention is to provide the basis for understanding how to make the best use of ACCC conductors in any situation.

The factors discussed include the nature of projects (as each project can have unique constraints), a host of electrical considerations, a discussion and description of conductor mechanical characteristics, the nature of spans of conductors joined in a series, the nature of heavy loads and galloping, the nature of long spans, the uniqueness of bundled conductors, and a very important discussion on Aeolian vibration management. After being armed with this information, the options and methodologies for sag-tension calculations and cost-based conductor selection are presented. Chapter 3 discusses modeling ACCC conductor sag and tension in various software programs and Chapter 4 offers several case studies for demonstration and reference.

2.1. Project Types

2.1.1. Capacity Increases on Existing Transmission Lines

Projects engineered to increase the capacity of existing line have been going on for several years, as the acquisition of rights-of-ways (ROW) for new lines has become increasingly more difficult. In many (but not all) cases, it has become more economically attractive to reconductor an existing circuit to increase capacity rather than to add a new circuit even if the improvement to the network is comparatively modest. In such cases, substation improvement costs also have to be considered. Nevertheless, the simple crowding of various land use interests within an area can make it difficult to build new lines and reconductoring projects are often considered.

Short of reconductoring there are a number of ways an existing transmission line can be "up-rated" (per the CIGRE definition) to effectively increase a line's capacity through the use of real-time monitoring devices, adjusting seasonal assumptions, increasing tower height, or other means. CIGRE Technical Brochure TB 294[14] provides a detailed overview of the subject and discusses available options. While various options exist, it is rare that they can offer significant improvements or improved system efficiency compared to reconductoring with ACCC conductor.

While increasing the capacity of an existing transmission line is generally driven by increased consumer demand or the addition of new generation assets, regulatory and reliability factors can also drive these requirements.

While the Cigre technical brochure suggests that "up-rating" a line via real-time monitoring or by establishing revised operating assumptions can achieve as much as a 25% increase in capacity, it also points out that the possible increase may be zero depending upon seasonal conditions. For instance, up-rating may allow an increase in capacity during winter conditions when the ambient air temperature is colder, but may not be available during summer conditions when the ambient air temperature is hotter and the lines are subject to increased thermal sag. The amount of increase that can be achieved is highly dependent upon the amount of excess strength and clearances available in the existing condition, the willingness to cut into or exploit that excess, and the cost of doing so. Achieving the maximum increases possible requires the maximizing of all three of these points.

When desired capacity increases cannot be achieved by real-time monitoring or other method, then physical modifications to the existing line may need to be performed to accommodate additional sag or the installation of a new larger/heavier conventional conductor or higher tensions. In some cases the existing structures may be 'de-rated' due to their condition. In either situation, the use of an equal or even smaller diameter/lighter ACCC conductor can be used to achieve capacity increases with little to no structural investment.

In theory, the choice of method to increase current is determined by a study that finds the highest added amperes/expenditure ratio from all possible options, or

---

[14] Cigre Technical Brochure TB 294 How Overhead Lines are Re-Designed for Uprating / Upgrading B2.06 (June 2006)

is determined by a quantified goal that is independent of the line's inherent potential for up-rating. In practice, only a few of the options are generally practical for any particular line. CIGRE Technical Brochures 207[15], 244[16], 450[17], 324[18], 331[19], 353[20] and 426[21] provide additional information on conductors and line uprating methods.

2.1.2. New Transmission Line Projects

As an alternative to increasing the capacity of an existing transmission line, or in cases where a new line has to be built to enable power delivery from a new source of generation or to a new or growing load center, a new transmission line must be developed. This is a relatively complex and time consuming process that requires a substantial investment of resources which is especially true on longer projects that cross state, country or other jurisdictional boundaries. Nevertheless, new transmission projects generally have clear objectives. Planners typically assess demand, load flow, generation assets, anticipated growth factors and other data that establish the electrical parameters of a new line. Transmission engineers, armed with survey and easement data (or proposed easement data), consider optimal pathways, structure placement, and structure type based on a number of variables including property lines, soil conditions, vegetation and esthetics. Line length, voltage, current type (AC/DC), conductor type and size, and many other factors are carefully considered to address potential line losses, line stability, voltage drop and other important factors, as discussed below.

---

[15] Cigre Technical Brochure TB 207 "Thermal Behavior of Overhead Conductors" SC 22 WG 22.12 (2002)

[16] Cigre Technical Brochure TB 244 "Conductors for the Uprating of Overhead Lines", SC B2 WG B2.12 (2004)

[17] Cigre Technical Brochure TB 450 "Grid Integration of Wind Generation C6.08 (Feb 2011)

[18] Cigre Technical Brochure TB 324 "Sag Tension Calculation Methods For Overhead Lines B2.12.3 (June 2007)

[19] Cigre Technical Brochure TB 331 "Considerations Relating to the use of High Temperature Conductors (2007),

[20] Cigre Technical Brochure TB 353 Guidelines for Increased Utilization of Existing Overhead Transmission Lines WG B2.13 (August 2008)

[21] Cigre Technical Brochure TB 426 Guide for Qualifying High Temperature Conductors for Use on Overhead Transmission Lines WG B2.26 (2010)

2.2. Project Economics

Conductor selection can have a significant impact on both the short and long term economic performance of transmission projects. Since conductors are one of the major cost components of a line design, selecting an appropriate conductor type and size is essential for optimal operating efficiency. To this end, a number of systematic approaches for conductor selection have been developed.[22] Methods of evaluation vary by author and case study; nevertheless, different approaches universally stress the importance of the same electrical and mechanical conductor properties as they pertain to project economics[23]. The ultimate goal is to select a conductor that provides the best value when viewed from an overall *systems* point of view. In this regard, ACCC conductor can provide T&D planners and systems engineers with a means to both reduce initial costs and increase long-term returns.

2.2.1. Conductor Selection

The choice of conductor type and size has a major impact on transmission line design and subsequent financial returns. For any given project, however, this choice is often limited to a narrow set that conforms to specified criteria; including (but not limited to):

- Electrical load requirements
- Load growth projections
- Network voltage requirements and/or accessible voltage ranges
- Support structure requirements, limitations, and/or the availability of extant infrastructure (towers)
- Environmental considerations
- Regulatory statutes

---

[22] Kennon, RE., and Douglass, DA., "EHV Transmission Line Design Opportunities for Cost Reduction," IEEE Paper 89 TD 434-2 PWRD

[23] Vajeth R and Dama D, "Conductor Optimisation for Overhead Transmission Lines", Inaugural IEEE PES Conference, July 2005

Some physical and economic consequences that affect the choice of conductor subject to these constraints include:

- Increasing conductor diameter yields increased wind and ice loads on support structures, increasing initial cost for towers and foundations
- Decreasing conductor diameter leads to a higher density radial field about the conductor, potentially increasing corona-induced noise
- Choosing a conductor with a higher resistance subsequently raises the cost of electrical losses over the life of the line, reducing the present worth of transmission assets
- Increasing conductor tension yields increased longitudinal loads and/or increased transverse tension loads on angle structures, also increasing initial investment

Consequently, a multivariate systems approach, such as those described above, must be followed to find an optimal solution for any proposed T&D project. Such an analysis should include an assessment of first-cost capital investment as well as the long term operating cost associated with various options.

2.2.2. Capital Investment Cost

The capital investment cost (CIC) associated with a T&D project is the sum of all expenses associated with component purchase, regulatory compliance, and project construction. Since each of these is significantly impacted by conductor selection, the conductor should be chosen on the basis of total systems cost – not simply the unit cost of the conductor.

In this regard, ACCC conductor provides substantial CIC advantages over conventional conductors. For new construction projects, the increased tensile strength and exceptional sag performance of ACCC conductor reduces the number and/or reinforcement cost of required support structures. These same performance advantages can be used to reduce right-of-way (ROW) requirements by limiting blowout clearance for new transmission corridors. For transmission line upgrades, ACCC conductor provides increased rated capacity without increased conductor size or weight – allowing transmission engineers to increase power delivery without modifying and/or expanding existing support infrastructure. ACCC conductor also provides planners with a variety of means to reduce CIC and, when the total costs of a transmission system are considered,

using ACCC conductor is often the lowest cost option for both new construction and existing line upgrades.

2.2.3. Life Cycle Cost

The Life Cycle Cost (LCC) associated with a transmission project is the sum of all recurring expenses, including annual capital costs and system line losses. Line losses can have a substantial impact on transmission line economics and should, therefore, always be considered when evaluating the economic value of a particular line design. (The significance of line losses is discussed in more detail in Sections 2.6 and 2.7). Since LCC, by definition, is dependent on dynamic market factors (escalating energy costs, load growth, etc.), a Net Present Value (NPV) analysis and an appropriate discount rate should be determined to provide the best estimate of long term project value.

2.2.4. Total Annual Cost

The methodology presented below is adapted from "Conductor Life Cycle Analysis" by Leppert & Allen[24]

The Total Annual Cost (TAC) is defined as the sum of the Annual Capital Cost (ACC) and the Annual Loss Cost (ALC).

$$TAC = ACC + ALC \qquad (2\text{-}1)$$

ACC is the product of a utility's annualized Carrying Charge (CC) for new investments and its unit Cost of Line (CL). Here, the utility's CC is defined as the sum of the interest rate of borrowed funds, operations expense, depreciation, and taxes, all expressed in decimal form.

ALC is the product of a system's Annual Energy Loss (AEL) and the Cost of Lost Energy (CLE).

---

[24] Leppert, SM et al., Conductor Life Cycle Cost Analysis; (pages C2/1 - C2/8) Presented at 39th Annual Rural Electric Power Conference, Nashville, TN, USA (April 30 – May 2, 1995)

Here AEL is defined as:

$$AEL = \frac{(Peak\ kW)^2 \times \frac{Resistance}{phase \times mile} \times Loss\ Factor \times \frac{8760\ hours}{year}}{(Voltage\ kV)^2 \times (Power\ Factor)^2 \times \#\ of\ Phases \times \frac{1000\ k\Omega}{\Omega}}$$

(2-2)

…and CLE is:

$$CLE = WEC + \frac{\frac{12\ months}{year} \times WDC \times Demand\ Adj.Factor}{\frac{8760\ hours}{year} \times Load\ Factor}$$

(2-3)

Where:

> WEC = Wholesale Energy Charge (in $ kW^{-1})
> WDC = Wholesale Demand Charge (in $ kW^{-1} Month^{-1})
> Demand Adj. Factor = *The sum of the square of the monthly peaks divided by the square of the peak month (for those months which exceed the ratcheted minimum), Plus, The per unit ratchet times the number of months the ratchet is paid, all divided by 12*
> Load Factor = Average Demand / Peak Demand

Loss Factor = $(0.84)^2$ * (Load Factor) + (0.16) * (Load Factor)   (2-4)

Coefficients (0.84 & 0.16) for the loss factor equation have been empirically determined for North American markets, but vary by region. For a discussion on loss factor coefficient determination, please see reference.[19]

2.2.5. Net Present Value

Net Present Value (NPV) is used as an indicator to determine how much value a particular investment will return over time. In financial theory, if there is a choice between two mutually exclusive alternatives, the one yielding the higher NPV should be considered preferable. In simplified terms, NPV can be described as the sum of any advantages produced by an investment over a specified period of time (referred to as Present Value or PV) minus the upfront capital cost or "investment" yielding the NPV. An NPV analysis requires the establishment of a *discount rate* (i) that considers the rate of return that could be earned on an investment with a similar risk / reward profile. In many cases, is estimated by a utility's cost of debt (i.e. the interest rate on borrowed funds) NPV is determined as follows:

$$\sum_1^t \frac{R_t}{(1-i)^t} \tag{2-5}$$

Where:

$R_t =$ the net cash flow (the amount of cash, inflow minus outflow) at time t. R_0 is commonly placed to the left of the sum to emphasize its role in the overall investment.

$t =$ service life of the asset in years

$i =$ discount rate

2.2.6. Present Worth Assessment

In economic comparisons of different conductor types and sizes, the costs of losses must be adjusted to reflect anticipated changes in load growth and wholesale power costs over the anticipated service life of the conductors. Since load growth, loss assumptions and the cost of wholesale power change at time-dependent rates, an "effective loss discount rate" – different from the standard discount rate – must be determined to assess how the "Present Worth" of transmission losses change over time. The formula used to derive the effective loss discount rate (i_e) in percentage form is:

$$i_e = \frac{\left(1+\frac{i}{100}\right)}{\left(1+\frac{\% \, rate \, escalation}{100}\right)} - 1 \tag{2-6}$$

Since line losses are not constant but increase at a rate proportional to the square of the growth rate, the formula is modified as:

$$i_e = \frac{\left(1+\frac{i}{100}\right)}{\left(1+\frac{\% \, rate \, escalation}{100}\right)\left(1+\frac{\% \, load \, growth}{100}\right)^2} - 1$$

$$\tag{2-7}$$

The Present Worth of a series of Annual Loss Costs (PWALC) and Annual Capital Costs (PWACC) may be approximated by:

$$PWALC = \left[\frac{(1+i_e)^n-1}{i_e(1+i_e)^n}\right] \times \left[\frac{1+i_e}{1+i}\right] \times ALC \tag{2-8}$$

25

$$PWACC = \left[\frac{(1+i)^n-1}{i(1+i)^n}\right] \times ACC$$

(2-9)

The Total Life Cycle Cost (TLCC) may then be determined as:

$$TLCC = CIC + PWACC + PWALC \qquad\qquad (2\text{-}10)$$

Comprehensive systems evaluations and TLCC analyses help T&D engineers and planners make more informed decisions in the line design and specification phase. In doing so, T&D professionals are able to optimize project economics and provide utilities with increased ROI.

2.3. Support Structure Considerations

Transmission line structures come in a wide range of materials, arrangements, functional types and sizes. The type, choices and locations of a transmission line's structures are based on terrain, land use, soil types, owner preferences, affected landowner preferences, easement width, clearance requirements, conductor size and tension and other factors.

Taller structures are generally used to increase span length to reduce the overall number of structures. Soil or other ground conditions will influence foundation requirements or direct embedment depth, which in turn leads to certain structure type preferences. Anticipated wind or ice loads also influence structure selection. While there are certain advantages to using a standard structure type, it is not uncommon to see various structures used in combination on any given line. In any situation, environmental conditions, electric and mechanical loads, structure and conductor types, all must be looked at with a systems approach, as each aspect affects the other and all impact short and long term economics. A structure's aesthetics is also playing an increasingly important role in project acceptance and approval.

The choice of conductor will do much to define the structure. The obvious conductor characteristics to define the structures are diameter, weight and design tension. The density (unit weight/diameter ratio) of the conductor can also define its range of motion with wind (galloping and blowout) which may impact phase spacing on the structures.

The condition, type, size, and location of existing structures can dictate or limit certain options. Voltage increase, for instance, generally requires increased clearance to ground and generous phase spacing. If reconductoring is being considered, the structures must be high and strong enough to support the weight (and added sag) of a larger / heavier conventional replacement conductor or a new high capacity, low sag conductor such as ACCC conductor, could be used to increase capacity and/or reduce line losses, with little to no structural modifications. In some cases, the condition of metal, wood, or metal reinforced concrete structures may not allow reconductoring with the same size conductor as these structures may be down-rated in terms of allowable loading. In such a situation, a smaller / lighter / higher capacity ACCC conductor could offer significant advantages, including the potential of substantially increasing capacity, while decreasing line tension to reduce stress on existing structures.

Overall, pre-determined (or existing) support structures can limit certain conductor options. Conversely, specific conductor choices can dictate structure features. Either way, these two major line components are intrinsically linked. The ACCC conductor offers greater design flexibility in either case.

2.4. Electrical Performance Considerations

Fundamental to any project is the determination of the electrical load that the transmission or distribution line will be called upon to deliver. While some lines (e.g., serving as independent links directly from a source of generation to the grid) may be relatively easy to consider, many other lines within the grid can be impacted in positive or negative ways depending upon how new lines or upgraded lines are connected. The seemingly simple question is not always easy to answer. The length of the line, voltage, current (AC / DC) and many other factors come into play; line losses, line stability, voltage drop and other important factors must be considered. Typically, the higher the voltage and the longer the line, the more complex the considerations become. In 2006, AEP replaced a 24 km (~15 mile) section of a 138 kV line in Texas. In addition to increasing the line's capacity and reducing thermal sag, AEP also reported a .9

MW reduction in line losses on the upgraded line. AEP also reported that the added efficiency of the ACCC conductor also reduced 'stress' on the interconnected system for an overall savings of 1.1 MW.

2.4.1. Electrical Clearances

The primary consideration of clearances is insulating the electrified conductors from any type of 'ground.' The fundamental insulation employed by overhead lines is the air surrounding each conductor. The airspace required must accommodate the voltage-to-ground (including during voltage surge conditions) space for vehicles, structures, under-built lines, human or animal activity, and the motion of the conductors caused by environmental conditions, among other things. Safety codes and owner standards from around the world address these clearance components with varied methods, but with similar concerns.

International, national, and state/ provincial safety codes specify minimum clearance requirements under a number of specified conditions. These are held to be legal requirements and it is unwise to challenge them with a very finely tuned design. Company standards generally include a clearance buffer on the local jurisdiction's legally required values and are thus larger to accommodate minor construction variations and other unforeseen variables.

2.4.2. Thermal Constraints

The capacity of most transmission lines under approximately 100 km (60 miles) in length is generally limited by Thermal Constraints rather than Voltage Drop or Surge Impedance Limits. Thermal constraints are dictated by either a conductor's maximum allowable operating temperature or the maximum thermal sag developed at some chosen design tension, given the structures' strength, height and placement.

In some cases, running a conductor hot may be useful because it will allow higher capacity with a smaller, less expensive set of conductors and support structures. In this instance, the ACCC conductor's low coefficient of thermal expansion offers excellent sag, capacity, and clearance advantages, however, higher temperature operation and line length will increase line losses. Nevertheless, the ACCC conductor's high aluminum content (and lower resistance of fully annealed 1350-O aluminum) helps reduce line losses by as much as 35% compared to other conductors of the same diameter and weight

under equal load conditions. While other conductor types also use trapezoidal shaped strands which can increase the aluminum content for a given conductor diameter, the lighter weight of the ACCC conductor's composite core compared to a steel core allows an added aluminum content without a weight penalty. The 25% increase in weight of an ACSS/TW "Suwannee" conductor (Drake diameter equivalent), can cause it to sag excessively before it reaches its maximum operating temperature/ampacity, compared to the more dimensionally stable and lighter Drake size ACCC conductor.

2.4.3. Inductive and Capacitive Reactance

In AC transmission lines, the current flowing through a conductor varies sinusoidally, so the magnetic field (associated with a current carrying conductor) which is proportional to the current also varies sinusoidally. This varying magnetic field induces an emf (or induced voltage) in the conductor. This emf (or voltage) opposes the current flow in the line, and is equivalently shown by a parameter known as inductance (L). The greater the amount of inductance, the greater the opposition from this inertia effect becomes. The induced voltage depends on the relative configuration between the conductor and magnetic field, and is proportional to the rate at which magnetic lines of force cut the conductor.

The opposing force which an inductor presents to the FLOW of alternating current is *INDUCTIVE REACTANCE* as it is the "reaction" of the conductor to the changing value of alternating current. Inductive reactance is measured in ohms and its symbol is X_L. Reactance increases with the increase in frequency.

In the calculation of inductance, the magnetic flux inside and outside of the conductor are both considered in the total inductance. The formula for inductance and inductive reactance of a single conductor are as follows:

$$L = L_{int} + L_{ext} \quad \text{and} \quad X_L = 2\pi f L \tag{2-11}$$

Where:

X_L is inductive reactance in ohm
2π is 3.1416 constant x 2 (~6.28)
f is frequency of the alternating current in Hz
L is inductance in Henry

L_{int} = $(\mu_r\mu_o/8\pi)*\iota$ is the internal inductance due to internal flux linkage, with μ_r and ι being the relative magnetic permeability of conductor core material and conductor length (meter) respectively.

L_{ext} = $(\mu_o/2\pi)*\iota*\ln(D/r)$ with r being the conductor radius and D being the distance to the conductor where inductance is assessed.

It can be readily shown that the L_{ext} is typically dominant as it is about an order of magnitude higher than L_{int} if the conductor core is made with non-magnetic material ($\mu_r=1$), such as ACCC conductors.

For three-phase transmission lines, the inductance per phase can be simplified into the following equation for conductors with non-magnetic core materials:

$$L_{phase} = (\mu_o/2\pi)*\iota*\ln(GMD/GMR_{cond})(H) \qquad (2\text{-}12)$$

$$X_{Lphase} = \mu_o*f*\iota*\ln(GMD/GMR_{cond})(Ohm) \qquad (2\text{-}13)$$

Where GMD is the geometrical mean distance for a three-phase line, and GMR_{cond} is the geometrical mean radius of the conductor.

For medium and long distance lines, the line inductive reactance is more dominant than resistance. It should be noted that the core materials of some conductors are highly magnetic. For example, the Invar steel core contains about 36% Ni, which makes it highly magnetic with a relative magnetic permeability approaching 1750 to 6000[25]. This significantly increases the internal inductance and overall inductance (and inductive reactance) by at least two orders of magnitude, with significant implication to power quality, voltage drop as well as circuit stability (VAR consumption).

Capacitance of a conductor (or ability to store an electric charge) also offers real opposition to current flow. This opposition arises from the fact that, at a given voltage and frequency, the number of electrons that cycle back and forth is limited by the storage ability or *capacitance* of a conductor. As the capacitance

---

[25] Section 2.6.6, Magnetic Properties of Materials, Kaye & Laby Tables of Physical and Chemical Constants, National Physical Laboratory.

is increased, a greater number of electrons flow per cycle. Since current is a measure of the number of electrons passing a given point in a given time, the current is therefore increased. Increasing the frequency will also decrease the opposition offered by a capacitor. This occurs because the number of electrons which the capacitor is capable of handling at a given voltage will cycle more often. As a result, more electrons will pass a given point in a given time (greater current flow). The opposition which a capacitor offers to AC is inversely proportional to frequency and to capacitance. This opposition is called *CAPACITIVE REACTANCE* (X_C). Capacitive reactance decreases with increasing frequency or, for a given frequency, the capacitive reactance decreases with increasing capacitance. The symbol for capacitive reactance is. X_C varies inversely with the product of the frequency and capacitance. The formula is:

$$X_C = 1 / 2\pi fC \qquad\qquad (2\text{-}14)$$

Where:
X_C is capacitive reactance in ohm
f   is frequency in Hertz
C   is capacitance in farad
2π is 6.28 (2 × 3.1416)

X_C and X_L affect the characteristic impendence of the line, which in turn affects voltage drop, surge impendence loading and the load-ability of a transmission circuit. While determining the X_c and X_L for the system is shown in several publications, the values for overhead conductors that are typically published are the inductive and capacitive reactance at 1 ft (0.3m) radius. These values published for ACCC conductors are calculated by the typical equations:

$$X_a = 0.2794 \left(\frac{f}{60}\right) \; log \left(\frac{1}{GMR}\right) \qquad\qquad (2\text{-}15)$$

$$X'_a = 0.6822 \left(\frac{60}{f}\right) log \left(\frac{1}{r}\right) \qquad\qquad (2\text{-}16)$$

Here, *GMR* is the geometric mean radius of the conductor and *r* is the radius of the conductor in inches.

2.4.4. Impedance

Impedance (Z) is the expression of the opposition that an electronic circuit offers to AC or DC current. It is a vector quantity (two dimensional), consisting of the two independent scalar (one-dimensional) phenomena: resistance and reactance discussed in previous section.

- As discussed before, the resistance is a measure of the extent to which a substance opposes the movement of electrons among its atoms or ions in molecules. It is observed with both Alternating Current and with Direct Current, expressed in positive real number (ohms).
- Reactance (X) is an expression of the extent to which an electric circuit or system stores or releases energy with each AC cycle. Reactance is expressed in imaginary number (Ohms). It is observed in AC, but not for DC. When AC passes through conductors, energy might be stored and released in the form of a magnetic field (in which case the reactance is inductive, $+jX_L$), or an electric field (in which case the reactance is capacitive, $-jX_C$). Reactance is conventionally multiplied by the J operator.
- The conductor impedance Z, is then expressed as a complex number of the form: $R + jX_L - jX_C$.

In an AC circuit which contains only resistance, the current and the voltage will be in phase and will reach their maximum values at the same instant. If an AC circuit contains only reactance, the current will either lead or lag the voltage by one-quarter of a cycle or 90 degrees. In practical circuit, the current will not be in step with the voltage nor will it differ in phase by exactly 90 degrees from the voltage, but it will be somewhere between the in-step and the 90-degree out-of-step conditions. The larger the reactance is, compared with the resistance, the more nearly the phase difference will approach 90º. The larger the resistance compared to the reactance, the more nearly the phase difference will approach zero degrees.

2.4.5. True, Reactive and Apparent Power

Reactive loads such as inductor and capacitors dissipate zero power, yet the fact that they drop voltage and draw current gives the deceptive impression that they

actually dissipate power. This 'phantom' power is called reactive power, Q, measured in unit of VAR (Volt-Amps-Reactive), rather than watts. The actual amount of power being used or dissipated in a circuit is called true power (i.e., real power), P, measured in unit of watt. The combination of reactive power and true power is called Apparent Power, S, measured in unit of VA (Volt-Amps), and the Apparent Power (S) is the product of a circuit's voltage and current without reference to the phase angle (see power triangle in Figure 8).

- True Power (P) is a function of a circuit's dissipative elements, e.g., resistance (R): $P = I^2R$ or V^2/R
- Reactive Power (Q) is a function of a circuit's reactance (X): $Q = I^2X$ or V^2/X
- Apparent Power (S) is a function of a circuit's total impedance (Z): $S = I^2Z$ or V^2/Z or IV
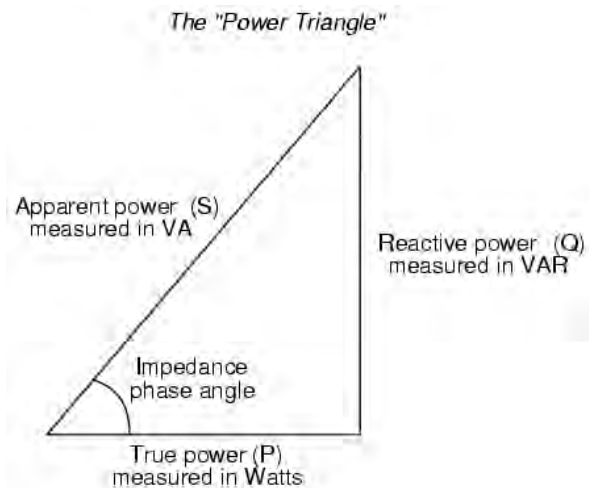
Figure 8 – True power, Reactive power and Apparent power relationship

Conductor and practical loads have resistance, inductance and capacitance, so both real and reactive power will flow to real loads. Apparent power is measured as the magnitude of the vector sum of real and reactive power. Apparent power is important, because even though the current associated with reactive power does no work at the load, it does heat the conductors and wasting energy. Conductors, transformers and generators must therefore be sized to carry the

total current, not just the current that does useful work. The ACCC conductor's lower resistance decreases both real and apparent power losses.

The ACCC conductor's lower resistance is based on four factors. 1) The ACCC conductor typically incorporates about 25% more aluminum using compact trapezoidal shaped strands (with generally little or no weight penalty to the conductor); 2) the ACCC conductor uses annealed aluminum which offers the lowest resistance (i.e., highest degree of conductivity) compared to other aluminum alloys; 3) the ACCC conductor operates at cooler temperatures compared to other conductors under equal load flow, which further improves efficiency as lower temperatures reflect reduced conductor resistance; 4) the ACCC conductor's composite core is non-conductive and non-magnetic, thus no power is lost due to hysteresis.

2.4.6. Power Factor

The ratio between the real and apparent power are linked by the *power factor* which is given by:

$$Power\ Factor = \frac{active\ power}{apparent\ power} = \frac{UI\ cos\emptyset}{UI} = cos\emptyset \qquad (2\text{-}17)$$

The power factor is a practical measure of the efficiency of a power distribution system. For two systems transmitting the same amount of real power, the system with the lower power factor will have higher circulating currents due to energy that returns to the source from energy storage in the load. These higher currents produce higher losses and reduce overall transmission efficiency. A lower power factor circuit will have a higher apparent power and higher losses for the same amount of real power.

The power factor is considered 'one' when the voltage and current are in phase. It is 'zero' when the current leads or lags the voltage by 90 degrees. Power factors are usually stated as "leading" or "lagging" to show the sign of the phase angle, where leading indicates a negative sign. They are also generally described in a decimal fashion (i.e. power factor of .95)

Purely capacitive circuits cause reactive power with the current waveform leading the voltage wave by 90 degrees, while purely inductive circuits cause reactive power with the current waveform lagging the voltage waveform by 90

degrees. The result of this is that capacitive and inductive circuit elements tend to cancel each other out. Where the waveforms are purely sinusoidal, the power factor is the cosine of the phase angle (ϕ) between the current and the voltage sinusoid waveforms.

2.4.7. Voltage Drop

On an AC line, voltage drops proportionally with line length primarily as a result of electrical phase shifting and conductor impedance. Voltage drop is usually limited to 5 to 10 percent along a line, which becomes increasingly difficult to control as line length increases. Voltage drop generally impacts the power flow on transmission lines between 60 and 180 miles (100 and 300 km) in length. Appropriate conductor selection can reduce voltage drop allowing longer lines between fewer substations and reduce the need for substations.

These aspects include non-uniform current density due to the skin effect and transformer effect (particularly with steel-cored conductors) that influence conductor inductance[26]. Inductive impedance decreases as frequency increases. The presence of steel will give rise to magnetic hysteresis, eddy currents and the redistribution of current density between the nonferrous wires which impacts resistance and impedance. Highly magnetic steel alloys such as invar can exacerbate these effects. The selection of a conductor that does not incorporate a magnetic core such as ACCC conductor can reduce voltage drop constraints. The addition of shunt capacitors at the ends of the transmission line can also be used to reduce these constraints, which can allow greater levels of current to flow at higher operating temperatures.

In AC lines, impedance (Z) depends on the spacing and dimensions of the conductors, the frequency of the current and the magnetic permeability of the conductor and its surroundings, as discussed in previous section. Voltage drop in an AC line is the product of the current and the impedance of the circuit, E = I*Z. Over longer distances, extremely large conductors may not be economically attractive. It is usually preferable to move to higher voltages. Higher voltage circuit requires less current to transmit the same power, which also serves to reduce line losses. Deploying ACCC conductor can further

---

[26] Karady, GG, Transmission System "*The Electric Power Engineering Handbook*" Ed. L.L. Grigsby Boca Raton: CRC Press LLC, 2001

improve efficiency with line loss reduction by as much as 35% due to its inherently lower resistance.

2.4.8. Surge Impedance Loading and Loadability

As power flows along high voltage transmission lines, there is an electrical phase shift that increases proportionally with the length of the line and its electrical current. As the phase shift increases, the system in which the line operates becomes increasingly less stable and more susceptible to electrical disturbances. While longer lines exhibit greater susceptibility than shorter lines, these stability limits typically govern operating limits, especially on lines exceeding 180 miles (300 km) in length.

For a loss-less line, its impedance simply becomes:

$$Z_o = \sqrt{\frac{L}{C}} \ (ohms) \tag{2-18}$$

This is called the *surge* or *characteristic* impendence. This impendence can also be expressed in terms of the surge impendence load (SIL), or *natural loading*, which occurs when a transmission line is loaded such that no net reactive power flows into or out of the line. The SIL is given by:

$$SIL = \frac{V_{LL}^2}{Z_o} \ (MW) \tag{2-19}$$

Where: V_{LL} is the line voltage.

When the line is loaded below its SIL, the line *supplies* (lagging) reactive power. If the line is loaded above the SIL, it *absorbs* reactive power.

The loadability of a transmission line can be evaluated knowing not only the SIL as a function of the length of the line, but also setting the voltage drop tolerances and limitations of the steady-state stability value (such as the allowed maximum phase shift the system can handle), one can evaluate how a line will perform and be able to remain stable without the need for shunt capacitors and other devices to keep the line voltage from collapsing. Figure 9 illustrates a

typical loadability curve. Reference[27] is an excellent paper on the subject of loadabilty of transmission circuits. With ACCC® conductor being used on the line, the loadabilty of the lines can be improved for the reasons discussed in section 2.4.5
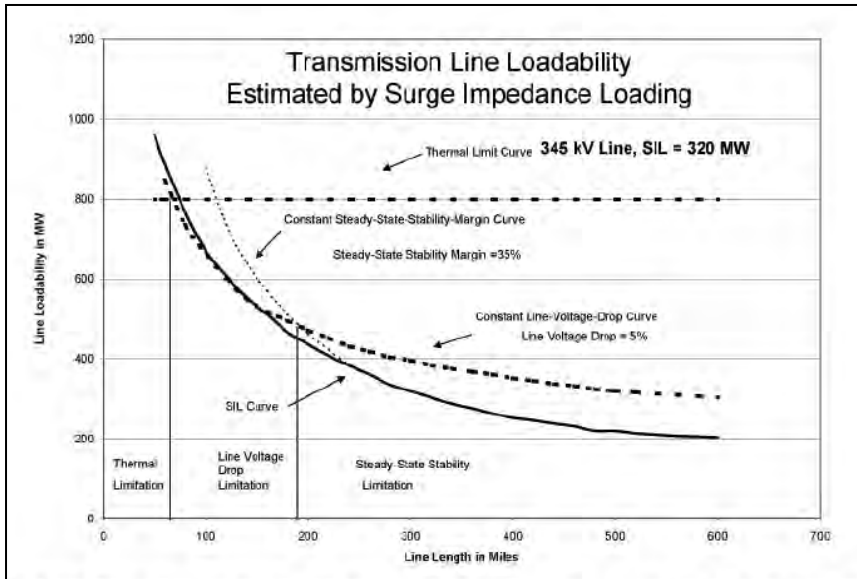
Figure 9 - Thermal, voltage drop, and stability load limits as a function of the line length[28]

2.4.9. Electric and Magnetic Field Considerations

Voltage on a transmission line creates an electric field. The current flowing through a conductor creates a magnetic field. The levels of magnetic field associated with any transmission line are primarily a function of the conductor spacing, geometry of the phase conductors, and current flow. The presence or

---

[27] Gutman, R, "Analytical Development of Loadability Characteristics of EHV and UHV Transmission Lines" IEEE Transactions on Power Apparatus and Systems; Vol.PAS-98 No. 2 March/April 1979

[28] Cigre Technical Brochure TB 425 Increasing Capacity of Overhead Transmission Lines Needs and Solutions. B2/C1.19 (August 2010)

absence of a ferromagnetic (steel) core within a conductor does not alter the magnetic fields outside of the conductor.

2.4.10. Corona, Audible & Radio Noise, and Ozone

Corona is a phenomenon where the localized electric field near an energized conductor can be sufficiently concentrated to produce an electric discharge that can ionize air (causing it to become conductive), create plasma and produce ozone. This electrical discharge can also cause small amounts of sound and radio interference ("radio noise"). The discharges and noise also result in unfavorable power losses. While this phenomenon is generally associated with voltages above 200 kV, sufficient conductor diameter/surface area (especially through the use of multiple "bundled" conductors in each phase) can provide the appropriate level of mitigation.

Several other factors, however, can exacerbate the problem. Conductor surface irregularities caused by scratches, nicks, debris, or water droplets can affect the conductor's surface gradient and cause an increase in corona. Higher altitudes (lower air density) will increase corona discharge because the insulating value of air decreases with its decreasing density. The ACCC conductor's smooth trapezoidal strands may slightly improve corona performance compared to round wire designs of the same diameter[29]. Mineral-based production lubricants (or grease), typically used for conductors stranded with hard Aluminum or Aluminum alloys, can cause dirt and debris to build up on the surface of a conductor. The ACCC conductor's high-purity trapezoidal-shaped aluminum strands are pre-annealed (soft) which allows vegetable/water-based lubricants to be used during manufacturing. This less hydrophobic option, combined with ACCC non-specular finish may help minimizing sediment build up and corona discharge.

---

[29] Corona and Field Effects of AC Overhead Transmission Lines IEEE Power Engineering Society July 1085
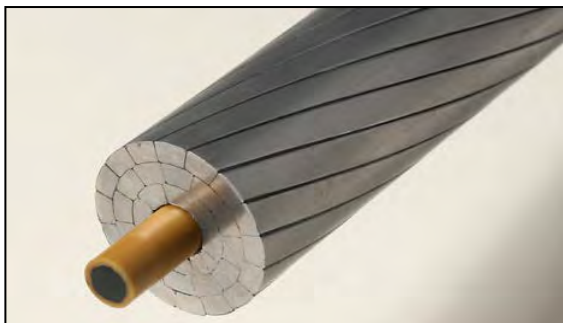
Figure 10 – ACCC conductor with smooth trapezoidal shaped strands and 'non-specular' surface finish which can reduce corona and radio noise

As with any conductor, especially those using annealed aluminum such as ACSS, and ACCC, care must be taken during installation to ensure that the conductor surface is not scratched or damaged.

Because power loss is uneconomical and audible and radio noise is undesirable, corona on transmission lines has been studied by engineers since the early 1900's. Many excellent references on the subject of transmission line corona and discharge exist.[30] Consequently, corona is well understood by engineers and steps to minimize it are one of the primary factors in transmission line design for high voltage transmission lines (typically above 200 kV), especially in inclement weather conditions or at high altitudes where reduced air density can have a detrimental effect.[31] A conductor selected for a project's transmission line must therefore be of sufficient diameter (and offer a suitable surface gradient) to lower the localized electrical stress on the air at the conductor's surface so that little or no corona activity will exist under normal or inclement operating conditions. In many cases, the use of bundled phase conductors can be used to decrease the overall surface gradient to minimize corona discharge.

---

[30] Renew, D; Kavet,R; Charging and Transport of Aerosols near AC Transmission Lines: A Literature Review, EPRI, Palo Alto, CA, and National Grid Transco Plc., London, England: 2003. 1008148.

[31] Chartier, V.L., L.Y. Lee, L.D. Dickson, and K.E. Martin."Effect of High Altitude on High Voltage AC Transmission Line Corona Phenomena;"IEEE PWRD-2. pp. 225-236, January, 1987

The spacing and orientation of bundled conductors can also influence corona performance.[32]

While the primary concerns regarding conductor corona relate to audible and radio noise, (and power loss in extreme circumstances), corona activity on bare overhead electrical conductors can also produce very small amounts of gaseous effluents including ozone (O_3) and nitrogen oxide (NO_X). However, the effluents generated are barely measurable over ambient levels.[33]

Though ozone in the stratosphere is naturally occurring in concentrations of approximately 6,000 parts per billion (ppb) - which serves to favorably absorb UV radiation - at ground level, typical rural ambient levels are normally measured at about 10 to 30 parts per billion (ppb) at night, and up to 100 ppb during daylight hours. In urban areas, concentrations greater than 100 ppb can occasionally be measured due to the influence of hydrocarbons and other pollutants. After a thunderstorm, ground level air may contain 50 to 150 ppb of ozone. While the presence of water droplets can increase corona activity on AC transmission lines, the presence of moisture inhibits the production of gaseous effluents, so there is essentially no net increase in ozone or nitrogen oxide generation under these conditions. Moisture on DC lines also serves to decrease corona discharge.[34]

---

[32] Chartier, V.L., D.E. Blair, R.D. Stearns, and D.J. Lamb. "Effect of Bundle Orientation on Transmission Line Audible and Radio Noise." IEEE PWDR-9. pp. 1538-1544. July. 1994
[33] EPRI 2005 "EPRI AC Transmission Line Reference Book – 200 kV and Above, Third Edition" Electric Power Research Institute, Palo Alto, California
[34] B. Henning, "Corona Effects in High Voltage DC Lines", Direct Current, December 1952
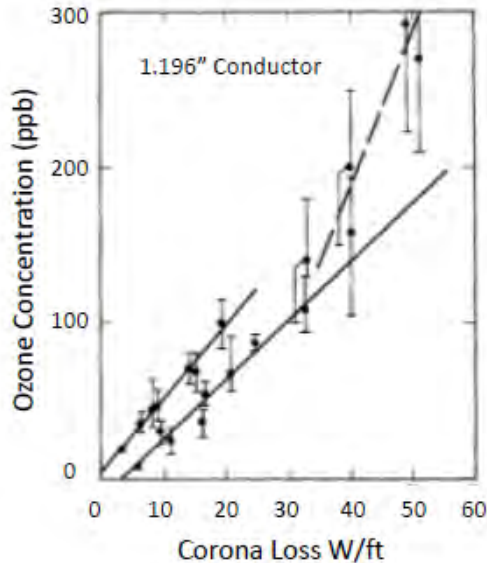
Figure 11 – Ozone generated by overhead conductors is
rarely greater than ambient levels. [35]

Because of its potential environmental impact, a substantial effort went into
assessing ozone production and dispersion at or near, UHV overhead conductors
in both lab and field conditions. A particularly interesting study was performed
by J.F. Roach, V.L. Chartier, and F.M. Dietrich of the Westinghouse Electric
Corporation in conjunction with American Electric Power.[36]   While field
measurements were only able to record approximately 2 to 5 ppb of ozone above
ambient levels of approximately 20 to 60 ppb, lab tests were able to record ozone
concentrations ranging from about 5 to nearly 300 ppb during the assessment of
several conductors in single and bundled configurations.   Figure 11 (from

[35] Roach, J.F., V.L. Chartier, F.M. Dietrich, H.J. Nowak; "Experimental Oxidant Production
Rates for EHV Transmission Lines and Theoretical Estimates of Ozone Concentrations Near
Operating Lines" Power Apparatus and Systems, IEEE Transactions on Page(s): 647 – 657
Issue Date: March 1974 Volume: PAS-93 Issue:2

[36] Roach, J.F., V.L. Chartier, F.M. Dietrich, H.J. Nowak. 1978."Ozone Concentration
Measurements on the C-Line at the Apple Grove 750 kV Project and Theoretical Estimates
of Ozone Concentrations Near 765 kV Lines of Normal Design," IEEE-PAS-97. pp. 1392-
1401, July/August.

Reference 35) shows ozone concentration on a 1.196 inch (30.4mm) diameter conductor versus corona loss data.

While controlled lab testing measured fairly substantial values (up to 300 ppb), wind and other field conditions play a substantial role in dispersion, actual concentration, and decay rates. The half-life of ozone ranges from about 10 to 40 minutes depending on a number of factors. Typically, concentrations of ozone at ground level below 230 kV and lower voltage transmission lines during heavy rain are significantly less than the most sensitive instruments can measure (which is about one ppb), and many times less than ambient levels. Nitrogen oxides are even less. Since ozone and other oxidants adjacent to overhead conductors exhibiting corona have not been measured at values much greater than ambient levels, they have not been considered to be an issue for AC or DC EHV line design, and are not considered to be an issue for the ACCC conductor, as ozone also tends to migrate away from the surface of a conductor even when no wind is present.[37]

To prove the ACCC conductor's resistance to ozone-induced degradation, Denver University, funded by the Western Area Power Administration and Bonneville Power (two of the three US government owned utilities) and TriState, conducted lab testing of the ACCC conductor's composite core at an ozone concentration of 1%.[38] A 1% ozone concentration is the equivalent of 7,284,000 ppb. This is several orders of magnitude greater than anything that could possibly be expected due to corona generated from a bare overhead conductor in any environment and is 24,000 times higher than the highest concentration of 300 ppb measured in the controlled lab environment described in Reference 35. Nevertheless, very little change in core mechanical properties was observed even after 90 days of immersion at this extremely high concentration level.

2.5. Ampacity & Line Ratings

---

[37] US Environmental Protection Agency Report #520179501 "Evaluation of Health and Environmental Effects of Extra High Voltage (EHV) Transmission (ITT Research Institute, Chicago, IL) May 1978

[38] Middleton, Burks, and Kumosa, "Aging of a High Temperature Epoxy under Extreme Ozone and Temperature Conditions" Annual Report to WAPA, Tri-State and BPA, April 2011.

Ampacity can be defined in simple terms by the conductor's electrical resistance and thermal and/or sag constraints in a given environmental condition. Environmental factors, such as ambient air temperature, wind speed, and other variables can dramatically impact a conductor's ampacity. In rating a particular line, utilities must make certain assumptions about ambient conditions based on the project's location, statistical data, real-time monitoring, or other available data. CIGRE Technical Brochure TB 299[39] is a good reference on this topic.

Lower voltage lines may be thermally constrained due to clearance limitations and/or the conductor's material properties. Type 1350 H-19 aluminum commonly used in ACSR conductor, for instance, begins to anneal at temperatures above 93°C. Annealing can cause a loss of conductor strength that may not be acceptable. The temperature capability of hardware components must also be considered when higher operating temperatures are considered. The ACCC conductor's dead-ends, splices and suspension clamps are all designed for high-temperature capability and have been rigorously and extensively tested.

Type 1350-O aluminum used in the ACCC conductor has the lowest electrical resistance (63% IACS) of any aluminum currently used in bare overhead conductors (See Table 2). Decreased electrical resistance coupled with added aluminum content, higher allowable operating temperatures, and resistance to thermal sag allows the ACCC conductors to carry approximately twice the current of conventional conductors such as AAC, AAAC, and ACSR without violating clearance limits. Under equal load conditions, the ACCC conductor's decreased electrical resistance allows a reduction in line losses by as much as 35% or more.

Line ratings can include adjustments for time of day (or night), seasonal changes in temperature, or varied wind parameters. Typically, variations due to solar heating reflect an ampacity variation of less than a 5%. However, as shown in Table 7, a change in ambient air temperature of only 10°C can impact a conductor's rating by nearly 10%, and relatively small increases in wind speed (1 to 4 ft/sec) can provide ampacity increases of 10 to 15%. The angle of incidence of wind to a conductor, and the conductor's temperature itself, can also have substantial impact. Wind blowing at 4 ft/sec or 1.2 meters/sec (~2.7

---

[39] Cigre Technical Brochure TB 299 (2006) WG12, TF6 "Guide for the Selection of Weather Parameters for Bare Overhead Conductor Ratings", SC B2 WGB2.12

mph / 4.3 km/h) nearly parallel to a conductor at a 10 degree angle yields a 10 to 15% lower rating than wind blowing at 2 ft/sec (~ 1.4 mph / 2.3 km/h) at 90 degrees or perpendicular to the line. As such, the temperature of a conductor can be considered sensitive to sunlight, wind, and other factors[40].

Air Temperature (°C)	Wind Speed (fps)	Wind Direction (90 degrees = perpendicular)	Time of Day (Solar Radiation)	Ampacity at 100°C	Percent Change	Ampacity at 180°C (Rating)	Percent Change
40	2	90	noon	1132	---	1702	---
40	2	10	noon	856	-32%	1197	-42%
40	3	90	noon	1242	9%	1840	8%
40	3	10	noon	932	-21%	1455	-17%
40	4	90	noon	1328	15%	1949	13%
40	4	10	noon	991	-14%	1527	-11%
30	2	90	noon	1230	8%	1755	3%
30	2	10	noon	934	-21%	1406	-21%
30	3	90	noon	1348	16%	1899	10%
30	3	10	noon	1015	-12%	1499	-14%
30	4	90	noon	1441	21%	2013	15%
30	4	10	noon	1079	-5%	1574	-8%
20	2	90	noon	1319	14%	1806	6%
20	2	10	noon	1004	-13%	1444	-18%
20	3	90	noon	1445	22%	1955	13%
20	3	10	noon	1090	-4%	1541	-10%
20	4	90	noon	1544	27%	2073	18%
20	4	10	noon	1158	2%	1619	-5%
40	2	90	6:00 PM	1170	3%	1722	1%

Table 7 - Impact of wind speed and angle to the line axis on ampacity
(Drake size ACCC used for example)

The ACCC conductor's high-capacity, high-efficiency, and low-sag performance make it ideally suited for operation in year round hot climates found in the Middle East, Africa, India, South America and other hot climates.

2.5.1. Line Rating Methodology

Bare overhead conductor line rating calculations are performed by setting the heat input from Ohmic losses and solar heating equal to the heat losses due to

---

[40] CIGRE WG 05 - Conductors, The Thermal Behavior of Overhead Conductors, 22 81 (WG05), December, 1981

convection and radiation. The various formulas used to determine heat balance vary slightly between the IEEE method, the CIGRE method, and the EPRI method[41], but, given the same assumptions, the thermal ratings found with each of the three methods is nearly identical (see IEEE Standard 738[42]; CIGRE TB 207[43]; EPRI Dynamp[44]). As a number of conductors have been introduced that are capable of operating at temperatures well above 100°C, and it is recognized that conductor resistance at higher operating temperatures is not completely linear, revisions to these methods are being made (previously resistance values were simply extrapolated). It has also been discovered that the temperature of inner core and conductive strands of ACSR or ACSS conductor can be as much as 30°C to 40°C hotter than the outer aluminum strands, so considerations for increased electrical resistance and thermal sag are being factored in for the upcoming 2012 revision of the IEEE 738 Standard[45]. In testing a 3 layer Bittern size ACCC conductor at 220°C (above its rated emergency temperature of 200°C), it was noted that the core reached equilibrium at 226°C, while the inner 2 layers were about 2°C hotter per layer than the layer surrounding it[46]. The low thermal conductivity of the composite core coupled with the increased surface area and compact nature of the trapezoidal strands help the ACCC conductor dissipate heat more efficiently than other conductors, even when the strands are relatively loose above the conductor's thermal knee-point, as described in Section 2.8.6.

---

[41] Watt, George; "Comparisons of CIGRE & IEEE Ampacity Rating" CIGRE / IEEE Joint Panel Session Las Vegas, Nevada; Feb. 2011

[42] Working Group on the Calculation of Bare Overhead Conductor Temperatures; Standard for Calculating the Current-Temperature of Bare Overhead Conductors, IEEE 738 Standard, 2003

[43] Cigre Technical Brochure TB 207 "Thermal Behavior of Overhead Conductors", SC 22 WG 22.12 (2002)

[44] W.Z. Black, R.A. Bush; DYNAMP- A Real-Time Ampacity Program for Overhead Conductors, Proceedings of Seminars on Effects of Elevated Temperature Operation on Overhead Conductors and Accessories & Real Time Ratings of Overhead Conductors, 20-21 May 1986, pp: 169 – 187, Atlanta, GA, USA, May 1986

[45] IEEE 738 Standard 2006 "IEEE Standard for Calculating Current-Temperature Relationship of Bare Overhead Conductors"

[46] C.J. Pon, M.J. Kastelein, HIGH TEMPERATURE SAG-TENSION CHARACTERIZATION AND AMPACITY TESTS ON 1572 KCMIL "BITTERN" ACCC/TW CONDUCTOR FOR COMPOSITE TECHNOLOGY CORPORATION Report No.: K-422163-RC-0002-R00, Sept 2005

2.5.2. Static & Dynamic Line Ratings

There are two methods of rating the ampacity of a line. The first is a "static" (or "steady-state") method, wherein a maximum allowable conductor temperature is coupled with a "worst-case" (or "conservative") ambient weather condition(s). The second, "dynamic" method relies on real time weather data that is gathered by different types of apparatus or is assumed from historical data. In either case, the calculation of thermal ratings is typically based on heat balance methods mentioned above.

Historically, static ratings were (and continue to be) used to determine the capacity of a transmission or distribution line during the design phase. These ratings then allowed operators to utilize the lines to their thermal limits when the determining design conditions occurred (albeit rarely).

More recently, in an effort to increase the capacity of existing lines, dynamic methods (that utilize real-time monitoring equipment) have also been developed. While a review of historical weather data may enable a re-evaluation of ambient conditions that might redefine "worst-case" assumptions, real-time weather and/or conductor monitoring can widen the operating window without temperature or clearance violations. However, the magnitude of the increase gained varies from very little to modest compared to other forms of change to the circuit. See CIGRE TB 425[47].

2.5.3. Transient Thermal Ratings

Many circuits in a network exist to accommodate a situation when another circuit is out-of-service for a planned or unplanned reason. A single contingency outage event (N-1) and even a double contingency outage event (N-2) can be the basis for a circuit's design ampacity. For example, if two similar circuits are in parallel in a network, each carrying 300 A and one fails, the surviving circuit could be instantly carrying 600 A. If each circuit is to be designed to handle this N-1 condition, its design ampacity is 600 A. If there are three such circuits in parallel carrying 200 A each for a total of 600 A, the loss of one circuit puts 300 A on the two remaining circuits. The N-1 design ampacity of these circuits is 300 A and the N-2 design ampacity of these circuits is 600 A. The need for

---

[47] Cigre Technical Brochure TB 425 Increasing Capacity of Overhead Transmission Lines Needs and Solutions. B2/C1.19 (August 2010)

deeper security than N-1 capacity depends on the purpose and value of the circuits to the owner and customers.

Once an N-x situation initiates, the objective is to reinstate the normal condition of all network functionality as quickly as possible. In well-equipped networks this can take a matter of minutes as the operators redirect power via switching or revising the deployment pattern of generating facilities on the system. In some networks, under unusual conditions, the loss of a circuit can take months to reinstate and there may be no ability in the meantime to shift loads around to alleviate the N-x load on certain circuits.

Figure 12 (from Reference 42) illustrates that the temperature of a conductor rises fairly slowly in response to the instant increase in current flowing through it. It can take 10 minutes or more for a conductor to reach a new and higher steady state temperature (thermal balance). If the time taken to reinstate the normal condition from an N-x condition is less than about 20 minutes, then the conductor temperature for the N-x condition requires a transient thermal calculation. If it takes more than about 20 minutes, then the N-x ampacity relates to a simpler steady-state thermal calculation. A transient thermal calculation is used to determine one of two values based on the other being assumed. The values in play are the time of transition from N-x back to normal (generally within 20 to 30 minutes), the starting (pre-event) conditions of amperes (I_i) and temperature, (T_i), and the target (N-x) amperes (I) and temperature (T_f). Typically, the pre-event ampacity is a percentage of normal condition design ampacity, say "75% of" and the pre-event temperature is the maximum or a slightly lower value. With the pre-event values declared, the calculation will find either the final temperature or the final ampacity provided the other is assumed.

The transient thermal calculations to addresses the situation:

- Given that the start amperes and start temperature are I_i and T_i, and you want to allow the conductor temperature to reach T_f in X minutes, the amperes that will do that is calculated to be A. This situation says that if you allow the conductor's N-x temperature to reach T_f, then the ampacity of the line is A.

- Or, given that the start amperes and start temperature are I_i and T_i as above, and you want to deliver A amperes for X minutes, the temperature of the conductor will reach after those X minutes is calculated to be T_f. This situation says that if you want N-x capacity of the circuit to be A amperes for X minutes, then the thermal design temperature of the circuit is T_f.
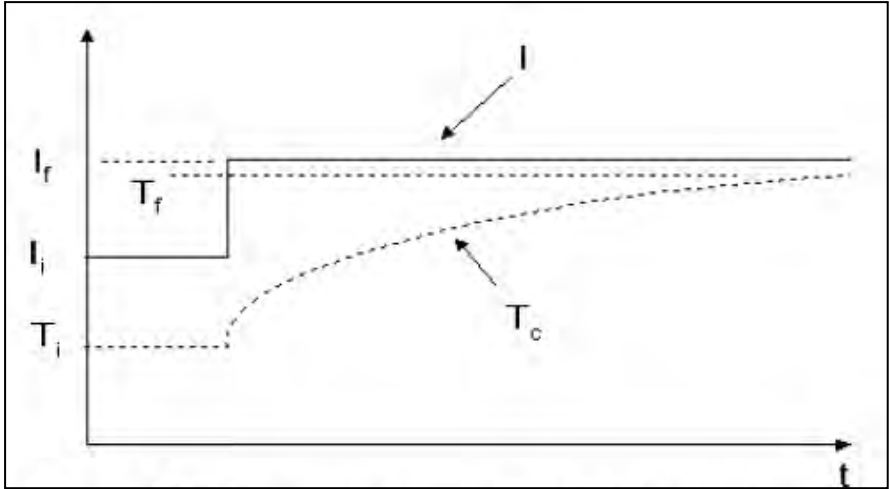
Figure 12 - An example of a temperature response of a bare overhead conductor due to a step-change in current.

The N-x thermal limit for a line is not always considered in sag and clearance calculations but to not do so is to risk clearance violations during N-x events. The thermal conductivity of the ACCC conductor's composite core is about five times less than a steel core, so it takes slightly more time to heat the composite core compared to a steel core.

In 2008, Yu, Hong-yun, Director Power Engineering Technology Lab, China State Grid, conducted testing of a Drake size ACCC conductor[48]. Initial conductor temperature ranged from 50° to 90°C with corresponding initial

[48] Yu, Hong Yun, Director Power Engineering Technology Lab, China State Grid "Conductor Double Capacity Comparison and Discussion" (2008)

current ranging from 741 to 1164 amps. The load was then instantaneously increased by 1.5X and 2X. Table 8 and Figure 13 show the time it took for the conductor temperatures to rise above various initial conditions (no wind lab conditions).

Initial Condition:		741 Amps at 52° C		852 Amps at 60° C		996 Amps at 70° C		1063 Amps at 80° C		1164 Amps at 90° C	
Increase Amps by:		1.5 X	2.0 X	1.5 X	2.0 X	1.5 X	2.0 X	1.5 X	2.0 X	1.5 X	2.0 X
time (1.5 x)	time (2 x)	Conductor Temperature Increases °C *(at stated number of minutes)*									
1	2	54	56	63	69	77	80	87	94	95	107
2	4	56	62	66	78	82	92	93	108	103	125
3	6	59	68	70	86	87	102	98	122	110	141
4	8	62	74	72	94	91	112	103	134	116	156
5	10	64	79	76	101	95	121	108	146	121	170
6	12	66	83	78	107	99	130	112	156	126	183
7	14	68	88	80	112	102	137	116	166	131	194
8	16	69	91	82	117	105	144	119	173	135	205
9	18	70	94	84	122	107	151	122	180	138	214
10	20	72	98	85	127	110	136	125	186	142	221
11	22	73	101	87	130	112	161	128	193	145	229
12	24	74	104	88	133	114	166	130	198	147	236
13	26	75	106	89	136	116	169	132	203	150	241
14	28	76	108	90	139	117	173	135	207	152	246
15	30	77	110	92	141	119	176	136	210	154	250
graph reference numbers:		1	2	3	4	5	6	7	8	9	10

Table 8 - Temperature response of an ACCC Drake conductor when the current was increased by either 1.5 or 2 times the current that produced the initial condition temperatures.
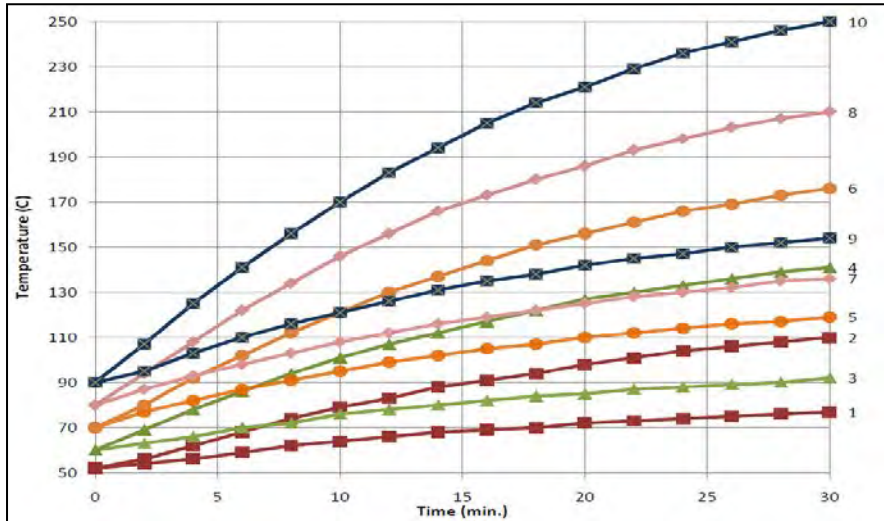
Figure 13 – Plotted results showing the temperature response of an ACCC Drake conductor. The numbers on the right side of the graph refer to the scenarios described in Table 8.

2.5.4. Short Circuit Events

Short circuit events lead to an instantaneous jump (Figure 14) in conductive strand temperature. The extent of the temperature jump is dependent upon the conductor's initial temperature, its aluminum content, and the extent and duration of the event.
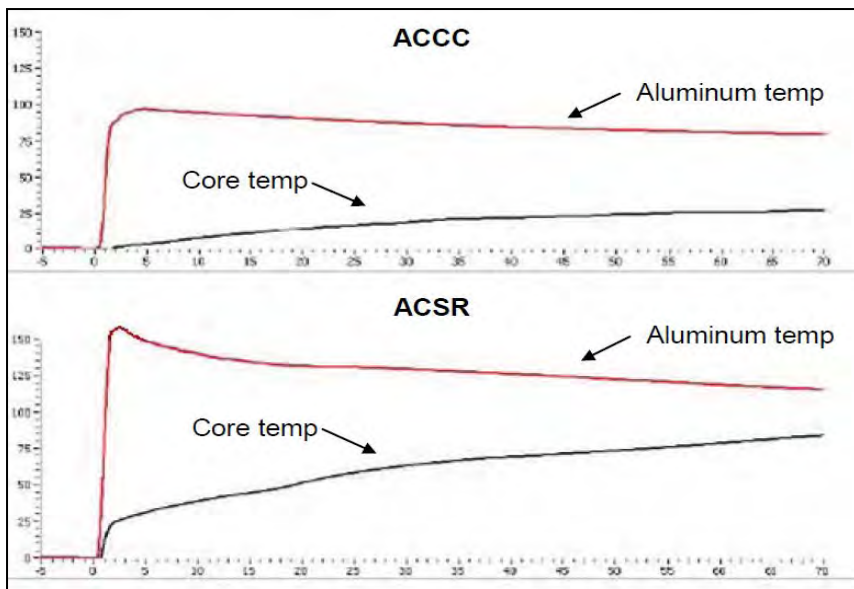
Figure 14 - Temperature response comparison of an ACCC and ACSR Drake
conductor to a short circuit event[49.] Note the cooler peak temperature in the ACCC
conductor's aluminum strands and the limited impact of the event on core
temperature.

As with any conductor, a short circuit event can cause very rapid expansion of
the conductive strands which can lead to birdcaging. The soft, fully annealed
aluminum used in ACCC® conductors improves the relaxation characteristics of
the strands and birdcaging has been seen to dissipate after subsequent thermal
cycles. Nevertheless, if extreme damage occurs to the ACCC® conductor's
aluminum strands, a repair sleeve can be utilized.

2.6.   Line Losses

Real line losses are primarily a function of conductor resistance, current, and
line length.   A conductor's resistance depends on the conductivity of the

---

[49] Pon, C.J. Short Circuit Performance Test on 1020 kcmil ACCC/TW Conductor
Kinectrics North America Inc. Report No.: K-422159-RC-0001-R00

constituent materials, the amount of material used (normally measured in kcmils or mm²), and its temperature (as resistance increases with temperature).

Reactive line losses are attributed to system inefficiency as described by *Power Factor* (Section 2.4.6) wherein higher circulating currents (due to energy that returns to the source from energy storage in the load) produce higher line losses. A lower power factor circuit will have a higher apparent power (which does no real work) and higher losses for the same amount of real power used. Utilities add capacitor banks and other components (such as phase-shifting transformers; static VAR compensators; physical transposition of the phase conductors; and flexible AC transmission systems ("FACTS") throughout the system to control reactive power flow for reduction of losses and stabilization of system voltage. The ACCC conductor's decreased electrical resistance (compared to other conductors of the same diameter and weight) can also reduce reactive line losses. The improved efficiency of the ACCC conductor may be able to reduce the Utilities' reliance on VAR compensators or other devices. Any potential reduction would require a system analysis.

Ohmic power loss per unit length of conductor is simply a function of conductor resistance per unit length *at a specified temperature* times the square of the current in amps.

$$P_L = R_{cdr} * I^2 \qquad (2\text{-}20)$$
Where:

I = current per phase in amps
R_{cdr} = conductor resistance at given temperature T_{cdr} in Ohms

While Ohmic and reactive losses are the most substantial, other losses can be attributed to corona, skin effect, frequency, current density, as well as each phase conductor's proximity to other conductors and the ground. Additionally, magnetic hysteresis and eddy current effects can substantially increase the resistance of steel-cored conductors used in AC lines. As conductive strands are helically wrapped around a steel core, the current follows the helical path which produces an axial magnetic field. If the conductor contains an even numbered layer of strands, this effect is essentially cancelled out. If, however, the conductor contains an odd number of layers (such as 1, 3, or 5), core magnetization losses can be substantial as current levels increase. A single layer conductor can see losses increase by 20% or more even at relative low load

levels, while a three layer conductor loses about ½ of that amount. Considering the ACCC conductor does not use a steel core; it exhibits no magnetic hysteresis losses[50]. Invar steel on the other hand, has very high magnetic permeability and is particularly impacted by this effect.[51]

2.7. Economic & Environmental Impact of Line Loss Reductions

While line losses can be attributed to each of the mechanisms described above, the length of the line and load factor are significant as it relates to the overall economic and environmental impact. Load factor is defined as the mean of the actual load on the line over a period of time divided by its capacity.

2.7.1. Line Losses and Load Factor

Using a 100 km (62 mile) 230 kV case study, line losses were assessed as a function of load factor at a peak current of 1,000 amps. Drake size equivalent (diameter and weight) conductors are used for comparison. While an ACSR Drake conductor would operate at 95°C compared to 82°C for an ACCC Drake conductor in an ambient temperature of 35°C (using other common operating assumptions[52]), a reduction in line losses of over $1,000,000 per year would be realized at a load factor of 53%. It is important to note that the conductors would operate at much cooler temperatures during off-peak or normal load conditions. Considering that many utilities operate ACSR conductors at temperatures above 95°C during peak conditions[53], an even greater savings in I^2R losses could be realized, especially considering that load factors often increase over time. As a

---

[50] Douglass, Dale A., and Rathbun, L.S., AC Resistance of ACSR - Magnetic and temperature effects, IEEE Paper 84 SM 700-1

[51] D.G. Rancourt and M.-Z. Dang. Relation between anomalous magneto-volume behavior and magnetic frustration in Invar alloys. *Physical Review B* 54 (1996) 12225–12231

[52] IEEE 738 assumptions include: 35°C; 2fps perpendicular wind (.61mps); 0' elevation; clear atmosphere; 38°N latitude; July 21st noon; N/S azimuth; 0.5 emissivity; 0.5 absorptivity; 1024 watt/m² solar radiation.

[53] Please note that ACSR conductors are generally limited to a maximum operating temperature of ~100°C. Nevertheless several US utilities operate at higher peak temperatures when clearances allow. Please refer to EPRI "Performance of Transmission Line Components at Increasing Operating Temperatures" Interim Report 1002094 (December 2003). Several other EPRI reports are also available on this topic.

reference point, most transmission lines in the United States operate at a load factor of approximately 60%.
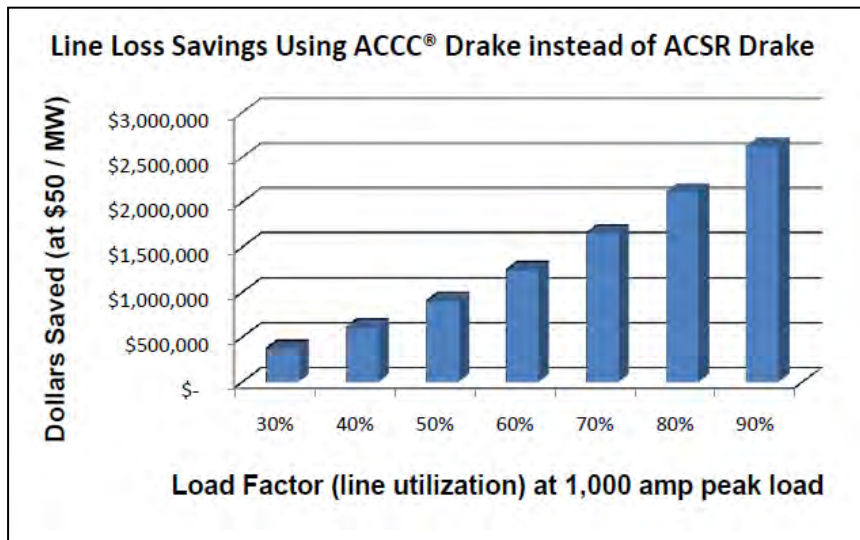
Figure 15 - depicts how line loss savings using ACCC Drake conductor compared to ACSR Drake conductor increase with load factor using 1,000 peak amps for comparison on a 100 km (62 mile) 230 kV line.

In a higher-capacity scenario, comparing ACCC Drake to ACSS Drake conductors of the same diameter and weight (using the same ambient assumptions as above) and a peak load of 1,600 amps, an ACSS conductor would operate at a peak temperature of 194°C while an ACCC conductor would only reach 156°C under peak conditions. The savings using ACCC conductor compared to ACSS conductor based on load factor are shown in Figure 16.
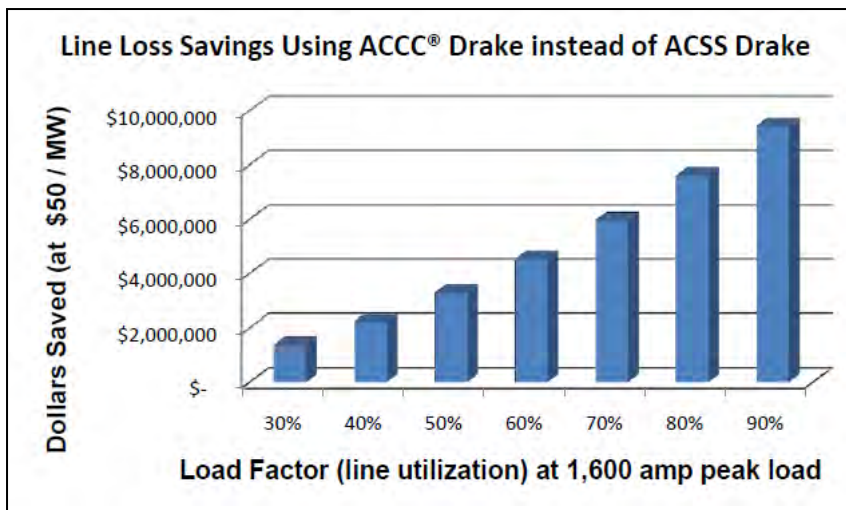
Figure 16 - depicts how line loss savings using ACCC Drake conductor compared to ACSS Drake conductor increase with load factor using 1,600 peak amps for comparison on a 100 km (62 mile) 230 kV line.

2.7.2. Impact of Line Loss Reductions on ACCC Economics

Assuming a load factor of 53% in the scenario described above, the ACCC conductor would save over $3.6 million dollars per year compared to an ACSS conductor of the same diameter and weight, assuming a cost of energy of $50/MWh.

From a conductor perspective, if one considers that a three phase 100 km AC line would require ~300,000 meters (~984,250 feet) of conductor, and that the annual saving in line losses (assuming a load factor of 53% and a peak current of 1600 amps) is about $3.6 million per year, the annual savings using ACCC conductor instead of ACSS conductor would equate to $12.21 per conductor meter (or $3.72 per lineal conductor foot). *In other words, the reduction in line losses the ACCC conductor provides compared to ACSR or ACSS conductors of the same diameter and weight will essentially allow it to pay for itself in a time frame that can be measured in weeks or months depending upon peak current and load factor.*

	Peak Amps	Temperature at peak amps (C°)	Load Factor	MVA	Annual Line Losses (MWh)	Line Loss Reduction	Value of Reduction (at $50/MWh)	Value of Reduction per lineal conductor (meter)	(foot)
ACSR	1,000	96	53%	398	76,989	—	—	—	—
ACCC®	1,000	83	53%	398	56,628	20,362	$1,018,085	$3.40	$1.04
ACSS	1,600	196	53%	637	252,407	---	---	—	—
ACCC®	1,600	158	53%	637	179,284	73,122	$3,656,119	$12.21	$3.72

Table 9 - Line loss comparison of Drake size conductors showing value of line losses per conductor unit length at 1,000 and 1,600 peak amps at a 53% load factor

In addition to the annual line loss savings reflected in either scenario presented above (which are generally associated with reductions in fuel consumption), *a significant reduction in generation capacity costs can also be realized*. In the 1,000 amp ACSR comparison, a reduction in line losses equates to a generation capacity savings of 2.33 MW. In the 1,600 amp ACSS comparison, a reduction in line losses equates to a generation capacity savings of 8.34 MW. Assuming the cost of building new generation is $1 million per MW[54] (conservative number), a reduction in line losses offered by the ACCC conductor compared to ACSR conductor of the same diameter and weight (using the 1,000 amp scenario) provides a value equivalent to $7.78 per conductor meter or $2.37 per conductor foot. In the 1,600 amp scenario, the generation capacity savings offered by the ACCC conductor's reduction in line losses can be translated into a $27.86 per conductor meter value which is equivalent to $8.49 per lineal foot. This is more than twice the cost of the ACCC conductor itself and reflects substantial overall project savings.

---

[54] US Energy Information Administration "Updated Capital Cost Estimates for Electricity Generation Plants" November, 2010

Table 10 - Line loss comparison of Drake size conductors showing the value of
generation capacity savings per conductor unit length at 1,000 and 1,600 peak amps
at a 53% load factor

Considering the ACCC conductor also offers high-strength, low-sag, high-capacity, and excellent self-damping characteristics, the ACCC conductor can often be used to further reduce upfront capital costs by taking advantage of existing structures (without requiring modifications on re-conductoring projects) and reduce structural costs on new projects by increasing spans between fewer and/or shorter structures - should environmental conditions and terrain allow.

2.7.3. Reduced Losses Reduces Fuel Consumption and Emissions

While increased capacity, improved mechanical characteristics and reduced line losses offer a number of advantages, an additional advantage relates to *emission reductions* associated with reduced fuel consumption. As discussed above, the generation savings from the 1,000 peak amp and 1,600 peak amp scenarios (both at 53% load factors) represent generation savings of 20,362 MWh and 73,122 MWh respectively. Based on the combined fuel sources used to produce electricity in the US (see Figure 17), the average CO_2 emissions produced from all fuel sources equates to 1.372 pounds of CO_2 per kWh.
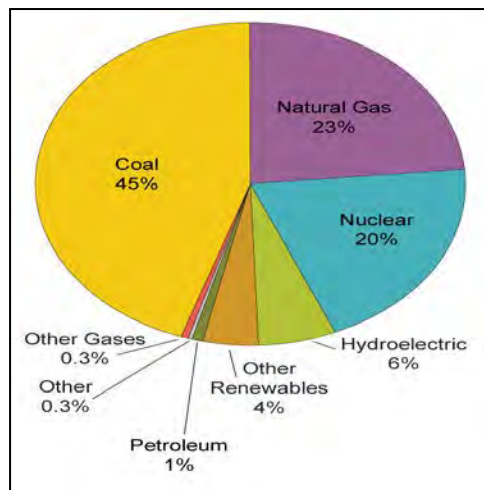
Figure 17 - US Net Electricity Generation by Fuel Type[55]

This average includes all non-fossil fuel, nuclear, and renewable resources. Considering the two 100 km (62) mile scenarios described above and the US national average CO_2 emissions, a reduction of 12,633 and 45,349 metric tons of CO_2 could be realized, respectively. These numbers can vary greatly depending up on specific project variables, fuel mix and other factors, and are offered in that context. A list of emissions from all fuel sources is provided in Table 11.

Fuel/Energy Source	Net Generation	CO2		SO2		NOx	
	(kWh)	(Metric Tons)	Pounds/kWh	(Metric Tons)	Pounds/kWh	(Metric Tons)	Pounds/kWh
Coal	2,014,172,634,000	2,001,236,871	2.190	9,498,910	0.010	3,135,149	0.0034
Natural Gas	751,549,111,000	381,927,374	1.120	2,048	0.000	383,138	0.0011
Petroleum	121,910,223,000	115,943,800	2.097	587,474	0.011	221,068	0.0040
Combined Fossil Fuels	2,903,275,650,000	2,499,108,045	1.898	10,088,432	0.008	3,739,355	0.0028
Geothermal	15,124,491,000	373,675	0.054	0	0.000	0	0.0000
Municipal Waste	23,996,556,000	14,127,685	1.298	0	0.000	0	0.0000
All/Average (for the above)	2,942,396,697,000	2,513,609,405	1.883	10,088,432	0.008	3,739,355	0.0028
Total Net Generation*	4,037,988,722,000	2,513,609,405	1.372	10,088,432	0.006	3,739,355	0.0020

Table 11 – Emissions based on fuel sources[56]

---

[55] US Energy Information Administration, "International Energy Outlook 2010"

[56] Paul Hesse, U S Energy Information Administration, www.eia.doe.gov/cneaf/electricity/epa/emission_state.xls

From an alternate perspective, the average American automobile produces 5.2 metric tons of CO_2 per year. Thus, the energy and potential emissions saved using ACCC conductor instead of ACSR or ACSS conductors in the scenarios described above would be equivalent to removing 2,429 or 8,721 cars from the highway, respectively.

2.7.4. Global Perspective of Line Loss Reductions using ACCC

While the scenarios described above demonstrate how substantial line loss reductions can be when ACCC conductor is utilized on a specific project, it may also be worthwhile to consider the impact the ACCC conductor might have on a global basis.

CTC Global believes that utilities, consumers, and regulators all recognize that access to affordable, reliable, and renewable energy is essential for the future health of our planet, economy, and security in general. Without it, water cannot be pumped to support growing populations, products cannot be economically manufactured to maintain viable economies, and poverty cannot be mitigated in underdeveloped countries that are economically dependent on more developed countries facing their own challenges. Considering that the world consumes over 20 Trillion kWh of electricity every year and that more than 1.4 Trillion kWh are lost in the inefficient transmission of that energy[57], CTC Global believes the time has come to consider the importance of investment, not just in more efficient clean generation, but also in improved transmission technologies. As several key industry executives have stated "It is cheaper to save a 'Negawatt' than it is to produce a Megawatt."[58]

From a fuel conservation or environmental perspective, there are an estimated 1.2 Trillion Metric Tons of CO_2 created annually as a by-product of transmission line losses. If that number could be reduced by one-third (or more) by deploying ACCC conductors *worldwide*, a reduction in CO_2 emissions of over 290 Million Metric Tons could be realized every year, based on the US average of all fuel sources including hydro, renewables, and fossil fuels. Using the average value of 1.372 lbs CO_2/kWh, this is comparable to removing 55.8 Million cars from the road. This hypothetical one-third reduction in transmission losses also

---

[57] United States Energy Information Administration, "International Energy Outlook 2010"

[58] The term Negawatt was coined by Amory Lovins of the Rocky Mountain Institute in 1989

reflects 466,620,000 MWh of electrical savings. This is the energy equivalent of 53,267 MW of generation,[59] or the amount of generation required to power nearly 48 million homes. From an oil-energy perspective, at a Btu conversion efficiency rate of 42%, the energy saved would equal over 1.9 billion barrels of oil annually.[60]

Potential Global Savings using ACCC® Conductor		
Global Consumption	20,000,000,000,000	kWh
T&D line losses (7%)	1,400,000,000,000	kWh
1/3 reduction	466,620,000,000	kWh
MWh equivalent	466,620,000	MWh
Generation equivalent	53,267	MW
US Average CO2 Emission	1.372	pounds per kWh
metric tons CO2 potentially reduced using ACCC® conductor	290,341,333	Metric Tons
equivalent cars removed	55,834,872	cars
equivalent houses powered	47,940,411	houses
equivalent barrels of oil saved at 42% Btu conversion efficiency	1,915,878,107	barrels

Table 12 - Summary of potential impact of line loss reductions through the global use of ACCC conductor, using the US national average from all fuel sources (including renewables) as a basis for comparison.

---

[59] This does not take capacity factor into account.

[60] The Union of the Electric Industry (EURELECTRIC) "Efficiency in Electricity Generation" July 2003

2.7.5. Impact of Line Loss Reductions on Coal Generation

While the figures provided in Table 11 reflect US average CO_2 emissions, a review of Figure 17 points out that 45% of electric energy produced in the US is based on coal-fired generation. The CO_2 emissions generated from coal are approximately 60% higher than the US average referenced. Thus, from an environmental perspective, the use of ACCC conductor on transmission lines that link coal generation would have an even greater environmental impact and could reduce the overall CO_2 footprint, if transmission line losses are factored in.

For instance, considering the two 1,000 and 1,600 amp scenarios presented in the 100 km (62 mile) 230 kV case studies above, and a CO_2 emission value of 2.19 lbs/kWh (per US EIA) a 20,227 metric ton reduction in CO_2 could be realized in the 1,000 amp scenario, while a 72,638 metric ton reduction could be realized in the 1,600 amp scenario. Recall that these scenarios considered very conservative load factors of 53%. Additionally, a reduction in SO_X and NO_X of 92 metric tons and 31 metric tons, respectively, for the 1,000 amp case study and 332 and 113 metric tons, respectively, for the 1,600 amp case study could potentially be realized based on reductions in fuel consumption that may be achieved via the ACCC conductor's reduction in line losses in the case studies presented. Keep in mind that these values are based on simple calculations using basic assumptions and that other variables will impact line losses, reductions in fuel consumption, and any emission reductions achieved. Nevertheless, the numbers presented using the 1,000 and 1,600 amp 100 km (62 mile) examples demonstrate how substantial potential reductions in line losses, fuel consumption, and associated emissions can be. Table 13 summarizes.

▶ Value of Emission Reductions	Peak Amps	Load Factor	MVA	Line Loss Reduction (MWh)	CO₂ Reductions (Metric Tons)	SOₓ Reductions (Metric Tons)	NOₓ Reductions (Metric Tons)	Value of CO₂ Reduction per lineal conductor (meter)	(foot)
ACSR	1,000	53%	398	----	—	—	—	---	—
ACCC®	1,000	53%	398	20,362	20,227	92	31	$1.69	$0.52
ACSS	1,600	53%	637	----	---	—	----	---	—
ACCC®	1,600	53%	637	73,122	72,638	332	113	$6.07	$1.85

Table 13 – Potential emission reductions and CO_2 value (per conductor unit length) using ACCC conductor on a 1,000 or 1,600 amp tie line to a coal-fired power plant at a 53% load factor. CO_2 value assumption is $25/metric ton. Metric ton calculation based on 2.19 lbs/kWh.

Regarding potential emission reductions in a "cap and trade" environment,[61] this could translate into several hundred thousand dollars annually. In the case of a coal-fired generation tie line, as described above in the 1,000 amp scenario, a 20,227 metric ton CO_2 reduction at a value of $25 per metric ton would translate into $505,675 per year. This is equivalent to $0.52 per conductor foot or $1.69 per conductor meter. In the 1,600 amp comparison, a reduction in 72,122 metric tons at $25 per ton would translate into $1,803,050 which is equivalent to $1.85 per conductor foot or $6.07 per conductor meter.

Using an "offset" credit mechanism rather than a cap and trade mechanism, credits may be awarded for specific projects that reduce emissions against a defined project-specific baseline, which can then be traded. An offset credit represents one metric ton of CO_2 emission reductions that have been achieved by a specific abatement project or activity and which have been verified by a qualifying program. To generate offsets from a CO_2 emissions reduction project, the project must be validated, registered, verified, and issued offset credits.[62]

2.7.6. Impact of Line Loss Reductions on Renewable Generation

While hydro, wind, solar and other renewable resources are essentially emission-free, they generally operate at capacity factors quite a bit below their rated capacities due to the limited availability of associated resources.[63] In the discussions above it was demonstrated that higher transmission line 'load factors' increased the economic or environmental savings associated with a reduction in line losses achievable using an ACCC conductor instead of an ACSR or ACSS conductor of the same diameter and weight.

At first glance it is apparent that reduced load factors will increase the amount of time it might take to recover any added costs that might be incurred as a result of using an ACCC conductor instead of an ACSR, ACSS or other conductor, based on line loss reductions alone. However, when considering the higher cost of renewable generation compared to the typically lower costs associated with

---

[61] Emissions Offsets: The Key Role of Greenhouse Gas Emissions Offsets in a U.S. Greenhouse Gas Cap-and-Trade Program. EPRI document #1019910 (2010)

[62] A Comprehensive Overview of Project-Based Mechanisms to Offset Greenhouse Gas Emissions." EPRI document #1014085(2007)

[63] Capacity Factor is defined as the ratio of the actual output from a power plant over a period of time compared to its potential output if it had operated at its full rated capacity.

fossil fuel generation, one can begin to consider the overall economic advantage the ACCC conductor might offer in addition to line loss reductions or reductions in structural costs due to the ACCC conductor's mechanical attributes. For example:

Consider a 100 MW wind farm located 50 km (31 miles) from the grid that provided 500 peak amps (at 115kV) at a load factor of 30%. A reduction in line losses using ACCC Hawk conductor vs. ACSR Hawk conductor would save 1,385 MWh at an annual savings of roughly $138,500 (at $100/MWh). Based on the load factor, peak current and other common operating assumptions, this equates to a generation capacity savings of 1.3 MW. At an average installed cost of wind generation of $1.75 million per MW, an upfront capital savings of approximately $2.275 million could be realized. Translated into dollars per conductor unit length, this would equate to $4.62 per lineal conductor foot or $15.16 per lineal conductor meter, which would more than pay for any potential differences in conductor costs.

2.8. Conductor Mechanical Characteristics

The mechanical characteristics of bare overhead conductors define their sag and tension response to external wind, ice, point loads, temperature change and time. ACCC conductors are sufficiently different from all other conductors in their material makeup that their sag and tension response to loads, temperature and time is equally unique. To understand these differences, mechanical conductor characteristics are discussed in general and the ACCC conductor is placed in that context.

2.8.1. Rated Strength

The Rated Tensile Strength (RTS) (sometimes referred to as Rated Breaking Strength or RBS) of conductors is defined in the US by ASTM Standards. Other countries have their own standards and many adopt IEC Standards. The methods for calculating RTS are not consistent in detail or principle around the world, and thus it is important to understand how the strength of the conductor is determined depending on the region the wire will be used in.

It is useful to understand how RTS values are calculated and to recognize that it varies between conductor types and the variation has impact on how the different conductors are used with adequate safety margins.

The RTS of ACSR conductors is defined in the US by ASTM Standard B 232[64]. ACSS conductor RTS is defined in ASTM standard B 856[65] and ACCC conductors have an ASTM standard currently in development. The RTS of ACSR is calculated as the sum of the stated strength of the aluminum strands and of the steel strands all at 1% strain. The 1% strain limit is chosen because it safely approximates the breaking strain of the hard (1350-H19) aluminum strands. The strength of steel core peaks at 3% to 4% strain. Once aluminum strands begin to break, the load transfer to the steel core strands, overloading the steel core fairly quickly. It is interesting to note that in most ACSR conductor designs, the aluminum strands contribute to approximately 50% of the conductor's rated tensile strength at room temperature when the tests are conducted and the RTS calculations are made.

For ACSS, ASTM B 856 indicates that the RTS is calculated as the sum of the stated strength of the annealed aluminum strands and of the steel strands at ultimate tensile strength. According to ASTM standards B 498[66], the ultimate tensile strength of the steel strands is about 10% to 15% greater than the strength at 1% strain and it occurs at more than 3-4% strain. The difference between these two calculations is as follows:

The rated strength of a conductor is based on the strengths of components achieved without breaking either component. In the case of the ACSS, the breaking strain of the 1350-O annealed aluminum strands is over 20% strain. Thus, the ACSS rated strength is determined by the lower strain limitation of the steel, whereas with ACSR, it is determined by the lower strain limitation of the aluminum. This leads to the logical calculation method for the ACCC conductors. Since the ACCC conductors also use very pliable 1350-O aluminum

---

[64] American Society for Testing and Materials (ASTM), 1991 Annual Book of ASTM Standards Section 2, Nonferrous Metal Products, Volume 02.03, Electrical Conductors B-232

[65] American Society for Testing and Materials (ASTM), 1991 Annual Book of ASTM Standards Section 2, Nonferrous Metal Products, Volume 02.03, Electrical Conductors B-856

[66] American Society for Testing and Materials (ASTM), 1991 Annual Book of ASTM Standards Section 2, Nonferrous Metal Products, Volume 02.03, Electrical Conductors B-498

strands. The less pliable (elastic) composite core determines the RTS (via its ultimate tensile breaking strain).

Figure 18 illustrates the failure mechanism of Drake ACSR. The combined aluminum/steel strand strength plotted in blue builds to 1% strain when the aluminum strands begin to break. This represents 100% of the conductor's RTS. As the hardened aluminum strands yield and break, the conductor's strength drops to that of the core only (shown in red). This strength holds to approximately 3.5% strain, when it subsequently breaks. Note that the strength of the aluminum strands and the strength of the steel core each contribute approximately 50% to the overall conductor's rated strength.
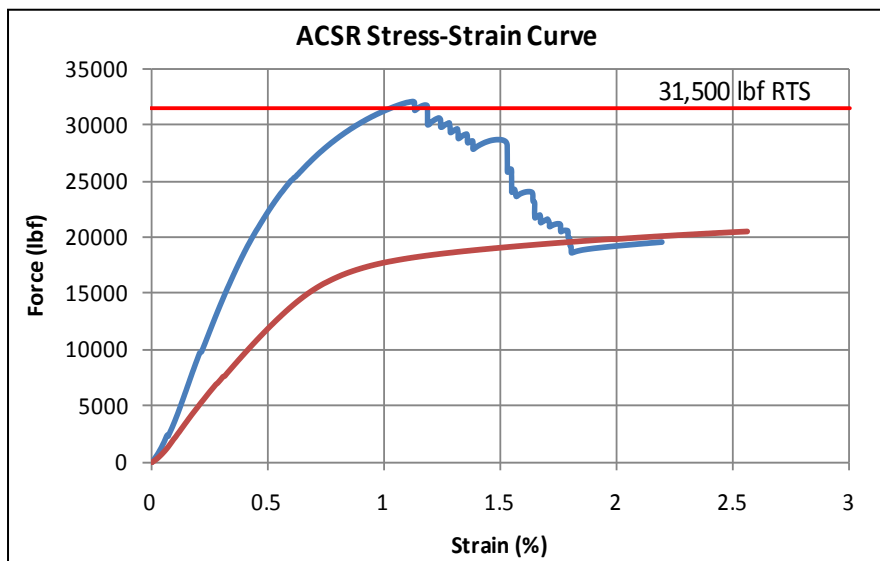
Figure 18 - ACSR Stress-Strain Curve. The lower line represents the ACSR core-only (stress and strain). The upper line shows the core and aluminum stress and strain.

Figure 19 compares the stress-strain nature of a steel core and the ACCC conductor core. The ACCC conductor core is purely elastic showing no permanent elongation up to its rupture at ~2% strain. The steel core does not break until above 2.5% strain but begins to yield at approximately 0.6% strain.
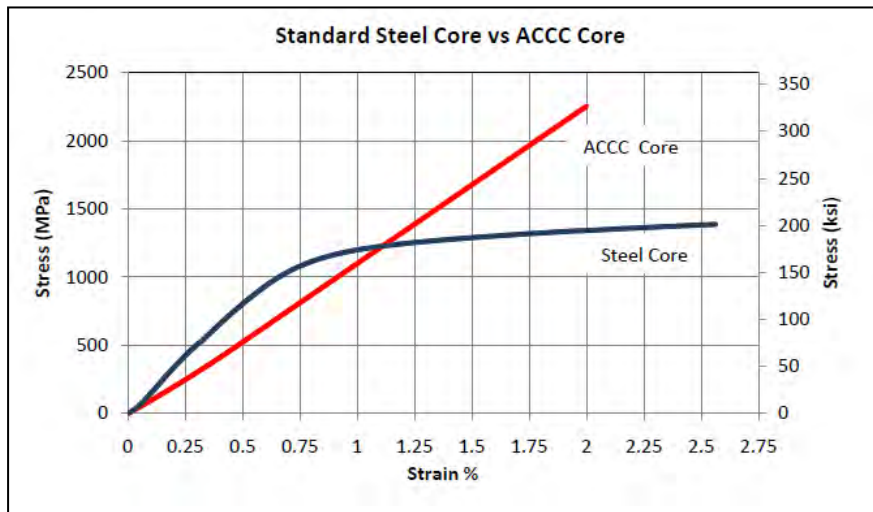
Figure 19 - Steel Core & ACCC Core Comparison – Note that the ACCC core (shown in red) does not yield, while the steel core will yield and plastically deform before it reaches its overall conductor's rated strength (100% RTS) at 3 to 4% strain.

Conductor testing performed at Kinectrics, NEETRAC and other labs show that the core of ACCC conductors breaks very consistently at ~2% strain. Thus, the ACCC conductors' RTS is the sum of the stated strengths of the aluminum strands and of full ultimate tensile strength of the core, *similar to how ACSS conductors are rated*. Table 14 illustrates several differences between the three conductor types. First, each conductor type will be stretched by different amounts to challenge its rated strength. Second, the load sharing between the two materials (aluminum and core) is very different between the conductor types.

Conductor	Diameter	kcmils	Weight (lbs)	RTS (lbs)	Strain at RTS	RTS Contribution from Core
Drake ACSR	1.108	795	1.094	31,500	1%	17,500 (56%)
Drakes ACSS	1.108	795	1.094	25,900	3-4%	20,000 (77%)
Drake ACCC®	1.108	1026	1.047	41,100	2%	34,570 (84%)

Table 14 - Drake Conductor Strength & Strain Comparisons

The cores of the Drake ACSR and standard ACSS use the same type of steel core (sometimes with different coatings) but, as defined by ASTM, the rated core strength of the lower strength ACSS conductor is greater, but at a triple to quadruple the ACSR strain. The core of the ACCC Drake is twice the strength of the ACSR core but at twice the strain. The 1350-H19 aluminum of the ACSR contributes greatly to the ACSR RTS while the annealed 1350-O aluminum of the ACSS and ACCC conductors contributes very little. As the temperature of the conductor drops, the load in the aluminum increases so the ACSR strength relies on the integrity of the aluminum quite a bit when it matters most. The relaxation of the soft annealed aluminum means that it will never contribute greatly to the strength of the ACSS or ACCC conductors so the integrity of these conductors' strength is highly dependent on the core. The high degree of tension and strain on the ACSR conductor's aluminum strands also limits it resistance to Aeolian Vibration, strand fretting and fatigue failure as discussed in Sections 2.13.

An argument can be made that all three of these conductors should be installed at approximately the same tension. There is also an argument that can be made that the ACSS and the ACCC conductors could be installed to a higher tension. If we assume the three conductors are installed at 6,000 lbs (everyday final tension), then it can be seen that the *reserve strength* (Table 15) against tension increasing events such as ice or a tower failure are:

Conductor	Final EDT	% RTS @ EDT	RTS (lbs)	Reserve Capacity
Drake ACSR	6,000	19%	31,500	25,500
Drakes ACSS	6,000	23%	25,900	19,500
Drake ACCC®	6,000	15%	41,100	35,100

Table 15 - Equivalent Drake conductor reserve strength comparisons.

This *reserve strength* is a form of security against extreme events. If this capacity is completely used up by an extreme load event, the permanent deformation in the ACSR core will be up to 0.8%, in the ACSS core about 3.5%, due to the steel yielding and not returning to its original length after the load is relieved. For the elastic ACCC conductor, there will be no permanent deformation of core, although the aluminum strands will yield. In addition to the elastic attributes of the composite core, the ACCC conductor can also tolerate a much larger load event than ACSR or the ACSS conductors. The reserve structural capacity of ACCC conductors is of much greater magnitude than that of comparable size ACSR and ACSS conductors. This is a valuable feature that is rarely measured or considered in conductor selection. Table 16 compares a number of additional conductor types.

Drake Size Equivalents / 1,000 ft Ruling Span	ACCC®	ACSR	ACSS	GAP	INVAR	ACCR	AAAC
Conductor Diameter (inches)	1.108	1.108	1.108	1.095	1.000	1.128	1.108
Al cross-sectional area (kcmil)	1,026	795	795	815	694	824	927
Conductor Weight (lbs/kft)	1,052	1,094	1,093	1,086	1,097	930	865
Rated Tensile Strength	41,100	31,500	25,900	33,500	31,500	32,200	30,500
Initial Tension (at 15°C / 60°F)	11,870	7,263	8,393	8,874	9,458	7,562	9,767
Initial Catenary (ft)	11,272	6,620	7,660	8,156	8,600	8,116	11,210
Percentage of RTS	29%	23%	32%	26%	30%	23%	32%
Tension (NESC Heavy) (lbf)	14,159	13,164	12,422	15,197	15,213	14,000	16,000
Percentage of RTS	34%	42%	48%	45%	48%	43%	52%
Sag (NESC Heavy) (ft)	21.9	24.0	25.4	20.6	20.1	21.2	18.0
Percentage of RTS	34%	42%	48%	45%	48%	43%	52%
Tension (1 in. ice) (lbf)	15,913	15,664	14,561	17,598	17,599	16,800	17,600
Sag (1 in. ice) (lbf)	29.1	29.9	32.2	26.4	25.7	26.8	25.0
Percentage of RTS	39%	50%	56%	53%	56%	52%	58%
Final EDT Tension (After NESC Heavy) (lbf)	7,876	6,381	6,211	8,736	8,428	6,287	8,061
Final EDT Sag (After NESC Heavy) (ft)	16.7	21.5	22.1	15.6	16.3	18.6	13.5
Final EDT Catenary (ft)	7,470**	5,811	5,659**	8,028**	7,659	6,742	9,248
Percentage of RTS	19%	20%	24%	26%	27%	20%	26%
Sag (ft) at 1200 A (after NESC Heavy)	17.1	29.4	27.2	19.6	24.1	25.4	27.9
Notes: Primary Design Objective: Tension not to exceed 17,600 lbf under 1" ice load / Sag not to exceed ACSR							
Assumptions: 25°C Ambient temp, Sea level, 30° North latitude, June 21, Wind 2 ft/sec, 0.5 absorptivity/emissivity, Solar Radiation 96 W/ft2							
Comments: *Exceeds Recommended Thermal Limit **No Load on Al							

Table 16 - Shows a comparison of different Drake equivalent conductor types. Section 7.5 of the Southwire Overhead Conductor manual[67] is used as the basis for sagging in the conductors for this comparison.

The goal of this comparison was to establish equality of tension under a 1" ice load condition. Note how initial, during load, and after load values vary considerably. Since these different types of conductors have mechanical attributes that are quite different from each other, it is important that design engineers strive to understand these differences when using them in the design of transmission line projects. In other words, the rules that are employed when using ACSR or other conductors may not serve the engineer well when using ACCC conductors. It is therefore important to start by understanding the fundamental strand/core interaction of ACCC conductors. ACSR is used as a basis for comparison.

2.8.2. The Stress-Strain Relationship

When tensile load is initially applied to a new bi-material (non-homogeneous) conductor, the load is shared by both the core and conductive strands. Over time,

---

[67] Thrash, R, et al; "Overhead Conductor Manual" 2nd edition, Southwire Company (2007)

each material responds differently to tension and temperature. As such, their load sharing will shift as a result. As will be discussed in greater detail in Section 2.13, reduced load or stress on the aluminum strands serves to improve self-damping qualities at higher conductor tensions.

To understand the stress-strain relationship, standardized stress-strain (load) and creep tests are performed to provide information used in sag-tension calculations for line engineering. Figure 20 provides a plot of a typical ACSR Stress vs. Strain test.
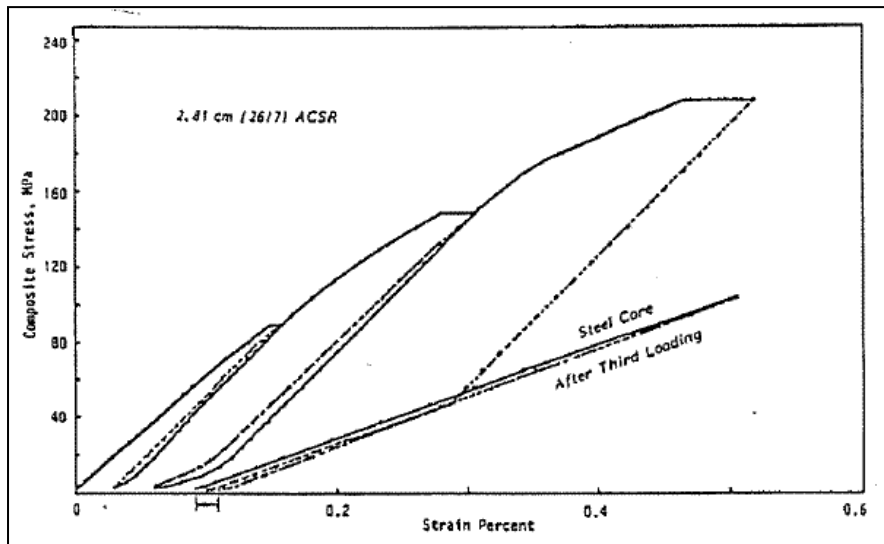
Figure 20 - Aluminum Association stress strain plot of ACSR conductor and steel core[68].

Since RTS is a calculated value, it is known before the test begins, although tensile tests are generally performed to confirm calculated values. Even though the RTS value is a calculated value, it represents the actual breaking strength of the conductor quite well. A conductor sample of approximately fifty feet (16 meters) in length is placed in a load frame. A small amount of tension (~2 to 5% RTS) is applied for a brief period of time to allow for initial loose strand settling.

---

[68] Aluminum Electrical Conductor Handbook, Aluminum Association 1989

The load is increased to 30% RTS and held for 30 minutes. The load is released back to zero then raised to 50% and held for one hour. The load is then released back to zero then raised to 70% of RTS held for an hour, and released to zero.

The plot of load-strain data in Figure 20 shows the three steps at the 30%, 50% and 70% holds (IEC and EN standards require an additional hold at 85% RTS for 1 hour). At each hold, the strain increases while the tension is held constant. Some permanent deformation (elongation) of the conductor occurs as illustrated by the curving of the plot to the right as the load is increased. The release of load after each hold reveals the permanent deformation, as the plot does not retrace along the initial plot, but falls away at a constant slope each time, but further and further to the right.

A second test of the core alone is run and plotted along what appears to be the base of the conductor plot. Compared to the conductor as a whole, the core (in the case of this figure: a steel core), does not deform much. It is very close to elastic within the range of load and strain applied, given the RTS based on a particular standard as described above. Relate this plot of the core to what is observed in Figure 18 and Figure 19 (above) where the steel core's plastic behavior (yielding) at strains above 0.6% strain are seen. A steel core is close to elastic in behavior up to about 0.5% strain, but then yields at higher strains. The characteristics of conductors that dictate the shape of these plots are described below.

Figure 21 shows a stress-strain curve for a Drake size ACCC conductor when subjected to the same stress-strain test protocol. It can be seen that the fully annealed aluminum yields at a relatively low load, and then plastically elongates. Also notice that as the load is increased, and then relaxed, it relaxes along the conductor final modulus lines (2 and 3, 5 and 6, and 8 for example). Thus, when the conductor was first subjected to the 30% RTS load of 12,330 lbf (54.8 kN), the aluminum was carrying some of the tensile load. After the conductor was held at 50% RTS or 20,550 lbf (91.4 kN), and then returned to 30% RTS, it can be see that the aluminum is no longer carrying load, and all the load is carried by the core alone. This unique aluminum load shedding will be explained in more detail in later sections. For the core, a stress-strain curve is shown in Figure 18. Notice, that while the core is subjected to the same testing protocol, there are no horizontal lines at each of the % RTS values. This shows not only that the *composite core is perfectly elastic*; it also shows that *it does not*

experience any creep that would cause permanent deformation or elongation to the core.
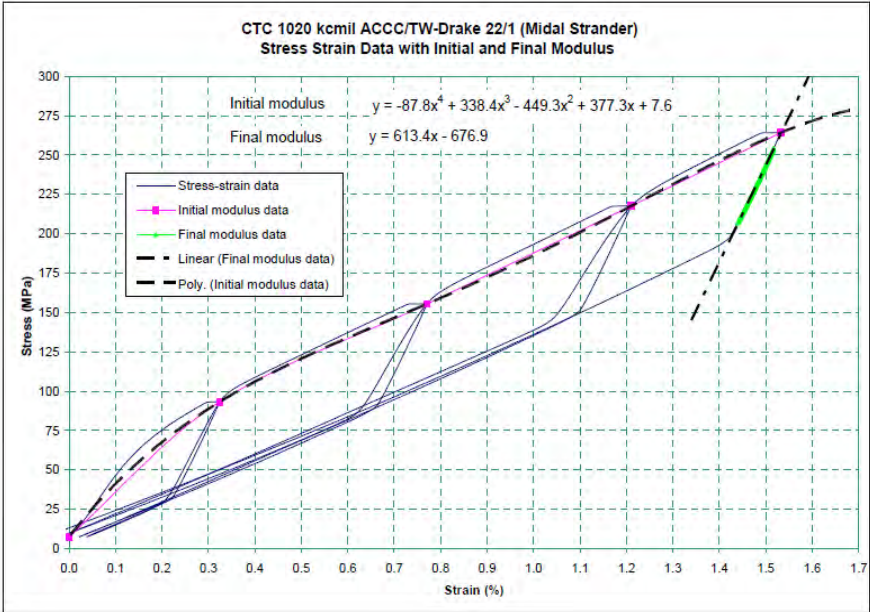
Figure 21 - Typical stress-strain curve for ACCC® conductors.
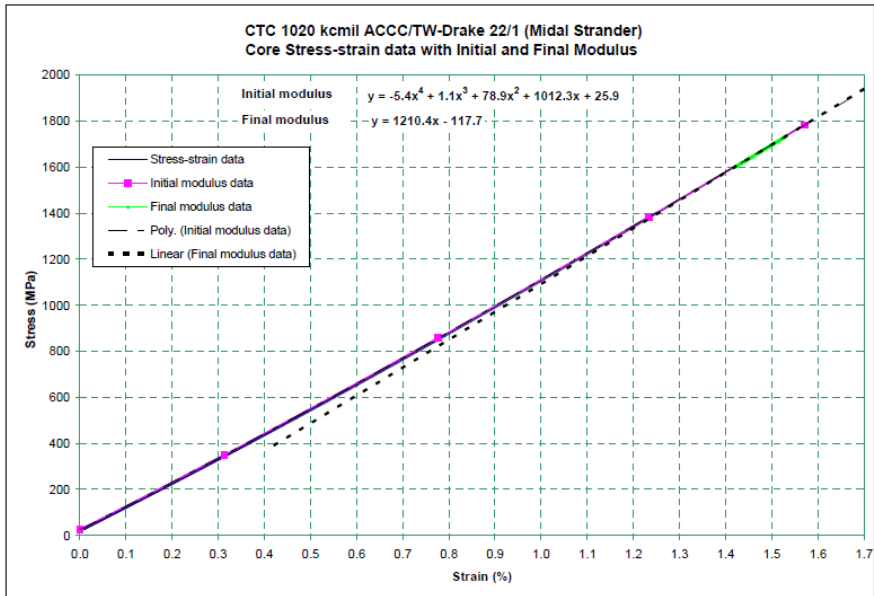
Figure 22 - Stress-strain curve for a composite core used in ACCC®

2.8.3. Material Elasticity

If the conductor's two constituent materials (conductive strands and core) were purely elastic and exhibited no permanent elongation under load for any reason, the conductor and the core plots would be straight lines and the plot, while the load is being applied, would be retraced as the load is being removed. This is almost the case for the steel core up to about 0.5% strain (or approximately 60% of the overall conductor's RTS for ACSR), beyond that it changes due to deformation/yielding (Figures 19 and 20). Referencing Figure 21, the slope of the 'unload' and 'reload' plots is the same after all three holds. This slope is defined as the *final* modulus of elasticity (MOE) of the conductor, and is considered to be a single value that is always applicable at tensions below the maximum tension that has ever been imposed on the conductor. A review of test data for ACCC core stress-strain plots (example shown in Figure 22) shows that it is elastic up to the point of rupture at ~2% strain (100% RTS).

When calculating the final modulus (MOE) and coefficient of thermal expansion (CTE) of the whole conductor, be it ACCC, ACSR, or other conductor type, the following equations can be used which are taken from IEC 61597 (section 5.2 for the CTE and section 5.4 for the final modulus).

$$E_{cond} = E_{Al}\left(\frac{A_{Al}}{A_{cond}}\right) + E_{core}\left(\frac{A_{core}}{A_{cond}}\right) \tag{2-21}$$

$$\alpha_{cond} = \alpha_{Al}\left(\frac{E_{Al}}{E_{cond}}\right)\left(\frac{A_{Al}}{A_{cond}}\right) + \alpha_{core}\left(\frac{E_{core}}{E_{cond}}\right)\left(\frac{A_{core}}{A_{cond}}\right) \tag{2-22}$$

For ACCC conductors, the values for the modulus and CTE of the aluminum and composite cores that can be used are:

- E_{Al} (aluminum final modulus) = 7.4 to 8.2 Msi (51 to 56.8 GPa) – this value is lower than the typical 10 Msi (69 GPa) reported for aluminum metal[69]. The aluminum wires are helically wrapped around the conductor core (not straight), and it is this twist that reduces the effective aluminum modulus when it is measured during a stress-strain test of the conductor. If one were to look at the PLS-CADD™ wire files for ACSR and ACSS conductors, for instance, and back calculated the actual aluminum final modulus from the virtual ones shown in the files, the range of aluminum modulus values would be between 6.9 to 8.5 Msi (48 to 58.6 GPa).
- α_{Al} (CTE of aluminum) = $12.8 \times 10^{-6}/°F$ ($23 \times 10^{-6}/°C$) a typical value for 1350 aluminum, which is not dependent on the aluminum's temper
- E_{core} (modulus of composite core) = is either 16.3 or 16.8 Msi (112.3 or 116 GPa) (see ACCC conductor spec sheet for details)
- α_{core} (CTE of composite core) = is either $8.94 \times 10^{-7}/°F$ or $8.06 \times 10^{-7}/°F$ ($1.61 \times 10^{-6}/°C$ or $1.45 \times 10^{-6}/°C$) (see ACCC conductor spec sheet for details)

From these values, Equations 2-21 and 2-22 can be used to calculate the modulus and CTE of the whole ACCC conductor, with the following exceptions noted below:

---

[69] "ACSR Graphic Method for Sag-Tension Calculations," Aluminum Company of Canada, LTD, Montreal, Canada, 1950.

It should be noted that the contributions of the aluminum modulus and CTE values is only valid over a small range of strains for conductors that use fully annealed aluminum such as ACSS and ACCC conductors. The effective conductor modulus and CTE value will change depending upon whether or not the aluminum has either fully unloaded its load to the core (above the thermal knee point of the conductor which will be discussed further in 3.3.6), or if the fully annealed aluminum wires have yielded (under high strain situations such as heavy ice or wind events).

The fully annealed, type 1350-O aluminum has a tensile strength of only 8,500 psi (60 MPa). Thus, unlike 1350-H19 aluminum used in ACSR conductors, the fully annealed aluminum yields at very low strains, of approximately 0.3%. Figure 23 shows a typical stress-strain curve for an ACCC conductor, in this case *ACCC Delhi*, which uses the 8.76 mm diameter composite core. The initial conductor curve is fitted through the points at the end of the holds seen in Figure 21. The composite core is perfectly elastic all the way to failure, which occurs at strains equal to or greater than 1.9%. The green curve in Figure 23 shows the initial aluminum curve, which is determined by taking the initial conductor curve and subtracting it from the core curve. After 0.5% strain, the modulus of the aluminum is essentially zero out to 2% strain, where the composite core fails. Once the fully annealed aluminum wires yield, they plastically deform with increasing strain, but do not break until they reach an elongation of 20% or greater. The actual polynomial that describes the initial aluminum curve <u>from 0 to 0.5% strain</u> is given by:

$$y(initial) \ (MPa) = 0 + 101x - 54.4x^2 + 349.8x^3 - 606.4x^4 \qquad (2\text{-}23)$$

(accurate to 0.5% strain)

This equation, at 0.5% strain, then has a slope that accurately can be extrapolated out to the 2% strain where failure in the ACCC conductor occurs. This slope (or modulus) is essentially zero between 0.5 and 2% strain. The reason for the curve being only accurate from 0 to 0.5% strain, is that PLS-CADD™ only uses the these curves to 0.5% strain, and from there, extrapolates a straight line, with a slope that is calculated at the 0.5% strain point in the aluminum and core curves, out to the breaking load of the conductor (as discussed in section 3.3.2). A discussion on using PLS-CADD™ for calculating the sag/tension results for ACCC conductor can be found in section 3.3 along with the reason a 4th order polynomial is used to describe the aluminum stress-strain curve.
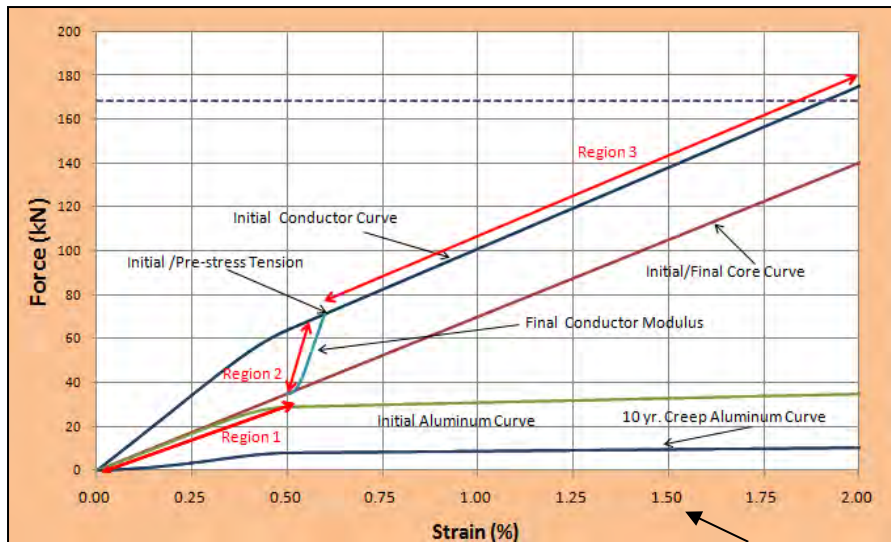
Figure 23 - Typical stress-strain curve for ACCC conductors, this example is for ACCC Delhi

For an ACSR conductor, the 1350-H19 aluminum and steel wires are nearly elastic for most of the stress-strain range where the conductor normally operates. Only at strains higher than 0.5% will the aluminum and steel cores begin to experience significant yielding (as observed in Figures 18 and 19). The aluminum and steel wires will also be sharing the tensile load throughout the ACSR operating temperature range (typically up to 100°C maximum). With the two components in the ACSR being elastic and always sharing the load between them, using the whole conductor modulus and CTE values calculated by Equations 2-21 and 2-22 are sufficient to give reasonable values for these parameters that can then be used to perform sag/tension calculations without knowing the exact stress-strain behavior of the ACSR conductor.

Due to the fully annealed aluminum yielding in the ACCC conductor in strain ranges the conductor is expected to be operating in, there is only a small region in which the aluminum and core are experiencing their elastic states together (final conductor modulus shown in Figure 23). Otherwise, the aluminum is either carrying no load (at temperatures above its thermal knee point which is ~60°C to 80°C for ACCC conductor region 1 in Figure 23) or has yielded (region

3 in Figure 23). This breaks the stress-strain curve of the ACCC into three distinct modulus and CTE regions, as labeled in Figure 23. Depending upon which region the conductor is in will determine which value of E_{cond} and α_{cond} are used to calculate the sag/tensions.

Region 1

- In strain region 1 shown in Figure 23, between 0 and ~0.5% strain, the initial conductor curve in this region is ignored. When load is initially applied to the conductor, the tension will travel up this initial conductor curve, but will never travel back along this curve again, and thus has no relevance in the sag/tension calculations. In the rest of region 1, the lower Initial/Final core curve is where the aluminum has completely unloaded its entire load. This occurs when the conductor is above its thermal knee point. In this region, above the thermal knee point, only the core modulus and CTE dictate the sags. Therefore, in region 1, the following values for calculating the conductor effective modulus and CTE value are:

Aluminum Values	Composite Core Values
$E_{Al} = 0$	$E_{core} = 116$ GPa
$\alpha_{Al} = 0$	$\alpha_{core} = 1.45 \times 10^{-6}/{}^\circ C$

Table 17 – Region 1 modulus values

- $E_{cond}(1) = 0 + 116$ GPa $* (60.3 \text{mm}^2/738.6 \text{ mm}^2) = 9.5$ GPa

- $\alpha_{cond}(1) = 0 + 1.45 \times 10^{-6}/{}^\circ C * (116$ GPa $* (60.3 \text{mm}^2/738.6 \text{ mm}^2))* (1/9.5 \text{ GPa}) = 1.45 \times 10^{-6}/{}^\circ C$

  o Thus, the effective modulus and CTE of the conductor is just the values from the core, and its these $E_{cond}(1)$ and $\alpha_{cond}(1)$ that

are used to calculate the sags from the thermal knee point temperature to 200°C (the emergency temperature of ACCC conductor).

Region 2

- Region 2, is the classical final modulus of the conductor, and is the location where both the core and aluminum are both exhibiting elastic behavior. Here, the point that intersects the initial conductor curve is the highest load value the conductor has been exposed to (which can be either the initial, pre-stressed tension or other high load event). As the conductor heats up, the load will travel down the final modulus curve, and once the load reaches the lower point intersection with the Initial/Final Core curve, the aluminum no longer carries any tensile load. The values used to calculate the conductor final modulus and CTE are as follows:

Aluminum Values	Composite Core Values
$E_{Al} = 56.8$ GPa	$E_{core} = 116$ GPa
$\alpha_{Al} = 23 \times 10^{-6}/°C$	$\alpha_{core} = 1.45 \times 10^{-6}/°C$

Table 18 – Region 2 modulus values

- The conductor modulus for Region 2 for *ACCC Dehli* would be calculated as follows:

  - $E_{cond}(2) = 56.8$ GPa $(678.4$ mm$^2/738.6$ mm$^2)+116$ GPa $(60.3$ mm$^2/738.6$ mm$^2) = 61.6$ GPa

- The conductor CTE value for Region 2 *ACCC Dehli* would be calculated as follows:

- α_{cond} (2) = 23x10^{-6}/°C * (678.4 mm^2/738.6 mm^2) * (56.8 GPa/61.6 GPa) + 1.45x10^{-6}/°C * (60.3 mm^2/738.6 mm^2) * (116 GPa/61.6 GPa) = 19.7x10^{-6}/°C

- Thus, between the installation temperature and the thermal knee-point, the conductor sag/tension will look similar to an ACSR conductor, because an ACSR conductor will have similar conductor modulus and CTE values, and it is this region where the largest changes in sag/tension will occur for a newly installed ACCC conductor.

Region 3

- For Region 3, if the conductor experiences a higher load than the initial or pre-stressing tension, the load will climb up along the conductor initial curve, and then decrease along the new final conductor modulus curve. For instance, if the load during a wind or ice event reaches 18,000 lbf (80 kN). The bright red line would then represent the new location of the Final Modulus of the conductor when the load is removed. It is important to note, that in Region 3, the aluminum wires have already yielded, and thus the modulus essentially becomes zero. Therefore, in this region, the conductor modulus and CTE calculation would be the same as in region 1, even though the aluminum is essentially carrying its full tensile stress of 8,500 psi (60 MPa) as the load increases from the Initial/Pre-stress tension of ~15,700 lbf (~70 kN) to the higher 18,000 (80 kN) load in this example.

- The aluminum and core values for Region 3 are:

Aluminum Values	Composite Core Values
$E_{Al} = 0$	E_{core} = 116 GPa
α_{Al} = 23x10^{-6}/°C	α_{core} = 1.45x10^{-6}/°C

Table 19 – Region 3 modulus values

- $E_{cond}(3) = 0 + 116$ GPa $* (60.3\text{mm}^2/738.6 \text{ mm}^2) = 9.5$ GPa

- $\alpha_{cond}(3) = 0 + 1.45\text{x}10^{-6}/°\text{C} * (116$ GPa $* (60.3\text{mm}^2/738.6 \text{ mm}^2))* (1/9.5$ GPa$) = 1.45\text{x}10^{-6}/°\text{C}$

- Thus, if the tension is expected to increase above the initial/pre-stress tension value of the conductor, the values for the whole conductor modulus and CTE would be $E_{cond}(3)$ and $\alpha_{cond}(3)$ would then be used to calculate the sag/tension during the high load event.

- This distinction is important, because if the values $E_{cond}(2)$ and $\alpha_{cond}(2)$ are used to calculate the tension in the conductor due to high load event, then the tension calculated would be higher, and the total sag lower, which would be incorrect for ACCC conductors.

  - Using $E_{cond}(2)$ and $\alpha_{cond}(2)$ to calculate the change in length of the conductor when the tensions are expected to go higher than the starting highest tension, would result in a smaller change in length of the conductor, leading to the higher tensions and lower total sags
  - Using $E_{cond}(3)$ and $\alpha_{cond}(3)$, from the starting point of the highest tension used in the calculations, would allow the conductor to stretch as expected with the higher tensions, leading to a larger change in length of the conductor, resulting in sag/tension values that would be closer to what would be calculated in PLS-CADD™.

The process of calculating the sag/tensions using numerical methods is ultimately an iterative mathematical process. Knowing the correct modulus and CTE values of the conductor is very important, so that the programs that calculate the sag/tensions can accurately calculate the change in length of the conductor for any given span length. PLS-CADD™ uses a graphical method (which uses an EPE model for the conductor stress-strain) for predicting sag/tensions. This program shifts the stress-strain curves as a function of temperature in order to determine the sag/tension for any particular temperature or other weather event. Ultimately, the graphical method employed by PLS-CADD™ and SAG10®, should produce results that are consistent with

numerical based calculations. Therefore, having a good understanding of the specific conductor stress-strain properties, and how the modulus of the conductor changes with strain, will allow numerical calculations to predict sag/tensions that are nearly the same as the graphical sag/tension programs.

2.8.4. Strand Settling and Creep

Strand settling is essentially the result of the individual conductor strands in each layer seating themselves into the layer below as tension is applied. Each layer of strands is wound around the layer beneath the wire in the opposing direction causing each layer to cross the other at an angle of twice the lay length angle. Only the central 'king' strand wire (e.g., the ACCC composite core) at the center of a conductor is straight. Each point of strand-to-strand crossing becomes a point of compression between the strands as each helically shaped strand tries to straighten out and force its way towards the center of the conductor. Such compression can effectively restrain tensile stretching of the aluminum strands during loading, and lengthen the strand's helical path/length after loading (upon relaxation). While strand settling can be significant in ACSR conductors, it is expected to be negligible in ACCC conductors as the product is designed with high packing density (*i.e., less room available for improper strand settling*) with TW strands of fully annealed 1350-O aluminum (*i.e., much more readily able to stretch during loading, and less likely to create significant compression at contact points due to the 'softness' of aluminum and greater contact areas between trapezoidal shaped strands*).

After a conductor is first installed, a certain amount of strand settling and initial creep will occur as the aluminum strands adapt to their new position and stress. To assess initial strand settling and creep, a Drake size ACCC conductor was mounted in a 60 foot (18 meter) load frame and tensioned to 15% RTS (6,165 lbs or 27.4 kN). Tension drop was recorded (Figure 24). The tension drop observed followed the classic power law in creep[70], and quickly dropped by 4% during the first 15 minutes and 5% in the first hour. By the 4th hour the tension had dropped by 7% (and substantially leveled off). This equates to drop in tensile stress in aluminum strands from an initial 3.37 ksi (23.2 MPa) to 2.99 ksi (20.6 MPa) in 1st hour, and 2.84 ksi (19.58 MPa) (for a 16% reduction in aluminum stress) by the 4th hour. This relaxation in the aluminum strands

---

[70] Ishikawa, K. Et al., Creep of Pure Aluminum Materials at a Low Temperature, Journal of Materials Science Letters, Vol. 17 (1998) pp.423-424.

improves self-damping performance and more importantly, improves resistance to fretting fatigue as described further in Section 2.13.4. This unique behavior of the ACCC conductor also serves to further improve thermal sag performance by transferring tensile load to the more dimensionally stable composite core. Pre-tensioning to some degree as discussed further in Sections 2.15 and 3.3 can offer additional benefits. A similar test was performed in a shorter load frame with nearly identical results (Figure 25).
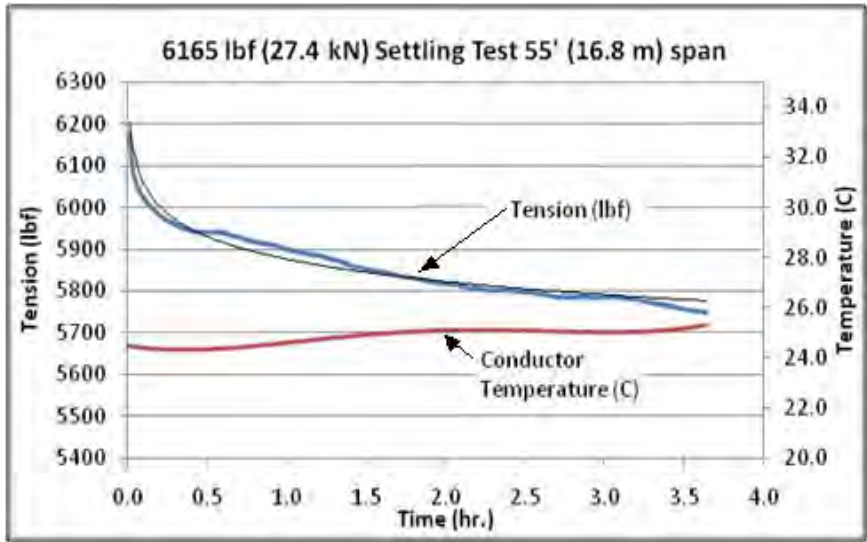
Figure 24 - ACCC Drake conductor exhibiting 7% reduction in tension during the initial 3.5 hours after 'stringing.' This equates to a 16% reduction in tensile stress in aluminum strands).
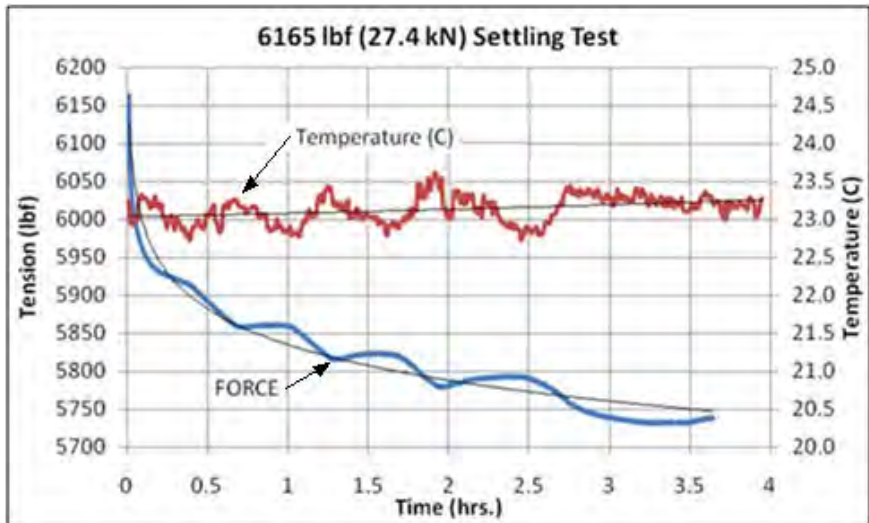
Figure 25 - ACCC Drake conductor in a test frame with a sample length of approximately 5 ft (1.5 m) during a 3.5 hour period after 'stringing in' showing a 7% reduction in the conductor tension, representing a reduction of stress in the aluminum strands by 420 lbs (1.8 kN) (16% reduction). The waviness in conductor tension is caused by temperature fluctuation in the test lab.

There are basically three sources of stress that contribute to metallurgical creep. These are based on thermal, elastic and plastic elongation. The terms used to define the stress at which plastic deformation begins are:

- Yield Strength is typically defined as the stress at which a pre-determined amount of permanent deformation (0.2%) occurs. When yield strength is reported, the amount of offset used in the determination should be stated. For 1350-O aluminum, the yield strength is about 4 ksi (27.6 MPa) at 0.2% offset.
- The Proportional Limit (PL) is defined as the stress at which stress strain curve first deviates from a straight line. Below this limiting value of stress, the material is elastic and obeys the Hooke's law (i.e., stress *proportional* to strain). The PL is generally not used in specifications because the deviation begins so gradually that controversies sometimes arise as to the exact stress at which the line begins to curve.

83

In soft metals such as fully annealed aluminum or copper, plastic deformation begins at stress levels significantly below their yield strength, as shown in Figure 26.
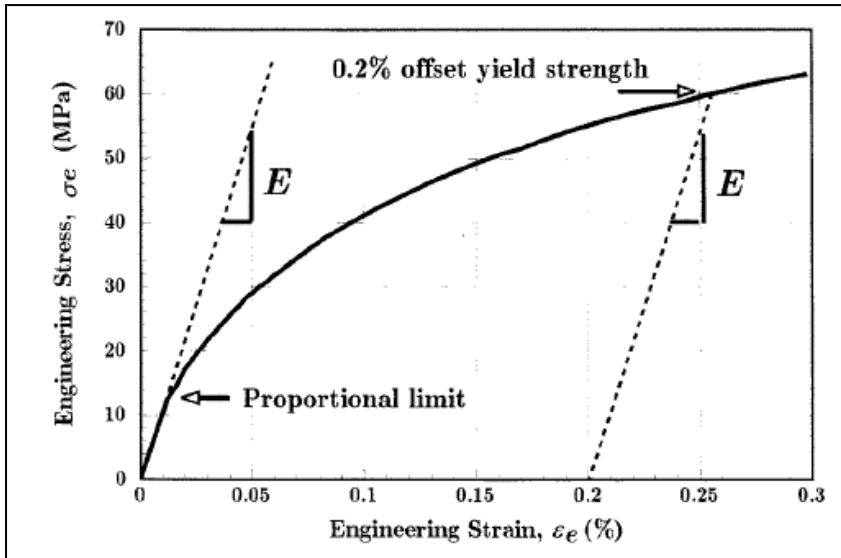
Figure 26 – Proportional limit & yield strength in conductor metals (copper and aluminum)

A standard creep test for conventional conductors holds a length of conductor at a constant tension for 1,000 hours and measures the length of the wire over that time. Creep typically follows the power law relationship during steady state conditions. The elongation with time, when plotted on log-log paper, is typically a straight line. The plot is then extrapolated to 100,000 hours (~10 years) to obtain the projected creep elongation during conductor life. Figure 27 compares the creep in ACSR and ACCC conductors.
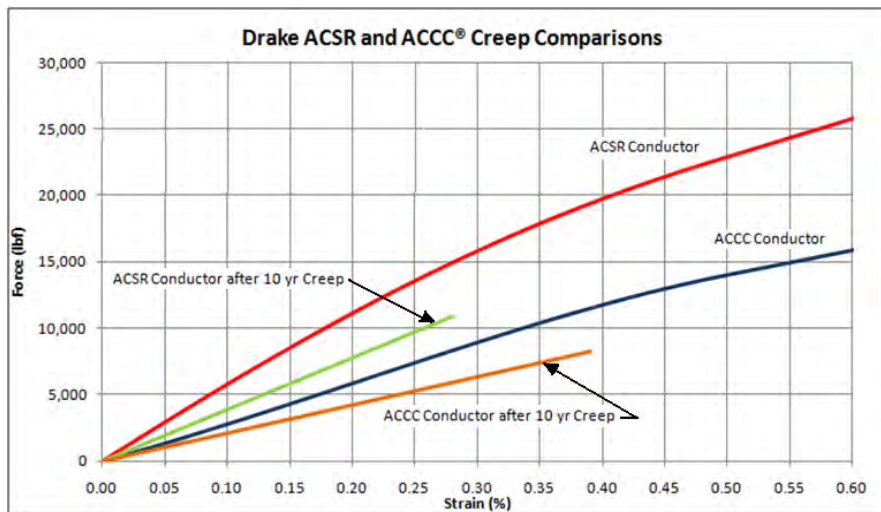
Figure 27 – Comparison of creep between ACSR and ACCC conductors

Sag from creep in conventional conductors (with a metal core) is related to both creep in the aluminum strands, which gradually sheds tensile load to the metal core, as well as the inherent creep in the metal core under load (i.e., accumulating conductor elongation). The plastic deformation associated with creep in both the aluminum strands and the metal core continues throughout the conductor's life. The steel core typically loses about 7% in modulus from room temperature to high temperatures (~250°C), which can contribute to additional creep. Heavy ice or wind load can also lead to increased (not fully recoverable) sag in conventional conductors due to plastic deformation. Sag associated with creep and permanent conductor elongation in metal core conductors can be underestimated because the creep in conventional conductors will continue beyond the 10 years where sag and creep are projected based on 1,000 hours of laboratory creep testing.

A creep test for ACCC conductors, executed per Aluminum Association test protocol or the IEC 61395 protocol will confirm that a reduction in stress in the aluminum strands does occur, but also confirms that the ACCC conductor's core *does not* exhibit creep. Therefore creep should not be considered an important design criterion when designing with ACCC conductor, and is essentially irrelevant.

For example: When an ACCC conductor with an "every day tension" (EDT) of about 7,250 psi (50 MPa) is subjected to an ice load of 21,750 psi (150 MPa), the load would follow the final conductor modulus line (Figure 23), then travel down the final core line after the load. When the conductor returns to the EDT of 7,250 psi (50 MPa) stress, aluminum strands would no longer be carrying any tension load, and there will be no additional creep in the conductor as the ACCC core is elastic. Similar to ACSS, "*creep is not a factor*" with ACCC conductor, especially at temperatures above the thermal knee-point or after any 'relatively light' ice or wind loads that plastically deform the very pliable aluminum strands. Creep should be even less of a factor with ACCC conductors compared to ACSS conductors due to the elasticity nature of the ACCC composite core compared to the steel core used in ACSS that is still subjected to creep over time.

2.8.5. Thermal Elongation

If not for the impact of large ice loads, strand settling, or creep, conductor length changes would primarily be a function of the Coefficient of Thermal Expansion (CTE) of the conductor's core and aluminum strands. Conductor temperatures range from the location's coldest ambient temperature to the conductor's maximum operating temperature. In non-homogeneous conductor designs, the core material has two purposes for being part of the conductor. First, it is there to increase overall conductor strength. Second, it is there to lower the CTE of the overall conductor by offering a CTE much lower than the unavoidable high CTE of aluminum.

As discussed previously, the tensile load sharing between a conductor's aluminum strands and its core can be calculated. If we assume a conductor is manufactured in a way that puts no stresses into its individual wires during the process, then we can say that the load sharing between the materials will be known for the temperature of the factory that made the conductor. It is easy to believe that the zero-stress manufacturing of a conductor is not precisely the case, but the assumption is reasonable.

As a conductor is subjected to various electrical loads that cause the conductor to heat up, the dissimilar coefficients of thermal expansion of the core strands and conductive strands cause a change in tensile load sharing. The aluminum strands expand at a higher rate than the core as temperature rises which relaxes

the aluminum strands and shifts the tensile load to the core. Even though the overall tensile load is decreasing, it is also moving to the core. At some temperature, the tensile stress in the aluminum is overtaken by thermal expansion of the aluminum, and all tensile load is transferred to the core, leading to no tensile load in the aluminum strands. The apex of this transition is called the *thermal knee point*.

A review of Figure 21 shows that the mechanical point of complete off-load of tension in the aluminum occurs when then final plot of the conductor being off-loaded from the 50% and 70% holds changes slope and tracks along the core's plot. The bend in that plot is called the *mechanical knee-point*.

It can be noted that when the conductor gets very cold, the aluminum shrinks more than the core and takes on a higher percentage of the tension in the conductor - a tension that is increasing as well. Stresses in the aluminum are maximized with cold temperatures and with large ice loads, but reduced over time via creep and/or events that cause additional strand settling or plastic elongation. After the load event passes and, over time, the load sharing will have permanently shifted away from the aluminum strands to the conductor's core.

2.8.6. Thermal Knee Point

At high temperatures, all tensile load is carried by the composite core. The thermal knee point of a conventional steel reinforced aluminum conductor such as ACSR can range from around 80°C to over 90°C[71]. The knee-point temperature is dependent upon the ratio of aluminum to core in a particular conductor and on the tension in the conductor. A tighter conductor needs to be taken to a higher temperature than a loose conductor to allow the thermal expansion to relieve the tension in the aluminum. So, tighter installations generally have higher initial knee-point temperatures. Regardless of the design tension for an ACSR installation, there is little temperature difference between the knee-point temperature and an ACSR thermal limit. Thus, the characteristics of an ACSR conductor at temperatures above its thermal knee-point temperature are of limited interest.

---

[71] Barrett, J.S., Ralston, P. And Nigol, O., Mechanical Behavior of ACSR Conductors, CIGRE International Conference on Large High Voltage Electric Systems, September 1982.

As the aluminum strands elongate over time based on load history, elastic deformation, strand settling and creep, their contribution to tensile load sharing under normal mechanical load conditions decreases and shifts the thermal knee-point to lower temperatures. This improves thermal sag characteristics, conductor self-damping performance and also reduces stress in the aluminum strands that can contribute to strand fatigue failure as is further discussed in Section 2.13. A comparison of the initial thermal knee-points between ACSR and ACCC Drake size conductors is shown in Figure 28. This data was acquired from a 65 meter (215 ft) test span wherein the current of the conductors wired in series was gradually raised to 1,600 amps. The ACCC conductor's added aluminum content allowed it to carry the same current at cooler operating temperatures. The sag of the ACCC conductor (shown in red) increased by 11.4 cm (4.5 inches), while the sag of the ACSR conductor increased by 153 cm (60.3 inches). The test was performed by Hydro One at Kinectrics lab in Toronto as part of a High Temperature Low Sag conductor evaluation[72].

In this particular test, the thermal knee-point was observed at about 50^0C for the ACCC Drake conductor and about 80^0C for the ACSR Drake conductor (Figure 28). Knee-point values can vary as a function of conductor type, tension, span length and conductor 'age' as ice, cold weather, and wind loads (high tension conditions) can stretch the aluminum strands, which allows them to subsequently relax (reduce stress) and shift load to the conductor's core (reducing the thermal knee point to at or below the stringing in temperature). The thermal knee-point of a non-homogeneous conductor can intentionally be lowered by pre-tensioning (as discussed further in Sections 2.13.5 and 3.3.4). The ACCC conductor's elastic core, pliable aluminum strands, and low CTE make the exercise of pre-tensioning relatively easy to accomplish and more productive than with other less elastic or higher CTE conductor types.

---

[72] Pon, C; "High Temperature – Sag Characterization Test on 1020 kcmil ACCC/TW Conductor" Kinectrics North America Inc. Report No.: K-422024-RC-0003-R00 February, 2004
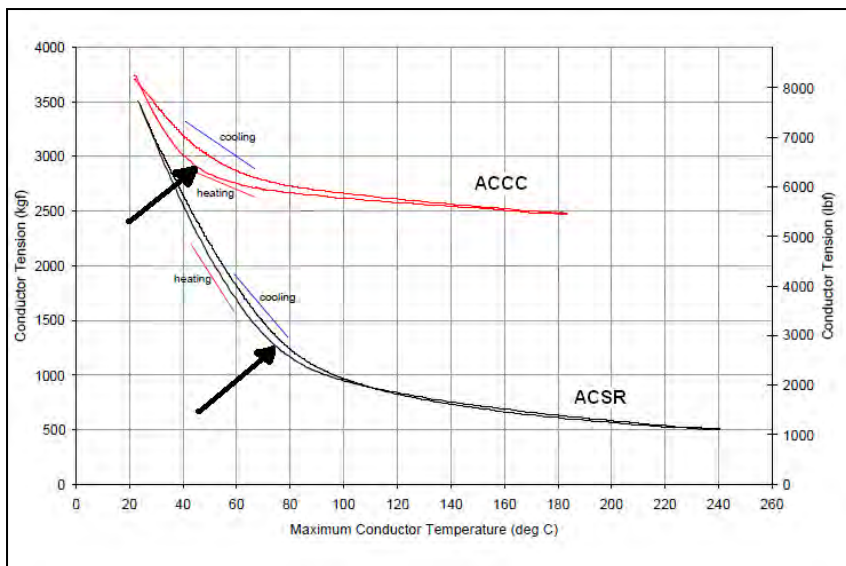
Figure 28 - Thermal knee-point comparison by Hydro One and Kinectrics Lab of Drake size ASCR and ACCC conductors.

2.8.7. High Temperature Aluminum Compression

A study conducted by the Canadian Electricity Association (CEA) in 1978 concluded that the aluminum strands in an ACSR conductor would expand and "go into compression" (as a result of thermal expansion) and that the expansion would create an equal and opposing tension in the core that would increase a conventional ACSR conductor's sag. The study was published as report 78-93[73] "Development of an Accurate Model of ACSR Conductors for Calculating Sags at High Temperatures". The work was done in association with the Research Division of Ontario Hydro (now Kinectrics and Hydro One, respectively).

The report stated that there was a limit to the expansive or "compressive forces" that the aluminum strands were capable of developing before they subsequently buckled or "birdcaged." The compressive stress at which birdcaging takes place

---

[73] CEA report Bare Overhead Aluminum Conductors Item # WCWG-03 (95) Ottawwa, Ontario, Canada

is dependent on the lay length of the stranding, the number of layers of aluminum and, as such, is quite variable and practically incalculable. The report stated a range from 870 psi (6 MPa) to 1700 psi (12 MPA), and suggested using a universal value of 1,450 psi (10 MPa). This value, however, was obtained when the conductor was at room temperature. The thermal expansion (or compressibility) of the outer strands decrease as a function of temperature - which limits the overall impact. The essence of the mechanics is that the compressed helical strands of inner layers are constrained from buckling at near zero stress by the layer above (outside) that are somewhat cooler and may be under a lower compressive stress.

Many recognize that this compressive action is occurring, but not necessarily to the degree that the CEA work suggested[74]. An alternate theory suggests that other things such as mill practices, stranding practices, and a reduction in the steel core's modulus of elasticity by 10 to 15% at high temperatures may be the reason for the higher than understood sags at temperatures above the thermal knee-point for ACSR conductors. Real time sag measurements of ACSR conductors made against rising and falling conductor temperatures also show hysteresis, which could be attributed to internal strand friction.

It is also important to note that recent studies of ACSR and ACSS conductors have demonstrated that the temperature of the conductor's internal core and aluminum strands can actually be 30 to 40°C hotter than the outer strands, which could further explain the discrepancies in steel core conductor sag[75]. Extensive testing of the ACCC conductor has only observed a difference in strand/core temperature of ~2°C per layer even at temperatures above the recommended short term emergency temperature of 200°C. While some hysteresis is noted in the ACCC conductor as temperatures rise and fall (from one extreme to another) during testing, the very low Coefficient of Thermal Expansion (CTE) of the ACCC conductor's composite core limits this hysteresis to a few inches or mm.

2.9. Ice Load Events

Based on the equation:

---

[74] Rawlins, C.B. Assessment of the Nigol-Barrett Theory of Compression Stress in the Aluminum Part of ACSR Due to Maximum Loading

[75] Douglass, D; "Radial Temperature Difference for Bare Stranded Conductors" CIGRE / IEEE Joint Panel Session Las Vegas, Nevada; Feb. 2011

$$D = \frac{w \cdot S^2}{8 \cdot H}$$

<div align="right">(2-21)</div>

If sag D could remain constant, a doubling of the weight of a conductor would double its tension, H. But, the increase in tension causes an elastic stretching of the conductor and that increases the sag. The amount of increase depends on the modulus of elasticity (MOE) of the conductor. Recall that a strain change wants to cause a sag change independent of the span length. A 1 lb/ft conductor strung to 5,000 lbf (122.2 kN)tension will have sags of 14 ft (4.3 m), 56 ft (17.1 m) and 156 ft (46.5 m) in spans of 750 ft (229 m), 1,500 ft (457 m) and 2,500 ft (762 m) respectively, according to this same equation. If we assume that an ice load event increases sag by 5 ft (1.5 m), the sags in these three spans will become 19 ft (5.8 m), 61 ft (18.6 m) and 161 ft (49 m) respectively. These are increases in sag of 19%, 9% and 3.2% respectively causing a reciprocal tension increase of the same percentages. A 19% change in tension involves considerably more strain change than does a 2.3% tension increase so the direct relationship between the iced weight / bare weight ratio and tension increase ratio is imperfect for short spans, but improves substantially with longer spans.

This means that for longer spans, the increase in ice loaded conductor tension is closely related to the weight change ratio (Figure 29). For a 2,500 ft (762 m) span the bare wire tension of 5,000 lbf (22.2 kN) would approach 10,000 lbf (44.5 kN) if 1 lb/ft (1.5 kg/m) of ice were placed on the conductor. But, the tension would increase to much less than 10,000 lbf (44.5 kN) if the same amount of ice were added to the 750 ft (229 m) span. The sag changes with short spans are dramatic while the tension increases are less dramatic. This is why very small conductors survive icing events on short spans reasonably well, but, in doing so, they develop large sags. The sag changes with long spans are minor but the tension increases are much greater, approaching the equation's simple suggested value. External loading issues (ice and wind) are why long spans need high-strength conductors.

If experience, standards, or regulations in a particular region requires that a line be designed for a particular thickness of ice, then understanding the equation above will suggest preferred conductors.   Table 20 shows the NESC requirements in the US. The weight of ½" (13 mm) of radial ice on a 1" (25 mm) diameter conductor is close to one pound per lineal foot (0.93 lb/ft, or 1.4 kg/m). As noted, if the conductor weights 1 lb/ft (1.5 kg/m), then the weight change is

a factor of 2.0 and the tension increase tries to be 2.0 times the bare tension. If the conductor weighs 0.8 lbs/ft (1.2 kg/m) the tension increase wants to be 2.25 times the bare weight [(1 + 0.8)/0.8]. If the two conductors are strung to the same tension, the lighter conductor will have less sag and develop a larger tension than the heavier conductor. If the two conductors are strung to the same sag, as is the general nature of line design, the lighter conductor will have a lower bare wire tension (80% of the heavier conductor) but will adopt an iced tension practically equal to the heavier conductor with greater sag. Thus, a heavier conductor tempers the tension increase imposed by ice (or wind).
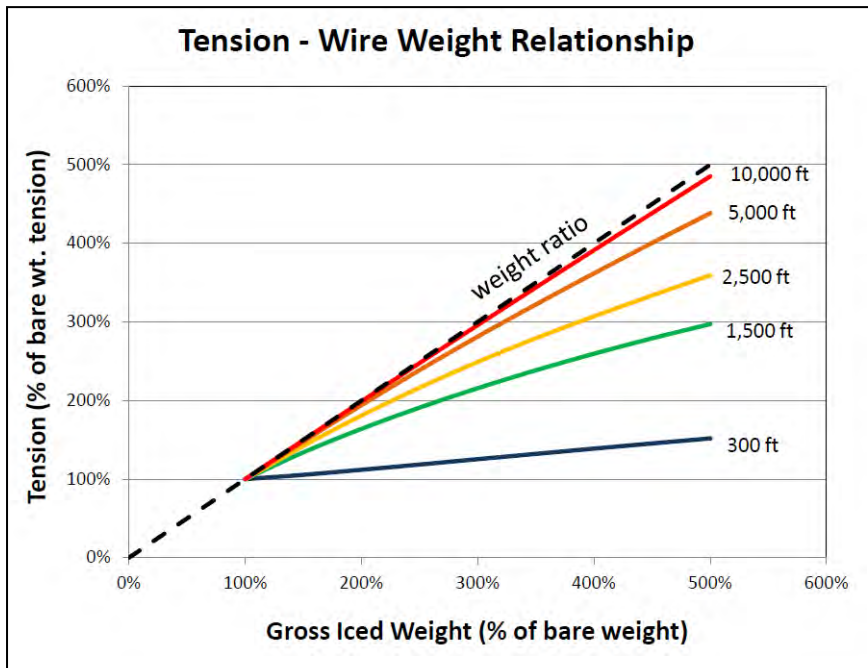
Figure 29 - Conductor / Ice Weight Ratios

NESC Load Cases - Rule 250 B				
	Ice (inches)	Ice (mm)	Wind (mph)	Wind (km/h)
Light	0	0	60	96
Medium	0.25	6.35	40	64
Heavy	0.50	12.7	40	64

Table 20 - Table of National Electric Safety Code (NESC) load case rules for evaluating conductor sag/tension results.

A conductor with a 50% larger diameter (1.5" or 38 mm) will typically weigh 2.0 to 2.25 times the 1" (25.4 mm) diameter conductor and the weight of the ½" (12.7 mm) ice will be about 1.25 lb/ft (1.9 kg/m), only 33% heavier. If strung to the same sag as the 1" (25.4 mm) conductor and with double the bare weight, its tension would be 10,000 lbf (44.5 kN) and the iced tension approximately 16,250 lbf (72.2 kN) [10,000 * (2.0+1.25)/2.0], a 62% increase, not a 100% increase. Here we see that larger diameter conductors temper the tension increase imposed by ice when the ice is expressed by thickness.
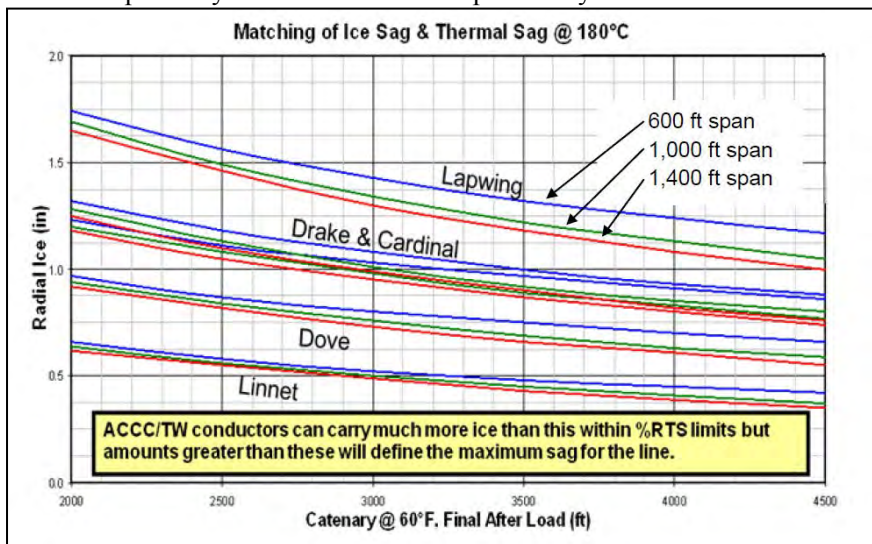
Figure 30 - Matching Thermal & Ice Load Sag with ACCC Conductor

Figure 30 describes the ice thicknesses 'above which' will define a line's maximum design sag using the ACSR/AAAC derived Catenary Constant (H/w) approach, as discussed in Section 2.13.2. The figure also shows the radial thickness of ice that can be applied to representative 'standard' ACCC conductors without exceeding the sags of the conductors operating at 180°C. Recall that the fully annealed 1350-O aluminum used in ACCC conductors causes the strength of the conductor to be 70% to 87% dependent upon the core. The MOE of the ACCC cores is about 60% of that of a steel core. Iced sags therefore grow faster with ACCC conductors than with steel core conductors assuming the initial conductor tensions are equal.

The very high strength and elasticity of the ACCC conductor cores means that under extreme ice load events, the conductor is at much less risk of breaking compared to other conductor types. The ACCC conductor core is so strong in fact that higher conductor tensions can be utilized to mitigate heavy ice load sag, assuming the structures can support higher tensions and consideration is given to Aeolian vibration, as discussed in Section 2.13.

Figure 30 is a reminder that smaller size conductors carry much less ice than the larger conductors before the iced sag defines the clearance requirements. A low tension design may be able support more ice than a tighter design. Finally, longer spans support slightly less ice than shorter spans before the iced conductor sag defines the clearances. Most lines will be designed to a Catenary Constant, C value of less than 8,000 ft (2,500 m) so an easy to remember rule of thumb is:

> *An ACCC conductor can support two to three times its own weight*
> *of added ice before the iced conductor sags are larger than the*
> *maximum possible thermal sags and will most likely define*
> *clearances (span lengths and/or structure heights). At these large*
> *ice loads, the strength of the conductor is not challenged.*

For example, at a C value of 7,200 ft (2,200 m) and using a 1,400 ft (425 m) span, the ice that can be carried is 2.1, 2.6, 2.9 and 3.0 times the weight of Linnet, Dove, Drake and Lapwing, respectively. Shorter spans and looser tensions will allow greater capacity without adding cost to the line with taller structures or shorter spans. For the reasons described above, very long spans and very tight lines will carry less weight without penalty, but such designs are rare.

For the heavy ice / long span scenarios, a higher ratio of structural core area to aluminum area will create greater resistance to iced conductor sag increases. In the case of ACCC conductors, several standard designs utilize larger cores to provide added strength and reduced ice load sag (conductor elongation). A higher modulus ACCC core is also available to accommodate particularly long spans which may be exposed to extreme ice load events. Pre-tensioning ACCC conductors is another way to effectively reduce ice load sag, as described in more detail in Section 2.15.3. Due to the ACCC conductor's high strength, elasticity, low coefficient of thermal expansion, and unique self damping characteristics, it is important that sag and tension considerations (and comparisons) be based on anticipated ice / wind load sag rather than solely on thermal sag - as other conductor types are more prone to thermal sag and permanent deformation under heavy ice load events. Therefore:

> *At even high loads of ice, ACCC conductors should be sag/tensioned per the ice load. This then needs to be compared to the worst sag of the other conductor types where the sag limit might be driven by thermal load and creep or compounding effects of ice and creep*

2.9.1. Full Span Radial Ice Loads

For mathematical simplicity, ice accreted onto conductors is assumed to be a uniform radial shape centered on a conductor. Despite the radial simplicity, this is often far from the actual condition. Freezing precipitation typically forms a very lopsided shape on the conductor, often with hanging icicles and accurately understanding its actual unit weight and resulting wind load is very difficult to calculate and usually overstated. Very large diameter rime ice accretions have the added complexity of a less but unknown density compared to the relatively well understood density of clear ice.

It should be noted that the ACCC conductor generally has a strength-to-diameter (or weight) ratio much higher than conventional all-aluminum or steel-reinforced conductor types. This can provide a greater margin of safety against conductor breakage under dramatic loading events. As with any conductor, the short-term but large sag may be accommodated by clearance, or exceptions to clearance, criteria, but the recovery of ACCC conductors to the pre-event sag level will be better than any other conductor type because the core is purely elastic exhibiting no permanent deformation after being loaded to near the

breaking point. Table 16 in Section 2.8.1 (above) offers several comparisons under varied conditions.

2.9.2. Ice Shedding Events

Ice that accumulates on a conductor eventually falls off. The industry's modeling of this event is concerned with the dynamic response of a long, elastically stretched wire to the instantaneous reduction in weight and tension or to the odd sags that result after partial unloading occurs. Generally, we are more concerned with electrical and ground clearance reasons than we are for structural reasons[76]. Instantaneous unloading of whole spans of ice is rare, as most ice shedding events are of minor lengths of ice falling off over a period of time.

The IEC standard for structural loadings[77] acknowledges that partial shedding occurs and suggests a static, unbalanced ice load condition for structural loadings and perhaps clearances. It recommends and employs different percentages of RTS accumulation on adjoining spans. If a line is in a location where ice or wet snow accumulations are large or frequent and considered problematic, the easiest fix is to configure circuits such that one phase is not above another or ample space is provided if they are vertically stacked.

2.10. Conductor Galloping

Conductor galloping usually occurs during modest wind conditions when some ice has accumulated on the conductor, usually in an uneven pattern causing an airfoil effect. As with Aeolian vibration, galloping is a resonant phenomenon wherein the energy from a constant / uniform wind couples with the conductor's natural frequency - given its condition (shape / tension) at the time. Bare conductors are generally considered to be uniform in their top surface and bottom surface shape (and texture), and an upward and downward lift differential caused by passing wind will not create low amplitude galloping, but can produce high frequency Aeolian vibration as discussed in Section 2.13. A minor ice coating on the conductor can impact the uniformity of its shape and textural equality, and galloping can ensue. Larger thicknesses of ice can

---

[76] Fengli Yang; Jingbo Yang; Dongjie Fu; Qinghua Li; Dynamic responses of the conductors in transmission lines under two typical impact loads Power System Technology (POWERCON), 2010

[77] Design Criteria of Overhead Transmission Lines", IEC Publication 60826

maintain the actions, but eventually very large ice accumulations mean that more mass has to be put in motion. This larger mass may tend to reduce the ability to gallop, but, should the line have the energy input to continue galloping, catastrophic events can result.

To date, only one galloping event of ACCC conductor has been reported. This occurred on a Hawk size conductor in the state of Kansas (in the US) where a relatively light ice load of 6 to 12 mm (1/4 to 1/2" thick) coupled with very constant wind velocity over open farmland caused substantial galloping that subsequently broke 40 cross-arms and/or insulators (Figure 31). The ACCC conductor was not damaged and did not hit the ground between the relatively short ~450 ft (50 m) spans. Structural repairs were quickly made and the line was back in service within a few days[78].

Figure 31 - Galloping Damage

2.10.1. Electrical Concerns

Galloping events are generally identified by flashover occurrences rather than visual sightings. Galloping is much more of a vertical motion than a lateral motion so putting conductors one above another certainly puts them more in each other's way compared to when placed beside each other. As with ice

---

[78] Hart, Ira; Report to CTC Cable of Conductor Galloping; e-mail communication December, 2007

shedding, galloping is a dynamic action that is difficult to accurately predict. As such, the industry's focus remains on electrical and clearance concerns, more so than structural loading concerns. Nevertheless, both need consideration.

The difficult-to-predict, mostly vertical and somewhat lateral motion of galloping is generally regarded as occurring within the confines of an elliptical shaped envelope that is described in size and location in a variety of ways by different organizations. All are based on varied amounts of analysis and should be considered empirically based. Each seems to work well enough and the ellipse is meant to say that with some acceptable probability, the conductor will remain within the elliptical bounds.

There is one empirical guideline that seems challenged by data. That is the rule stating that spans over 600 to 700 ft (180 to 220 m) in length will not gallop in a single loop but only in a double loop producing much smaller elliptical envelopes above this span length that require addressing. Those who believe in this guideline, may consider extending spans to longer than this limit to access the smaller double loop ellipse dimensions and the accompanying tighter phase spacing relative to the span's sag. Those who believe that single loop galloping does occur on longer spans may avoid longer spans because of the large phase spacing required.

The US RUS standards[79] suggest the guideline is valid. Dr. David Havard, of Havard Engineering, points out in reference[80] that single loop galloping, as recorded over a number of years on Ontario Hydro's (now Hydro One's) system, knows no span limit. Dr. Havard offers a way to predict phase spacing needs and may have useful guidance to offer for long spans[81].

A number of ancillary devices have also been employed with varied degrees of success to mitigate the effects of conductor galloping. These devices include:

- Inter-phase or bundled conductor spacers

---

[79] REA 'Galloping Conductors', Design Report No. 1, Rural Electrification Administration, Transmission Branch, 1962, Rev. 1982.
[80] Havard, D.H., Analysis of Galloping Conductor Field Data, the 8th International Workshop on Atmospheric Icing of Structures, IWAIS 1998
[81] Lilien, J.L., Havard, D.G., "Galloping Data Base on Single and Bundled Conductors Prediction of Maximum Amplitudes" IEEE TRANSACTIONS ON POWER DELIVERY, VOL. 15, NO. 2, APRIL 2000

- Pendulum de-tuners
- Windampers®
- Torsional Damper De-tuners
- AR Twister®
- Air Flow Spoiler®

As galloping involves the rotation of the conductor or conductor bundle, many of these anti-galloping devices attempt to decrease rotation. While no known device can completely prevent galloping under every condition, inter-phase spacers can reduce incidences of electrical faults between phases. It has also been suggested that double bundled conductors are more prone to galloping than triple or quad-bundled conductors, due to their relatively poor rotational resistance.

2.10.2. Structural Concerns

The largely ignored effects of galloping are the mechanical or structural effects on the conductors themselves and on the support structures. Some papers have reported the large motion-induced (dynamic) loads on conductor attachments as multiples of static loads[82]. The vertical load increase at suspension points can be 1.5 times the static load and tensile load increases at terminations can be 2 times static loads. However, these factors need very careful scrutiny because a ratio requires a 'denominator' that is the static load. In some reports, that static load is of the bare wire, not of the iced wire without the motion.

If the bare wire weighs 1 lb/ft (1.5 kg/m) and the iced wire weighs 2 lb/ft (3 kg/m) as used in an example above, when discussing tension increases the choice of weight use in the denominator to calculate the dynamic effects of galloping will be radically affected. Unless a structural load case for structural design purposes involves a very heavy ice load, the dynamic loads of the load case will typically not design the structure. Most galloping analyses for electrical clearance reasons use a modest ice weight and a ratio of 1.5 or 2.0 applied to this ice weight will not likely affect the structure design.

---

[82] Cigre Technical Brochure TB 322 State of the Art Conductor Galloping B2.11.06 (June 2007)

However, motion can be damaging if sustained or if accompanied by either very large galloping motions or heavy ice weights. The sustained galloping of an ACSR conductor on large 400 kV towers in the UK some years ago tore the towers apart after several days of occurrence.

Since our concern lies primarily with conductors, it is noted that large ice loads can cause large sags which causes large departure angles out of suspension clamps. Excessive galloping in combination with excessive bending and tension can cause problems. The stresses on the outer strands of a conductor at the interface of conventional suspension clamps can be large enough to cause strand damage. The protection must be clamps with a sufficient radius for seating the conductors in terms of both radius and angle to minimize the stresses under this condition. CTC Global recommends AGS suspension clamps (or equivalent) and armor rods to help dissipate stress. When departure angles are substantial, the use of double suspension clamps with yoke plates is preferred. In some cases, it may be more preferable to use dead-end structures.

2.11. Long Span Considerations

The longest transmission line span in the world is the 132 kV Ameralik Fjord Crossing in Greenland at 5.374 km[83]. Long spans cause huge sags since sag varies with the square of the span length. To counter the large sag, tensions are typically as high as can be tolerated by the conductor strength, vibration mitigation technology, and local rules. Long spans challenge the engineering of installed conductors on strength and vibration concerns so these spans invariably use very strong conductors and employ careful and extensive vibration damping systems. A secondary concern is for multi-loop galloping.

Long spans are often wholly or partially very high above the ground. Spatially small gusty winds cannot load the span so the wind load must account for the extraordinary height above ground and also be limited to synoptic speeds. Ice loads may be severe but the likelihood of dropping large portions of ice all at once decreases with the span length.

Conventional steel-reinforced conductors often rely on the use of many more steel core strands to achieve the higher strength so that some of the large sag can

---

[83] Cigre Technical Brochure TB 396 Large Overhead Line Crossings WG B2.08 (October 2009)

be removed from the design. When the tensions are inordinately high, vibration will be enhanced and a vibration damping study is routinely necessary. The added steel content also adds weight. The use of ACCC conductor greatly reduces the overall conductor weight and extremely high tensile strengths can be achieved in relatively compact conductor designs.

2.12. Bundled Conductors

Bundled conductors are commonly used to increase electrical capacity and reduce corona and radio noise at voltages above 200 kV[84]. Though the extent of corona and radio noise is impacted by elevation (air density), and other factors such as conductor surface condition and moisture, the bundle dimensions are the primary factor in mitigating the onset of corona. While increased aluminum content serves to reduce line losses and increase power flow, increased diameter also increases the conductor's surface area. Bundling phase conductors can effectively do both with greater efficiency. Generally, bundled conductors are used at 200 kV or above and range from double bundled to six or even eight bundle designs.

American Electric Power (AEP), one of the first utilities in the US to build 765 kV lines currently uses a six bundle conductor design, while China has built 1,000 kV lines with 8 bundle conductors. Bundled ACCC conductors have been utilized on UHV transmission lines due to their high strength and improved conductivity.

2.12.1. Electrical Benefits

In addition to reducing corona, audible and radio noise (and associated electrical losses), bundled conductors also increase the amount of current that can be carried compared to a single conductor of equal aluminum content due to the skin effect (for AC lines). Bundled conductors also lower reactance and reduce voltage gradients.

2.12.2. Structural Impact

---

[84] EHV Transmission Line Reference Book. New York: Edison Electric Institute, 1968.

As discussed, large conductors adopt lower percentage tension increases than smaller diameter conductors when coated with the same radial thickness of ice. With ½" (12.7 mm) of radial ice applied, a pair of 1026 kcmil (1.1" or 28.14 mm diameter) ACCC Drake size conductors adopts 1 lb/ft (1.5 kg/m) of weight each (doubling their weight to 4 total pounds) while the closely equivalent 2004 kcmil (1.5" or 38.1 mm diameter) slightly less than 2 lbs/ft (3 kg/m) ACCC Berlin conductor adopts only 1.25 lb/ft (1.9 kg/m) for a total weight of 3.2 lbs (1.5 kg) - an increase of ~60%. The wind area of the Berlin ACCC conductor is about 70% of the pair of the Drake ACCC conductors.

As the number of sub-conductors increases (with comparable aluminum content to a single conductor), ice loads increase measurably. As the electrical attraction to a bundle with more sub-conductors increases, so increases the structural loads. If a small conductor has a greater difficulty supporting a large ice load than a large conductor, there is a sag cost associated with more subconductors as well. The cost-effectiveness of a bundle design and its component subconductors is a project-specific calculation.

2.12.3. Vibration in Bundled Conductors

Up-wind sub-conductors can create oscillation on down-wind sub-conductors by casting a wind shadow that is understood to affect the leeward sub-conductor up to 20 diameters away. Aeolian vibration (as discussed in Section 2.13) is generally less pronounced on bundled conductors due to the effect of spacers and/or spacer dampers installed at relatively close intervals along the line. As discussed in CIGRE TB 273[85], *increased tension* on bundled conductors appears to decrease their propensity for wake induced oscillation and galloping.

2.12.4. Short Circuit Events and Bundled Conductors

During short circuit events, an electromagnetic attraction between sub-conductors causes them to slap together, exerting compressive forces on spacers and spacer dampers, which induces bending stresses on the conductor at the interface of the spacers[86]. Conductor tension can also increase measurably (for

---

[85] Cigre Technical Brochure TB 273 (2005), "Overhead Conductor Safe Design Tension with Respect to Aeolian Vibrations", SC B2 TF B2.11.04

[86] Hanamuri, M., et al Mechanical characteristics related to fault currents in bundle conductors Electric Engineering in Japan Volume 113, Issue 6, pages 61-70 1993

a few milliseconds) on shorter spans. Spacers, and their attachment methods, must therefore consider these forces and be designed in such a way as to not damage the conductors or spacers. It is recommended that elastomeric-lined clamps on all spacers and spacer dampers be used. Armor rods can also provide additional protection.

At the exact location of a short circuit, a conductor's aluminum strand temperature can jump substantially and nearly instantaneously. While it generally takes time for a conductor's core's temperature to rise, the nearly instantaneous increase in strand temperature can cause localized birdcaging in the aluminum strands of any conductor type. While the ACCC conductor's core is much less thermally conductive than aluminum or steel, as with any conductor, in extreme cases a repair sleeve may be required to repair damaged strands. However, in most cases any birdcaging in the soft (previously annealed) aluminum strands will dissipate over a short period of time during thermal cycling. While the aluminum strands may loosen slightly for some period of time due to such an event, unlike non-annealed conductors, no loss of overall conductor strength or loss of core integrity will occur.

2.13. Aeolian Vibration

Aeolian vibration is a resonant phenomenon wherein a steady stream of wind blowing across a conductor causes eddies or vortices (Figure 32) on the downwind side of the conductor which break away in an alternating pattern (from the top to the bottom) and subsequently exerts a periodic force on the conductor that is determined by the velocity of the wind and the geometry of the conductor. When frequency of the wind-induced forces matches one of the natural frequencies of the conductor, resonant vibration occurs, causing the amplitude of that particular harmonic motion to grow and increased stress at the two ends of the conductor (i.e., conductor hanging points)[87].

---

[87] Hagedorn, P. and Karus, M. (1991). "Aeolian Vibrations: Wind Energy Input Evaluated from Measurement on An Energized Transmission Line", IEEE Tractions on Power Delivery, 6(3), 1264-1270
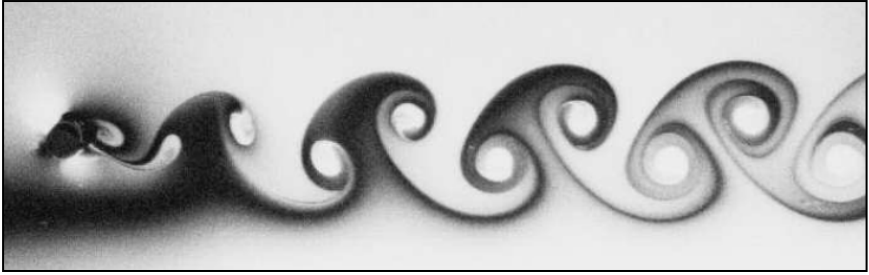
Figure 32 - Wind Induced Vortices

The amplitude or "anti-node" (height of the wave in Figure 33) and frequency (wave length or "loop length" between nodes) of the vibration depend upon the energy input from the wind - balanced against the self-damping characteristics of the conductor at a particular tension/condition.
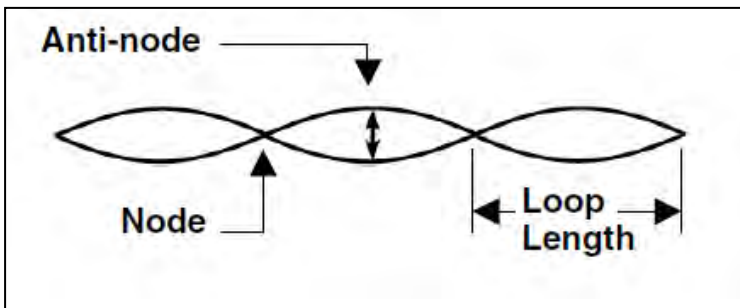
Figure 33 - Wind Induced Vibration

Aeolian vibration is typically between 8 to 60 Hz (from typical wind speeds of 3 to 25 km/hr), which occur almost exclusively in the vertical direction, and the amplitude is about one conductor diameter. Energy input from the wind grows with the diameter and length of the conductor. Large conductors in long spans receive more energy than smaller conductors on shorter spans. Vibration damping or energy dissipation is available in two forms: from the natural self-damping characteristics of the conductor itself, and supplementally, from special apparatus ("dampers") that can be attached to the conductor when the self-damping capabilities of the conductor are considered insufficient.

2.13.1. Impact of Aeolian Vibration

Aeolian Vibration in a conductor causes cyclic bending and tensile stresses that are two primary components of fatigue failure. These stresses have been studied extensively and, to some degree, correlated with field experiences in an effort to offer tensioning guidelines - *above which dampers may be required*. In addition to tensile and bending stresses, tight / highly compressed strands exacerbate the impact of inter-strand rubbing, particularly in round wire conductor designs, that can cause mechanical damage known as fretting. Looser (or trapezoidal-shaped) strands generally do not create high compressive forces that lead to strand fretting. Fatigue failure resulting from strand fretting is generally observed at the interface of suspension or other clamped-on devices where stresses are concentrated and compressive forces can be particularly high[88].

In addition to the mechanical damage to the strands caused by inter-strand rubbing when compressive forces are high, conventional compression fittings can also mechanically damage a conductor's strands by compressive deformation. From these mechanically damaged points, micro-fractures can develop. In the presence of cyclic mechanical stress, micro-fractures can propagate and lead to strand fatigue failure. While bending and tensile stresses in a conductor's strands can be minimized to some degree by decreased conductor tension, and/or the utilization of dampers which dissipate bending stresses, the use of AGS[89] (Armor Grip) suspension clamps (or equivalent) with armor rods will substantially prevent compressive strand deformation and reduce bending stress by as much as 60% (Figure 34).

---

[88] Fricke, Jr., W.G. and Rawlins, C.B., "The Importance of Fretting in Vibration Failure of Stranded Conductors", IEEE Trans. on Power Apparatus & Systems, Vol. PAS-87, No. 6, June 1968, pp. 1381-1384.
[89] PLP White paper "ARMOR-GRIP® Suspension - Still the Best After 56 Years" Preform Line Products White Paper
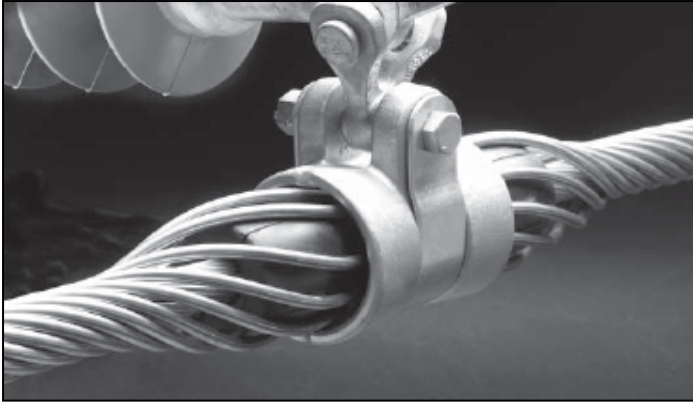
Figure 34 - AGS Suspension Clamp & Armor Rod

As stated above, the use of Armor Grip (AGS) Suspension clamps and armor rods (or equivalent) can reduce bending stress by as much as 60%. While these suspension clamps do not serve as mechanical dampers, the rubber grommet within them prevents compressive strand deformation, reduces strand fretting, and, with equal importance reduces bending stress at their interface where fatigue failure generally occurs[90].

Testing of ACCC conductors using the AGS units and armor rod has revealed no fatigue failure of the strands or composite core at over 100 million cycles of vibration *under high tensile load* and *at high amplitudes*[91]. Two such tests performed in association with American Electric Power (AEP) also included an additional 100 thousand cycles of galloping, with no breaks, cracks, failure, birdcaging, or discoloration (representative of degradation) observed[92]. The significance of these findings is discussed in more detail in Sections 2.13.3 to 2.13.5.

---

[90] P. R. Mehta, Preformed Line Products, Experimental Evaluation of Compressive Stresses in Stranded Conductors TR-551-E Oct 1969

[91] C.J. Pon, M.J. Kastelein, M. Colbert "Aeolian Vibration Test on 1572 kcmil "BITTERN" ACCC/TW Conductor" Kinectrics North America Inc. Report No.: K-422163-RC-0005-R00

[92] Zsolt, Ladin, Kastelein, Brown; SEQUENTIAL MECHANICAL TESTING OF 1020 KCMIL "DRAKE" ACCC/TW CONDUCTOR Kinectrics North America Inc. Report No.: K-419138-RC-0001-R00 December 2009

2.13.2. Aeolian Vibration & Industry Recommendations

For several decades, IEEE, CIGRE, EPRI and other entities such as Alcoa, have studied the impact of vibration on conventional all-aluminum or steel-reinforced bare overhead conductors. Many lab tests have been performed, bending amplitudes and stress levels characterized, and a number of transmission lines monitored over a period of decades. Based on the data gathered, various recommendations have been offered regarding acceptable limits of conductor tension in an effort to mitigate strand fatigue failure, as higher conductor tensions are generally associated with increased vibration amplitude and potentially higher bending stresses at the interface of suspension clamps.

In the early 1960's, CIGRE recommended that a maximum conductor tension of 18% of its Rated Tensile Strength (RTS) could be used as a conservative limit, above which they suggested dampers may be required[93]. The % RTS guideline was broadly accepted, not only as it related to minimizing the effects of Aeolian vibration, but also as it related to acceptable safety factors - should a conductor be exposed to heavy ice or wind load event. Such % RTS approaches are still in effect today. Specifically, the National Electric Safety Code (NESC)[94] states that maximum conductor tension should not exceed 60% RTS under the worst anticipated ice/wind load condition; nor should it exceed 25% RTS under "every day conditions" *after* an anticipated load event occurs. They further state that an initial stringing tension of 35% RTS is acceptable, assuming that appropriate consideration is given to mitigating vibration (through the use of dampers or other means). Different regions, countries and utilities utilize other rules, some of which allow the conductor to be loaded to as high as 90% RTS or more under extreme ice load conditions. More conservative limits are commonly imposed when warranted (such as over major roadways or in highly populated areas).

As described in CIGRE Technical Brochure 273[72], it was noted in the 1980's that 45% of the 40 (ACSR, AAC, AAAC, or ACAR) lines included in the study that were installed at tensions equal to or less than 18% RTS (without AGS suspension clamps or dampers) suffered some degree of strand fatigue failure after 20 years of service.   Unfortunately the extent of strand fatigue failure that

---

[93] Cigre Technical Brochure TB 273 (2005), "Overhead Conductor Safe Design Tension with Respect to Aeolian Vibrations", SC B2 TF B2.11.04

[94] National Electric Safety Code, 1997 Edition, C2-1997.

was observed, and the conditions that may have led to or prevented strand fatigue failure from occurring, was not clarified. In other words, any data about the load history of the conductor that could have relieved stress in the aluminum strands was not presented, nor was any additional data about specific environmental conditions, temperature, wind speed, etc. Nevertheless, a new recommendation or guideline for conductor tension, *above which dampers would be required*, was proposed.

The new guideline was based on the "Catenary Constant" *C,* which is essentially the tension of a conductor divided by its mass, in units of length (feet or meters). The CIGRE C value recommendations came with a caveat *"that they only apply to round wire designs (not trapezoidal strands) and only to conventional AAC, AAAC, ACSR and ACAR type conductors mounted in conventional suspension clamps*." The Catenary Constant guidelines therefore cannot be used solely to assess tension limits (above which dampers may be required) for modern conductors such as ACCC that have performance characteristics and strength to weight ratios that are substantially higher than all-aluminum or steel-reinforced round wire conductors. Nevertheless, it is useful to understand the differences between the % RTS and Catenary Constant guidelines.

In the ratio T/m, *T* is the conductor tension and *m* is mass per unit length, i.e. lbs/ft or kg/meter. In a span of conductor, the tension, *T* at the ends is slightly greater than the horizontal component, *H* of the tension that occurs at the low point of the span. Except for extraordinarily long or steep spans, T and H are very near equal and can therefore be considered same for practical purposes. Also, mass and weight are related by a constant (gravity) so unit weight can be substituted for unit mass. Thus, T/m can be labeled H/w, which is a combination of values also associated with sag equations. The ratio H/w is called the Catenary Constant *C* and has the unit of length in feet or meters.

Two conventional conductors: one weighing 1 lb/ft (1.5 kg/m) and the other 2 lbs/ft (3 kg/m) and strung to tensions of 5,000 lbf (22.2 kN) and 10,000 lbf (44.5 kN) respectively will have the same sag in the same span. A school of thought promoted since the early 1980s suggests (with some laboratory and field test confirmation of conventional conductors) that certain conventional conductors of different weights that are strung to common sags (or a common C value) will exhibit the same vibration intensity as each other. The suggestion (*to keep things simple)* was that a C value could be identified that could represent a rational

threshold of tension below which vibration damage *should* not occur without the use of dampers.

This is the premise and the suggestion presented in CIGRE TB 273. As CIGRE acknowledges, it should be noted that the vibration characteristics of trapezoidal-stranded conductors are different than those of round wire conductor designs. Additionally, ACCC conductors are substantially different than any other round or trapezoidal conductor designs due to their unique self-damping characteristics, dissimilar natural frequencies (between the composite core and aluminum strands - which resist resonant coupling), and bending amplitude (fatigue) limits.

Comparing two different conductor types with established matching C values (sag) does not produce equal % RTS results. Thus, the two vibration guidelines are different. This is not consistent with the understanding that wind energy input into a span (that must be dissipated) increases with span length. Alcoa has done considerable work on this subject for decades and offers additional insight. ACA offers a software program, VIBREC® that makes Alcoa damper recommendations. It includes defining the threshold above which dampers may be required. In other words, Alcoa makes a recommendation for the self-damping capabilities of many conventional conductor types. Studying Alcoa's recommendations allows comparison to CIGRE's simple Catenary Constant recommendations. They are very dissimilar as Figure 35 (with associated terrain category in Table 21) and Figure 36 illustrate.
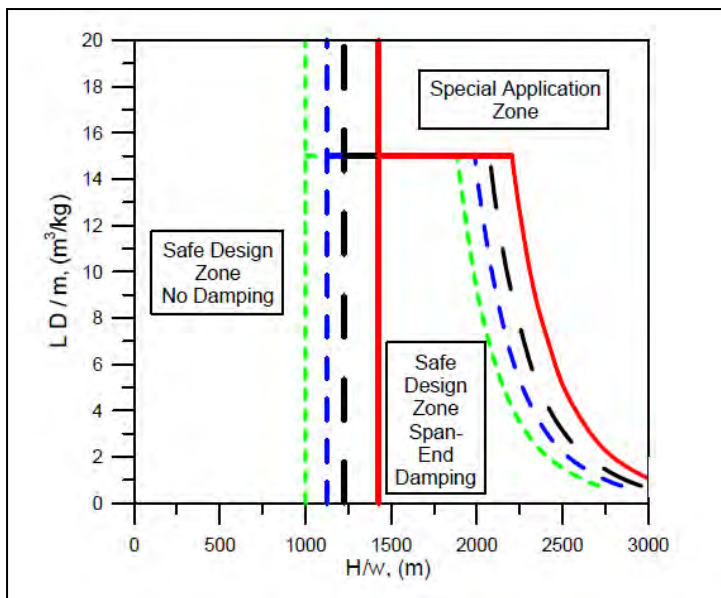
Figure 35 - Safe design tensions per CIGRE TB 293.

Terrain Category	
----- (green dashed)	#1 : Open, flat, no trees, no obstruction, with snow cover, or near/across large bodies of water or flat desert.
--- (blue dashed)	#2 : Open, flat, no obstruction, no snow; *e.g.* farmland without any obstruction, summer time.
--- (black dashed)	#3 : Open, flat, or undulating with very few obstacles, *e.g.* open grass of farmland with few trees, hedgerows and other barriers; prairie, tundra.
─── (red solid)	#4 : Built-up with some trees and buildings, *e.g.* residential suburbs; small towns; woodlands and shrubs. Small fields with bushes, trees and hedges.

Table 21 - CIGRE TB 293 terrain categories.

The Alcoa data points lie on rather discrete lines that curve downward from top-left to bottom right. This is a reflection of the knowledge that shorter spans can tolerate tighter tensions (higher C values) than longer spans. Close examination shows that the different sizes and types of conductors do not share the same

curves (limits). The green, dashed line box in Figure 32 defines the range of most typical use. LD/m values below 4.0 imply spans that are quite short and conductor C values above 7400 ft (2,250 m) imply designs that are getting very tight (LD/m is the ratio of the product of the span length *L* and the conductor diameter *D* to the conductor mass *m* per unit weight). Within this box, the data appears completely scattered either side of the CIGRE C limit of 4,600 ft (1,400 m) that is associated with the lowest of four wind exposure categories. On the face of it, the two systems seem to disagree radically.
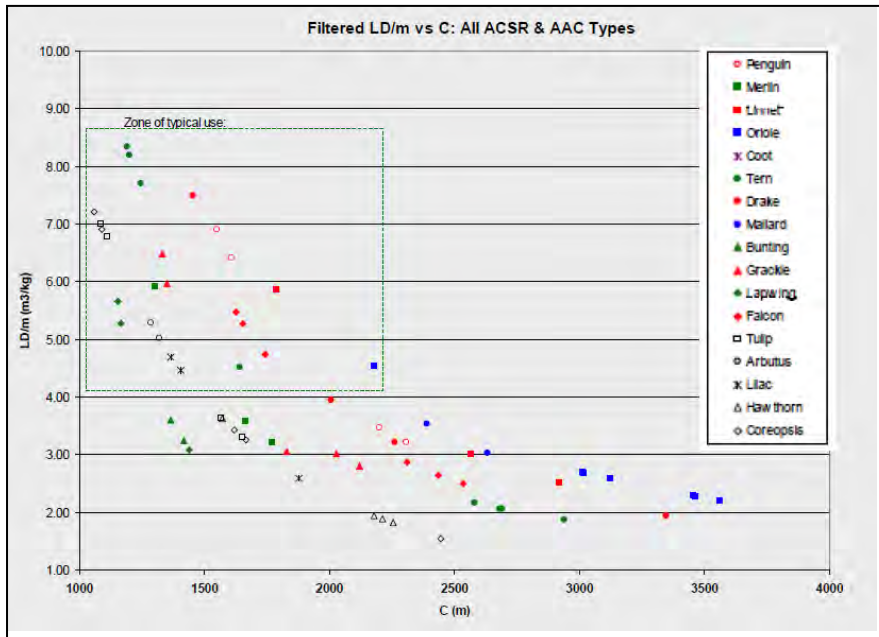
Figure 36 - Alcoa Safe Design Tension Data

Current CIGRE work is admittedly conservative, so that it can be employed world-wide without much concern for causing problems with conventional conductors mounted in conventional suspension clamps. The Alcoa method may be considered slightly less conservative, but it is also based on substantial experience. There are occasions (as with situations) that plot high in Figure 36 (long span designs) where Alcoa appears to recommend a C limit lower than CIGRE suggests. There are occasions as with certain conductor types and shorter spans where Alcoa suggests that the CIGRE limits can be exceeded.

111

There is an important point to make about damper recommendations. The threshold up to which a first damper is needed on a span of conductor is calculated differently by different damper manufacturers. They have chosen slightly different views of the subject and, at times, have been accused of seemingly been interested in selling dampers regardless of the span's conditions. They can rightly argue that their recommendations are being made in the absence of full knowledge of the line's exposure or anticipated load and in the absence of control over how their product is actually applied to the conductor, or knowledge of how quickly a conductor's strands will shift their load to the core reducing stress that is a primary component of fatigue failure.

In spite of varied damper recommendations, it seems logical, at a minimum, to select suspension clamps that offer the most conductor protection as most vibration damage occurs at the interface of suspension clamps. In addition to the use of dampers, as may be required, CTC Global strongly recommends the use of AGS suspension clamps and Armor Rod[95] or equivalent. When horizontal or vertical angles exceed 30 degrees, CTC Global also recommends the use of double AGS units (or equivalent) with a yoke plate (Figure 37). At angles above 50 to 60 degrees, CTC generally recommends the use of dead-end structures).

Figure 37 - Double AGS suspension clamp and armor rod.

---

[95] Whapham, B. ARMOR-GRIP® Suspension – Still the Best After 56 Years

While the Catenary Constant (H/w) and % RTS guidelines have been developed in an effort to simplify the determination of whether or not dampers should be used at some particular conductor tension (or catenary), a 2005 EPRI Report on "Updating the EPRI Transmission Line Reference Book: Wind-Induced Conductor Motion ('The Orange Book')" stated that "No satisfactory criterion is available yet to evaluate analytically the fatigue behavior of conductors from the fatigue properties of the materials used in their construction and the stresses that occur in them. *Thus, fatigue characteristics of conductors must be determined by fatigue tests of conductors themselves*. These tests should be performed on conductor-clamp systems reproducing as closely as possible the field loading conditions. In such tests, the fatigue life of the conductor must be determined as a function of some measure of vibration intensity, rather than of the stress or stress combination *that causes the failure,* since that stress is not accessible." [96]

2.13.3. ACCC Conductor and Aeolian Vibration

There are significant differences between ACCC conductor and conventional conductors in terms of vibration self-damping and strand fatigue resistance to Aeolian vibration. Since conductor core in bi-material conductors is rarely a fatigue damage concern, the conductor performance in Aeolian vibration relates to two key principals: a) the remnant vibration energy from wind that must be absorbed by the conductor strands, which is dependent on the energy input from wind (e.g., minimizing wind energy input) and the **self-damping** from the conductor system (e.g., maximizing self-damping from the conductor and damping from dampers); b) the capacity of the aluminum strands to absorb the remnant vibration energy without **fatigue** damage.

2.13.4. Self-Damping in ACCC Conductors

Self-damping tests were performed on numerous ACCC conductors. Comparison tests were also performed to establish base lines and offer perspective. ACCC Drake conductor (which uses annealed trapezoidal shaped strands) and ACSR Drake (hard aluminum - round strand design) conductors

---

[96] EPRI Progress Report on "Updating the EPRI Transmission Line Reference Book: Wind-Induced Conductor Motion ('The Orange Book')" 2005

were tested at Kinectrics Lab in Toronto[97]. Vibration testing was performed through a range of frequencies that reflect wind conditions ranging from 10 to 30 km/hr (~6 to 19 mph). The conductors were assessed at 15, 20, 25, 30, and 40% RTS. The results showed that under this variety of conductor tensions and varied frequencies representing varied wind speeds, the ACCC conductor dissipated vibration energy more effectively (as much as an order of magnitude better) than an ACSR conductor of the same diameter and weight. Figure 38, Figure 39 and Figure 40 are from that testing effort.
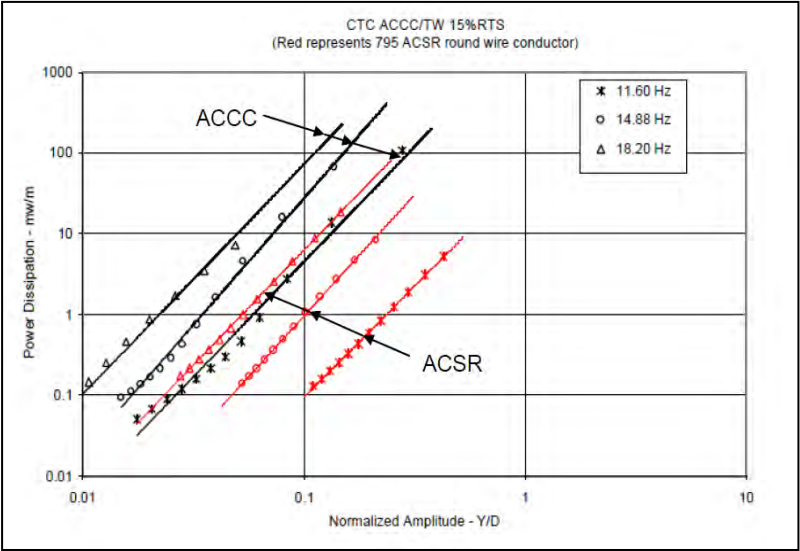
Figure 38 - Self damping comparison of ACSR and ACCC at 15% RTS.

---

[97] Pon, C; "Self Damping Test on 1020 kcmil ACCC/TW Conductor" Kinectrics North America Inc. Report No.: K-422024-RC-0008-R00 October 15, 2004
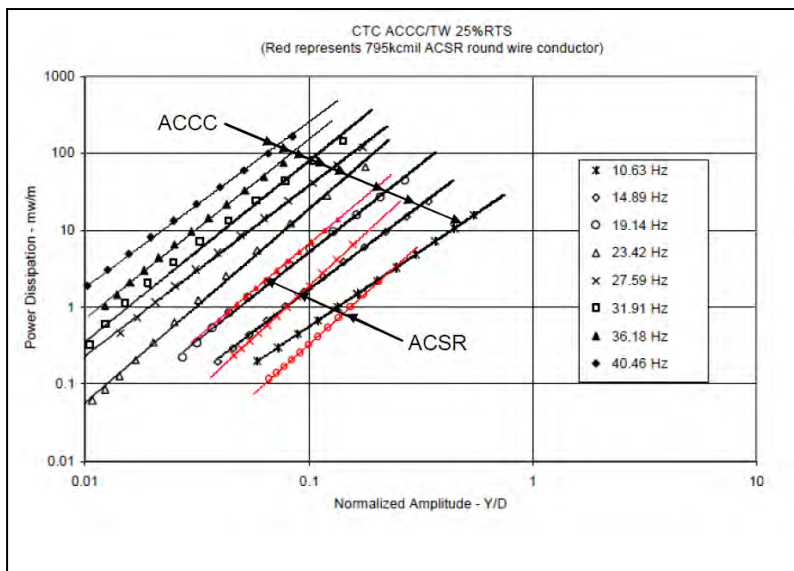
Figure 39 - Self damping comparison of ACSR and ACCC at 25% RTS.
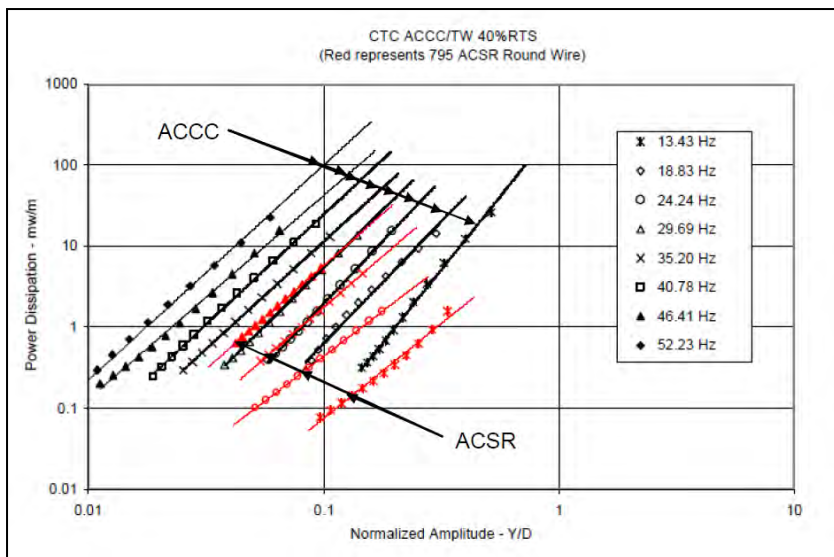
Figure 40 - Self damping comparison of ACSR and ACCC at 40% RTS. Notice the sharper slope in ACCC conductors toward higher amplitude.

In these tests, a new (un-aged) conductor was held at a constant tension in a temperature controlled room. On an actual span with sufficient time (hours to days), the natural relaxation of the aluminum strands would result in a modest reduction in conductor tension and a significant reduction in aluminum stress. These tests were performed with the target tension (% RTS) maintained throughout the tests. Although it is known that polymer matrix composites have better material damping properties, as reflected in their *Vibration Decay Loss Factor* (~ three to five times greater than that of steel[98] due in part to its lower modulus in resin matrix materials and the interaction between the microfibers and matrix within the core that converts kinetic energy into heat)[99], it is unlikely that this is principally responsible for the better self-damping in ACCC

---

[98] Michael C.Y. Niu; Aircraft Design Book Composite Airframe Structures – Practical Design information and Data

[99] Crane, Roger. David Taylor Research Center Characterization of the Vibration Damping Loss Factor of Glass and Graphite Fiber Composites, Composites Science and Technology 40 (1991) 355-375

conductors as higher conductor tension actually resulted in less effective overall self-damping.

2.13.5. ACCC Conductor Fatigue Resistance to Aeolian Vibration

While there is strong evidence that the natural self-damping capabilities of the ACCC conductors is extraordinarily good, self-damping tests do not necessarily address the issue of survivability of the aluminum strands against cyclic bending/tensile stress. It is one thing to predict or recognize the amount of vibration that a conductor will exhibit in a particular environment, but it is another thing to predict the material's ability to survive the action.

To empirically address this question, American Electric Power (AEP) developed a Sequential Mechanical Test[100], wherein several conductor types were pulled through a series of sheave wheels to replicate installation, tensioned to 20% RTS and subjected to 100 million cycles of vibration, followed by 100 thousand cycles of galloping. A ~45 ft (15 m) section of each "aged" conductor was then placed in a load frame and tensioned from 15 to 70 or 85% RTS five times. The conductors were then pulled to failure. After completing the test series, the conductors were carefully inspected. Both the ACSR and ACSS conductors showed signs of fretting and fatigue failure as evidenced in Figure 41 and Figure 42.

Neither the ACCC core nor its aluminum strands exhibited any sign of fatigue failure when supported by an AGS (cushioned) suspension clamp and armor rod. At 20% RTS, the tensile loads of the ACSR, ACSS, and ACCC conductors were 6,300 lbf (28.0 kN); 5,180 lbf (23.0 kN); and 8,220 lbf (36.6 kN), respectively (catenaries of 5,760 ft (1755 m), 4,740 (1444 m) and 7790 ft (2,370 m), respectively). In other words, the ACCC conductor was installed at a tension that was 60% higher than the ACSS round wire conductor (that also uses fully annealed aluminum strands) and saw no fatigue failure. The respective stress in the aluminum strands are shown in Table 22 and are calculated from the known stress-strain curves of these tested conductors.

---

[100] Freimark, B., et al, Sequential Mechanical Testing of Conductor Designs 2009 Electrical Transmission and Substation Structures Conference Technology for the Next Generation November 8-12, 2009 Ft. Worth, Texas, USA
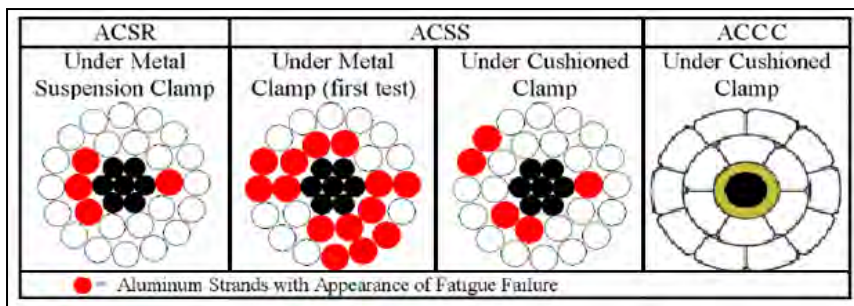
Figure 41 - Fatigue Failure Comparison ACSR, ACSS, ACCC

Figure 42 - Strand fretting and fatigue failure of round stranded ACSS Conductor

Test Condition	Conductor Type:	ACSR	ACSS	ACCC®
20% RTS; 0.5 dia Y/D; ~29.5 Hz	Conductor Tension, lbf (kN)	6,300 (28.0)	5,180 (23.0)	8,220 (36.6)
	Catenary Constant ©, ft (m)	5,700 (1,760)	4,730 (1,440)	7,810 (2,380)
	Aluminum Stress, ksi (Mpa)	4.6 (32)	4.0 (28)	4.1 (29)

Table 22 - Stress in Aluminum Strands during AEP Aeolian Vibration Tests

As Table 22 shows, while the tension in the ACCC conductor was higher, the stress in the aluminum strands for all conductors was nearly the same. The higher catenary (and substantially higher conductor tension) that the ACCC conductor was tested at did not affect the fatigue life of its aluminum strands.

Following the Sequential Mechanical Test (performed at Kinectrics' Lab in Toronto), AEP cut the tested ACCC conductor core into approximately 30, 3

118

feet (1 m) long samples and shipped them to their in-house lab in Dolan, Ohio. While approximately four one (1) meter long core samples were severely stressed from the "pull-to-failure" test at Kinectrics (when the core section broke at approximately 102% RTS), the core samples directly adjacent to the tensile failure zone still exhibited over 100% RTS during subsequent testing. This was considered fairly remarkable considering the arduous test protocol and the fact that the adjacent core samples has seen an instantaneous 35,000 lbf (155.6 kN) drop in tension and associated shockwave.

One of the core samples from the initial protocol (that was not included in the load frame portion of the test) was tensioned to 50% of its rated strength and cycled 25 times to 95% RTS. It subsequently pulled to failure at 104% of its rated strength. This was after putting that piece of conductor through the sheave test series, 100 thousand cycles of galloping and 100 million cycles of vibration. The vibration frequency of the conductor test was targeted at 29.5 Hz which would correspond to the frequency produced by a wind of 4.5 m/sec or 14.8 ft/sec (~10 mph). The peak-to-peak anti-node amplitude was 14.07 mm (0.554 inch) which was equivalent to one-half of the conductor's diameter. Data from the complete test protocol for the ACCC conductor was summarized in a joint AEP / CTC Report[101].

Standardized Aeolian Vibration tests generally aim for peak amplitude of one-third of the conductor's diameter[102], so the AEP test was considered to be relatively severe. The factor fy_{max}, that appears in the vibration equations for these tests was on average equal to 29.5 Hz for each conductor times one half of the peak-to-peak amplitude, 0.277 in. (7.035 mm), giving 8.14 in./s (207 mm/s). This value of fy_{max} is in excess of what the endurance limit is considered to be for ACSR conductor which is 4.6 in/s (118 mm/s)[103] and the maximum allowed bending stress (σ_a) for the top surface of an aluminum strand for ACSR is considered to be 1.2 ksi (8.5 MPa).

---

[101] Bryant, D; Engdahl, E; Pon, C. ACCC Conductor Combined Cyclic Load Test Report American Electric Power & CTC Global January 2009

[102] CIGRÉ Study Committee 22, Working Group 04, "Recommendations for the Evaluation of the Lifetime of Transmission Line Conductors", Electra No. 63, March 1979, pp. 103-145.

[103] EPRI Transmission Line Reference Book: Wind-Induced Conductor Motion (Nov 2006)

$$\sigma_a = \pi d E_a \sqrt{\frac{m}{EI}} f y_{maz} \qquad (2\text{-}22)$$

In this test value of fy_{max}, the value for σ_a would have been about 3.2 ksi (22 MPa), which is also in excess of the recommended allowable bending stress. While these values are considered conservative limits, the ACSR and ACSS round wire conductors showed numerous aluminum strand failures, even when an AGS clamp was installed on the ACSS conductor.

For ACCC Drake size conductor, the frequency was tuned to 31.13 Hz, giving a fy_{max} of 8.6 in/s (218 mm/s). Therefore, from the equation above, the theoretical σ_a is about 4.4 ksi (30 MPa). This result also gives a value for the peak-to-peak bending amplitude Y_b measured at 3.5 in. (89 m) from the first point of contact with the suspension clamp of 31 mils (0.79 mm). Referencing equation 3.2-15 in EPRI Transmission Line Reference Book on Wind-Induced Conductor Motion, this is much higher than the 9 mils (0.22 mm) recommendation for the ACSR Drake at its testing tensions.

2.14. Fundamental Analysis of ACCC Conductor Vibration

The following section will review and discuss fundamental aspects and experimental vibration test data on ACCC conductors, and provide design recommendations for leveraging ACCC unique characteristics to mitigate the potential impact of Aeolian Vibration.

2.14.1. Resonance and Self Damping in ACCC Conductors

When a conductor is exposed to wind, the shedding of vortices produces an alternating pressure difference that causes the conductor to move up and down at right angles to the direction of air flow. When the shedding frequency becomes almost equal to one of the frequencies of the conductor, a 'lock-in' phenomena takes place and the conductor response to the vortex induced alternating force become enhanced. This increases the amplitude of the

oscillation until the damping power equals the input power to the conductor and the limiting amplitude of roughly one conductor diameter is reached[104-105].

In the lock-in range where wind energy input to the conductor is maximum, the vortex shedding frequency coincides with the conductor natural frequency.

- The vortex shedding frequency 'f' is given by the Strouhal number (S), conductor diameter (D_{cyl}) and normal wind speed (V): $f = S\ V/D_{cyl}$.
- The wind energy input relates to the vibration frequency by:

$$(P'_w)_{cyl} = P\left(\frac{A}{D_{cyl}}, V_r\right) D_{cyl}^4 f^3$$

(2-23)

- Assuming a cohesive solid for the conductor, its natural frequency can be calculated as:

$$f_r = \frac{r}{2L}\sqrt{\frac{T}{m} + \left(\frac{r\pi}{L}\right)^2 \frac{EI}{m}}$$

(2-24)

where the second term is typically negligible[106].

It should be noted that the aluminum strands and the conductor core are not 'tightly bonded/fastened' together as a cohesive structure such that all the constituent components have to move in unison (e.g., individual aluminum strands can slip against each other, independently of the core, to provide damping). Incidentally, steel and aluminum have almost identical specific modulus (E/ρ) and similar T/m. This makes it possible for bi-metallic ACSR or ACSS conductors to exhibit coherent resonant vibration among all of their constituent components. This unique situation makes it easier for the wind to lock into resonant frequencies of all constituent components (i.e., the core and

---

[104] Harvard, DG et al., Aeolian vibration excitation of bundled conductors, Vol I and II, CEA 177 T50, March 1989.

[105] Vecchiarelli, J., Aeolian Vibration of a Conductor with a Stockbridge-type Damper, PHD Thesis, University of Toronto, 1997.

[106] DIANA, G. & FALCO, M. 1971 On the forces transmitted to a vibrating cylinder by a blowing fluid,
Meccanica 6, 9-22.

all the aluminum strands) in ACSS and ACSR conductors for maximum impartation of wind energy to these conductors.

In ACCC conductors, the specific modulus for the composite core is almost 2X that of aluminum. This makes it less likely for wind to lock in to resonant frequencies of both the core and the aluminum strands at the same time, potentially limiting the wind energy imparted onto the conductor during lock-in and conductor oscillation.

In order to assess a conductor's resistance to fatigue failure from Aeolian vibration, one must understand and evaluate a conductor's self-damping characteristics. When a conductor oscillates, there is material damping associated with micromechanical cyclic stretching at the microscopic level (especially with low elasticity materials such as the resin matrix in ACCC core). However, the frictional force from the relative motion of conductor strands slipping against each other provides the principal self-damping mechanism[107]. The vibration induced cyclic stress is responsible for the creation and propagation of fretting fatigue cracks. Although the initiation and propagation of fretting cracks contribute to the energy absorption in vibration damping, it also leads to fatigue damage in the aluminum strands in conductors, especially adjacent to or within clamp assemblies where compressive forces can exacerbate geometric deformation and create higher stress concentrations. One needs to understand and minimize the remnant energy (after self-damping) from wind on the conductor that can be absorbed by the aluminum strands in the process of fretting fatigue.

High conductor tension typically results in less effective self-damping. As conductor tension increases, the helical wound strands tend to lock down, resulting in reduced slippage. As a result, conductor self-damping decreases and the severity of Aeolian vibration increases, thereby increasing the risk for fatigue damage.[108] It is for this reason that tensions of un-damped conventional conductors are kept relatively low. The Kinectrics test data (summarized in Table 23) clearly demonstrate that ACCC conductors have the potential to be used at much high tension levels (or catenaries) as ACCC conductors at 30%

---

[107] Rawlins, CB., Flexural self-damping in overhead electrical transmission conductors, Sound and Vibration 323 (2009), 232-256.

[108] Fadel AA. Et al., Effect of high mean tensile stress on the fretting fatigue life of an Ibis steel reinforced aluminum conductor, International J. of Fatigue, (2011). In press.

RTS load still exhibit very good and comparable power dissipation as that of ACSR conductors at only 15% RTS load. Unlike ACSR conductors where self-damping, as measured by power dissipation, precipitously drops from 8 mw/m (at 15% RTS tension) down to 0.5 mw/m at 25% RTS tension, the ACCC conductor under 40% load still exhibits good self-damping (power dissipation of 3 mw/m). ACCC conductor also seemed to be more effective in damping the more dangerous high amplitude vibrations at 40% RTS than the ACSR conductor. A 2005 study by FCI in France drew a simple conclusion by stating that "the ACCC conductors' superior self-damping characteristics will limit the need for damping hardware based on their testing"[109].

---

[109] Lombard, R., Hamilton, D., Lievin, A.; Self Damping Analysis ACCC Drake Diameter 28.14 mm per IEEE 664 Cigre SC N°22 and IEEE – Electra N°62 FCI TD 000429 January 2005

Test Condition	Conductor Type	ACSR	ACCC
15% RTS; 0.1 Y/D; 18.24 Hz	Tension (lbs)	4725	6165
	Cat Constant (ft)	4319	5860
	Al Stress (ksi)	3.34	3.03
	Power Dissipation (mw/m)	8	80
25% RTS; 0.1 Y/D; 19.14 Hz	Tension (lbs)	7875	10275
	Cat Constant (ft)	7198	9767
	Al Stress (ksi)	4.59	5.15
	Power Dissipation (mw/m)	0.5	8
30% RTS; 0.1 Y/D; 21.1 Hz	Tension (lbs)	9450	12330
	Cat Constant (ft)	8638	11721
	Al Stress (ksi)	5.57	6.01
	Power Dissipation (mw/m)		7
40% RTS; 24.2 Hz	Tension (lbs)	12600	16440
	Cat Constant (ft)	11517	15627
	Al Stress (ksi)	7.51	6.60
0.1 Y/D	Power Dissipation (mw/m)	0.6	3
0.2 Y/D	Power Dissipation (mw/m)	1	10

Table 23 - Effect of Conductor Tensions (various % RTS) on vibration power dissipation for the respective conductors. ACCC has much better self-damping than ACSR across the test regime.

The superior self-damping in ACCC conductors is partially attributable to the extensive frictional damping associated with high density packing of TW strands (where the TW strands make contact over a wider area than the very small contact area provided by round wires.[110]

Another important reason for the superior self damping performance in ACCC conductors relates to the relatively loose strands of 1350-O aluminum. Claren

---

[110] K. Munaswamy and Asim Haldar, Self-Damping Measurements of Conductors with Circular and Trapezoidal Wires, IEEE Transactions on Power Delivery, Vol. 15, No. 2, April 2000, pp 604-609.

and Diana[111] suggested that tension in the aluminum strands could be an important parameter. Harsanyi[112] has argued that a common error is to ignore the effect of aluminum strand tension on the damping properties of the conductor, because the power dissipation in the core is negligible compared to the power dissipation in the aluminum strands and damping is more affected by the tension in aluminum than the tension in the conductor. For ACSR conductors, Harsanyi experimentally determined that the power dissipation in ACSR Drake conductor is inversely proportional to $\sigma_{Al}^{0.3}$ (σ_{Al} is the tensile stress in aluminum), and lower tensile stress in aluminum should be beneficial for conductor self-damping.

Table 23 includes the initial aluminum stress at the various tension levels for ACSR and ACCC Drake conductors, calculated using PLS-CADD™. The 1350-O aluminum has low yield strength of about 4 ksi, significantly below some values of the Al stress levels calculated. It is highly likely that the aluminum strands are experiencing creep while the tension is maintained during vibration testing, as shown in Figure 43 and Figure 44. The extent of stress relaxation in 1350-O TW strands are time dependent, and further improved self-damping could be expected on ACCC conductors if it is 'aged' in the laboratory under the test tension conditions (to allow for complete relaxation) for several hours before vibration damping test.

- Stress relaxation in aluminum strands allows the ACCC carbon fiber core to carry more load, and it also moderates the compressive stress at the contacting surface of aluminum strands that facilitates highly effective damping strand slip/sliding motion (i.e., kinetic energy dissipation) without creating excessive shear stress that could lead to fretting cracks. The self-damping characteristics of a conductor are typically highest when its strands are relatively loose.

- As conductor tensions rise (during cold ambient conditions, for instance) the self-damping capability can diminish to some degree

---

[111] Claren, R and Diana, G, Dynamic strain distribution on loaded stranded cables, IEEE Transaction, Vol. PAS 88 (11), 1969, pp. 1678-1690.

[112] Adam Harris-Harsanyi, Temperature Effects on the Aeolian Vibration of High Tension Transmission Lines, PHD Thesis, Tulane University, 1973.

as the strands lock tightly down onto each other in conventional conductors.

- Strands of a conductor operated at higher temperatures (above the thermal knee-point) tend to relax as a result of the dissimilarities of coefficients of thermal expansion between the core and aluminum strands. Temperature effects on damping, other than those caused by redistribution of the loads between the aluminum and the steel strands, were not observed by Harsanyi.

- An 'aged' conductor whose aluminum strands have loosened over time due to an ice, wind, or extreme cold temperature event (or intentional pre-tensioning), will typically exhibit better self damping characteristics than a conductor that has not experienced such strand loosening[113]. The experimental data in Figure 43 and Figure 44 demonstrate that ACCC conductors do not have to rely on the 'aging' event to exhibit excellent self-damping, as required in ACSR conductors.
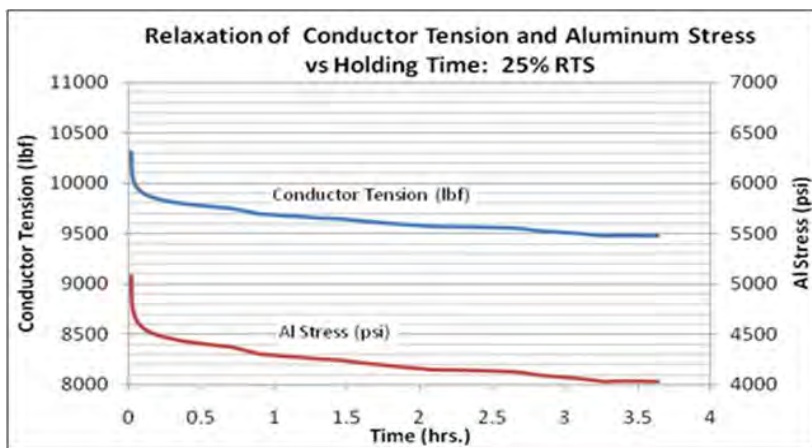
Figure 43 - Relaxation of Conductor tension and tensile stress in aluminum strands in ACCC Conductors at 25% RTS. The Aluminum strands might be initially loaded

---

[113] Rawlins, C.B., "Fatigue of Overhead Conductors", Chapter 2 of "Wind-Induced Conductor Motion", EPRI Transmission Line Reference Book, Electric Power Research Institute, Palo Alto, California, 1979.

above its yield strength (4 ksi), but creep in aluminum strands quickly (within hours) relieves its tensile stress level to that of its yield strength.
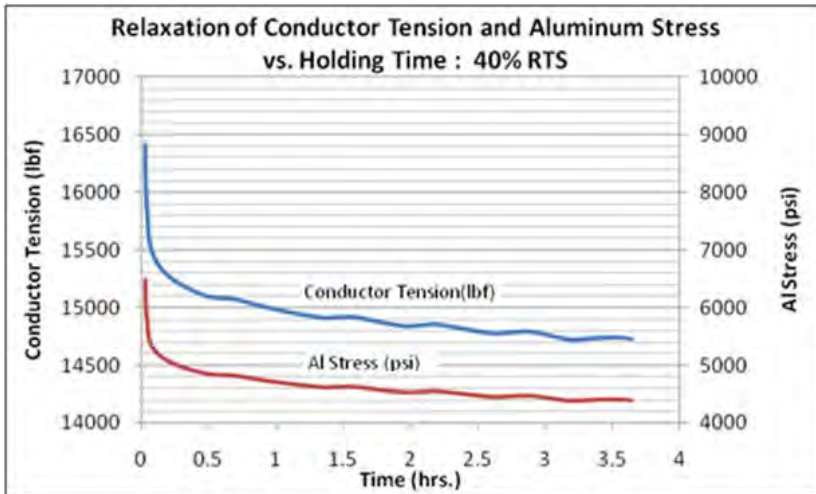
Figure 44 - Relaxation of Conductor tension and tensile stress in aluminum strands in ACCC Conductors at 40% RTS. The Aluminum strands might be initially loaded above its yield strength (4 ksi), but creep in aluminum strands quickly (within hours) relieves its tensile stress level to that of its yield strength.

Superior self-damping coupled with a lack of cohesive resonance coupling between its aluminum strands and the composite core keeps the remnant energy (which must be absorbed through damaging initiation and growth of fretting cracks in aluminum strands) from wind to a minimum in ACCC conductors. This makes it possible for ACCC conductors to be highly tensioned without compromising the self-damping of its aluminum strands, by leveraging the tension drop in 1350-O aluminum as a result of its low yield strength and creep. The creep in Aluminum does not create risk and lead to higher sag because the elastic composite core controls and completely mitigates the impact of aluminum creep on conductor design sag.

The diminished remnant wind energy in the conductor reduces the need for the aluminum strands (especially those constrained under clamps) to experience fretting crack formation and propagation (i.e., fatigue failure). Conductors whose strands have loosened show *reduced stress in the aluminum strands*. The

significance of reduced stress in aluminum strands is further discussed in detail below.

2.14.2. Managing Fretting Fatigue in Aluminum Strands

Conventional round conductor strands cross in relatively small elliptical areas. Trapezoidal conductor strands generally offer a wider contact area which reduces stress concentration and strand fretting (Figure 45). Increased contact surface area of trapezoidal shaped strands serves to improve self damping characteristics by increasing the contact area and reduce contact stress between the strands[86]. Conductor strand fatigue failure under clamps is a classical high cycle fatigue (low amplitude), complicated by fretting between strands or strand and clamp (Figure 46). Studies of fretting fatigue in overhead conductors have been mostly limited to ACSR type of conductor with less focus on the effect of the type of aluminum strands (TW or alloy type) used.[82,84,85,93,114,115,116]
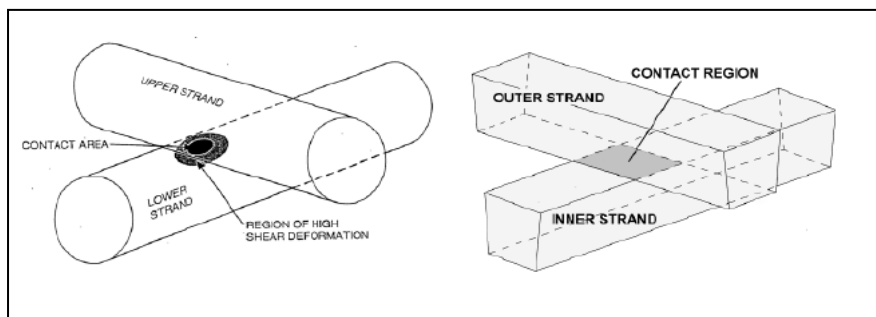
Figure 45 - Contact Differences between Round & Trapezoidal Strands

[114] Levesque F. et al., Finite element model of the contact between a vibrating conductor and a suspension clamp, Tribology International, 44 (2011) 1014-1023.

[115] Zhou ZR et al., Single wire fretting fatigue tests for electrical conductor bending fatigue evaluation, Wear 181-183 (1995) 537-543.

[116] Zhou ZR et al., Fundamental investigation of electrical conductor fretting fatigue, Tribology International, 29 (3) (1996) 221-232.
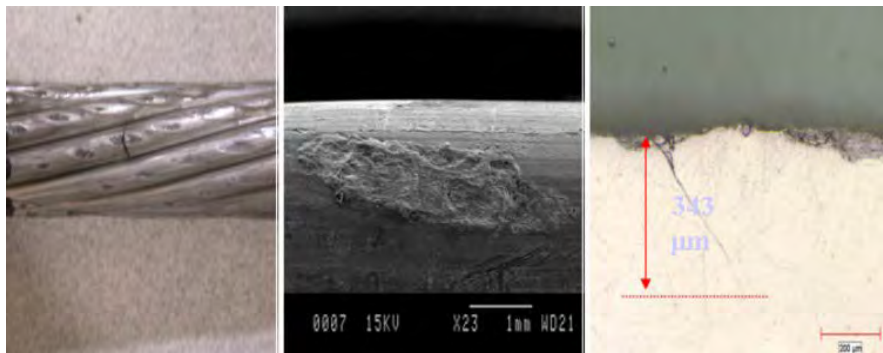
Figure 46 - Images of strand fretting and micro-fracture propagation in aluminum strands of ACSR conductor[117]

The aviation industry is one area in which fretting failure is often observed. Fretting fatigue in aerospace aluminum structures can be safety critical, and has

---

[117] Cloutier, L. and Leblond, A., Fatigue Endurance capability of Conductor/Clamp Systems Update of Present Knowledge, Technical Brochure presentation to SC B2, Helsinki, July 2007.

been extensively studied. [118,119,120,121,122,123,124,125,126] Although none of the aerospace research covered aluminum materials used for conductor applications, many varieties of aluminum alloys have been experimentally studied and modeled, and the principals and understanding are quite applicable for understanding aluminum fretting fatigue in overhead conductors.

Fretting can be described as a combination of three processes: wear, corrosion and fatigue with fatigue being the principal process. Fretting occurs between two contacting surfaces subjected to a relative motion of small magnitude (such as vibration), through the process of adhesive contact of asperities on contacting surfaces, that results in formation of debris or breaks of oxide layer on the material. Fretting can nucleate fatigue cracks at very low stress. Maximum reduction in fatigue strength occurs when the fretting process and cyclic stress are applied together.

The major parameters in fretting fatigue include: Cyclic Stress (i.e., cyclic fatigue load); Normal Force, Tangential Contact Stress & Stress Distribution; Slip Amplitude; Number of Fretting Cycles; Geometry, Contact Condition,

---

[118] Dowling, NE et al., Strain based fatigue for high strength aluminum alloys, American Helicopter Society 65th Annual Forum, Grapevine, Texas, May 27-29, 2009.

[119] Scott-Emuakpor, OE, Development of a Novel Energy Based Method for Multi-Axial Fatigue Strength Assessment, PHD Thesis, The Ohio State University, 2007.

[120] Munoz, S. et al., Prediction of the crack extension under fretting wear loading conditions, International Journal of Fatigue, 28 (2006) 1769-1779.

[121] Barrois, W., Repeated plastic deformation as a cause of mechanical surface damage in fatigue, wear, fretting-fatigue, and rolling fatigue, International Journal of Fatigue (1979) pp 167-188.

[122] Shah, AH, The Effect of Fretting on Fatigue Characteristics of a Mechanically Fastened Aircraft Joints, PHD Thesis, University of Utah, 2002.

[123] Shinde, SR, A Study of Fretting Fatigue Damage Transition to Cracking in 7075-T6 Aluminum Alloy, PHD Thesis, University of Utah, 2005.

[124] Navarro C. et al., On the use of multiaxial fatigue criteria for fretting fatigue life assessment, International Journal of Fatigue, 30 (2008) 32-44.

[125] Smith KN et al., A stress-strain function for fatigue of metals, J. Mater, JMSLA 1970 (5) 767-778.

[126] Araujo JA et al., The effect of rapidly varying contact stress fields on fretting fatigue, International Journal of Fatigue, 24 (2002) 763-775.

Surface Roughness and Friction Characteristics;[127] Materials (e.g., hardness) and Microstructure;[128] and Environment[129,130,131]. Depending upon the magnitude of the normal force and the displacement, there are three characteristic fretting regimes: partial slip regime (i.e., stick regime as in contact points between outer layer and clamp and wire-wire contacts in a conductor where relatively high normal load is present); slip regime (i.e., high relative slip at contact points with lower normal load such as outside of clamp zone); and mixed fretting regime. Unlike the stick regime *(requiring large number cycles to initiate fretting crack)* or the slip regime *(little consequence in terms of crack initiation despite severe worn 'bath tub' appearance because the wearing process removes the fretting cracks and the normal stress exerted by contact also diminishes when the 'bath tub' depth below surface increases),* mixed fretting regime is the most critical regime in terms of crack initiation,[93,132,133,134] where small discontinuities are nucleated at points of high stress concentration near contacting asperities in the boundary between slip and nonslip areas in the contact region (Figure 47).

[127] Proudhon, H et al., A fretting crack initiation prediction taking into account the surface roughness and the crack nucleation process volume, International Journal of Fatigue, 27 (2005) 569-579.

[128] Ambrico, JM et al., The role of macroscopic plastic deformation in fretting fatigue life prediction, International Journal of Fatigue, 23 (2001) 121-128.

[129] Poon, CJ., Environmental Effects on the Mechanism of Fretting Fatigue in 7075-T6 Aluminum, PHD Thesis, University of Missouri.

[130] Voris, HC., The Effect of a High Humidity Environment on the Fatigue Life of Aluminum Alloy 2024-T351, MS Thesis, CSU Long Beach, 1988.

[131] King, WG, Critical Corrosion Pit Depth for Fatigue Crack initiation in 2024-T3, 6061-T6 and 7075-T6 Aluminum Alloys, MS Thesis, Oklahoma State University, 2006.

[132] Blanchard P. et al., Materials effects in fretting wear: application to iron, titanium and aluminum alloys, Met Transaction A, 22A (1991) 1535-1544.

[133] Farcy L. et al., Factors of crack initiation and microcrack propagation in aluminum lithium 2091 and in aluminum 2024, Journal of Physics, C3 48 (9) 1987.

[134] Hoeppner, DW and Uhlig, HH., Fretting, cavitation and rolling contact fatigue – critical introduction' corrosion fatigue: chemistry, mechanics and microstructure, NACE-2 conference, June 14, 1971.
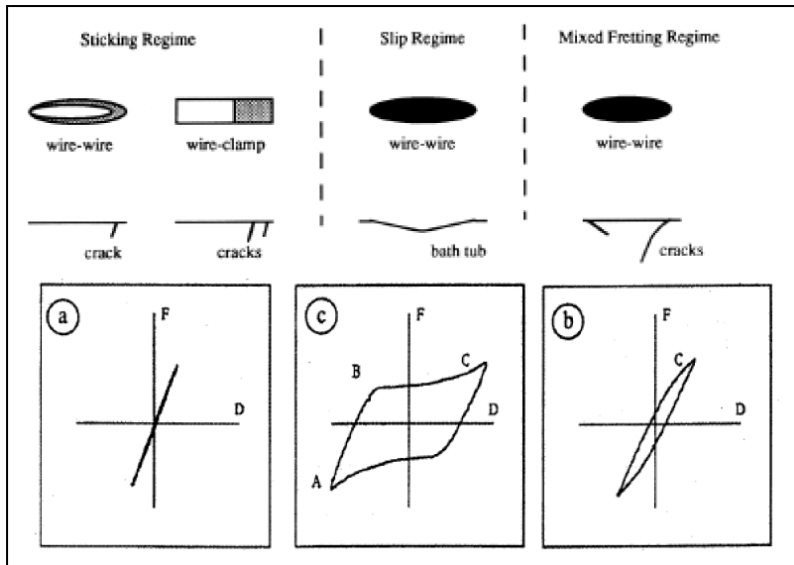
Figure 47 - Three regimes in fretting.

The steps in fretting fatigue are illustrated in Figure 48. Fatigue life is the total number of cycles to failure, and may be considered as the sum of the numbers of cycles for crack nucleation (i.e., resistance to fretting crack initiation in stage I) and the number of cycles for crack propagation (i.e., resistance to fretting crack growth in stage II). In low stress high cycle fatigue, a large portion of the life is consumed in crack initiation. However, the presence of fretting (surface damage and surface/sub-surface stress) significantly reduces the endurance limit and fatigue life due to the relatively rapid crack initiation in aluminum alloys with fretting.
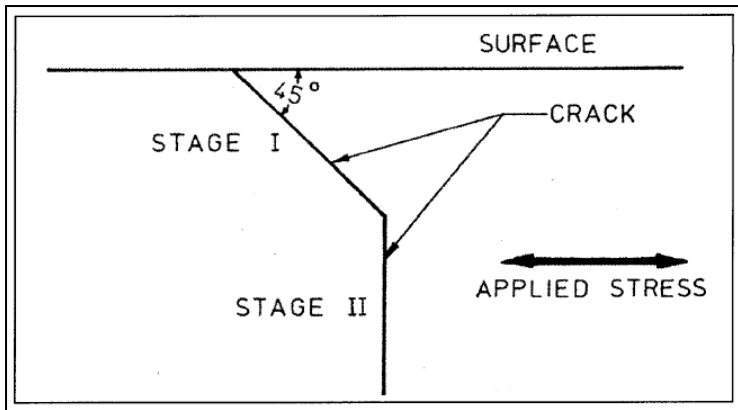
Figure 48 - Stages I and II during fatigue crack growth. Stage I growth is related to fretting crack initiation and the (small) crack growth occurs along the maximum shear direction (45°), which typically extends to about 0.1 to 0.5 mm for aluminum alloys; Stage II growth occurs perpendicular to the applied stress.[135]

<u>Fretting Crack Initiation & Growth (Stage I):</u>

- 1st few fretting cycles involves gross slip of surface oxide layer → oxide removal
- The fresh materials (after oxide removal) begins to stick together → reducing slip displacement and accommodating slip elastically
- Sticking + fretting displacement → induces high **shear stress** in the materials due to the normal and tangential forces at the contact area:

  o High shear stress at surface asperity (especially at small contact area).
  o High shear stress → dislocations move along the preferred slip plane in Aluminum; → Sub-surface material under high strain → plastic deformation → increased dislocation density and work hardening.
  o There is a 'fretting damage threshold' observed for aerospace aluminum alloys, below which irreversible fretting damage does not occur. This suggests that a minimum amount of

---

[135] Waterhouse RB, Fretting Fatigue, Applied Science Publishers, Essex, UK, 1981.

fretting damage is required before any reduction in fatigue life.[136][137][138]

For example, for 7075-T6 alloy under maximum fatigue stress of 20 ksi, the first 20-30% of fatigue cycles are said to be fretting fatigue threshold.

- ▪ Higher stress level might transition the fatigue from high cycle to low cycle where no fretting damage threshold was observed.
- • Formation of multiple fretting cracks. Time to initiate fretting cracks depends on material toughness and rate of cyclic strain hardening.
  - o The critical tangential load (related to shear stress) for fretting crack nucleation is the load that makes the first crack to appear, which depends on the normal load to the contact area as well as its frictional characteristics.
  - o Growth of these fretting cracks is driven by the shear stress, and fretting cracks may be arrested at certain depth as the shear stress decrease with distance from fretting surfaces. Higher shear stress (from high tangential load) causes longer fretting cracks as the shear stress level needed for propagation of the small fretting cracks is preserved deeper under the surface.
  - o These fretting cracks are relatively small (in the range of grain size or less), and they tend to grow along slip band at a constant rate until it reaches an obstacle that forces it to stop or change direction, and the crack can continue to grow if there is another slip direction it can easily change to.
- • Fretting cracks may also be driven to grow by the continued cyclic tensile stress, and propagate along the slip bands which are at 45° to the tensile axis, thus also planes of maximum shear stress. This is known as the fretting fatigue growth in stage I.
  - o One fretting crack near the stick-slip boundary of the trailing edge of the fretting region will typically grow into the dominant fatigue crack for Stage II.

[136] Hoeppner, DW and Goss GL, A fretting fatigue damage threshold concept, Wear, 27 (1974) 61-70.

[137] Adibnazari S and Hoeppner D, Characteristics of the fretting fatigue damage threshold, Wear 159 (1992) 43-46

[138] Sato K, Damage formation during fretting fatigue, Wear 125 (1988) 163-174.

- o Fretting also causes wear of the surface which competes with crack growth. If the wear rate is higher than the crack growth rate, the initial crack will be eliminated and thus fatigue failure will be delayed (as in the slip regime discussed above).
  - o When cracks in Stage I reaches a critical length, the crack driving force is high enough that the crack is no longer retarded by microstructural obstacles, and the crack growth transitions into Stage II.
- Fretting primarily affects the crack initiation and short crack growth as in Stage I. Fretting was found to contribute about only 10-13% of overall fatigue life (due to rapid crack initiation under fretting). Alloys most affected are those with best S-N fatigue strength as their superior resistance to crack initiation is negated by fretting.
  - o There seemed to be no significant difference among alloys in similar class (e.g., 2000 series aluminum alloys) in terms of resistance to fretting crack initiation (nucleation of fretting cracks and growth of such small cracks).

There are also studies showing tougher Aluminum (2024-T351) has better resistance to fretting crack initiation than 7075 (T651) Aluminum alloy, including higher values in the critical tangential load (by 70%) as well as shorter crack depth under same tangential load for similar numbers of fretting cycles, as shown in Figure 49.
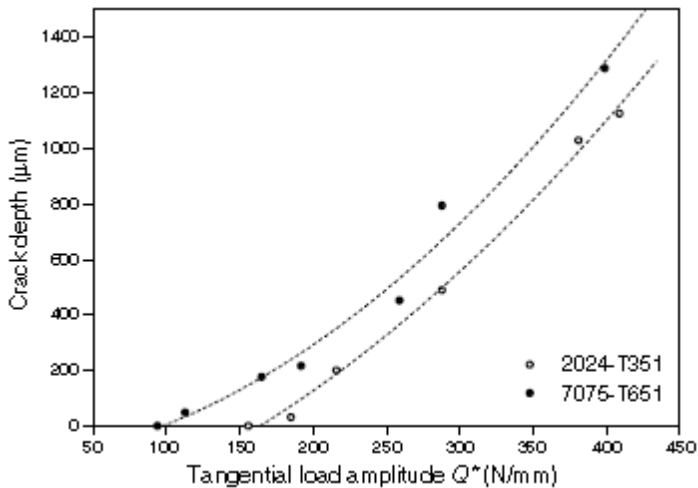
Figure 49 - Crack depth as a function of tangential load for 2024 and 7075
aluminum alloys[139]

The better fatigue performance in ACCC conductor system (with AGS) might be
attributed to the tougher Aluminum strands (1350-O) in TW configuration from
the perspective of resistance to fretting crack initiation:

- Lower compressive force (i.e., normal load)
- Compressive Stress/load to the inner strands from helical winding in
  ACCC conductor should be considerably less (as compared to ACSR)
  as these soft aluminum strands readily yield which reduces the normal
  load.
- The other significant factor of reduced load is the large strand to strand
  surface contact area in TW strands as compared to the round wires in
  ACSS.
- The AGS clamp limits the compressive force/load to the aluminum
  strands (especially the outer layer under the clamp). The maximum
  load/stress in the normal direction is limited to the yield strength the
  AGS elastomeric material can support. This should result in a

---

[139] Munoz, S. et al., 'Prediction of the crack extension under fretting wear loading
conditions', International Journal of Fatigue 28 (2006) 179-1779.

substantially lower stress than in direct metal to metal contact configuration in conventional clamps.

- Lower Tangential Load/Stress which reduces the shear stress in the aluminum strands that lead to fretting cracks.
- The soft aluminum might be also beneficial in avoiding hard asperity on strand surfaces which could lead to high stress concentration and fretting crack formation.
- The performance comparison between 7075 and 2024 alloy seemed to suggest that a tougher aluminum such as Type 1350-O (with high tensile elongation) offers better resistance to fretting crack initiation.

Fatigue Crack Growth (with fretting):

- During stage II of crack growth (Figure 48), the crack propagates smoothly along the direction perpendicular to the maximum principal stress (i.e., the applied tensile stress in Aluminum strands) as the shear stress is no longer relevant for such (long) cracks that are much deeper under the surface.
- Crack growth proceeds by a repeated plastic blunting and sharpening process at the crack tip (e.g., microscopic striation on the fracture surface).
- Fatigue life in a material is related to the (long) crack growth rate via the Paris equation. If the stress intensity at the (long) crack tip is less than the threshold value, (long) cracks don't propagate. It should be noted that there is no such threshold for small crack propagation, as in fretting (Stage I).
  - o 87-90% of fatigue life takes place in this stage for aluminum alloys when fretting is present.
- *The superior fatigue performance in ACCC conductor may also be related to the 1350-O material during fatigue crack growth:*
  - o *The low yield strength and the propensity of plastic deformation in the 1350-O aluminum strands limits the tension stress in aluminum strands to a relatively low level (i.e., 4 ksi). The laboratory tension test shows that conductor tension in ACCC quickly relaxes as the soft aluminum strands creep, and the stress level in aluminum approaches that of its yield strength level within hours after stringing.*

- *Lower tensile stress in aluminum is highly desirable as it limits crack growth rate, thereby increasing the fatigue life.*
  - *The propensity of 1350-O aluminum to plastically deform is attractive in blunting the tip of fatigue crack. It reduces the stress intensity near the crack tip area, and inhibits fatigue crack growth and increases fatigue life.*

2.14.3. Fatigue Life Modeling

One approach in structural fatigue design is to keep the stress (or strain) below the endurance limit. This works well for materials such as titanium and ferrous alloys that exhibit an endurance limit where application of stress below this limit seems to produce infinite life. Aluminum alloys, similar to most non-ferrous metals, do not have a fatigue limit (i.e., lack of a sharply defined knee in the S-N curve and no true endurance limit). Fatigue strength for these materials is often defined as the stress level at which failure will occur for some specified number of cycles (e.g., 500 million cycles). These values are typically set to be conservatively low, including the endurance limit established for ACSR conductors per EPRI.

The S-N curve is a plot of either the alternating stress or maximum stress vs. the respective numbers of cycles to failure (typically on a semi-logarithmic scale). Other tools for assessing fatigue properties is the Goodman diagram, which is popular for failure-free design in critical aircraft structural design, and it plots the alternating stress vs. mean stress for fatigue properties for a given number of cycles of a given material. Both S-N curves and Goodman diagrams are constructed with uni-axial fatigue data. For fretting fatigue involving high cycle fatigue such as Aeolian vibration in conductors, data are often not available or incomplete especially for new conductor materials, as expensive and time consuming test is often required.

Strain Energy based design approach for fatigue life assessment is also gaining popularity. It is built on the premise that strain energy required to fracture a material monotonically is the same as the energy accumulated during a cyclic

fatigue procedure.[95,96,140,141] Scot-Emuakpor[96] extended the approach for multi-axial load fatigue, and the total strain energy from a monotonic fracture, W_f, is equivalent to the W_{cycle} *(the strain energy of one cycle from a fatigue process)*, times N, the number of cycles to failure in the fatigue process that developed W_{cycle}. The effect of an applied mean stress on fatigue life is analyzed by considering that some of the strain energy required for monotonic fracture has already been dissipated and the total energy required for fatigue process is proportionally reduced. For example, in Figure 50, the gray area under the stress-strain curve from the origin to the point of mean stress represents the strain energy associated with mean stress (i.e., conductor or aluminum tension load). The total strain energy is defined by the area under the entire stress-strain curve. Thus, the remaining strain energy available for fatigue is obtained by subtracting the mean strain energy from the total strain energy.
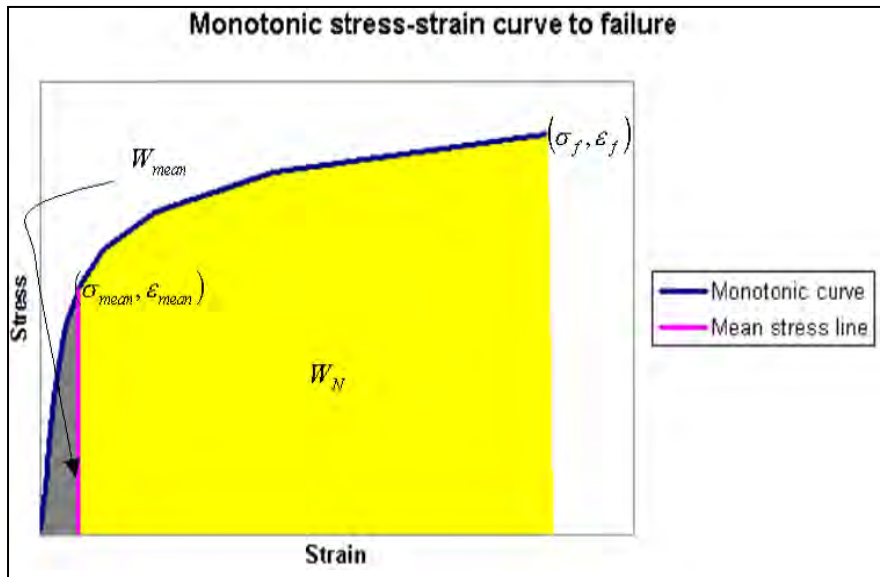
Figure 50 - Stress-strain curve in energy based fatigue life modeling.

---

[140] Feltner CE and Morrow JD, Microplastic strain hysteresis energy as a criterion for fatigue fracture, ASME Paper No. 60-MET-2, 1960.

[141] Stowell E, A study of the energy criterion for fatigue, Nuclear Engineering and Design, 1966, pp 32-40.

This approach allows good qualitative assessment on the fatigue performance of the various aluminums used in conductor applications without having to rely on extensive testing data. Figure 51 and Table 24 exhibit the materials properties and their strain energy. It is quite evident that 1350-O aluminum strands should have far more superior fatigue resistance in Aeolian vibration environment, as the strain energy is about 6 times bigger than 1350-H19. The data also suggest that Al-Zr alloy may not be an ideal choice for Aeolian vibration sensitive applications, and 6201 might have good fatigue resistance. Table 24 shows the effect of mean stress (i.e., conductor tension or Aluminum stress) on the respective fatigue resistance of various aluminum strands. For example, increasing conductor tension from 20% RTS to 30% RTS in an ACCC Drake conductor, only consumes an additional 0.5% remaining strain energy, while the same tension increase in ACSR Drake would have consumed over 2% of the remaining strain energy, resulting in a much greater impact on fatigue life. This is consistent with laboratory testing in ACCC conductors where higher tension does not appear to impact ACCC conductors as much as the other conductors (ACSS and ACSR).
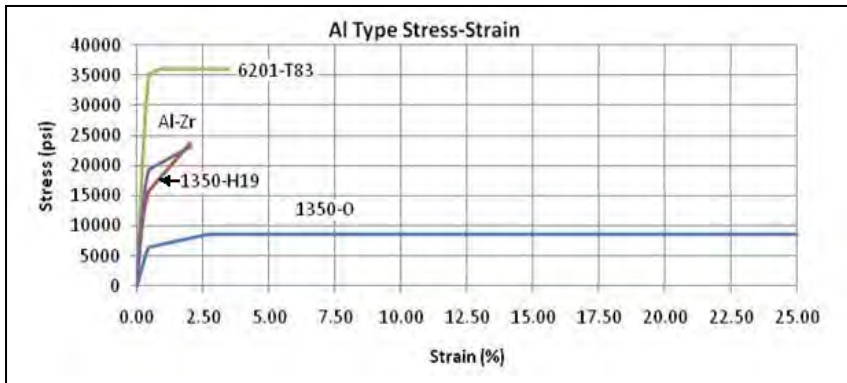
Figure 51 - Strain energy of typical aluminums used for conductor applications. The toughness (large tensile elongation) in 1350-O makes it an outstanding candidate for conductors to be used in Aeolian vibration sensitive areas.

	1350-O	1350-H19	6201-T83	Al-Zr
Tensile Strain	25%	2%	3.50%	2%
Total Strain Energy	190743	30319	118423	38015
20% RTS (Al strain)	0.27%	0.12%		
Remaining Strain Energy	190274	30096		
Impact of stress on on fatigue	-0.25%	-0.74%		
30% RTS	0.42%	0.18%		
Remaining Strain Energy	189926	29687		
Impact of stress on on fatigue	-0.43%	-2.08%		

Table 24 - Effect of mean stress and tension load on a conductor and aluminum strands in a Drake sized conductor. Increasing line tension in conductors using 1350-O has negligible effect on its ability to manage fatigue; however, conductors using 1350-H19 are more significantly impacted, making it necessary to keep conductor tension low in conductors such as ACSR types.

2.15. Recommendations for Aeolian Vibration Design for ACCC

The superior performance (self-damping and resistance to fretting fatigue) in ACCC conductors allows the opportunity of considering higher tensions and catenary constants in transmission projects using ACCC conductors for significant savings in capital and infrastructure costs. This is supported by both experimental test data and a fundamental understanding of material fatigue and vibration damping. The unique features in ACCC conductors include fast stress relaxation (within hours) in aluminum strands to minimize the tensile stress in aluminum even after the conductor is subjected to much higher tension levels. Reduced aluminum tensile stress not only improves self-damping, it reduces the shear stress that leads to fretting crack initiation. The toughness and significant strain energy from 1350-O aluminum offers the ACCC conductor with the best resistance against fatigue crack growth.

Relaxation of aluminum does shift the conductor load burden to the composite core in ACCC conductors. Unidirectional hybrid carbon composites, as used in the ACCC conductor core, has one of the best fatigue performance properties among all material options and is a much better option as compared to the other core materials such as steel or aluminum (as shown in Figure 52). It provides an ideal solution in ACCC conductors as the shifted load from aluminum strands does not impact the overall longevity of conductor, which optimal for long span

applications including river/ocean crossing where Aeolian vibration and steel core corrosion in the conductor has to be mitigated while managing high conductor tension and high capital expenditures. CTC Global recommends that designers give full consideration for higher initial and/or higher every day tension with ACCC conductors for substantial savings in project costs, It is also prudent to work with damper manufacturers to conduct additional testing (e.g., self damping test) at proposed tensions levels, especially when long spans are envisioned.
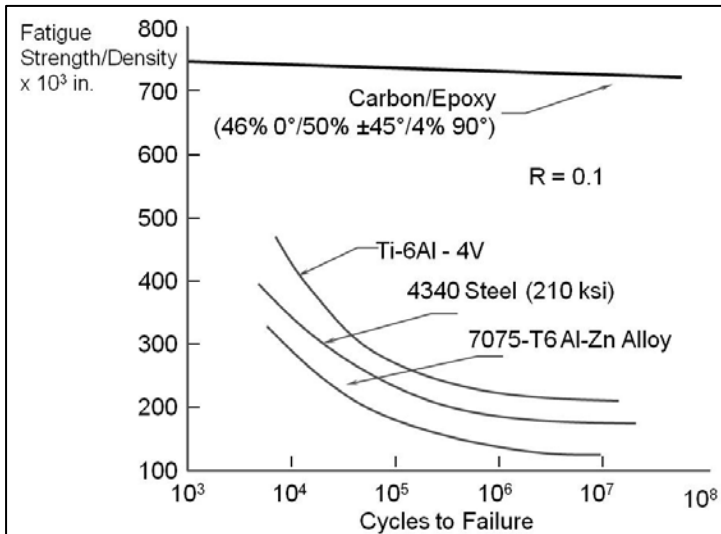
Figure 52 - Fatigue resistance of candidate materials for conductor core. Both aluminum and steel experience substantial reduction in tensile strength when high cycle fatigue is present as in overhead conductor in Aeolian vibration sensitive areas (long span and river crossing). Carbon composite core is virtually immune from fatigue effect, and making it an ideal choice for demanding applications.

2.15.1. Use of AGS Suspension Systems

CTC Global and others have compiled considerable evidence that ACCC conductors have the ability to endure and dissipate Aeolian vibration at higher than typical installation tensions with the use of AGS suspension clamps and armor rod (or equivalent). On a minimum, the AGS suspension is expected to reduce the vibration amplitude near the clamping/conductor contact area and

will limit the extent of compressive force from the clamps onto the conductor aluminum strands. Both of these effects are helpful in managing fatigue from Aeolian vibration.

2.15.2. Relevance of Tensile Stress in the Aluminum Strands

It is highly advisable that design engineers consider the effective stress level in aluminum strands as this is the most relevant and important parameter that impacts fatigue failure. While overall conductor tension and catenary constant are important design parameters for new conductors such as ACCC conductors, they are not quite as pertinent as they are for ACSR or other conductors where T/m for the steel core and aluminum strands are virtually identical.

An attempt was made to re-analyze the field performance table of ACSR conductors provided in CIGRE TB 273.[142] Extrapolated stress levels in aluminum strands were developed. Table 25 shows the analysis with most of the known conductor types depicted in the CIGRE report where the stress – strain curves was evaluated at -10°C to determine force, and thus the stress, in the aluminum strands. The reproduced CIGRE table shows that the failures occurred for the 6/1 ACSR conductor at 1029 meters, suspended by a pin-type insulator. The next failure occurred at just below a 4600 ft (1400 m) catenary. The aluminum stress based analysis did not substantially change the conductor ranking.

---

[142] Cigre Technical Brochure TB 273 (2005), "Overhead Conductor Safe Design Tension with Respect to Aeolian Vibrations", SC B2 TF B2.11.04

Conductor Diameter (mm)	Aluminum Strand Count	Steel Strand Count	Span (meters)	Catenary H/W (meters)	Conductor Tension @ -10° C (N)	-10C Initial Al Tension (N)	-10C Initial Al Tension (lbf)	Stress in Al x-section (MPa)
21.9	24	7	200	707	6384	5280	1187	21.80
24.2	54	7	137	934	13225	9473	2130	24.80
21.9	24	7	395	844	7621	6084	1368	25.20
8.0	6	1	61	1029	1369	1039	234	30.90
18.8	30	7	396	1511	11620	5794	1303	31.20
18.8	30	7	350	1554	11950	5937	1335	32.00
16.5	30	7	310	1405	8332	4202	945	32.00
21.8	26	7	183	1358	12996	8391	1886	34.70
25.9	30	7	396	1655	24196	11918	2679	36.70
26.4	32	19	655	2095	33939	13781	3098	38.00
26.4	32	19	445	2108	34150	13851	3114	38.20
18.8	30	7	270	1908	14673	7104	1597	38.30
26.4	32	19	520	2116	34279	13901	3125	38.30
22.4	30	7	333	1747	19060	9326	2097	38.60
21.0	30	7	390	1761	16835	8222	1848	38.80
22.4	30	19	475	2154	29531	11920	2680	38.90
18.8	30	7	360	1959	15065	7272	1635	39.20
26.4	30	19	475	2176	31378	12646	2843	39.20
22.4	30	7	340	1865	19974	9699	2180	40.70
21.8	26	7	274	1638	15676	9839	2212	40.70
25.4	54	7	346	1735	24568	16156	3632	42.30
21.8	26	7	326	1723	16489	10283	2312	42.50
19.9	26	7	170	1738	13869	8623	1939	42.80
19.6	30	7	350	2001	16588	7977	1793	43.50
19.6	30	7	350	2001	16588	7977	1793	43.50
10.7	12	7	300	1607	5962	2252	506	43.70
12.7	6	1	107	1772	5724	3886	874	46.30
25.1	26	7	580	2162	27609	16648	3743	51.70
11.7	12	7	264	1996	7405	2688	604	52.10
18.3	26	7	440	2279	15383	9203	2069	54.00
31.7	114	37	425	2297	45113	28611	6432	54.10
31.7	114	37	415	2300	45172	28647	6440	54.20
31.7	114	37	374	2382	46782	29525	6637	55.90
21.9	24	7	315	2243	20254	13867	3117	57.40
22.4	30	7	350	2861	30641	14211	3195	59.60
14.4	12	7	194	2458	14674	4973	1118	61.70

Table 25 - Re-analyzed data from CIGRE TB 273. The data is sorted by calculated aluminum stress from the lowest to the highest. The highlighted rows depict conductors with no noted fatigue failure.

Looking at the expected stress in the round wire aluminum in Table 25, it would appear that a safe stress level in the aluminum would be 25 MPa. To put it into perspective, the vibration testing performed on ACCC® conductor at tensions much higher than the tensions imposed on ACSR and ACSS conductors tested by AEP, had stress in the aluminum strands of 28.5 MPa without fatigue failure. This also supports the notion that higher tensions and thus higher catenaries for ACCC® conductors should be permissible, as long as the tensions stay within regulatory limits. It might also be possible that the more comprehensive information on the data analyzed could indicate the fatigue failures below 45

MPa aluminum stress is attributable to other causes (e.g., inappropriateness in clamp choice and clamp installation).

2.15.3. Levels of Pre-Tensioning

Longtime suppliers of ACSS conductor have stated that there is considerable plastic deformation of the aluminum strands in the first hours of applied tension[143] and tests performed on ACCC conductor suggests the same. Field and lab testing of ACCC conductor has found that plastic elongation and a minor degree of strand settling causes conductor tension to drop by approximately 5-7% in the first few hours, and then to about 10% over a period of 24 to 48 hours after it is initially pulled to a desired "clipping-in" tension.

To offset this drop and stabilize the conductor no matter how long it may have been in the air prior to being clipped in, the conductor can be pre-tensioned by an additional 2% RTS above the desired initial tension, held for 30 minutes, lowered back to the desired clipping tension and clipped it. Conversely, it can simply be clipped in at a 2% RTS higher tension and allowed to relax over a period of a day or two. (1% RTS of ACCC Drake example = 410 lbs (~4.45 kN))

- For example, an ACCC Drake conductor with a desired initial tension of 20% RTS, or 8,200 lbs (36.5 kN), was pre-tensioning to ~9,000 lbs (40.0 kN), and held for 30 minutes. It was then reduced back to 8,200 lbs (36.5 kN) and clipped in. After the conductor is either allowed to relax on its own, or after a 30 minutes hold, the tension will stabilize at ~8,200 lbs (36.5 kN) (not including changes in tension due to temperature fluctuations). This process will reduce strain in the aluminum strands by about 10% at the initial stringing temperature.

- Creep is rarely a controlling factor with conductors using Type 1350-O annealed aluminum. This means that designs will have sags defined by the high load events defined for the project (ice, very low temperatures, or very high winds). Modest pre-tensioning to varied degrees can overcome creep, improve self-dampening characteristics, and reduce stress in the aluminum strands to enable higher initial conductor

---

[143] BICC Brand TransPowr™ ACSS Brochure (2001)

tensions while reducing the possibility of strand fatigue failure due to Aeolian vibration.

Higher levels of pre-tensioning may be used to eliminate tensile stress in Aluminum strands and to overcome the elongation that large loads may eventually cause, and, in effect, drive the conductor's state to at or near its final state, with the thermal knee-point temperature driven to the installation temperature or lower. Driving the knee-point to the "Average Annual Minimum Temperature" (AAMT), can also ensure the conductor has the maximum self dampening properties, no matter what the operating or environmental temperature might be.

- High levels of pre-tensioning that may be required to achieve this very attractive level of a further reduced sag range, may require pulling the conductor at up to nearly twice its sagging-in tension. This extreme level of pre-tensioning may not be practical or safe for the crew, construction equipment, or the support structures, unless certain provisions are made and the line is relatively straight. Any level of pre-tensioning, that might be considered useful, should be approached with an appropriate degree of caution.

- If conditions allow, a recommended level of pre-tensioning that will substantially reduce stress in the aluminum strands, lower the thermal knee-point, and improve ice load sag performance is 4 to 5% RTS or ~30% above the desired clipping-in tension. For example, if the clipping-in tension at 15°C is 6,000 pounds (26.7 kN), a pre-tensioning to 7,800 pounds (34.7 kN) would be appropriate. Maintaining the conductor tension at this pre-tension level for 30 minutes, and then reducing back to the desired clip in tension is recommended.

Figure 53 shows the stress-strain curve and the load sharing between the core and aluminum with no pre-tensioning. If the conductor is initially clipped in at 6,000 lbf (26.7 kN) (without pre-tensioning), the aluminum would initially be carrying 2,425 lbf (10.8 kN), of tension, or 3,000 psi (21 MPa) of stress, and the core 3,575 lbf (15.9 kN) of tension, placing the thermal knee point at approximately 65°C. By pre-tensioning to 7,800 lbf (34.7 kN) (Figure 54), holding at that tension for 30 minutes, and then relaxing the conductor back to 6,000 lbf (26.7 kN), the tension in the aluminum strands can be reduced to 1,770 lbf (7.9 kN), or 2,200 psi (15.2 MPa), which significantly reduces its initial

stress level and virtually overrides strand settling and initial process of creep. This would have the effect of lowering the thermal knee-point by approximately 15°C which will improve thermal sag at lower operating temperatures.
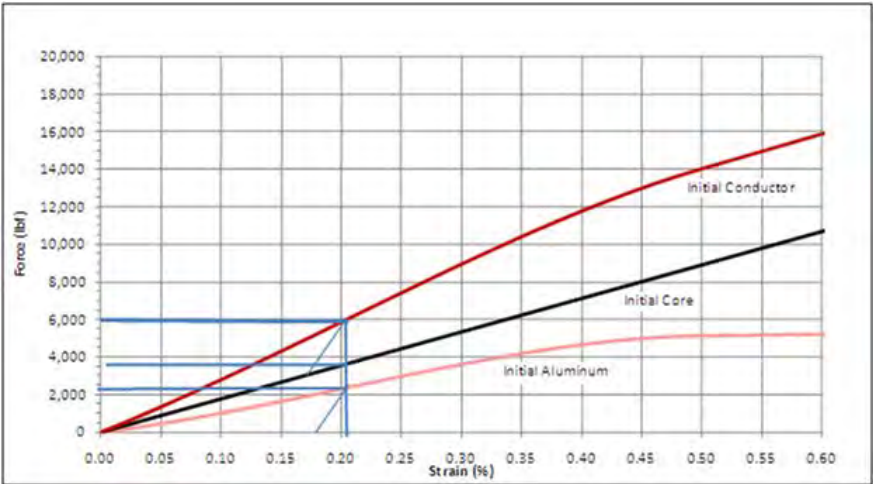
Figure 53 - Stress-strain curve of ACCC® Drake conductor with no pre-tensioning showing core and strand load sharing
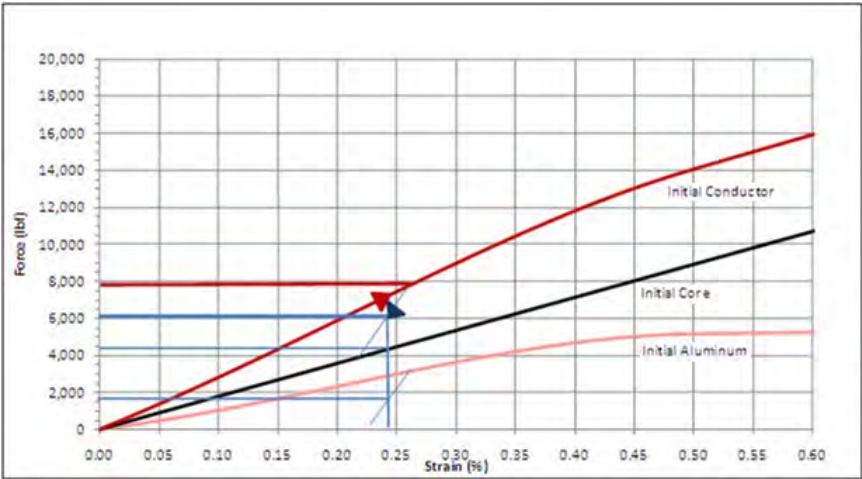
Figure 54 - Stress-strain reduction after pre-tensioning to 7,800 lbf (34.7 kN)

147

Table 26 shows that in order to relieve the aluminum completely from any load at the -10°C AAMT temperature (used for example), a pre-tensioning up to 32% RTS would be required. While the 32% RTS needed to do this is not unusually high and within the NESC limits, the additional force needed to drive the knee-point to this very cold AAMT condition is significant, and care should be taken to determine if this type of pre-tensioning can be done safely given the capabilities of the structure, pulling equipment and other factors.

After Pre-tensioning, clip in tension of 6,000 pounds at 15°C (60°F) (ACCC® Drake)						
Pre-tension Force (pounds)	6,000	7,800	9,000	10,200	12,000	13,200
% RTS	15%	19%	22%	25%	29%	32%
Aluminum Tension at 15°C	2,545	1,772	1,369	869	125	0
Aluminum Tension at -10°C (AAMT)	3,010	3,253	2,917	2,417	1,670	434
Knee point Temperature (C)	65°C	50°C	41°C	29°C	17°C	-5°C

Table 26 - Levels of pre-tensioning ACCC® Drake conductor to lower the thermal knee-point and relieve stress on the aluminum strands to improve fatigue resistance

Pre-tensioning has also been performed with ACCC conductor in some instances to move the conductor's sag closer to its final condition (lower) so it drops further below OPGW wire. The directions necessary to model pre-tensioning in PLS-CADD™ are provided in section 3.3.

2.15.4. Cautionary Statements

Pre-tensioning has to be approached cautiously. The dead-end and corner structures have to be strong enough to accommodate the temporary, higher pulling tensions. In a case where conductors exist on the opposite sides of a dead-end, the opposing conductor may offer sufficient reinforcement. In the case where no other conductor exists, temporary cross arm bracing or guy wires may be required. Using a tensioner itself to pre-tension the conductor may also create excessive down force at the dead-end structure equipment must be placed suitably. Larger stringing blocks should also be employed and additional bracing may be required. Light to moderate levels of pre-tensioning can often be accomplished with little to no additional bracing, but only after a thorough engineering analysis is performed and the structures assessed. Pre-tensioning is most easily accomplished between to dead-end structures on a relatively straight

pathway. Please refer to CTC Global's Installation Guidelines for additional information.

3. Calculating ACCC Conductor Sag & Tension

3.1. Conductor Sag & Tension Analysis

While the primary function of conductors is to transfer electrical load (and provide functionality related to line stability, system reliability/redundancy and other factors), conductors must also be strong enough to support their own weight as well as any other weight (or stress) caused by ice, wind or other loads. Higher strength conductors might enable a reduction in the number or height of structures required to support the line, which can produce very favorable economic and environmental results. Conductor sag to some degree can be mitigated by installing the conductor at a higher initial tension but higher tensions tend to increase the conductor's susceptibility to premature fatigue failure due to Aeolian vibration. For this reason, most conductors are installed at relatively low initial tensions ranging from 15 to 25 percent of their overall rated strength, or at a relatively low "catenary constant" (tension divided by weight, per unit length, as described above). Some conductor types/sizes adopt larger sags with imposed loads or high temperatures than others. This can impact span length and support structure combinations dramatically. The choice of conductor, based on its sag and tension characteristics, have a large impact on overall project costs.

3.1.1. The Catenary

A flexible wire of uniform weight suspended between supports and subjected to uniform gravity takes a shape called a *catenary*. The conductor catenary is very nearly a *parabolic* shape defined by the conductor's Weight per unit length (w) and the Horizontal tension (H), as shown in Figure 55. The sag of the conductor (D) is a function of w and H, the span length (S), and the difference in elevation between the span supports.
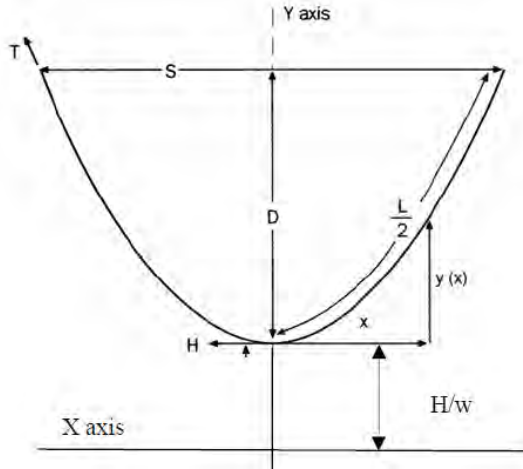
Figure 55 – Catenary curve for level spans.

The catenary equation for a conductor between supports is expressed in terms of the horizontal distance (x) from the lowest point (or vertex) of the catenary to a point on the catenary that is y (x) above the vertex.

$$y(x) = \frac{H}{w} \cdot \left[\cosh\left(\frac{w \cdot x}{H} \right) - 1 \right] \cong \frac{w \cdot x^2}{2 \cdot H}$$

(3-1)

The expression on the right side of equation is an approximate parabolic equation based upon the first term of the MacLaurin expansion of the hyperbolic cosine. The approximate parabolic equation is valid as long as $x^2 * w^2 / 12H^2 \leq$ 1.

For a level span with the vertex in the center the sag (D), is found by substituting $x = S/2$ in the previous equation. The exact catenary and approximate parabolic equation for sag becomes:

$$D = \frac{H}{w} \cdot \left\{ \cosh\left(\frac{w \cdot S}{2 \cdot H} \right) - 1 \right\} \cong \frac{w \cdot S^2}{8 \cdot H}$$

(3-2)

151

The ratio, H/w, is commonly referred to as the *catenary constant*, C. An increase in the catenary constant causes the catenary curve to become less pronounced (decreased sag). While the catenary varies as a function of conductor temperature, ice and wind loading, and time, the catenary constant typically has a value in the range of 500-2000 meters for most transmission catenaries under most conditions.

The horizontal component of tension (H) as measured at the vertex is the same at all points within the catenary, but the total tension increases as the support points are approached, due to the added vertical component. Given a level span at the supports, the vertical component (V) of tension is equal to one half of the weight of the conductor.

$$V = w \cdot L / 2 = H \cdot \sinh\left[\frac{w \cdot S}{2 \cdot H}\right]$$

(3-3)

At the end supports, the conductor tension is the vector sum of the horizontal and vertical tension.

$$T^2 = H^2 + (\frac{w \cdot L}{2})^2$$

(3-4)

Substituting the equation for length (L) from above and taking the square root of both sides from this equation, we find:

$$T = H \cdot \sqrt{1 + \sinh^2\left(\frac{w \cdot S}{2 \cdot H}\right)} = H \cdot \cosh\left(\frac{w \cdot S}{2 \cdot H}\right)$$

(3-5)

To relate the total tension to sag in a level span, the equation can be rearranged to:

$$T = H + H \cosh\left(\frac{w \cdot S}{2 \cdot H}\right) - H$$

<div align="right">(3-6)</div>

$$T = H + w \cdot \left(\frac{H}{w} \cosh\left(\frac{w \cdot S}{2 \cdot H}\right) - \frac{H}{w}\right)$$

<div align="right">(3-7)</div>

Substituting the sag (D) equation above gives us:

$$T = H + w \cdot D$$

<div align="right">(3-8)</div>

For inclined spans in Figure 56, in each direction from the vertex, the conductor elevation y(x), relative to the low point is:

$$y(x) = \frac{H}{w} \cdot \left[\cosh\left(\frac{w \cdot x}{H}\right) - 1\right] \cong \frac{w \cdot x^2}{2 \cdot H}$$

<div align="right">(3-9)</div>

The sags relative to the supports is:

$$D_L = D_R + h$$

<div align="right">(3-10)</div>
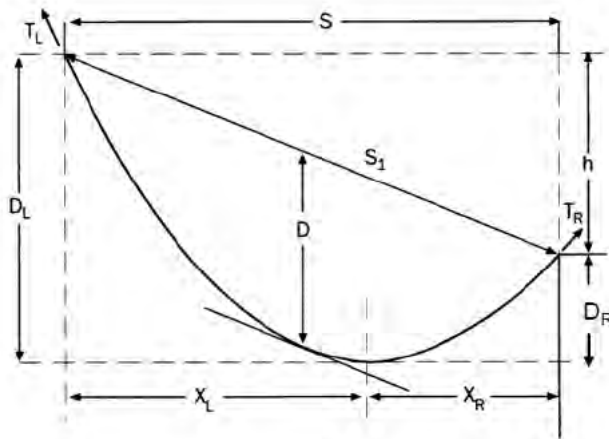
Figure 56 - Inclined catenary span

The position of the low point in an inclined span can be calculated by:

$$x_R = \frac{S}{2} - \frac{H}{w} \sinh^{-1} \left[\frac{h/2}{\dfrac{H}{w} \sinh \dfrac{S/2}{H/w}} \right]$$

(3-11)

3.1.2. Mechanical Coupling of Spans

With occasional exceptions, transmission lines are usually comprised of numerous tangent structures located between dead-end or strain structures. The strain structures prevent longitudinal movement of the conductor at its attachment points. Tangent structures are used within the line section to support the conductors. Insulators and suspensions clamps used at suspension structures are generally able to move both transversely and longitudinally to the line. This combination of fixed attachment points at dead-end structures (or horizontal post insulators) and movable attachment points at the ends of suspension insulators is important to understanding in order to properly manage the behavior of a series of spans.

Consider the simple equation from above:

$$T = H + w \cdot D$$

This states that in a pair of adjoining spans, the conductor tension at each side of the shared attachment point equals *the common horizontal tension in the spans plus the weight of the wire times the elevation difference between the lowest point in each span (the location where T = H) and the attachment.* If the low point elevation of one span is different than the low point elevation of the adjoining span, then the tensions on either side of the attachment they share will be unequal. A line of several spans rising up a slope or a combination of long spans and short spans will cause span low point inequalities, so this inequality of tensions at structure attachments is very common and they are unequal by a calculable amount.

For example, if the conductor weighs 1 lb/ft (~1.5 kg/m), was strung to a horizontal tension of 5,000 lbf (22.2 kN) and the sag low points of two adjacent spans are 50 ft (15 meters) and 20 ft (6 meters) below the common attachment point, the tensions at the attachment are 5,050 lbf (22.5 kN) and 5,020 lbf (22.3 kN) for a tension unbalance of 30 lbf (0.13 kN). Something must occur during design and construction to make the two spans H values equal at 5,000 lbf (22,2 kN) because, when the conductor is in travelers (sheave wheels) during installation, the travelers will feel the 30 lb (0.13 kN) imbalance and turn until the tensions on either side of it at the attachment are equal. If they equalize at 5,035 lbf, (22.4 kN) then the H values in the two spans must be 5,015 lbf (22.3 kN) and 4,985 lbs (22.17 kN). While in travelers, the horizontal tensions at the low points of a series of spans are NOT equal as desired when span low points are unequal. If the two spans are 1,500 ft (457 meters) and 750 ft (229 meters) in length, the sag differences between balanced and unbalanced H values are 0.06 ft (1.8 cm) and 0.15 ft (4.5 cm). This modest situation is no cause for alarm but the calculation of elevation differences of 50 ft or more can be much more pronounced. In rough terrain, sag errors of many feet or centimeters are not uncommon.

Thus it is useful to have equal horizontal tension values (H) in all spans in a series between dead-end structures. Without that equality, the alternative is nearly incalculable. Imagine trying to engineer a line (calculate the sags and the structure loads) when the catenary constant is unique in every span, when the tension in the line is high on the high ground and the sags are large in the low elevation spans. Not only are the sag and tension calculations more cumbersome

and complex but managing structure designs would be extremely challenging. Managing tension limits and having acceptable sags at the bottom of slopes would also be extremely difficult.

When you consider that the calculations of sags and tensions and structure loads was a tabular process until as recently as 15 years ago when computers took over the exercise, it is no wonder that span tension equality (H) was very attractive. The concern has always been, *"when are the minor inequalities worth accepting (as in the example above) and when should action be taken to change the natural inequalities that are in place in the travelers into a state of equality in all spans?"* The construction action required to change from inequality of H in sheaves to equality of H values in suspension clamps is referred to as "clipping offsets."

Tension differences between spans exist at the time of installation, as described above, and they are corrected by clipping offsets or they are not. As the length of the conductor in each span changes with external load, temperature and time, the tension unbalances change as well. There is a poorly understood phenomenon worth mentioning. Without providing the development of the formula, it is a fact that *the change in sag due to a strain change (unit length change) is independent of the span length.* Tensile stretch, creep and thermal elongation are all strain changes so, any change in tensile load, any creep and any change in temperature will, in theory, cause a sag change that is the same in all spans, regardless of the spans' lengths. In practice, the purity of the sag-strain change relationship gets modified by the elastic response of the spans and short spans adopt less sag change than longer spans. As spans become longer, the relationship becomes more pure. In other words, short distribution spans don't act this way.

As an example, consider two adjoining spans of 1,000 ft (305 m) and 1,600 ft (487 m). Assume the conductor is the 1 lb/ft (1.5 kg/m) conductor strung to 5,000 lbf (22.2 kN) tension. Using the formula:

$$D = \frac{H}{w} \cdot \left\{ \cosh\left(\frac{w \cdot S}{2 \cdot H}\right) - 1 \right\} \cong \frac{w \cdot S^2}{8 \cdot H}$$

(3-12)

The sags in the spans are 25 ft (7.6 m) and 64 ft (19.5 m). Assume a temperature change that causes a sag increase in the 1,000 ft span of 4 ft. The principle says that the sag in the 1,600 ft (487 m) span will increase 4 ft (1.2 m) as well. So, the sags become 29 ft (8.8 m) and 68 ft 20.7 m). Using the same formula, the H values with the new sags become 4,310 lbf (19.2 kN) in the shorter span and 4,705 lbf (20.9 kN) in the longer span causing an unbalance of 400 lbf (1.8 kN). This example shows that a temperature change (or any such strain change in the spans) changes the tensions in the spans un-equally. So, the presence of a common tension between all spans wants to exist only once (when you strung it perfectly) or when the strain in the spans happens to be equal to that strain by some future combination of load, temperature and time.

Minor differences in conductor tension between adjacent span in most cases is nearly equalized by very small movement along line of the suspension insulators. The movement effectively takes some conductor length out of the looser span and puts it in the tighter span. Rigid or short insulators do a poorer job of moving and equalizing these tension unbalances. Unbalances that remain will cause sag differences from those expected, based on the assumption that H is always equal in the spans. This also loads the structures, although usually without much consequence.

Tension equalization between suspension spans works reasonably well for modest changes in conductor temperature and small differences in ice and wind loading. With higher conductor temperatures, if the conductor has a relatively high coefficient of thermal expansion, the unbalances grow which can lead to unfavorable sag consequences. If very large temperature changes are part of the line design, the tension unbalances will be greatly reduced by a conductor such as ACCC that exhibits a very low coefficient of thermal expansion.

3.1.3. Conductor Slack

Conductor Slack is another important factor to understand before approaching sag and tension calculations. Conductor slack is the difference in length between the conductor and the chord (straight line) distance between its end supports.

For a level span, the distance between the supports (S) is the span length, while the total conductor length is (L). Slack can therefore be defined by[144,145]:

$$L - S = \left(\frac{2H}{w}\right) \sinh\left(\frac{wS}{2H}\right) - S \qquad (3\text{-}13)$$

While slack can be described in units of length, it can also be described as a percentage (i.e. 0.15% of the span length). The approximate parabolic equation above offers good insight, but cannot be considered precise on sloped spans. One of the reasons for this is the high degree of sensitivity of slack. The slack can also be approximated by the following equation:

$$L - S \cong S^3 \left(\frac{w^2}{24H^2}\right) \cong D^2 \left(\frac{8}{3S}\right) \qquad (3\text{-}14)$$

For any given H/w ratio (also known as the catenary constant), the slack in the conductor is related to the cube of the span and to the square of the sag. For a series of spans having the same horizontal tension (H), the slack of a 1,200 ft (365 m) span is eight times as large as the slack in a 600 ft (183 m) span. The cubic dependence of slack on span length is the primary reason the sag-tension behavior of multiple suspension spans is largely determined by the longest spans.

The equation for slack can also be converted to obtain equations showing the dependence of sag (D) and tension (H) on slack (L-S):

$$D \cong \sqrt{\frac{3S(L-S)}{8}} \qquad (3\text{-}15)$$

and

$$H \cong \frac{wS}{2} \sqrt{\frac{S}{6(L-S)}} \qquad (3\text{-}16)$$

---

[144] "ACSR – Graphic Method for Sag-Tension Calculations," Aluminum Company of Canada, Ltd., Montreal, Canada, May 1950.

[145] CIGRE Guide 324, "Sag-Tension Calculation Methods for Overhead Lines", Task Force B2.12.3.

As the slack of the span becomes very small, the tension becomes very high. Equations 3-15 and 3-16 are known as the catenary equations.

The chart below (Figure 57) depicts conductor tension (H) and Sag (D) vs. Slack ($100*(L-S)/S$); where L = conductor length and S = Span length based on the catenary equations.
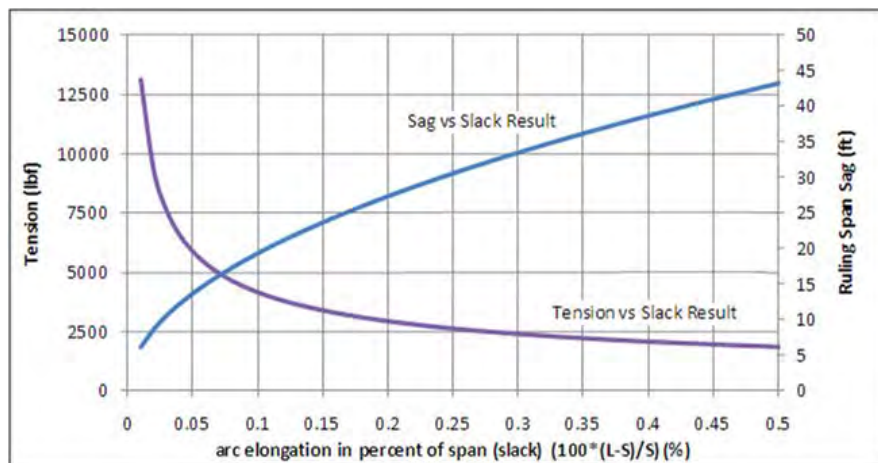
Figure 57 - Conductor tension, sag and slack[146] for a 1000 ft (304.8 m) span

These catenary equations relate to the change in the length of the conductor, either due to changes in mechanical tension or thermal elongation, that lead to a change in tension of the conductor which dictate sag and tension. Note that there are no CTE or modulus values in these equations. Therefore, for any conductor exhibiting a weight 'w', no matter what type of conductor it happens to be, a change in the length of the conductor, and thus the change in sag and tension, will be related through Equations 3-15 and 3-16.

Graphical sag programs use Equation 3-16 to draw tension / % slack lines for each weather condition at which the sag is to be determined. Note here, that only weight and tension influence the results of these curves. Thus, for a series of ice loads that need to be investigated, there will be separate catenary lines for

---

[146] Cigre Technical Brochure TB 324"SAG-TENSION CALCULATION METHODS FOR OVERHEAD LINES"; Task Force B2.12.3 (June 2007)

each ice case due to the change in the weight of the ice, or change in the radial thickness of the ice and if wind is added to the weight or not. There is only one curve though, that shows the change in tension with % slack when only the temperature is changed for a bare conductor. Sag / tensions are then determined by superimposing the stress-strain curve of the specific conductor that is being investigated, over the tension / % slack lines. This can be done because the percent increase in the arc length, for all practical purposes, is equivalent to the percent elongation on the conductor stress-strain. Therefore, the intersections of the stress-strain curve lines with the tension / % slack lines then provide sag / tension results[147]. For each temperature of the conductor that needs to be determined, though, a separate stress-strain graph for the conductor at the particular temperature is also needed. Reference[70] describes how this is done and can also be applied to ACCC conductors. An example calculation using the slack/stress-strain curves for determining the "thermal knee point" temperature for ACCC is discussed in 3.6.

3.1.4. Ruling Span Method

To simplify sag-tension calculations (and conductor installation), the assumption of a "ruling" span has been widely used. As tension equalizing between dissimilar spans becomes more efficient, the ruling span method of calculating sags and tension becomes more accurate. The ruling span method assumes that there is a span that "well represents" the behavior of the series of spans. That assumption depends on the easy equalizing of tensions between spans by the movement of suspension point attachments.

The span that best represents the series of spans is the span that has the same *rate of slack* as the series of spans. Realizing this point offers one of the reasons to recognize slack as a feature of spans on a transmission line. Consider an example of 3 spans: 600 ft (183 m), 900 ft (274 m) and 1,100 ft (335 m) strung with a 1 lb/ft (1.5 kg/m) conductor at 5,000 lbf (22.2 kN). According to the formula below, the ruling span that represents these three spans is 932.62 ft (284.3 m). The slack in these four spans is 0.36, 1.215 and 2.218 ft (0.11, 0.37 and 0.68 m) for the series of spans and 1.365 ft (0.42 m) for the ruling span. The *rate of slack* for the series is the sum of their slacks divided by the sum of their span lengths i.e. 0.001459 ft/ft (m/m). The *rate of slack* for the ruling span is its

---

[147] "Aluminum Electrical Conductor Handbook", The Aluminum Association, 3rd edition, pages 5-1 to 5-21.

slack divided by its span length. It is identical. Again, the correct ruling span is the span that has the same *rate of slack* as the series of spans.

The ruling span is defined as:

$$RS = \sqrt{\frac{S_1{}^3 + S_2{}^3 + \cdots + S_n{}^3}{S_1 + S_2 + \cdots + S_n}}$$

(3-17)

RS_1 = Ruling span for the line section containing n suspension spans
S_1 = Span length of first suspension span
S_2 = Span length of second suspension span
S_n = Span length of nth suspension span

In very rough terrain with large elevation changes between span end attachments, the formula gets an added component to account for the elevation differences. The approximate sag in any span can be calculated by:

$$D_i = D_{RS} \cdot \left(\frac{S_i}{S_{RS}}\right)^2$$

(3-18)

This squared ratio of the span lengths requires that the horizontal tension in the spans (H) is equal. Recall that a strain change causes a common sag change to all spans and therefore causes varied tension changes that are equalized by small movements of the attachment points. In other words, holding the horizontal tension in all spans equal requires small adjustments to the length of wire in the spans. If the attachment points could not move and you, in spite of that rigidity insisted that the tension always be equal, you would need to somehow constantly be moving bits of wire around between the spans. The ruling span method requires that the *amount* of conductor in all spans constantly adjust. On paper it does not, but in reality, it does to some degree by way of the attachment point freedoms of movement.

3.1.5. Finite Element Method

The introduction of computers into transmission line design that are programmed to calculate the complexities of mechanical actions has allowed

another approach to sag and tension calculations which may be considered a departure from the ruling span method. Nevertheless it is not a complete departure.

Finite Element Analysis (FEA) offers the user with a higher degree of sophistication in assessing sag and tension. Unlike the ruling span method, the FEA method assumes that the *amount* of conductor in each span is fixed. The amount of material in the span changes length due to tension, temperature and time changes, and the method allows the spans to adopt individual tensions in each span as was described as the nature of things above. The reaction of the attachment points, both in movement and force adoption to the calculated unbalances is part of the calculation effort albeit with different degrees of accuracy depending on the particular software program in use and the user's choices with it.

The presumed benefit of the FEA method is identification of more accurate sags and unbalanced loads at attachments based on the imperfection of the equalization caused by attachment movements. However, there are two points to make regarding this presumed benefit.

First, the FEA method requires the establishment of an *amount* of conductor in each span. The practice with most FEA calculations is to assume that all spans have the common tension, H value at the time of clipping in after pulling in and sagging the conductor. If H is common to all spans and the value of H is assumed to be accurate, then a length of wire for that condition allows the *amount* of conductor in each span to be locked down as fixed. This is the same assumption made by the ruling span method, but from that moment onward, the two methods diverge in their calculations. In either case, the assumption of a common H value is quite an assumption. If clipping offsets are not performed, then the accompanying conductor *amount* errors described above are incorporated into the span lengths (*amounts*). If clipping offsets are performed, the inaccuracies of the effort are adopted. Nothing is perfect and sometimes the imperfections will be larger than the accuracy of the FEA method itself is going to reveal.

Secondly, the accuracy of the FEA method depends greatly on the accuracy of the flexibility of the attachments. This flexibility is a function of the suspension insulator's length and weight and it must include an accurate modeling of the flexibility of insulators that are not suspension posts, braced posts, V-strings,

etc and it must include an accurate model of the support structure itself. This latter point is usually ignored completely which is reasonable for stiff latticed towers but not so reasonable for tall steel poles or any form of wood pole structure that can be considered extremely flexible or impacted by soil condition.

The real value of FEA methods is to model the unusual events such as uneven ice loads, point loads on a span, or extreme temperature diversions from the temperature of tension equality. Short of that, the method should potentially be considered capable of providing the wrong answer with excellent precision. The final thing to understand about FEA modeling is that is a static model. Dynamic actions are not generally modeled or understood by FEA.

3.2. Modeling ACCC Conductor Sag & Tension

The discussions above are intended to ensure that we have addressed all factors that play a role in setting goals and constraints in sag-tension calculations for transmission line conductors. This section describes the various models used to make these calculations. The intention is to be specific enough with each models' features that an understanding can be gained regarding the merits and pitfalls of each model with respect to ACCC conductor installations. Due to the propensity of the ACCC conductor's fully annealed aluminum strands to plastically deform under very little load, CTC recommends that the Experimental Plastic Elongation (EPE) model be used to evaluate ACCC conductor sag and tension.

CIGRE Technical Brochure 324[148] offers a high caliber discussion on the topic of sag, tension, and modeling methods. It is an excellent resource. There are three very different calculation methods described in that document: linear elastic (LE) model, simplified plastic elongation (SPE) model and experimental plastic elongation (EPE) model. All three are in use throughout the world. Figure 54 compares sag results in an example scenario between the EPE and SPE modeling methods. The LE model is ignored for reasons explained.

The LE model does not calculate in any way the permanent elongations of the conductor's materials due to elastic loading deformation, strand settling or

---

[148] Cigre Technical Brochure TB 324 Sag Tension Calculation Methods For Overhead Lines B2.12.3 (June 2007)

creep. It assumes the conductor is always completely elastic which they of course are not.

The SPE model also ignores permanent elongation and attempts to account for this by a somewhat standardized and estimated method usually involving adjusting the temperature to mimic the elongation of the conductor that has occurred for other reasons. For example, although the temperature may be 15°C, the permanent deformation is embraced by contemplating that the conductor temperature is hotter, say 90°C. Clearly, the more inelastic the actual behavior of a conductor and the less experience that the designer has with it, the lower the trust in either of these calculation methods should be.

The EPE model does account for all of the components of elongation, permanent and temporary using data elasticity and elongation data gathered from stress-strain and creep tests. As the CIGRE TB 324 states, the EPE model is the basis for almost all work performed in North America, including with such tools as the graphical Varney method and the popular software programs: PLS-CADD™ and SAG10®.
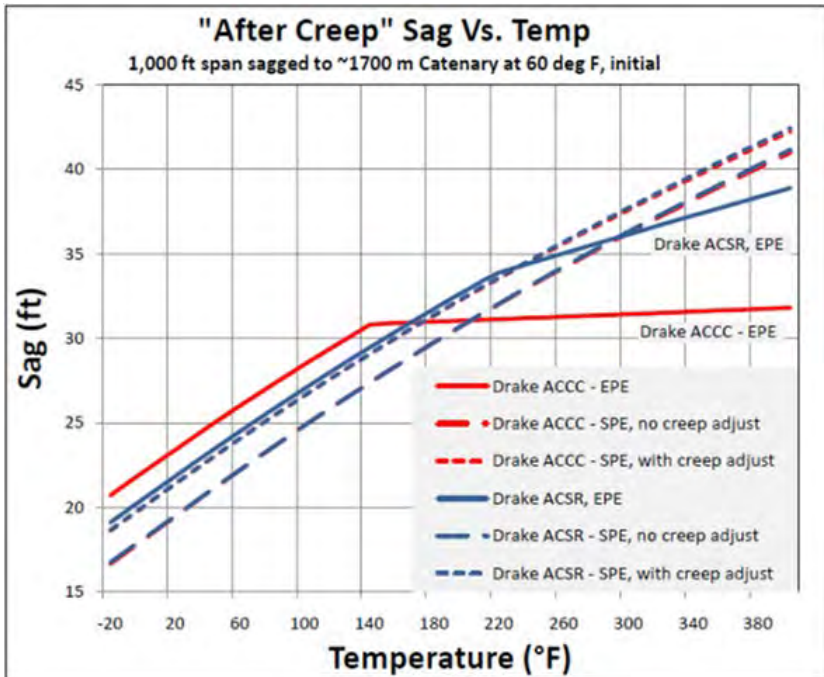
Figure 58 - Differences in calculated sag and tension of ACSR & ACCC conductor using different modeling methods. The EPE method is the most accurate method.

In Figure 58, the ACSR conductor plots in blue. Notice that differences between the EPE and SPE models do not show up in the SPE (or LE) modes at all and not until temperatures exceed the values applicable to the conductor type in the EPE model mode. However, for the ACCC conductor shown in red, the differences in sag between modes are huge at very applicable temperatures. The reason for the huge differences is enhanced by the very flat plot of the ACCC conductor (i.e., due to its very low CTE). The knee-point shown in the comparison graph will also change (decrease) substantially over time due to the ACCC conductor's very pliable aluminum strands. So, we see that it is very difficult to determine the extraordinary merits of ACCC conductors without a modeling method that can address the true behavior of conductors very well. The use of the EPE modeling mode is highly recommended for use with ACCC conductors.

165

3.3. Modeling ACCC Sag & Tension using PLS-CADD™

PLS-CADD™ is a transmission line analysis and design software program written and maintained by Power Line Systems, Inc of Madison, Wisconsin, USA. The program's calculations are done in a 3D environment with the subject transmission line's alignment placed on a 3D terrain surface. Linked structural programs allow the modeling and structural analysis of all types of support structures: lattice towers (PLS-TOWER™), wood, concrete, steel and fiberglass poles (PLS-POLE™), and drilled pier foundations (CAISSON™). PLS-CADD™ has been well received around the world and it is the most widely used software platform for transmission line engineering in the world today.

3.3.1. The Stress-Strain Relationship

PLS-CADD™ uses an EPE model for sag and tension calculations but can revert to the LE and SPE models, if desired. This discussion is of the EPE model. It is very useful to understand the stress-strain relationship so that EPE type sag-tension calculations can be interpreted properly. Figure 59 shows the load-strain plot of an ACCC conductor. The load tracks as described here. The numbered steps refer to the numbered arrows in the Figure 59.

1. Load tracks from zero up the initial curve to 30% RTS and is held for 30 minutes where the strain increases while the load is held steady.
2. Load is released back to zero
3. Load is taken up to 50% RTS. In doing so, it retraces the path of its unloading from the 30% RTS loading.
4. Once the load exceeds the previous maximum of 30% RTS, it continues to track along the initial curve to the 50 % RTS hold of one hour.
5. The load is released back to zero. It tracks along the composite (combined core and aluminum) MOE until the now deformed aluminum unloads all stress and the core carries all tension and the MOE of the core defines the slope of the plot to the origin.
6. The load is taken up to 70% RTS and, as before re-traces the path of its unloading from the 50% RTS loading.

166

7. Once the load exceeds the previous maximum of 50% RTS, it continues to track along the initial curve to the 70 % RTS hold of one hour.
8. The load is released back to zero and again, it tracks along the composite (combined core and aluminum) MOE until the elongated aluminum unloads all stress and the core carries all tension and the MOE of the core defines the slope of the plot to the origin.
9. After a large load has been applied, the stress-strain relationship of the ACCC conductor easily resides ever after on the core because the soft aluminum has been deformed to the point where it will never carry stress unless the extreme load is repeated.

There are two things to glean from this loading description.

1. The stress-strain relationship rides on the initial curve ONLY when the load is greater than it has ever been in the past. Otherwise, it resides on the composite slope (Region 2 as described in section 2.8.3) when above the mechanical knee-point or on the core slope (Region 1) when strain is below the knee-point strain. The composite slope is represented by lines 2,3,5,6 and 8, but can be located at any position within this area depending on the maximum load encountered. The slopes shown are based on increases in tension to 30, 50, and 70% RTS.
2. The stress at which the aluminum ceases to participate in the load sharing is the knee-point. The knee-point moves to higher and higher strains as the aluminum is increasingly deformed. Below the knee-point (as represented at any point on line 9) the aluminum is not engaged and therefore has little to no stress.
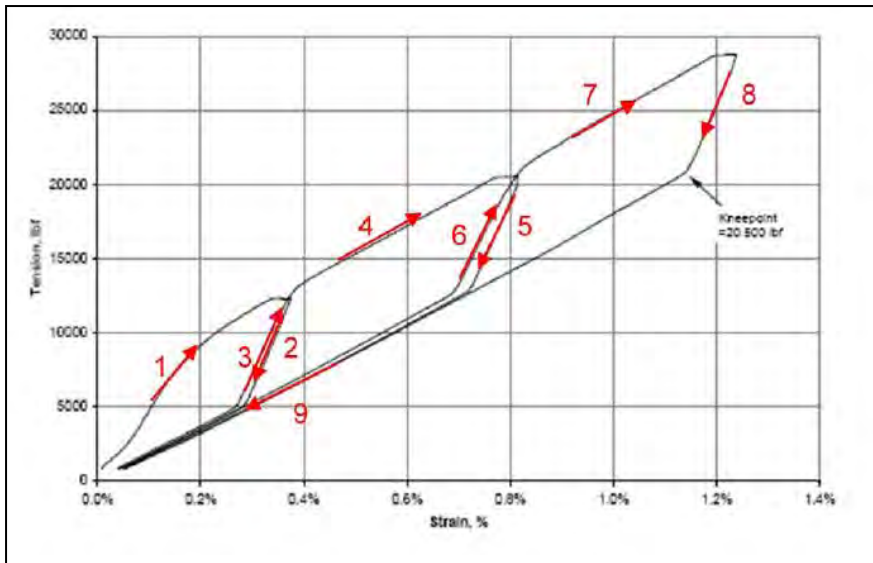
Figure 59 - Stress-strain and load sharing of ACCC conductor. Graph shows the mechanical knee point where the aluminum completely unloads its mechanical load to the core after excursions to increasingly higher tensions.

Figure 60 illustrates another point. This figure shows a repeated loading to a common tension. In the figure's case, the load is very large, at 85% RTS. Regardless of the load level, the pattern would be the same. On each application of the load, the track shows continued strain growth but at a decreasing rate. The figure shows that a hold longer than one hour, even in the form of a series of applications causes strand settlement, elastic and some creep deformation to continue. The point to notice is the shifting of the one-hour initial curve shown in red to a higher strain for a given stress as the hold time increases from one hour to, in this case: five hours. The five hour initial stress-strain curve is shown in green.

Figure 60 - Aluminum strands yield quickly under repetitive (or sustained) high loads.
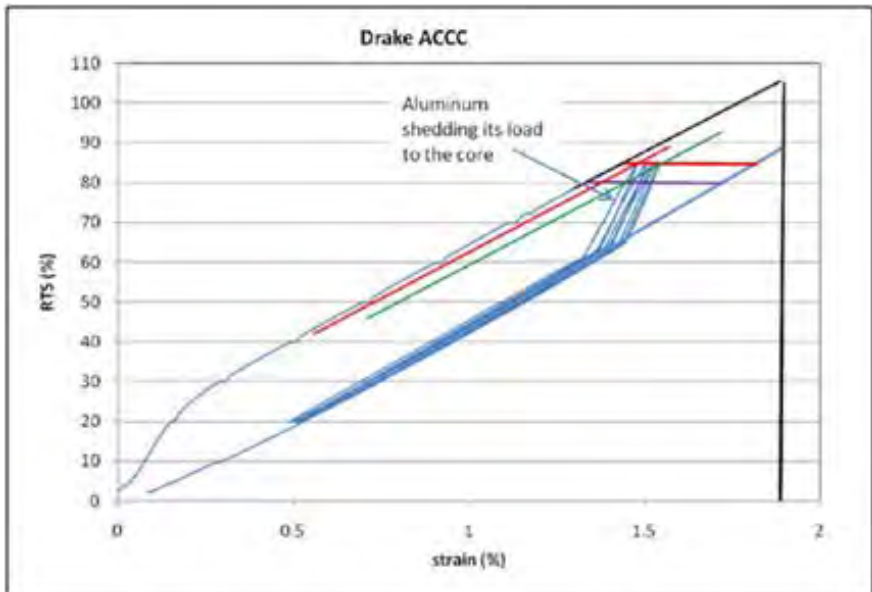
3.3.2. Development of Stress-Strain Curves and "Wire Files"

EPE sag-tension models have been developed to understand when the conductor is operating on the initial curve, the composite (combined) final curve, and the core's final curve. The purpose is based on the belief that understanding the conductor's state in this way provides more accurate sag and tension results based on snap shots of its load history or load expectations.

Recall that the LE model ignores creep and elastic deformations and the SPE model mimics them with a presumably suitable temperature shift as a substitute strain increase, and neither can accurately model the three regions of the ACCC conductor stress-strain curve as discussed in section 2.8.3. The EPE model uses a suitably correct initial curve derived from stress-strain test data and a 10-year creep curve to provide the understanding of these deformations. These initial and creep curves are defined for EPE models by 4th order quadratic equations in the form:

169

$$\text{Stress} = A + B \cdot \epsilon + C \cdot \epsilon^2 + D \cdot \epsilon^3 + E \cdot \epsilon^4 \qquad (3\text{-}19)$$

Where: ϵ is strain, and A, B, C, D and E are polynomial constants.

The four polynomial constant sets for the initial and creep curves for the core and for the aluminum have been published for common conductors for decades through the Aluminum Association of America, among other sources. It is important to recognize that the published values and the use of the 4th order equations are an established system that has been in place for decades and it has worked well for typical conductors but does have its limitations and peculiarities.

If you plot nearly any conductor's published curves you will find that the curve stops tracking properly at strains above about 0.6% to 0.7% strain. For conductors such as ACSR and AAC (all aluminum) that have breaking strains of about 1%, this is acceptable. To make calculations at strains above 0.6%, these equations fail. Since conductors like ACCC require the stress-strain relationship be accurately known at strains higher than 0.5%, PLS-CADD™ and it's near identical calculation engine, SAG10® (an Alcoa program now owned and maintained by Southwire Company), modified the stress-strain curves as follows. The slope of the initial and creep curves are calculated at 0.5% strain and the plots are projected forward to all greater strains at that slope. This works very well for ACCC conductors and can also make calculations for ACSS conductors more accurate.

Figures 61 shows that the initial curves for an ACCC 520 mm² (Dublin) conductor. Beyond about 0.5% strain the curves are straight due to the very strainable soft aluminum and elastic core. Still, the development of polynomial constants for ACCC conductors requires tracking the accurate initial curve at strains below 0.5% strain *while also* hitting a suitable slope for projection all the way to 2% strain. This also requires making an assessment of the one hour initial curves 'best fit' location at low strains. Laying the initial curve where desired matters most in the very low strain region.
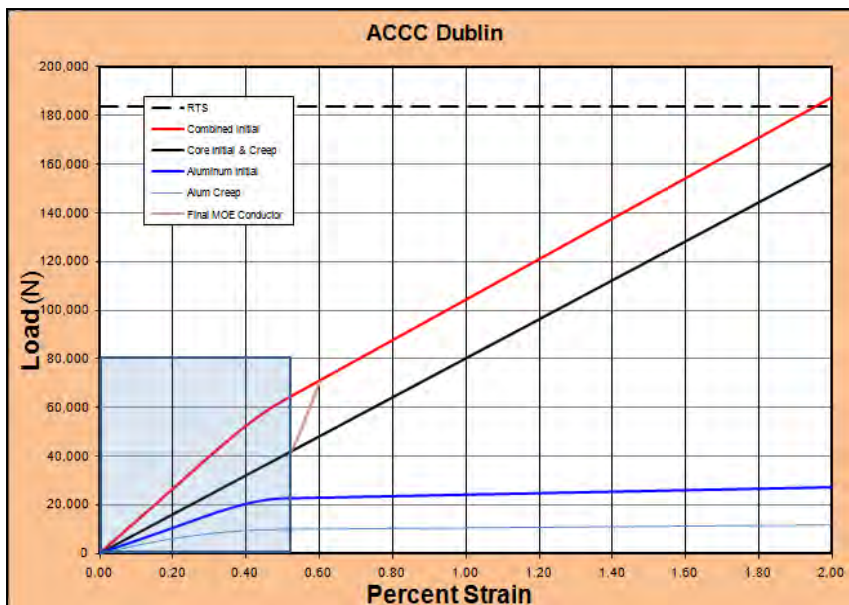
Figure 61 - Shows the stress-strain curve for ACCC Dublin size
conductor. The area in blue shows the strains (using PLS-CADD™),
wherein the initial and creep polynomials for the aluminum and core are
utilized. Above 0.5% strain, the slope calculated from the polynomial at
0.5% strain is projected out to 2% strain.

For new ACCC conductor sizes, generic stress-strain curves for the fully
annealed aluminum and composite cores have been developed that accurately
predict what has also be measured during stress-strain testing. Generic stress-
strain curves are developed as follows:

1) The proposed cross-sectional areas for the aluminum and core are
   assumed.
2) An intrinsic, initial modulus curve for the aluminum has been
   developed based on numerous measurements performed on conductor
   samples over the past several years by various ACCC conductor
   stranders. Equation 2-23 in section 2.8.3 is the intrinsic curve and is
   shown here again, which takes into account that, at 0.5% strain, the
   slope of the line is such that it will accurately represent the aluminum
   curve beyond the 0.5% strain.

171

$$y(\text{initial}) \ (MPa) = 0 + 101x - 54.4x^2 + 349.8x^3 - 606.4x^4 \quad (3\text{-}20)$$

(accurate to 0.5% strain)

$$y(10 \ \text{year creep}) = 73.9 \ x - 71.6 \ x^2 \quad (3\text{-}21)$$

where values are already divided by 100 so that they can be multiplied by the % strain.

3) The individual core intrinsic modulus values are shown in Table 4. With the exception of the 0.345" (8.76 mm) diameter core, all cores exhibit a 16.3 Msi (112.3 GPa) modulus, while the 0.345" (8.76 mm) core exhibits a 16.8 Msi (116 GPa) modulus. Thus, the equation that describes the core curve is:

$$y(MPa) = 11{,}230x \ (\text{all cores except } 0.345 \ \text{in } (8.76 \ \text{mm}) \quad (3\text{-}22)$$

$$y(MPa) = 11{,}600x \ (0.345 \ \text{in } (8.76 \ \text{mm core}) \quad (3\text{-}23)$$

where the values are divided by 100 so they can then be multiplied by the % strain. For the 10 year creep, since there is no creep in the composite core, the initial and final polynomials for the core are the same.

4) Since the conductor initial curve is the sum of the core and fully annealed aluminum curves, their intrinsic modulus values need to be turned into virtual ones.
   a. This is done by multiplying the initial and 10 year intrinsic aluminum and core equations by their percent of cross-sectional areas for the specific conductor the curves are being developed for.

5) PLS-CADD™ also calculates the final modulus of the conductor
   a. For aluminum, the intrinsic final modulus has been chosen to be 58 GPa (as explained in section 2.8.3)
   b. For the core, the intrinsic final modulus values are the same ones seen in Table 4.
   c. The aluminum and core final modulus values are then multiplied by their respective percentage of cross-sectional

area to get the virtual modulus values that PLS-CADD™ and other similar programs use.

6) Figure 62 shows a screen shot of a program developed by CTC Global that is used to calculate the values needed for PLS-CADD™ (and others) to accurately calculate sag/tensions for ACCC conductors.
   a. The values in the white cells inputted into the PLS-CADD™ Cable (wire) file menu.
   b. The polynomial values in the wire files are all 'virtual.'
   c. Note that PLS-CADD™ only needs the total cross-sectional area of the conductor, and in metric units, needs to know the weight of the cable in N/m, not kg/m.
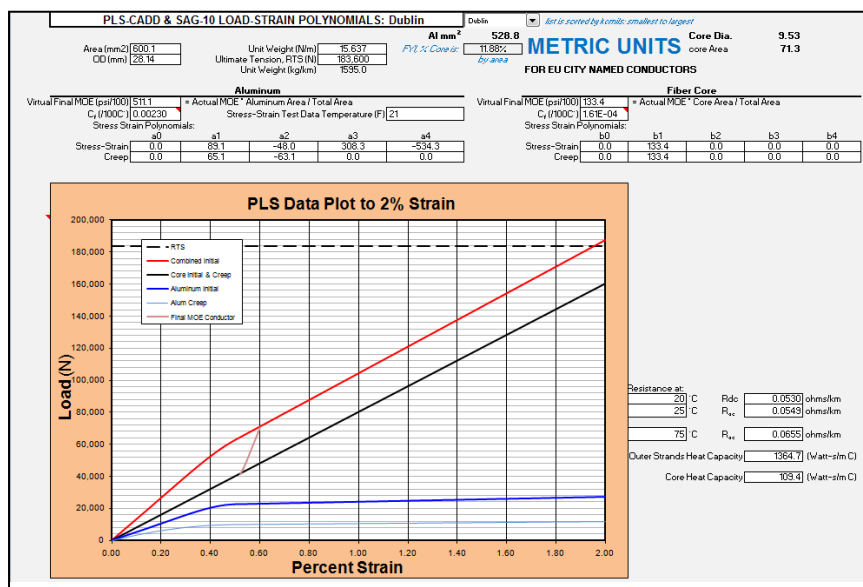
Figure 62 - Screen shot of a program used to develop generic wire files for ACCC conductors. The values in the white cells are inputted into the "Create New Cable file" menu and the file saved for the specific conductor.

7) Therefore, for the Dublin shown in Figure 62:
   a. The core has an area that is 11.88% of the total area of the conductor

173

b. Multiplying Equations 2-23 and 3-19 by 0.8812 gives the values for the Stress strain for the aluminum
    i. Taking 58,000 MPa for the final modulus of aluminum and multiplying by 0.8812 gives the value shown for the Virtual Final MOE of aluminum seen in Figure 62.
c. Multiplying Equation 3-20 or 3-21 by 0.1188 give the values for the Fiber Core stress-strain values, and the Virtual Final MOE as well.
d. The unit weight in kg/m is shown as 1595 kg/km. Taking this value and dividing by 0.102 and then again by 1000 gives 15.637 N/m for the weight.
e. All wire file temperatures are set to 21°C. PLS-CADD uses this "reference temperature" as the starting temperature where the aluminum and core curves are not shifted due to temperature, as will be discussed in section 3.6.

8) It is also important to note, that the same polynomial values can also be used in Sag10®. In Sag10® though, one needs to go to Tools/Options, and pick "Use Extrapolated Curves" and then choose 0.5%.

3.3.3. Load Sharing Between the Strands & Core

Notice that Figure 62 shows that at 30% RTS, or 12,400 lbf (55.1 kN) for the ACCC Dublin size conductor, the aluminum yield point occurs at about 0.4% strain. The typical installation tension for this conductor is 6,000 lbf (26.7 kN) to 8,000 lbf (35.6 kN) or 15% to 20% RTS or higher. Conductors are strung to initial values but clearances depend on final values so the mechanics of transition from the conductor's initial state to a final state is important. The quality of the mechanic's modeling determines an appropriate level of confidence in the final sags and tensions. The EPE modeling method is intended to overcome the less accurate assumptions required of the LE model and the SPE models.

Figure 63 shows the ACCC Dublin conductor's load-strain plot from PLS-CADD™. Since most other types of conductors cannot be strained to 1% without damage, it is the program's practice to display the relationships only to 0.6% strain. In the case of ACCC Dublin size conductor this is a plot to about 16,000 lbf (71.2 kN) or 39% RTS. As noted, this conductor is likely to be

installed to a bare wire tension of about 6,000 to 8,000 lbf (26.7 to 35.5 kN) so all activity with this conductor except the occurrence of a very large ice load will occur within the bounds of this figure.
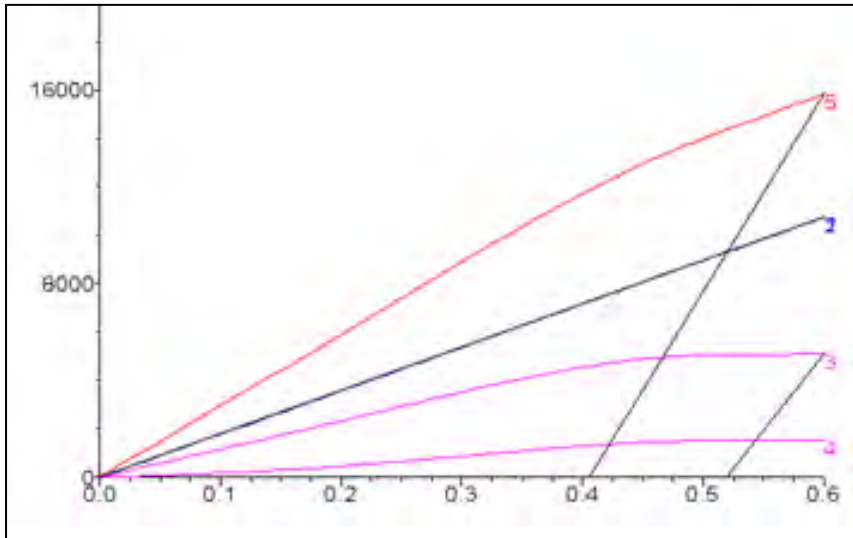
Figure 63 - ACCC Dublin size conductor PLS-CADD™ load-strain plot.

The uppermost red line (5) in Figure 63 is the initial curve for the conductor which is the sum of the black line (2, the core plot) and the aluminum curve (3). Curve 4 is the 10-year creep curve for the aluminum. The core exhibits no creep. Consider stringing the conductor at 6,000 lbf (26.7 kN) initial tension per Figure 64.
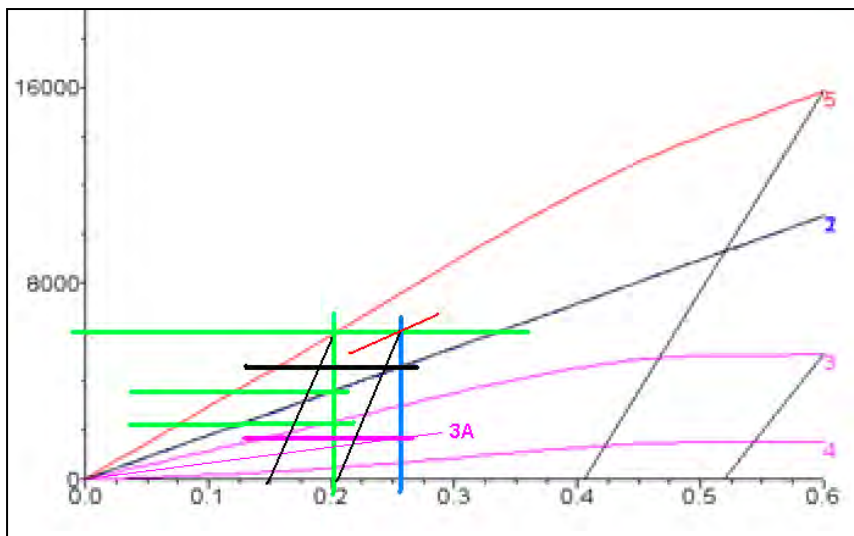
Figure 64 - ACCC Dublin conductor aluminum and core load sharing. Conductor strung in at 6000 lbf (26.7 kN) which demonstrates how the load is initially shared between the aluminum and core strands.

Assuming the initial curve (5) is correct, then the load sharing between the aluminum and core at sagging time is about 2,425 lbf (10.8 kN) and 3,575 lbf (15.9 kN) of tension, respectively, and the conductor strain is ~0.20% and the knee-point is at ~0.175% strain. Suppose the initial curve understates the permanent elongation that has taken place in the aluminum at this very early stage in the conductor's history and the aluminum is represented by curve 3A in lieu of curve 3. Now, the 6000 lbf (26.7 kN) tension is shared as expressed by the horizontal black and purple lines: 4,600 lbf (20.5 kN) in the core and 1,400 lbf (6.2 kN) in the aluminum. The conductor strain is 0.25% and the knee-point is at ~0.24% strain. All of these strain and load values are extracted from the figure visually so are approximate.

It is clear that the state of the conductor in terms of load sharing and knee-point strain is affected by the actual location of the aluminum's initial strain state at the time of measuring the installation sag.

Is the length of the core in the span different between the two calculations? The equations for the sag-tension relationship have no interest in the load sharing

176

between the conductor's core and aluminum, so the sag of both installations is the same. Therefore, the stressed length of the core is the same in both cases. Therefore, the unstressed length of the core cannot be the same between the two cases and will be different by the amount of Length of Wire * 0.05% strain in the case described here. This would be about 0.5 ft (0.15 m) difference in a 1,000 ft (305 m) span with the published curve (3) producing the longer unstressed core length compared to the possible curve, 3A.

If the elongation that may have already taken place in the aluminum at the time of sagging-in is understated, then the load in the core will be greater than calculated. This will cause the length of the core in the span to be less than calculated which will produce final sags that are less than expected.

This point is valid for all bi-material conductors but is especially important to understand for ACCC conductors because the aluminum is quite soft, yielding easily with little provocation and the core is quite elastic in response compared to a steel core. When in doubt about the amount of relaxation of the aluminum due to extended time in the travelers or by running it through many travelers, understand that the excess elongation will only result in final design sags that are *less* than expected. This is a built-in conservative feature to the ACCC conductor EPE polynomial set values.

3.3.4. Initial, After Creep & After Load Conditions

PLS-CADD™ sag-tension output reports offer three sets of data: *initials, after creep* and *after load* sags at corresponding tensions. It is important to understand the source of these values and how they relate to each other. *Initial* sag-tension values apply ONLY when the tensions are occurring for the first time, as noted above. In field conditions, these *initial* values will change rather quickly due to strand settling, creep and cold ambient conditions that can increase conductor tension causing the aluminum to stretch and subsequently shed load to the core effectively reducing overall conductor tension. It is not uncommon to see as much as a 10% reduction in conductor tension (and subsequent increase in sag) in a matter of hours or days after the conductor is first installed, because of the rapid initial creep rate of the extremely pliable aluminum. This is one reason slight pre-tensioning ~30% above the desired stringing tension can be very advantageous. The *after creep* values are based on the assumption that the conductor has experienced no loading history at all except for 10 years of a constant, bare wire tension. This would be as if the line was subjected to nothing

but a creep test with no hot or cold events, no wind events and no ice events. The *after load* values are based on the assumption that the conductor might be subjected to some defined 'heavy load' event as replicated to some degree in a typical stress-strain test. Whether the load event occurs today or 20 years from now does not affect the outcome very much.

Recall that the strains incurred by creep and by elastic deformation brought on by a large load are not additive. The strain in the conductor will be the greater of the two, but not the sum of the two. This odd reality is the reason that the *after creep* and *after load* calculations can be independent of each other in the calculation method. It is therefore incumbent on the engineer to review the output and select values accordingly.

The aforementioned program SAG10® does the same calculations but only reports the after creep *or* after load cases based on which of the two developed the greater sags. If creep developed the maximum (design) sags, the program reports that "Creep is a Factor." If a large load's sags are greater, those sags are reported along with the note, "Creep is NOT a factor." With either program, it is incumbent on the engineer to understand what caused the values to be as they are and to employ them accordingly.

The *after load* value set is defined by whatever load case that you select. Other load cases that develop higher tensions are reported for interest but they have no impact on the *after creep* or *after load* value sets. So, you can for example design the line's sags for compliance with a 1" ice load with that load case used to develop the after load sags, but you can also ask for the sags and tensions for a 2" ice case in the same calculation. But, understand that the 2" ice load will not be accounted for in the *after load* sags and tensions.

Similarly, it should be noted that, if the tension of the conductor was ever raised to a value greater than the sagging-in tension while still in travelers, then the sagging table sags and tensions are in error for all tensions below the sagging in tension. This is because the sagging table values are derived only from the *initials* value set. As described, the sags and tensions for all conditions below the maximum tension seen to date are to be derived from the *after load* value set provided the tension defining the *after load* set is the maximum tension seen to date.

Under normal construction sequencing, the conductor is pulled in at a tension below the sagging-in tension and will be pulled up to the sagging tension only at the last hour or so before being locked down. A tension spike could occur if the conductor has been left in the sheaves at a reasonable tension for a long period and subjected to very low temperatures, big wind or ice. This could be called an inadvertent pre-tensioning or pre-stressing.

3.3.5. Pre-Tensioning

The goal is to model an ACCC conductor that has experienced a pre-tension load and extract any necessary outputs. The specific goal is to pre-tension the conductor to a load that will eliminate stress on the outer layers of the conductor at the Average Annual Minimum Temperature 'AAMT' load case, as long as the contractor and structures can handle this maximized load in a safe manner. The example given could be considered relatively extreme, to help make certain points.

Technically, the goal is to place the conductor *completely* on its core's *after load* line at the AAMT case and therefore lies on this line for any condition with less tension (i.e.: with higher temperatures than the AAMT).

3.3.6. Define and Apply the Pretension Load Case

The pre-tension load case will consist of a weather case with a temperature equal to the temperature at which the pre-tensioning will take place. This is necessary to avoid including any unwanted thermal elongation differences between the pretension case vs. the AAMT case. It is necessary to develop tension with ice or wind only because PLS-CADD™ does not have the feature that allows the direct input of a tension. The pretension load must not be mimicked using a very cold condition, as this will cause havoc with the stress vs. strain values by differentially shifting these curves a great distance horizontally.

3.3.7. Setup

Place an ice load weather case in the "Criteria/Weather" dialog window to generate the pre-tension. Call it "Pretension." Use ice rather than wind because ice is an easier way to model conductor tensioning. Enter a nominal amount of ice by thickness or unit weight (Table 27). The actual ice load for this weather case is to be determined in the following steps, so initially set the ice load for

this weather case to the maximum design ice load. Even though you are placing ice on the conductor in this weather case, the temperature for the Pretension case MUST be an approximation of the pending pre-tensioning temperature.

Weather Cases

See Criteria/Code Specific Wind and Terrain Parameters for more information on height adjustments and gust response factors.

	Description	Air Density Factor (Q) psf/mph^2	Wind Velocity (mph)	Wind Pressure (psf)	Wire Ice Thickness (in)	Wire Ice Density lbs/ft^3	Wire Ice Load (lbs/ft)	Wire Temp. (deg F)	Ambient Temp. (deg F)
1	EDT	0.00256	0	0	0	0	0	60.0	60.0
2	AAMT	0.00256	0	0	0	0	0	14.0	14.0
3	MOT	0.00256	0	0	0	0	0	356.0	356.0
4	NESC Heavy	0.00256	39.5285	4	0.5	57	0	0.0	0.0
5	Heavy Ice 1"	0.00256	0	0	1	57	0	30.0	30.0
6	High Wind 90 mph	0.00256	90	20.736	0	0	0	60.0	60.0
7	Pretension	0.00256	0	0	0	57	0.5	60.0	60.0

Table 27 - Inserting an ice load weather case in the "Criteria/Weather" dialog window to generate pre-tensioning

Use this new pre-tension weather case in the "Creep-Stretch…" dialog box to define/control the final *after load* output (Table 28).

Table 28 - Naming a pre-tensioning load case

Now, use the AAMT, *after load* case as the ONLY tension controlling condition in the Automatic Sagging dialog box (Table 29)

Table 29 - Setting the AAMT, *after load* case as the ONLY tension controlling condition in the Automatic Sagging dialog box.

Although not universally used to help determine damper needs, the AAMT weather case is an important line item in all projects' criteria files. Assign the LOAD RS condition to the AAMT weather case and specify the tension limit to that which will become the tension on the line after relaxing from the pretension and when sagging the line in. Typically an AAMT tension limits uses an *initial* cable condition. When pre-tensioning, the goal is for the *after load* condition to reflect the *after pretension, that then becomes the initial* condition of the conductor.

Figure 65 graphically illustrates the pretension and the sagging (AAMT) tension on the Conductor's load-strain plot. In this plot, the aluminum and the core both pass through the origin. This is the case when the temperature is the testing laboratory temperature (stated in the wire file). At cooler temperatures, the aluminum curves shift to the left by the strain of thermal shrinkage, and to the right for warmer temperatures. So, if your pretension weather case temperature is different from the laboratory temperature, there will be an aluminum shift involved. This shift results in a difference in required pre-tension and is the rationale for the pre-tension weather case reflecting the expected pre-tension temperature.

The objective in selecting a pre-tensioning value via the pre-tension weather case is to place the knee-point on the core plot (line 2 in the Figure 63) to the right of intersect between the core plot and the AAMT tension. This indicates the off-loading of tension from the aluminum at this tension and all lower tensions to maximize the self-damping of the conductor and reduce stress in the aluminum strands to reduce susceptibility of the aluminum strands to fatigue failure.
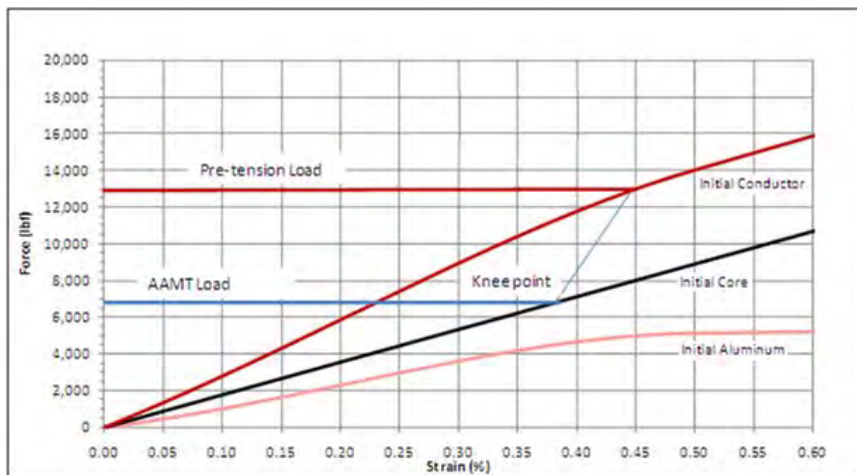
Figure 65 - Shows the pre-tensioning required to relieve all Aluminum tensile load
at the AAMT tension.

3.3.8. Iterative Sag-Tension Runs

With the above setup steps completed, you iteratively adjust the ice thickness or weight in the pretension weather case until you achieve the desired result of having no load on the outer strands (aluminum) at the AAMT weather case.

Automatically sag the conductors and review the resulting sag-tension report. Check that the AAMT weather case controlled the tension as intended. Look at the aluminum load in the *after load* column in the "tension distribution in inner and outer materials" (lower part) of the report. If the load is above zero and if you want to maximize the value of pre-tensioning, then you should increase the pretension weather case ice. This will increase the pretension and drive the load in the aluminum to lower values.

In Table 30, the tension is properly controlled by the AAMT tension limit, but the aluminum strands still carry 3,328 lbf (14.8 kN) of load at the AAMT case. In this instance the pretension ice load needs to be increased until this load is driven to zero or lower.

```
Section #1 from structure #1 to structure #2, start set #1 'de', end set #1 'de'
Cable 'r:\pls\pls_cadd\projects\113779\pretension\cables\drake_accc_tw_2010.wir', Ruling span (ft) 1000
Sagging data: Catenary (ft) 6196.8, Tension (lbs) 6487.43 Condition I Temperature (deg F) 60
Weather case for final after creep EDT, Equivalent to 15.3 (deg F) temperature increase
Weather case for final after load Pretension, Equivalent to 32.5 (deg F) temperature increase


Ruling Span Sag Tension Report

 ----Weather Case--- | --Cable Load-- | ----R.S. Initial Cond.---- | -----R.S. Final Cond.----- | -----R.S. Final Cond.----- |
                     |                |                            |  -------After Creep------ |  --------After Load-------- |
 # Description       | Hor. Vert Res. | Max. Hori.   %         R.S. | Max. Hori.   %        R.S. | Max. Hori.   %        R.S. |
                     | -----Load----- | Tens. Tens. UL    C   Sag | Tens. Tens. UL    C   Sag | Tens. Tens. UL    C   Sag |
                     | ---(lbs/ft)--- | (lbs) (lbs)     (ft) (ft) | (lbs) (lbs)     (ft) (ft) | (lbs) (lbs)     (ft) (ft) |
-----------------------------------------------------------------------------------------------------------------------------
 1 EDT           0.00 1.05 1.05    6506  6485 16  6195 20.19    6136  6164 15  5888 21.24    5871  5848 14  5586 22.39
 2 AAMT          0.00 1.05 1.05    6917  6397 17  6588 18.93    6898  6873 17  6570 19.03    6823  6803 17  6498 19.25
 3 MOT           0.00 1.05 1.05    4638  4608 11  4402 28.43    4338  4306 11  4113 30.43    4338  4306 11  4113 30.43
 4 NESC Heavy    0.70 2.05 2.46   10589 10517 26  4268 29.32   10589 10517 26  4268 29.32   10589 10517 26  4268 29.32
 5 Heavy Ice 1"  0.00 3.67 3.67   12843 12710 31  3465 36.14   12843 12710 31  3465 36.14   12843 12710 31  3465 36.14
 6 High Wind 90 mph 1.91 1.05 2.18 9594  9531 23  4368 28.65    9594  9531 23  4368 28.65    9594  9531 23  4368 28.65
 7 Pretension    0.00 1.55 1.55    7947  7909 19  5113 24.47    7947  7909 19  5113 24.47    7947  7909 19  5113 24.47


Tension Distribution in Inner and Outer Materials

 ----Weather Case--- | --Initial Condition- | --Final After Creep- | --Final After Load-- |
                     | Horiz. Tension (lbs) | Horiz. Tension (lbs) | Horiz. Tension (lbs) |
 # Description       |                      |                      |                      |
                     | Total  Core  Outer | Total  Core  Outer | Total  Core  Outer |
-----------------------------------------------------------------------------------------------
 1 EDT              6485   3652  2833    6164   3841  2323    5848   4025  1823 |
 2 AAMT             6897   3516  3380    6878   3493  3386    6803   3474  3328
 3 MOT              4608   4964  -356    4306   5487 -1181    4306   5487 -1181
 4 NESC Heavy      10517   5730  4787   10517   5730  4787   10517   5730  4787
 5 Heavy Ice 1"    12710   7710  5000   12710   7710  5000   12710   7710  5000
 6 High Wind 90 mph 9531   5466  4066    9531   5466  4066    9531   5466  4066
 7 Pretension       7909   4483  3426    7909   4483  3426    7909   4483  3426
```

Table 30 - PLS-CADD™ sag/tension chart and tension distribution chart, for
ACCC Drake conductor being used to model a desired level of pre-tensioning. The
tension is properly controlled by the AAMT tension limit, but the aluminum strands
still carry 3,328 lbf (14.8 kN) of load at the AAMT case. In this instance the
pretension ice load needs to be increased until this load is driven to zero or lower.

After increasing the pretension ice load, automatically sag the conductors and
review the resulting sag-tension report. This process is repeated until a
pretension ice load results in a sag tension report that shows tension properly
limited by the AAMT case and load removed from the aluminum strands at the
AAMT case, an example of this desired output is provided in Table 31. The
negative tension in the outer strands is related to allowing the aluminum strands
to go into compression.

```
Section #1 from structure #1  to structure #2, start set #1 'de', end set #1 'de'
Cable 'r:\pls\pls_cadd\projects\113779\pretension\cables\drake_accc_tw_2010.wir', Ruling span (ft) 1000
Sagging data: Catenary (ft) 11024.8, Tension (lbs) 11541.9  Condition I Temperature (deg F) 60
Weather case for final after creep EDT, Equivalent to 18.5 (deg F) temperature increase
Weather case for final after load Pretension, Equivalent to 166.3 (deg F) temperature increase


Ruling Span Sag Tension Report

----Weather Case--- | --Cable Load-- | ----R.S. Initial Cond.---- | -----R.S. Final Cond.----- | -----R.S. Final Cond.----- |
                    |                |                            | -------After Creep------- | -------After Load-------- |
# Description       | Hor. Vert Res. | Max. Hori. %          R.S. | Max. Hori. %          R.S. | Max. Hori. %          R.S. |
                    | -----Load----- | Tens. Tens. UL    C   Sag | Tens. Tens. UL    C   Sag | Tens. Tens. UL    C   Sag |
                    | ---(lbs/ft)--- | (lbs) (lbs)      (ft) (ft) | (lbs) (lbs)      (ft) (ft) | (lbs) (lbs)      (ft) (ft) |
-------------------------------------------------------------------------------------------------------------------------------
1 EDT               | 0.00 1.05 1.05 | 11554 11542 28 11025 11.34 | 10584 10571 26 10097 12.38 |  6769  6749 16  6446 19.40
2 AAMT              | 0.00 1.05 1.05 | 11853 11841 29 11311 11.05 | 11350 11839 29 11309 11.06 |  6824  6804 17  6499 19.24
3 MOT               | 0.00 1.05 1.05 |  8010  7993 19  7635 16.38 |  6481  6460 16  6171 20.27 |  6467  6446 16  6157 20.31
4 NESC Heavy        | 0.70 2.05 2.46 | 13778 13722 34  5569 22.46 | 13778 13722 34  5569 22.46 | 12723 12668 31  5141 24.33
5 Heavy Ice 1"      | 0.00 3.67 3.67 | 15575 15466 38  4216 29.68 | 15575 15466 38  4216 29.68 | 15574 15465 38  4216 29.69
6 High Wind 90 mph  | 1.91 1.05 2.18 | 13246 13201 32  6050 20.67 | 13246 13201 32  6050 20.67 | 10311 10253 25  4699 26.63
7 Pretension        | 0.00 3.95 3.95 | 15959 15835 39  4012 31.20 | 15959 15835 39  4012 31.20 | 15959 15835 39  4012 31.20


Tension Distribution in Inner and Outer Materials

----Weather Case--- | --Initial Condition- | --Final After Creep- | --Final After Load-- |
                    | Horiz. Tension (lbs) | Horiz. Tension (lbs) | Horiz. Tension (lbs) |
# Description       |                      |                      |                      |
                    | Total   Core  Outer  | Total   Core  Outer  | Total   Core  Outer  |
------------------------------------------------------------------------------------------
1 EDT               | 11542   6804   4738  | 10571   6918   3653  |  6749   7932  -1183
2 AAMT              | 11841   6848   4993  | 11839   6846   4993  |  6804   7977  -1173
3 MOT               |  7993   6985   1007  |  6460   7643  -1183  |  6446   7629  -1183
4 NESC Heavy        | 13722   8647   5076  | 13722   8647   5076  | 12668   9046   3623
5 Heavy Ice 1"      | 15466  10356   5110  | 15466  10356   5110  | 15465  10355   5110
6 High Wind 90 mph  | 13201   8190   5011  | 13201   8190   5011  | 10253   9500    753
7 Pretension        | 15835  10737   5098  | 15835  10737   5098  | 15835  10737   5098
```

Table 31 - Example of sag/tension and tension distribution chart when performing
pre-tensioning in PLS-CADD™. In this case the strands carry no load but have
gone into compression as discussed below

The amount of negative stress allowed in the outer strands is governed by the
value of "maximum virtual compressive stress" in the Bimetallic Conductor
Model of the cable file and/or criteria file (Table 32). In this instance the value
is set to 1.3 ksi. Selecting a different value will raise or lower the horizontal
line of the "outer strand after load" plot along the y-axis. Lowering the
compressive stress value will result in a reduced pretension load.

Whether ACCC conductors should be modeled as compression-capable or not
is a separate subject as discussed in Section 2.8.7 above. Here, we are only
pointing out that the choice impacts the pre-tensioning value modestly.

Table 32 - Bi-metallic compression option as discussed in Section 2.8.7

3.3.9. After Pre-Tension Outputs

With the pre-tension load case defined and selected as the after load weather case all PLS-CADD™ sag tension data taken from the *after load* condition refer to the after pre-tensioning behavior. The *after load* case essentially becomes the *initial* case and the PLS-CADD™ data listed as the *initial* values have been rendered irrelevant. They will never occur. Also, it is likely that the *after creep* sag values will result in less sag than this *after load* case. If this is the case, the *after creep* column can also be disregarded.

It is critical to understand that installation stringing charts now require *after load*, not *initial* outputs.   Likewise, the AAMT condition for damper recommendations should correlate to this *after load* case. Any further PLS-CADD™ analysis should consider the *after load* case.

It is expected that this procedure will result in a pre-tension load similar to the maximum design load, although if the maximum design load is much greater than the pre-tension load, consideration should be given to the additional stretch

in excess of the pre-tension load stretch for design value production. The *after load/pre-tension* case refers to the stress vs. strain behavior after pre-tensioning but prior to the occurrence of the maximum design load.   The *after load/maximum design load* case refers to final stress vs. strain behavior after this maximum design load occurs. This requires a second run of the sag-tension calculation with the larger, design ice load replacing the pre-tension ice load as the load case defining the after load values.

If field pre-tensioning will use sag to achieve the pretension load, be aware that the pre-tension weather case refers to sags of an ice-loaded conductor and will not provide the sags of a tight, bare conductor appropriate to achieve the pre-tension load during construction. The pre-tension sag will require further work to determine.

Determining the bare wire sag that will result in the pre-tension load requires some <u>temporary</u> changes to the PLS-CADD™ file for the desired "pre-tension" event sag output. First, create a new weather case, call it "Pre-tension Sag" (Table 33). This weather case will have the same temperature as the "Pre-tension" weather case.

Weather Cases

See Criteria/Code Specific Wind and Terrain Parameters for more information on height adjustments and gust response factors.

	Description	Air Density Factor (Q) psf/mph^2	Wind Velocity (mph)	Wind Pressure (psf)	Wire Ice Thickness (in)	Wire Ice Density lbs/ft^3	Wire Ice Load (lbs/ft)	Wire Temp. (deg F)	Ambient Temp. (deg F)
1	EDT	0.00256	0	0	0	0	0	60.0	60.0
2	AAMT	0.00256	0	0	0	0	0	14.0	14.0
3	MOT	0.00256	0	0	0	0	0	356.0	356.0
4	NESC Heavy	0.00256	39.5285	4.00001	0.5	57	0	0.0	0.0
5	Heavy Ice 1"	0.00256	0	0	1	57	0	30.0	30.0
6	High Wind 90 mph	0.00256	90	20.736	0	0	0	60.0	60.0
7	Pretension	0.00256	0	0	0	57	0.5	60.0	60.0
8	Pretension Sag	0.00256	0	0	0	0	0	60.0	60.0

Table 33 - Creating a 'temporary' pre-tension weather case

Next, revise the Automatic Sagging Criteria to consider this weather case and set the Maximum Tension to the pretension load, as in Table 34.

Automatic Sagging Criteria					
	Weather case	Cable condition	% of Ultimate	Maximum Tension (lbs)	Maximum Catenary (ft)
1	Pretension Sag	Load RS		16000.000	

Table 34 - Revising the Automatic Sagging Criteria

Auto-sag the section and extract the resulting pre-tensioning sag information for the desired temperature.

3.4. Alternate Modeling Methods

The PLS-CADD™ and SAG10® software packages are a computerized, mathematical simulation of the graphical Varney method. As noted, they both use the same wire data, including polynomial constants for the 4th order quadratic equations. Any other form of calculation, LE, SPE or EPE models that is not a Varney method mimic or does not use these particular polynomials is a different calculation with different inherent assumptions and accuracies.

It should be obvious that LE models will provide very inaccurate results for ACCC conductors. Once the temperature equivalency of ACCC conductors is studied and suitable values are developed, the SPE model might provide reasonable results. Certainly, the EPE model is meant to be the best mimic of the mechanical nature of conductors by addressing actual issues 'head on.' Still, the discussions above should reveal, as does the section on accuracies below, that sag-tension calculations should never be read to the third significant digit, regardless of the model.

3.5. Accuracy of Calculations and Clearance Buffers

CIGRE Technical Brochure 324[149] discusses at some length the various reasons why the results of a sag-tension calculation will be approximate at best, even for reasons other than the varied or suspect quality of the modeling methods described above. For example, the potential, even likely underestimation of the

---

[149] Cigre Technical Brochure TB 324 Sag Tension Calculation Methods For Overhead Lines B2.12.3 (June 2007)

conductor's unit weight and the effects of stiffness at the span ends (issues that tend to balance against each other) cause doubt about the actual sag by about 0.2 meters.

Other issues, such as uncertainty of the conductor's temperature under any moment's conditions of ambient, wind, electric load; uncertainly of the mechanics and modeling of high temperature aluminum compression require consideration of an appropriate buffer on clearances.

A very recent experiment at the Oak Ridge National Laboratory facility in the USA tracked the sag of a span of ACSR conductor as its temperature was raised and lowered repeatedly through a full range of temperatures[150]. Figure 66 shows by the blue tracing of sag against temperature and reveals two things: First, the sag at any given temperature was up to 0.3 m different depending on whether the temperature was rising or falling. Second, the sag exceeds the sags predicted by either aluminum compression models (the blue and green lines) by up to 0.5 m. at high temperatures. So, despite the best modeling methods in use today, any calculation of a conductor's actual sag should be considered representative. Appropriate clearance buffers should be considered especially when high temperature operation is anticipated or when ice loads are expected to be high.

---

[150] Seppa, T. "Errors in Calculating Line Ratings for Design and Real Time Purposes" IEEE TP&C/ESMOL/CIGRE Joint Panel Session, Feb 2011, Las Vegas, NV
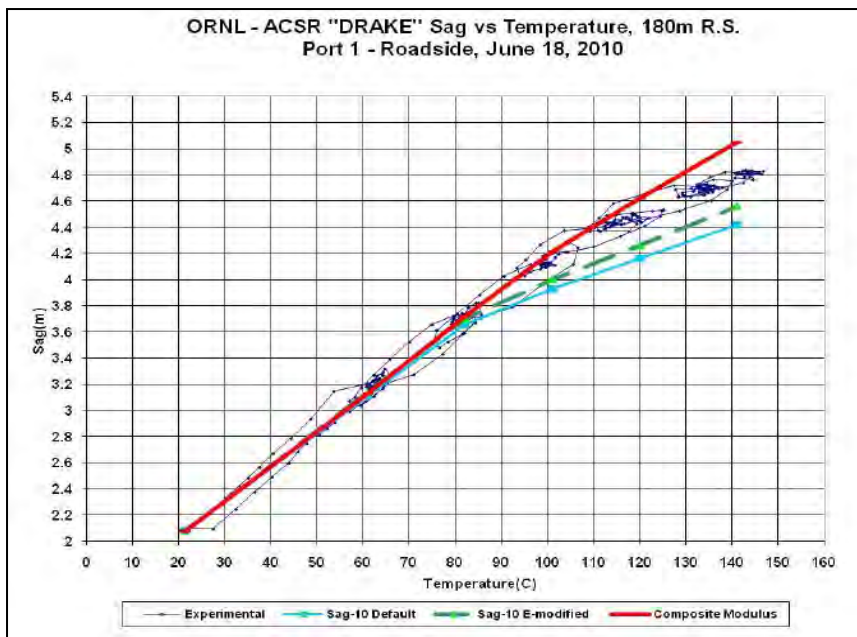
Figure 66 - Oak Ridge testing of ACSR conductor showing variation of sag and tension as the temperature is rising or falling - compared to calculated values
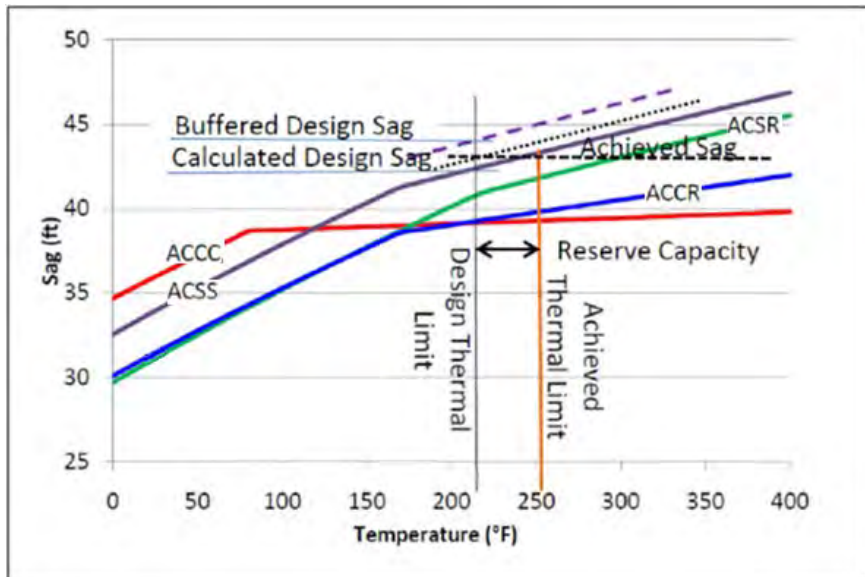
Figure 67 - Sag comparison between ACCC and other conductors showing
dimensional stability and reserve limits

The uncertainty of a span's actual sag compared to any calculations employed
leads to an opportunity that ACCC conductors are best poised to exploit. Figure
67 shows the sag vs. temperature plots of comparable ACSR, ACSS, ACCR and
ACCC conductors. The feature to observe is the slope of each plot at the high
temperatures, above the knee-points. The uncertainty of the sag at a temperature
equates to uncertainty about the temperature when the sag is known by
measurement or assumption. Uncertainty about temperature creates uncertainty
about ampacity at that sag.

Consider that a buffer is added to the calculated sag and it is deemed sufficient
to guarantee that clearances will not be less than *required* and could be as large
as *required + buffer*. This means that there is a temperature and an ampacity
value associated with the calculated sag that is guaranteed and an ampacity value
associated with the larger, buffered sag that is possible. If you were to survey
the sags after construction you should discover that the actual sag lies
somewhere between the calculated design sag and its larger, buffered value. The
actual sag intersects the sag-temperature plot at a higher temperature than the

design temperature. This is the design's reserve capacity and it was created by the buffer value chosen during design. Figure 65 illustrates that the line's reserve capacity is a function of the chosen buffer value and the slope of the conductor's sag-temperature plot. The flatter the plot, the greater is the inherent reserve capacity for a given buffer value.

The discussion above suggests that the buffer to protect against the unknowns and incalculable features of sag-tension calculations should be at least 1 ft (0.3 m). The buffer against survey and construction methods depends on the technologies used and the roughness of the terrain along the line and the type of structures being installed. One is taking a risk if the buffer for these considerations is less than about 3 ft (1 m) and if the buffer in total is less than 4.9 ft (1.5 m) for a new line design due to construction tolerances.

Figure 66 shows the difference in sag between 100°C and the ACCC conductor's maximum continuous operating temperature of 180°C which is only about 0.7 ft (0.2 m). This difference will change a bit with the design's span length and tension. If the design buffer incorporates this small sag difference between the design temperature and the conductor's thermal limits, then the reserve capacity of the line has the potential to become limited only by the thermal capacity of the ACCC conductor. No other conductor type has a sag-temperature relationship that is nearly this flat and therefore able to offer such large reserve capacity.

If the buffer for new line designs were intentionally healthy enough, the ACCC conductors offer the cost-effective ability to practically guarantee that the reserve or emergency thermal capacity of the line is the emergency thermal limit of the ACCC conductor. The sag-temperature slope of any other type of conductor prevents such a cost-effective, full use of its thermal capacity (especially after any substantial ice or wind load event that might increase the conductor's sag due to yielding).
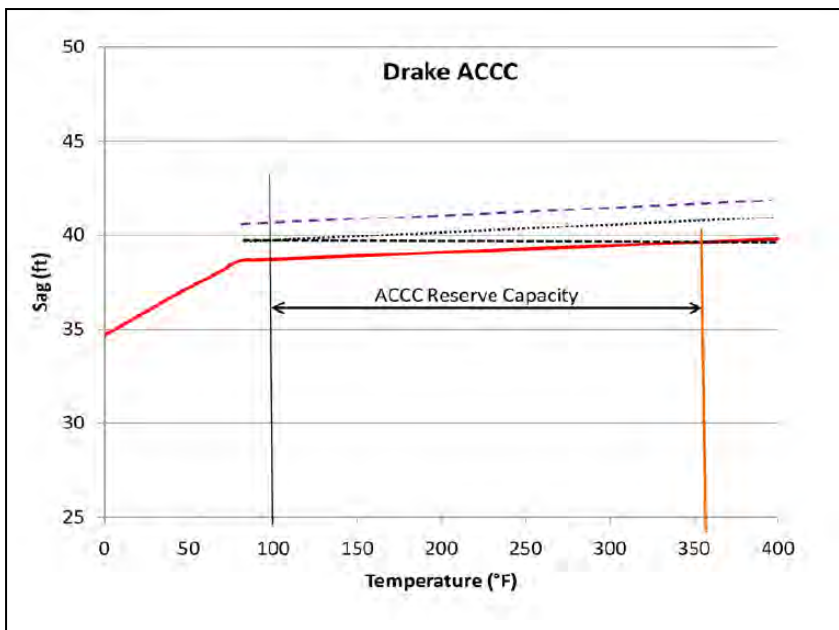
Figure 68 - ACCC conductor broadened reserve capacity defined by low thermal knee-point and low coefficient of thermal expansion of its core

3.6. Calculation of Thermal Knee Point in ACCC Conductors

To accurately determine the thermal knee-point of an ACCC conductor, it is recommended that the value is determined using EPE stress-strain models with the graphical methods as employed in programs such as PLS-CADD™ and Sag10®. The primary concerns are due to rapid aluminum yielding, and the fact that the stress-strain curve has three distinct regions where the aluminum properties are either contributing or not contributing to the coefficient of thermal expansion (CTE) and modulus of the ACCC conductor, as discussed in section 2.8.3. Therefore using basic linear equations to determine the thermal knee-points are not accurate.

To determine the thermal knee-point temperature of an ACCC conductor, when the initial stringing condition is known, i.e. 21°C at 20% RTS on a 1,000 ft (304.8 m) span, certain other conditions must be known. In this case, for an ACCC Drake size conductor, an initial tension of 8,220 lbf (36.6 kN) is used,

and the conductor weight of 1.052 lb/ft (1.565 kg/km) is known. It must also be assumed that the conductor stress-strain curve was developed at 21°C. Wire files for other common ACCC conductors are available on the Power Line Systems Inc. website (www.powline.com). Figure 69 shows the stress-strain curve of the ACCC Drake size conductor and core superimposed over the tension / % slack curve.
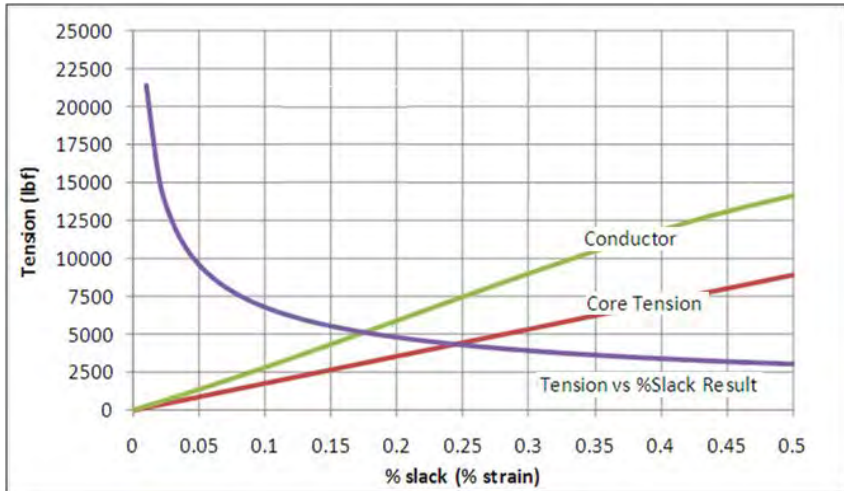
Figure 69 – Shows the ACCC Drake stress-strain curve (red for core, green for conductor) superimposed over the tension vs % slack result.

For the stated initial condition however, the stress-strain curve needs to be shifted, so that the conductor curve intersects the catenary curve at the conductor initial tension. In this case, the stress-strain curve needs to be shifted by -0.2103%, as shown in Figure 70. Thus, at 8,220 lbf (36.6 kN), the amount of slack in the conductor would be 0.0645%. The pink line represents the final conductor modulus. If the tension in the conductor was relieved, the tension would travel down the final modulus (MOE) curve until the tension reached the core curve, called the "mechanical knee point", and then travel back down the core curve until it reaches zero tension, as described in section 3.3.1.

194
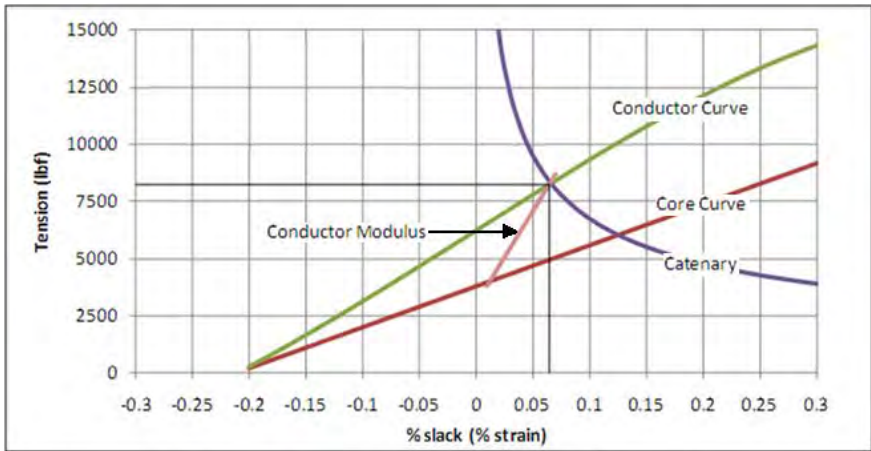
Figure 70 – ACCC Drake Stress-strain curve shifted by -0.2103% so
that the conductor curve intersects the catenary curve at 8,240 lbf (36.7
kN).

If the temperature were changed, then the aluminum and core curves would
change according to their respective CTE values[70] and change from the
reference temperature, T_{ref} (typically set to 21°C for all PLS-CADD™ ACCC
wire files). This would shift the core and aluminum curves, and thus the
conductor and final modulus curves to higher % slack values as temperature
increased, or lower % slack values if the temperatures were decreasing. For
simplicity, assume the core curve and conductor curves do not change with
temperature. If the final modulus curve, and thus the "mechanical knee point"
(@ T_{ref} in Figure 71) were to shift due to temperature only to a point where
"mechanical knee point" intersects the core curve/catenary curve, the
temperature at which this would occur would be considered the "thermal knee
point" temperature (@ T_1 in Figure 71).
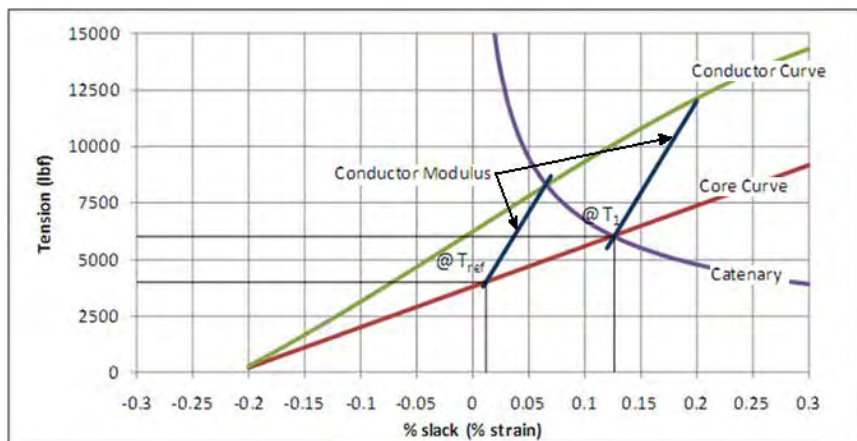
Figure 71 – Shows the change in the final modulus curve due to a
change in temperature. The new intersect point is at 0.1266% slack.

In this example, this shift would occur until a % slack of 0.1266% is reached (@ T_1), or the tension decreased to 6,036 lbf (26.8 kN) due to the thermal elongation of the conductor. In PLS-CADD™ and Sag10®, the temperature at which this point shifts to this intersection point, will show that the outer (aluminum) strands are no longer carrying load at that temperature. PLS-CADD™ and Sag10® also will shift the core curve with increasing temperature, and thus the final load on the conductor at the intersection point would actually be at a slightly higher strain than simply calculated here, or ~5,926 lbf (26.4 kN). Table 35 shows the PLS-CADD™ output for ACCC Drake size conductor, where the conductor is installed to the same initial conditions as described above.

```
PLS-CADD Version 10.79    12:45:04 PM Thursday, September 15, 2011
CTC
Project Name: '\thermal knee point determination\thermal knee point calcs.DON'

Criteria notes:
    This Criteria File is limited in scope.

Section #9 from structure #2  to structure #3, start set #4 'Left', end set #4 'Left'
Cable '\accc_drake_20110516', Ruling span (m) 304.8
Sagging data:  Catenary (m) 2387.3, Horiz. Tension (N) 36651.7 Condition I Temperature (deg C) 21
Weather case for final after creep 21C, Equivalent to 32.5 (deg C) temperature increase
Weather case for final after load 21C, Equivalent to 0.1 (deg C) temperature increase


Ruling Span Sag Tension Report

---Weather Case---  |  ---Cable Load---  |  -----R.S. Initial Cond.----  |  ------R.S. Final Cond.-----  |  ------R.S. Final Cond.-----
                    |                    |                              |  --------After Creep-------  |  ---------After Load--------
# Description       |  Hor.  Vert Res.   |  Max. Hori. Max        R.S.  |  Max. Hori. Max        R.S.  |  Max. Hori. Max        R.S.
                    |  -----Load------   |  Tens. Tens. Ten    C   Sag  |  Tens. Tens. Ten    C   Sag  |  Tens. Tens. Ten    C   Sag
                    |  ------(N/m)-----  |  (N)   (N) %UL     (m)  (m)  |  (N)   (N) %UL     (m)  (m)  |  (N)   (N) %UL     (m)  (m)
-------------------------------------------------------------------------------------------------------------------------------------
 1 21C          0.00 15.35 15.35    36717 36642  20  2387  4.87    29292 29198  16  1902  6.11    36717 36642  20  2387  4.87
 9 70           0.00 15.35 15.35    32231 32146  18  2094  5.55    26457 26353  14  1716  6.77    26609 26506  15  1726  6.73
10 71           0.00 15.35 15.35    32147 32061  18  2088  5.56    26450 26346  14  1716  6.77    26472 26368  14  1717  6.77
11 72           0.00 15.35 15.35    32062 31977  17  2083  5.58    26443 26339  14  1716  6.77    26443 26339  14  1716  6.77
33 200          0.00 15.35 15.35    25554 25446  14  1657  7.01    25554 25446  14  1657  7.01    25554 25446  14  1657  7.01


Tension Distribution in Inner and Outer Materials

---Weather Case---  |  --Initial Condition-  |  --Final After Creep-  |  --Final After Load--
                    |  -Horiz. Tension (N)-  |  -Horiz. Tension (N)-  |  -Horiz. Tension (N)-
# Description       |                        |                        |
                    |  Total   Core  Outer   |  Total   Core  Outer   |  Total   Core  Outer
-------------------------------------------------------------------------------------------------
 1 21C              36642  21968  14674      29198  25062   4137      36642  21968  14674
 9 70               32146  22956   9189      26353  26353      0      26506  26232    274
10 71               32061  22981   9080      26346  26346      0      26368  26334     34
11 72               31977  23005   8971      26339  26339      0      26339  26339      0
33 200              25446  25446      0      25446  25446      0      25446  25446      0
```

Table 35 – PLS-CADD™ output for an ACCC Drake showing that when the After Load Column calculations are set to the same weather case used for the initial stringing of the conductor, when the tension in the aluminum goes to zero, the weather case this occurs can be equated to the "thermal knee point temperature" of the conductor.

From Table 35, to determine the thermal knee point in PLS-CADD™, the 'After Load' column needs to be set to the same weather condition used for the initial stringing. In this case, it was 21°C, and can be done by looking at Table 28, looking at the "Weather Cases for After Load", and choosing the 21°C Weather Case. By doing this, this will force the final after load modulus to intersect the initial conductor curve at the tension in which the conductor was strung in at. Looking at the after load column in the "Tension Distribution in Inner and Outer Materials" table, when the tension in the outer (aluminum) shows zero, then look left to determine the weather case that gives this zero aluminum tension, and this will equate to the "thermal knee point temperature".

In Table 35, the thermal knee point occurs at a temperature between 71° and 72°C for this example for ACCC Drake. It is important to note though, that the thermal knee point will change with span and initial stringing tension. This point will also change after heavier events occur on the conductor, like high wind loads or ice conditions. This is because, load will build up along the initial conductor curve, and when the load is released, the final modulus would not be

starting at the new higher tension, and thus the knee point would have shifted and will occur at lower temperatures than the initial stringing temperature.

When programs like PLS-CADD™ or Sag10® are not available, and the "thermal knee point" needs to be determined, there is a numerical method that can be used to produce similar knee point temperatures and sag/tension results at temperatures above the initial stringing tension. The numerical method that can be used is call the Hybrid Sag Method, and is discussed in Reference.[151] Using this method, two simultaneous calculations are made, using the conductor composite properties, and the core only properties. Equations 3-13 through 3-16 are used in an iterative process to calculate change in the length of the conductor and core, separately, as a function of temperature.

The thermal knee point can be determined when the tension in the conductor matches the tension in the core from these iterative calculations. These equations can be programmed into Microsoft Excel, and the iterative calculations performed. When using the Hybrid Sag Method, the knee points that are calculated will typically be within a few degrees of what PLS-CADD™ would predict, as discussed in this section, as long as the starting stress-strain curves for the specific conductor are the same.

---

[151] A. Alwar, E.J. Bosze, S.R. Nutt, "A Hybrid Numerical Method to Calculate the Sag of Composite Conductors," Electric Power Systems Research 76 (2006), pg. 389-394.

4. Project Examples

Four project examples are offered for guidance. For the differences in approaches that exist, the first project presented is a conductor replacement project. The second project presented is a new line project. The third and fourth examples highlight the differences between ACCC and ACSS conductors. To highlight other differences, the replacement project uses parameters for spans and weather conditions that are quite different from the new line project.

4.1. Conductor Replacement Project

4.1.1. Input Data

- 115 kV circuit on wood poles, roadside construction with under-build
- Ruling span: 487 feet (148 m)
- Minimum temperature: -40ºC (-40ºF)
- AAMT: -20ºC (4ºF)
- Design ice load: ½" (12.7 mm) radial with 8 psf (383 Pa) wind @ -20ºC (4ºF)
- Conductor being replaced: Hawk ACSR
- Controlling tension: 4,850 lbs (21.6 kN) @ design ice load case, initial
- Existing ampacity: 707 A. based on 30ºC (86ºF), 4 fps (192 Pa) wind at 20º from parallel to line, latitude 47ºN.

The request is to achieve whatever ampacity can be reasonably achieved on a cost-benefit basis.

Poles are aged and classes are presumed. Corners are guyed. There are a few steel poles of unknown strength. Pole framing types are widely variable. Some poles will be replaced for age or framing arrangement or location reasons. The circuit is one of three between source and load substations. The line is about 5 miles (8 km) long.

A very good LiDAR survey of the existing line is available and a PLS-CADD™ model of the line exists with the survey as its basis.

While the expense of some structure changes can be allocated to maintenance or other capital cost subjects, there are sufficient unknowns surrounding the strength of wood poles, steel poles, guys and anchors that it is prudent for cost reasons to attempt a conductor replacement that causes no load increases on the structures.

Highly variable under-built circuits and the general premise of keeping the conductors high in an urban environment suggests that the maximum sag of the existing conductor should not be exceeded.

4.1.2. Steps

The following is a generic description of the analysis process:

1. Establish the design criteria for the analysis project. These include code and owner-based tension limits, clearances, load and strength factors for structural components, thermal limits for various conductor types, etc.

2. Establish the maximum tensions and maximum sags of the existing condition by applying criteria, noting source cases.

Establishing the maximum sag for the existing conductor requires knowledge of the original design intention. If that is unknown, then it can be calculated from the circuit's known or presumed allowable usage (MVA limit).

3. Review the clearances of the existing line condition. Flag clearance violations, if any.

4. Report structure usage of the existing condition. Flag overages.

5. Replace Hawk ACSR in model with replacement conductor.

To avoid increasing the structure over-usage, clearance violations and line design tension; the replacement conductor must (logically) be no larger in diameter, no heavier and have an equal or lower co-efficient of thermal expansion. There are only three logical candidates: Hawk ACSS, Hawk ACSS/TW or Hawk ACCC.

6. Fit each conductor type into the model. There are two choices for starting.

a. First, matching hot curves. This ensures no clearance violations (hot).

   i. In line with note 2a above, the proposed conductor can be set to a series of its own unique hot temperatures (and related catenaries) when there is no useful established limit for the ACSR for comparison. This turns the work into an exploratory venture to find a cost-effective balance between maximum sag for the proposed conductor and the cost of rehabilitating the clearance violations created by that temperature.

b. Or, match the design tension. This ensures no structure usage violations.

   i. The tension developed in the proposed conductor must be less than the highest tension that matters in the ACSR report. Note that *initial* tensions in the reports for both conductors matter and may control.

7. Check for maximum ice sag violations. This can be done with the sag-tension reports by comparing catenary constants, C. The hot limits C values will match and for ALL other cases that matter, the C value of the proposed conductor must be larger than it is for the ACSR.

8. Check the vibration damper requirement status of the proposed conductor. Do this against whatever criteria you choose: CIGRÈ, SAG10®, other vendor, etc.

9. With a namesake ACCC® conductor, it will be discovered that it creates no increases in structure usage (see caveat 9b below), no design tension increase and no increase in clearance problems when the maximum sag is matched to that of the ACSR.

a.　Depending on the hot temperature chosen for the ACSR, the ACCC® conductor may or may not reach its thermal limit. Since the sag of the ACCC® conductor rises very slowly with increasing temperature, it may be worth exploring higher temperatures to see if costly clearance violations are incurred. They should not be incurred at an alarming rate and pursuit of the ACCC® conductor thermal limit may be beneficial. If you do this, repeat steps 4 through 8 until satisfied.

b.　With guyed corner structures, a wind blowing into the bite of the angle will cause an increase in usage when the conductor tension is reduced. This may or may not be an actual concern.

10. With the high operating temperature of the proposed conductor established, run IEEE 738 ampacity calculations to establish the proposed line ampacity.

11. If you run more than one conductor type option, check the losses by comparing R_{ac} values of the options. The cost savings of a conductor option are quite related to the ratio of R_{ac} values. The lowest value provides the savings over the life of the line and this can help offset the capital cost of conductor change.

12. In making the final conductor choice with its associated operating limits, you will have accepted existing clearance and strength problems. To not do so means that you sacrificed some capacity (perhaps a great deal of capacity) to take the opportunity to correct these issues via the conductor change alone. This method of correcting existing problems is not likely to produce much circuit capacity increase.

a.　An existing line with no such problems is rare. This is not meant to be alarmist as most such problems are real but not imminently dangerous or costly to fix.

4.1.3. Results

(Table 35 relates to the input data and steps listed above)

Hawk conductor data:

Item	ACSR	ACCC	ACSS	ACSS/TW	ACCR
Diameter	0.858	0.858	0.858	0.789	0.852
Unit Wt.	0.656	0.623	0.656	0.655	0.533
RTS	19,500	23,200	15,600	15,600	19,200
kcmils	477	611	477	477	477
R_{ac} 75°C	0.2305	0.1796	0.2253	0.2247	0.2275

Table 36 - Comparative input data for Hawk size 115 kV re-conductor project

Note that ACSS/TW Calumet (not listed) matches the ACSR diameter at 0.858 inches (21.8 mm) but the weight is 10% higher at 0.7758 lb/ft (1.15 kg/m). The increased aluminum content yields an R_{ac} value of 0.1898 ohm/mile (0.1179 ohm/km) – still 5.6% above the ACCC® conductor. In other words, the ACSS family, including its TW version and the ACCR option do not show the overall advantages of the ACCC® conductor. This means the ACCC® conductor option shows most promise based on the basic parameter comparison.

The one unlisted feature is the conductor's co-efficient of thermal expansion (CTE). ACCC® conductors have a much lower CTE than all other options. If the knee temperature (the temperature at which the core carries all tension in the conductor can be made low enough compared to other conductor choices), the ACCC® conductor sags will remain very low.

Matching the Existing Conductor:

In our example in Table 35, we matched the design tension of 4,850 lbs under the ice and wind load. Key results are:

Item	ACSR	ACCC
Design Tension, lbs	4,850 (25% RTS)	4,850 (21% RTS)
Iced Sag, C (ft)	2,470	2,500
Hot Sag, C (ft)	1,857	2,177
Tension T, -40ºC	2,587	3,106
C_{AAMT}	3,279	4,381
Amperes, Hot	707	1,200
Amperes at 90ºC	707	779

Table 37 - Results of ACSR / ACCC® comparison

In this example, the known operating limit for the ACSR is 90ºC (193ºF). The assumed limit for the ACCC® conductor is 180ºC (356ºF).

In this example, the design tensions are matched and both the iced sag and the hot sag of the ACCC® conductor are less than that of the ACSR. This is evidenced by the higher C values for the ACCC® conductor. The hot sags exceed the iced sags and the ruling span sag of the ACCC® conductor is about 2.4 ft. less than that of the existing conductor. This indicates that we could match those sags and reduce the design tension of ACCC® conductor. This would be a reasonable option if structure strengths were a concern.

Initial Tension and Vibration Management:

The table above shows that by matching the tensions and pulling the ACCC® conductor as tight as possible without causing strength problems, we have caused increases in the cold tension and C_{AAMT} value. Both of these are initial state values. A review of the sag-tension output shows the predictable result with the ACCC® conductor. The *after load* case controls the final sags and tension. The *after creep* case does not.

204

Note: For states hotter than the knee-point temperature, the after load and after creep case results are identical. This is because the non-creeping core is doing all the work above this temperature.

As a result, the C_{AAMT} value that defines damper requirements needs our attention. The extreme cold tension is higher for this conductor but remains well below the design tension in this case. We can ignore it.

The C_{AAMT} value is also well below the threshold of concern. The no damper threshold is much higher. This is a very loosely strung line so we are not concerned about Aeolian vibration issues.

Cost of Losses:

We recognize from this data that the ACCC® conductor namesake replacement conductor can provide an ampacity increase with no structural work required. We can recognize that the ACCR conductor can do the same thing. We have not explored the results for that conductor when design tensions are matched. That is not the point of this document. Such work can be explored using the same steps described here. However, one point remains to review. The cost of losses between options will vary with the ratio of R_{ac} values. The ACCC® conductor will provide a 22% cost of losses savings over the ACSR conductor. If the line is heavily utilized, these savings are substantial and can pay for the installation depending on the owner's view of line losses.

4.2. New Line Project

For the new line project example, we look at a very different situation. We look at an EHV line that will not make use of the conductor's high temperature capabilities. This exercise is more complex than the one above.

4.2.1. Input Data

- 550 kV circuit in open terrain
- Assume 4-bundle Drake 795 kcmil conductor
- Power Transfer required: 3,000 Amperes capable
- Ruling span: 1,400 feet (427 m)
- Minimum temperature: -30ºC (-22ºF)

- AAMT: -10ºC (14ºF)
- Design ice load: 1½" (38 mm) radial 0ºC (32ºF)

Ampacity calculation basis: 35ºC, 2 fps (96 Pa) wind perpendicular to line, latitude 40ºN.

The request is to achieve a cost-effective line.

If we compare Drake namesake conductors, the size of the structures will be the first and best indicator of cost savings developed by the conductor choice. Operating savings are also important. Supplementary differences will be observed along the way.

The 4-bundle arrangement is chosen to enhance the challenge posed by ice loads.

4.2.2. Steps

Calculate the hot temperature for the ACSR and ACCC® conductor options (Table 38). This is used for sag interests although it may rarely occur as 500 kV lines are rarely thermally limited.

1. Set up the criteria and run sag-tension calculations for both conductors. The matching point is a common vibration criteria since ACCC® conductor and ACSR can be considered equally susceptible to damage at the same C value.

4.2.3. Results

Ampere – Conductor Temperature Relationship:

Item	4-Drake ACSR	4-Drake ACCC®
3,000 Amp. Temp (ºF)	162	150
R_{ac} at 75ºC	0.1390/wire	0.1086/wire

Table 38 - Conductor temperatures under 3,000 amp load

The larger aluminum content (1026 kcmils) of the ACCC® conductors allows it to run a bit cooler at the target amperes of 750 A per sub-conductor, as shown in Table 39.

Sag-Tension Results:

Item	4-Drake ACSR	4-Drake ACCC® Conductor
Control: C_{AAMT}, *initial*	5,000 ft	5,000 ft
Design Tension (DT), 1.5 inch ice	84,150 lbs	73,450 lbs
DT % RTS	67%	45%
DT Sag	71.0 ft	81.3 ft
Hot Sag	64.1 ft @ 72°C	64.1 ft @ 65°C
C_{AAMT}, *after creep*	4,848 ft	4,582 ft
C_{AAMT}, *after load*	4,284 ft	3,857 ft

Table 39 - Sag/tension comparison

Results of a sag-tension run in which the 1.5 inches (38 mm) of ice defines the *after load* case are shown in Table 38. The hot sags happen to match but the large ice sag rules for both choices. Vibration mitigation issues will be equal for this complex bundle. The design tension for the ACCC® is 13% lower than for the ACSR. The ACSR is pushed to a reasonable limit of 67% of RTS. The ACCC conductor still has room to move. The design (ice) sag is 10 ft (3 m) more for the ACCC® conductor

Overall, we could stop here. The ACCC® conductor could simply force towers that are 10 ft (3 m) taller but be lighter at corners and in broken wire cases based on the 13% reduction in tension. But, there is another choice. We could increase the ACCC® conductor design tension to near the ACSR value, get rid of its extra sag and address a potential vibration problem. This would eliminate the taller structure requirement that now stands.

> *Notice that in this second scenario we suggest is thinking in terms of matched tensions or sags even though the project is for a new line and is not about re-conductoring. It is a re-conductoring project for the moment.*

Since the problem is the 10 feet (3 m) of sag difference with ice, set the ACCC® conductor sag with the ice to match the ACSR sag with ice.

Sag-Tension Matched Sag Results:

Item	4-Drake ACSR	4-Drake ACCC/TW
Control: 1.5" ice, C, *initial*	3,459 ft	3,459 ft
Design Tension (DT), 1.5 inch ice	84,150 lbs	83,450 lbs
DT % RTS	67%	51%
DT Sag	71.0 ft	71.0 ft
Hot Sag	64.1 ft @ 72°C	46.8 ft @ 65°C
C_{AAMT}, *initial*	5,000 ft	8,867 ft
C_{AAMT}, *after load*	4,284 ft	5,318 ft

Table 40 - Sag/tension under equal ice load

By matching the critical (design) sag of the ACCC® conductor to that of the ACSR, its design tension also rises to nearly equal (Table 40). The benefits remain that the RTS usage of the ACCC® conductor is lower than that of that ACSR and the hot sag is lower.

The problem lies with the vibration indicator, C_{AAMT}, *initial*. It has become quite high and may be problematic. Managing this vibration level may require dampers unless laboratory testing proves otherwise. There is an alternative. Notice the dramatic reduction in C_{AAMT}, from the *initial* condition to the *after load* condition. If we override the initial condition with pre-tensioning during construction, we can decrease stress on the aluminum strands and further reduce the conductor's susceptibility to Aeolian vibration.

If we do not apply a pre-stressing activity during construction, the installing tensions will be about 5,500 lbf (24.5 kN) per sub-conductor for the ACSR and 9,000 lbf (40.0 kN) for the ACCC® conductor with matched ice sag. Suppose we apply a pre-stressing of 14,000 lbf (62.3 kN) during installation. This is done by defining the *after load* case as ¾" inch of ice because our work to date shows the tension of that load to be 14,000 lbf (62.3 kN).

Sag-Tension Pre-Tension Results:

Item	4-Drake ACSR	4-Drake ACCC®
Control: 1.5" ice, C, *initial*	3,459 ft	3,459 ft
Design Tension (DT), 1.5 inch ice	84,150 lbs	83,260 lbs
DT % RTS	67%	51%
DT Sag	71.0 ft	71.2 ft
Hot Sag	64.1 ft @ 72°C	46.8 ft @ 65°C
C_{AAMT}, *initial*	5,000 ft	NA
C_{AAMT}, *after load*	4,284 ft	6,148 ft

Table 41 - Effect of pre-tensioning ACCC® conductor in this example

The results in Table 41 for the ACCC® conductor come from the *after load* case with the pre-stressing applied. Notice that doing the work reduces the design load very slightly, increases the design sag very slightly but largely corrects the vibration problem indicator, C_{AAMT} from 8,867 ft (2703 m) to a manageable 6,148 ft (1874 m). Our competing ACSR conductor remains at 5,000 ft (1524 m).

The question is whether the pre-stressing is worth it compared to the taller, lighter structures. The answer to this will vary from project to project as the structure types vary and as the mix of tangents to corners varies with the alignment.

Cost of Losses:

Finally, we have the issue of cost of losses saving. For the Drake conductor comparison, the ratio suggests a savings on losses with the ACCC® conductor of up to 35%. With 1,000+ amperes flowing over an EHV line on average, this offers a significant savings.

As a minor point, we notice that the very light ice load sag of the ACCC® conductor in the matched large ice sag scenario with pre-stressing is about 75% of that of the ACSR option. The everyday bare sag is also equally less. At 20ºC, the sags are 61 ft (18.6 m). and 44 ft (13.4 m). for the ACSR and ACCC® conductor respectively. These sags play into many phase spacing calculations for clearances and galloping. If the lower sag ACCC® conductor leads to closer phase spacing, then the impedance of the EHV design is lowered and power flow capacity is increased.

If by this approach to engineering with ACCC® conductors, we find we can match the structure needs for a new line almost exactly, then the operating savings found in lower losses and lower impedance are the venue for paying for the higher cost conductor, plus.

4.3. 138 kV Transmission Line - Conductor Replacement Project

4.3.1. Input Data

- Based on "ACSS/TW – An Improved Conductor for Upgrading Existing Lines or New Construction[152]", by F.R. Thrash, Jr.
- 138 kV circuit on light duty wood pole H-frame construction in service for 30 to 40 years
- 600 ft (183 m) ruling span
- Design ice load: NESC Heavy 0.5 in (12.7 mm) radial ice with 8 psf (383 Pa) wind at -20ºC (4ºF)
- Conductor being replaced: 477 kcmil (241.7 mm2) -26/7 ACSR Hawk
- Controlling tension: NESC maximum tension of 7,350 lbf (32,700 kN)
- Existing ampacity: 710 A at 100ºC, based on 40ºC (104ºF) ambient, 2 ft/sec (0.61 m/sec) wind, 96 W/ft^2 (1033 W/m^2), 0.5 emissitivity/absorptivity, 500 ft (152 m) elevation

---

[152] Thrash, R; "An Improved Conductor for Upgrading Existing Lines or New Construction"; Transmission and Distribution IEEE Conference; New Orleans, LA; (April 1999)

The request is to achieve at least a 30% increase in the maximum ampacity of the ACSR Hawk operating at 100°C (212°F). This increase in capacity should be done with as little capitol cost as possible, and thus is prudent to attempt a conductor replacement that does not increase the load on the existing structures. The replacement conductor should also not exceed the sag of the ACSR Hawk at 100°C (212°F), which is calculated to be 15.24 ft (4.6 m). While the H-frame poles are 30 to 40 years old, they have been found to still be in good condition. The length of the line is 11.7 miles (18.9 km).

4.3.2. Steps

The following is a generic description of the analysis process.

1. Establish the design criteria for the analysis project. These include code and owner-based tension limits, clearances, load and strength factors for structural components, thermal limits for various conductor types, etc.

2. Establish the maximum tensions and maximum sags of the existing condition by applying criteria, noting source cases.

   Establishing the maximum sag for the existing conductor requires knowledge of the original design intention. If that is unknown, then it can be calculated from the circuit's known or presumed allowable usage (MVA limit).

3. Review the clearances of the existing line condition. Flag clearance violations, if any.

4. Report structure usage of the existing condition. Flag overages.

5. Replace Hawk ACSR in model with replacement conductor.
   To avoid increasing the structure over-usage, clearance violations and line design tension; the replacement conductor must (logically) be no larger in diameter, no heavier and have an equal or lower co-efficient of thermal expansion. There are only three logical candidates: Hawk ACSS, Calumet ACSS/TW or Hawk ACCC. Drake ACSR is shown since an increase in ampacity until recently meant increasing the diameter of the conductor.

6. Fit each conductor type into the model. There are two choices for starting.

a. First, matching hot curves. This ensures no clearance violations (hot).

   i. In line with note 2a above, the proposed conductor can be set to a series of its own unique hot temperatures (and related catenaries) when there is no useful established limit for the ACSR for comparison. This turns the work into an exploratory venture to find a cost-effective balance between maximum sag for the proposed conductor and the cost of rehabilitating the clearance violations created by that temperature.

b. Or, match the design tension. This ensures no structure usage violations.

   i. The tension developed in the proposed conductor must be less than the highest tension that matters in the ACSR report. Note that *initial* tensions in the reports for both conductors matter and may control.

7. Check for maximum ice sag violations. This can be done with the sag-tension reports by comparing catenary constants, C. The hot limits C values will match and for ALL other cases that matter, the C value of the proposed conductor must be larger than it is for the ACSR.

8. Check the vibration damper requirement status of the proposed conductor. Do this against whatever criteria you choose: CIGRÈ, SAG10®, other vendor, etc.

9. With a namesake ACCC® conductor, it will be discovered that it creates no increases in structure usage (see caveat 9b below), no design tension increase and no increase in clearance problems when the maximum sag is matched to that of the ACSR.

a. Depending on the hot temperature chosen for the ACSR, the ACCC® conductor may or may not reach its thermal limit. Since the sag of the ACCC® conductor rises very slowly with increasing temperature, it may be worth exploring higher temperatures to see if costly clearance violations are incurred. They should not be incurred at an alarming rate and pursuit of the ACCC® conductor thermal limit may be beneficial. If you do this, repeat steps 4 through 8 until satisfied.

b. With guyed corner structures, a wind blowing into the bite of the angle will cause an increase in usage when the conductor tension is reduced. This may or may not be an actual concern.

10. With the high operating temperature of the proposed conductor established, run IEEE 738 ampacity calculations to establish the proposed line ampacity.

11. If you run more than one conductor type option, check the losses by comparing R_{ac} values of the options. The cost savings of a conductor option are quite related to the ratio of R_{ac} values. The lowest value provides the savings over the life of the line and this can help offset the capital cost of conductor change.

12. In making the final conductor choice with its associated operating limits, you will have accepted existing clearance and strength problems. To not do so means that you sacrificed some capacity (perhaps a great deal of capacity) to take the opportunity to correct these issues via the conductor change alone. This method of correcting existing problems is not likely to produce much circuit capacity increase.

4.3.3. Results

Table 41 captures the input data. Figure 70 and Table 42 relate the current capacity with resultant sag as well as the associated temperatures.

	Base Conductor	Considered Replacements			
Conductor Type	477 kcmil 26/7 ACSR Hawk	795 kcmil 26/7 ACSR Drake	477 kcmil 26/7 ACSS Hawk	565.3 kcmil Calumet ACSS/TW	611 kcmil ACCC⊕ Hawk
Size kcmil (mm²)	477 (241.7)	795 (402.9)	477 (241.7)	565.3 (286.5)	611 (309.6)
Diameter in. (mm)	0.858 (21.8)	1.108 (28.1)	0.858 (21.8)	0.858 (21.8)	0.858 (28.1)
Weight lb/kft (kg/km)	655.4 (975.2)	1093.4 (1627.1)	655.4 (975.2)	775.6 (1154)	623.4 (931)
Weight increase %	--	67	0	18	-5
Tensile Strength lbf (kN)	19,500 (86.7)	31,500 (140.1)	15,600 (69.4)	18,400 (81.8)	23,200 (103.2)
Strength increase %	--	62	-20	-6	19
DC Resistance 20°C ohm/mile (ohm/km)	0.1882 (0.1169)	0.1129 (0.0702)	0.1829 (0.1136)	0.1540 (0.0967)	0.1448 (0.0900)

Table 42 - Comparison between conductors considered

Note that the ACSS Hawk, while having the same aluminum cross-sectional area as the ACSR Hawk, is rated to operate at temperatures up to 250°C in order to help increase the ampacity. The ACSS/TW Calumet is the OD equivalent to ACSR Hawk. It offers more aluminum than the ACSS Hawk, but at the cost of an 18% increase in the weight. The ACCC® Hawk, offers the same diameter, with slightly less weight, an improvement in the rated tensile strength (which will translate to higher factors of safety), and the lowest resistance of the OD ACSR equivalents. While Drake ACSR has the lowest resistance, it has 67% more weight and will need to have its tension increased to meet the 15.3 ft (4.7 m) sag requirement. Figure 72 shows the sag and ampacity as a function of temperature for each of the conductors considered.
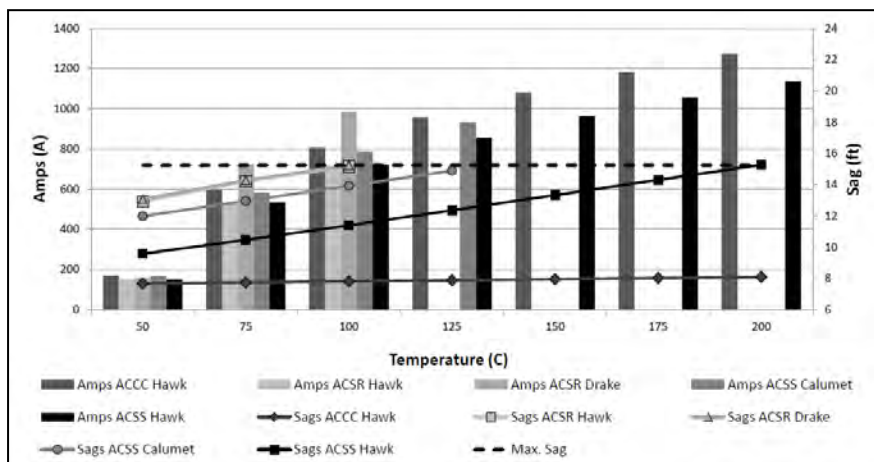

Figure 72 - Ampacity and sag comparison

The one unlisted feature is the conductor's coefficient of thermal expansion, CTE. The ACCC®conductors have a much lower CTE than all other options. If the knee temperature – the temperature at which the core carries all tension in the conductor can be made low enough compared to other conductor choices, the ACCC® conductor sags will remain very low.

Table 43 shows a comparison of the different conductor types that are expected to replace the ACSR Hawk. Note that while the Drake does offer improved capacity, it must have its NESC Heavy tension increased by 50% in order to ensure that at 100°C (212°F), its maximum operating temperature, that its sag does not exceed the 15.24 ft (4.6 m). Therefore, ACSR Drake does not meet the lowest capital cost investment criteria.

For the ACSS Hawk, it can meet the required 30% desired increase in capacity, but cannot be run to its full potential of 250°C (482°F), due to excessive sag at higher temperatures. The ACCC® Hawk, with its much lower CTE value for the core, allows this conductor to reach its maximum operating temperature of 180°C (356°F), without any violation of sag, and offers the highest capacity. The catenary of the ACCC® Hawk though initially looks very high, and would warrant attention, along with the catenary of the ACSS Hawk. It is important to note here that the ACCC® and ACSS use fully annealed aluminum.

Thus, these catenaries would not exist after the design load occurs. The aluminum will also undergo creep relieving the tension out of the aluminum when the cold temperatures occur, thus reducing the initial catenary and lowering the Aeolian vibration risk to the aluminum strands. The initial stress in the aluminum of the ACSS Hawk would be approximately 6000 psi (41 MPa) and 4860 psi (33.5 MPa) in the ACCC® Hawk. After load though, the stresses in the aluminum become nearly zero for both conductors, and which would reduce any concern for the aluminum fatiguing over time in these conductors.

Conductor Type	Base Conductor	Considered Replacements			
	477 kcmil 26/7 ACSR Hawk	795 kcmil 26/7 ACSR Drake	477 kcmil 26/7 ACSS Hawk	565.3 kcmil Calumet ACSS/TW	611 kcmil ACCC® Hawk
Maximum Sag 600 ft RS ft (m)	15.2 (4.6)	15.2 (4.6)	15.2 (4.6)	15.2 (4.6)	8.04 (2.45)
NESC Heavy Max. Tension lbf (%RTS)	7,350 (38%)*	10,250 (33%)**	7,350 (47%)	7,350 (40%)	7,350 (32%)
Installed Tension 20°C lbf (%RTS)	3,444 (18%)	5,300 (17%)	5202 (33%)	4,611 (25%)	6,071 (26%)
After Load Tension 20°C lbf (%RTS)	2,863 (15%)	4,615 (15%)	3438 (22%)	3,225 (17%)	3,708 (16%)
Initial Catenary at -10°C AAMT ft (m)	6902 (2104)	6210 (1893)	8868 (2703)	6929 (2112)	9893 (3015)
Catenary after NESC Heavy at -10°C AAMT ft (m)	5859 (1786)	5566 (1697)	5873 (1790)	4793 (1461)	6078 (1853)
Max Temp. @ Max. Sag (C)	100	100	200	~130***	180
Max. Amp at Max Sag‡	714	987	1138	958	1202
Ampacity increase %	--	38%	60%	34%	68%

†Based on "ACSS/TW - An Improved Conductor for Upgrading Existing Lines or New Construction" by F.R. Thrash, Jr.

* Design tension Hawk ACSR not to exceed 7350 lbf (32.7 kN) at NESC Heavy

** ACSR Drake needs to exceed design load of ACSR Hawk to achieve 15.2 ft (4.6 m) sag at max operating temperature

*** Is a lower temperature than reported in referenced report†

‡Amps based on 40°C Ambient, 2 ft/sec wind, 96 W/ft² sun, 0.5 emissity/absorptivity, 500 foot elevation

Table 43 - Sag/tension and ampacity comparison

While in this example, all conductors were allowed to reach the maximum tension limit under the NESC Heavy condition, the ACCC® Hawk could have its initial tension reduced by 10% to 6,615 lbf (29.4 kN), so that it does not have to reach the 7,350 lbf (32.7 kN) load when the ice is on the conductor. The NESC total sag will increase from 11.64 ft (3.5 m) to 13 ft (4 m), but will still not violate the 15.24 ft (4.6 m) sag requirement. This will reduce the tension to the towers, and only allow for a modest increase in the blowout from 4.4 ft (1.3 m) to 5 ft (1.5 m) during the NESC Heavy event. The high temperature sag will only increase to 10 ft (3 m), still well within the allowed maximum sag limit. Table 44 compares the ACCC® Hawk with the reduced overall tension to the other conductor types. This also helps reduce the initial catenaries to a more reasonable value, and after the load, drops below any catenary that would need to be concerned with. The aluminum would also be carrying no load, and thus eliminate any risk of Aeolian vibration damage to the aluminum.

Conductor Type	Base Conductor	Considered Replacements			
	477 kcmil 26/7 ACSR Hawk	795 kcmil 26/7 ACSR Drake	477 kcmil 26/7 ACSS Hawk	565.3 kcmil Calumet ACSS/TW	611 kcmil ACCC® Hawk
Maximum Sag 600 ft RS ft (m)	15.2 (4.6)	15.2 (4.6)	15.2 (4.6)	15.2 (4.6)	10.01 (3.1)
NESC Heavy Max. Tension lbf (%RTS)	7,350 (38%)*	10,250 (33%)**	7,350 (47%)	7,350 (40%)	6615 (29%)
Installed Tension 20°C lbf (%RTS)	3,444 (18%)	5,300 (17%)	5202 (33%)	4,611 (25%)	4485 (19%)
After Load Tension 20°C lbf (%RTS)	2,863 (15%)	4,615 (15%)	3438 (22%)	3,225 (17%)	2994 (13%)
Initial Catenary at -10°C AAMT ft (m)	6902 (2104)	6210 (1893)	8868 (2703)	6929 (2112)	7921 (2414)
Catenary after NESC Heavy at -10°C AAMT ft (m)	5859 (1786)	5566 (1697)	5873 (1790)	4793 (1461)	4857 (1480)
Max Temp. @ Max. Sag (C)	100	100	200	~130***	180
Max. Amp at Max Sag†	714	987	1138	958	1202
Ampacity increase %	--	38%	60%	34%	68%

Table 44 - Ice and thermal sag comparison

While the ACCC® Hawk may cost approximately twice the ACSS Hawk and 1.5 times the Calumet, the line losses savings that will be realized by the ACCC® will allow the initial capital cost of the ACCC® Hawk to be paid back within 2 to 7 years depending on the comparison and load factor. Table 44 summarizes the economic benefits of the ACCC® Hawk versus the other conductors considered for this reconductoring project.

Conductor Type	Base Conductor	Considered Replacements			
	477 kcmil 26/7 ACSR Hawk	795 kcmil 26/7 ACSR Drake	477 kcmil 26/7 ACSS Hawk	565.3 kcmil Calumet ACSS/TW	611 kcmil ACCC Hawk
First Year Line Losses (MWh)	--	--	20653	16594	15501
ACCC® Hawk Improvement in Lines Losses (%)	--	--	25%	7%	--
ACCC® Hawk First Year Savings ($50/MWh)	--	--	$258,000	$55,000	--
Savings per meter (3 ft) of conductor $	--	--	$13.70	$2.92	--
Payback Period Years	--	--	2	7	--

Table 45 - Line loss comparison

4.4. 4-Bundled 400 kV - Reconductor Project

4.4.1. Input data

- Increase capacity of existing quad bundled 400 kV right-of-way
- Prevent new conductor from sagging more than the ACSR Moose running at 85°C (185°F)
- Prevent new conductor from going above the allowed maximum tension of the ACSR Moose for a 29 psf (1383 Pa) maximum wind at 32°C (90°F)

217

- 45°C (113°F) Ambient condition, 2 ft/sec (0.6 m/sec) wind, 0.5 solar absorptivity, 0.45 emissivity, 111.5 W/ft² (1200 W/m²) solar radiation
- New conductor must be larger than 1.127 in. (28.62 mm) and no larger than 1.25 in. (31.77 mm) in diameter

The request is to increase the electrical capacity of the existing 400 kV, quad bundled Moose right-of-way with a conductor that can double the capacity, while not violating the high temperature sag of the Moose running at a maximum temperature of 85°C (185°F), or increase the load on the towers during the maximum wind event, which equates to 29 psf (1383 Pa) wind pressure on the conductor. ACSR Moose at 85°C (185°F) and running at this temperature under the inputted environmental conditions, can deliver 3,312 Amps. The new conductors must be able to reach 6,624 Amps, while operating at a temperature lower than its maximum continuous operating temperature. The diameter of the new conductor must also be nearly the same size as the old conductor, in order to help mitigate corona in the quad bundle configuration.

4.4.2. Steps

The following is a generic description of the analysis process.

1. Establish the design criteria for the analysis project. These include code and owner-based tension limits, clearances, load and strength factors for structural components, thermal limits for various conductor types, etc.

2. Establish the maximum tensions and maximum sags of the existing condition by applying criteria, noting source cases.

   Establishing the maximum sag for the existing conductor requires knowledge of the original design intention. If that is unknown, then it can be calculated from the circuit's known or presumed allowable usage (MVA limit).

3. Review the clearances of the existing line condition. Flag clearance violations, if any.

4. Report structure usage of the existing condition. Flag overages.

5. Replace Moose ACSR in the model with replacement conductor.

    To avoid increasing the structure over-usage, clearance violations and line design tension; the replacement conductor must (logically) be no larger in diameter, no heavier and have an equal or lower co-efficient of thermal expansion. There are only two close candidates: ACCC 1332 kcmil (675 mm^2) Budapest which is a 1.24 in. (31.5 mm) diameter conductor or ACCC 1338 kcmil (678 mm^2) Mumbai, which has the same diameter as a ACSR Moose of 1.25 in. (31.77 mm)

6. Fit each conductor type into the model. There are two choices for starting.

a. First, matching hot curves. This ensures no clearance violations (hot).

    i.In line with note 2a above, the proposed conductor can be set to a series of its own unique hot temperatures (and related catenaries) when there is no useful established limit for the ACSR for comparison. This turns the work into an exploratory venture to find a cost-effective balance between maximum sag for the proposed conductor and the cost of rehabilitating the clearance violations created by that temperature.

b. Or, match the design tension. This ensures no structure usage violations.

    i.The tension developed in the proposed conductor must be less than the highest tension that matters in the ACSR report. Note that *initial* tensions in the reports for both conductors matter and may control.

7. Check for maximum ice sag violations. This can be done with the sag-tension reports by comparing catenary constants, C. The hot limits C values will match and for ALL other cases that matter, the C value of the proposed conductor must be larger than it is for the ACSR.

8. Check the vibration damper requirement status of the proposed conductor. Do this against whatever criteria you choose: CIGRÈ, SAG10®, other vendor, etc.

9. With the ACCC® conductor, it will be discovered that it creates no increases in structure usage (see caveat 9b below), no design tension increase and no increase in clearance problems when the maximum sag is matched to that of the ACSR.

a. Depending on the hot temperature chosen for the ACSR, the ACCC® conductor may or may not reach its thermal limit. Since the sag of the ACCC® conductor rises very slowly with increasing temperature, it may be worth exploring higher temperatures to see if costly clearance violations are incurred. They should not be incurred at an alarming rate and pursuit of the ACCC® conductor thermal limit may be beneficial. If you do this, repeat steps 4 through 8 until satisfied.

b. With guyed corner structures, a wind blowing into the bite of the angle will cause an increase in usage when the conductor tension is reduced. This may or may not be an actual concern.

10. With the high operating temperature of the proposed conductor established, run IEEE 738 ampacity calculations to establish the proposed line ampacity.

11. If you run more than one conductor type option, check the losses by comparing R_{ac} values of the options. The cost savings of a conductor option are quite related to the ratio of R_{ac} values. The lowest value provides the savings over the life of the line and this can help offset the capital cost of conductor change.

12. In making the final conductor choice with its associated operating limits, you will have accepted existing clearance and strength problems. To not do so means that you sacrificed some capacity (perhaps a great deal of capacity) to take the opportunity to correct these issues via the conductor change alone. This method of correcting existing problems is not likely to produce much circuit capacity increase.

4.4.3. Results

Two ACCC options are considered and are shown in Table 46. The ACCC Budapest is a 1.24 in. (31.5 mm) diameter conductor, using the 0.375 in. (9.53 mm) diameter composite core and having an aluminum cross-section of 1332 kcmil (675 mm^2). The ACCC Mumbai, which has the same diameter of ACSR Moose of 1.25 in. (31.77 mm), is a 1338 kcmil (678 mm^2) conductor using the same 0.375 in. (9.53 mm) diameter composite core. Pre-tensioning of the conductor, that can help also reduce the load on the towers when the maximum wind occurs, can also be considered.

All sag/tension calculations were performed using PLS-CADD™ for a 1,150 foot (350 m) ruling span. The ACSR Moose installed a typical tension of 22% RTS, or 7,980 lbf (35.5 kN) at 32°C, has a tension of 15,000 lbf (66.6 kN) at the maximum wind load. This produces a tension on the tower of 59,900 lbf (266.4 kN) due to each phase being a quad bundle. At 85°C (185°F), it has an after creep sag of 37.6 ft (11.45 m).

The ACCC options without pre-tensioning them, and installing the conductor at nearly the same tension at 32°C (90°F) as the ACSR Moose, will actually lower the tension on the towers during the maximum wind event, to approximately 53,500 lbf (238 kN). If the high temperature sags wanted to be improved, so that only the core properties are dictating the sags at temperatures above ambient, then the conductor can be pre-tensioned to the maximum wind load tension, and then backed down to approximately 7,200 lbf (32 kN) at 32°C (90°F), and the thermal sags are decreased by about 5 ft (1.5 m).

The ACCC Mumbai and ACCC Budapest have similar results for either installing the conductors at approximately 7,900 lbf (35 kN), or after pre-tensioning the conductor to the maximum wind load tension of 15,000 lbf (66.6 kN) per conductor in the phase. The ACCC options can easily double the capacity, while operating at around 150°C (302°F). Both ACCC options also have spare capacity, and can operate at or near its 200°C (392°F) emergency temperature, increasing the emergency capacity to nearly 8000 Amps, without exceeding the sag of the ACSR Moose running at 85°C (185°F). If the conductors were all to run at the old capacity of 3312 Amps, then the ACCC options can reduce the line losses by 36% over the ACSR Moose at the same ampacity. For a typical $50/MWh cost of electricity, the first year line losses can be reduced by nearly $1M USD. After thirty years, this value increases to an NPV of approximately $17M.

Conductor Types	OD (mm)	Al Cross Section (mm²)	Weight (kg/km)	DC Resistance (ohm/km) at 20C	RTS (kN)	Average Tower Tension (kN)	Max Temp Req for 2X Capacity	Worst Sag (m)	Max Tension at Tower (kN)	Line loss Reduction	Reduced line loss in 1st year	Benefit from reduced line loss in 30 yrs (1 circuit)	Allowable Maximum Capacity
ACSR Moose	31.78	528.5	2005	0.054	165	128	85C (3312 A)	11.45 (85C, Creep)	266.4	baseline			3312 A
ACCC Budapest	31.5	674.9	2005	0.0416	192	119	151C (6624 A)	11.36 (151C, Load)	238.0	36%	$979,000	$16,270,000	7859 A (@195 C)
ACCC Budapest	pre-tension (266.4 KN for 1hr)					129	151C (6624 A)	9.63 (151C, Load)	266.4	36%	$979,000	$16,270,000	7983 A (@200 C)
ACCC Mumbai	31.77	678.2	2015	0.0414	192	111	150C (6624 A)	11.3 (150C, Load)	238.0	36%	$981,000	$17,400,000	7996 A (@ 200 C)
ACCC Mumbai	pre-tension (266.4 KN for 1hr)					130	150C (6624 A)	9.67 (150C, Load)	266.4	36%	$981,000	$17,400,000	7996 A (@ 200 C)

Assumption: 350 m span, 1000 m elevation, 170 Km/hr wind; 2X ACSR Moose Capacity; 22% RTS string tension at 32 C; Max Tension to tower not exceed ACSR Moose

Table 46 - Sag, temperature and line loss comparison

5. Additional References

Terminology References:

- North American Electric Reliability Corporation (NERC)—Glossary of Terms, 2005
- Australian Electricity Market Commission (AEMC)
- Institute of Electrical and Electronics Engineers (IEEE) Catalog Number 96 TP 110-0 "Glossary of Terms and Definitions Concerning Electric Power Transmission System Access and Wheeling"
- Union for the Co-ordination of Transmission of Electricity (UCTE) Operation Handbook, July 2003
- P. Kundur, J. Paserba, V. Ajjarapu, G. Andersson, A. Bose, C. Canizares, N.Hatziargyriou, D. Hill, A. Stankovic, C. Taylor, T. Van Cutsem and V. Vittal, *IEEE/CIGRE joint task force on stability terms and definitions,* "Definition and classification of power system stability", IEEE Transactions on Power Systems, Volume 19, Issue 3, Aug. 2004 Page(s): 1387 – 1401 (IEEE/CIGRE)
- Hiroshi Tanaka, University of Ottawa, Canada; Helmut Wenzel VCE Holding GmbH, Austria; "Glossary of Terms in Cable Dynamics" (Dec 2009)

6. Appendix

6.1. Installation Notes

Based on the experience gained supporting the installation of over 50,000 km of ACCC® conductor at over 500 project sites, CTC Global developed *and maintains* a document referred to as "ACCC® Conductor Installation Guidelines[153]." While it is important that installers refer to this document periodically to help avoid *'re-learning things the hard way'* and take advantage of CTC Cable's installation support, there are a few important points regarding correct installation procedures that are discussed below.

IEEE 524[154] and other similar guidelines describe correct installation practices and procedures for all conductor types, based on decades of experience, which apply to ACSR, ACSS, ACCC® and other conductor types. For example, IEEE 524 recommends that bull wheel tensioners be placed at a distance away from the first structure that is three times greater than the structure's height. Unlike AAC, AAAC, ACAR, ACSR, or other conventional conductor types - that rely on a few high-strength core or conductive aluminum strands themselves - the ACCC® conductor's core relies on tens of thousands of individual load-bearing fibers that, in many ways, reflect the intentionally redundancy of aerospace structures. From another point of view, not unlike a fiberglass fishing rod, the ACCC® conductor's composite core is very flexible and strong, but does have certain bending limitations that need to be understood.

When bent, the ACCC® conductor's composite core stores a fair amount of kinetic energy. It prefers to lay straight. While the aluminum strands effectively control kinetic energy and make the conductor very easy to handle, in certain cases a spring-like effect can be noted if the conductor becomes loose on a reel. It is therefore important to keep the conductor snug on the reel and well controlled during installation, which can be readily accomplished by having suitable reel holders *with suitable tensioning brakes*. When a conductor

---

[153] ACCC® Installation Guidelines Rev M 2011

[154] IEEE 524 "Guide to the Installation of Overhead Transmission Line Conductors" 2003

becomes loose on a reel, it can become entangled and damaged. Proper back tensioning, with the use of suitable reel brakes, can prevent this from occurring.

Similar to ACSS conductors, the annealed aluminum in the ACCC® conductor is relatively soft and can be damaged if pulled over rocks, fences, or other objects. Neoprene lined sheave wheels are preferred. Sheave wheels with adequate diameter should be in good condition and properly aligned. They should also be properly supported at large angle pulls. Oversized sheave wheels should also be used at the first and last structures, especially when pulling tensions are high, so the soft aluminum strands are not damaged. Pulling ACCC® conductor around angles greater than 30 degrees may require larger diameter sheave wheels or double sheave wheels and yoke plates, either one of which may need to be supported by a steel cable, nylon sling, chain hoist, or solid brace.

Dead-end structures are preferred at angles exceeding 50 to 60 degrees, even if the span to adjacent structures is relatively low. While the composite core has certain bending limitations, an undersized sheave wheel can also damage the aluminum strands when high pulling forces are combined with large angles, due to compressive stresses on the aluminum strands.

The ACCC® conductor's core bending limits are essentially a function of the core's diameter and aluminum content, with smaller ACCC® conductors of smaller diameter cores being more flexible. Attention should be paid when working with small core ACCC® conductors, as it does not take much load to create large stress in the conductor. Unlike metallic core, unidirectional composite material is superior on tensile properties (perfectly suited for overhead conductors), however, it is axial compressive strength is not as high as the tensile strength.

While compressive stress on the conductor is mostly absent when the conductor is properly tensioned during installation (and in service), installation personnel should *avoid sharp bend angles* working with smaller ACCC® conductors as this could present excessive compressive stress to the composite core, causing fiber buckling failure (e.g., fiber breaking under compression), which may not be apparent until the conductor is subsequently placed under high tension. This potential problem can be easily avoided by using appropriate installation equipment and procedures as described in the IEEE 524 Guidelines and

reiterated in the ACCC® Conductor Installation Guidelines: <u>1) adequate tension maintained on conductor, 2) avoid sharp bending angle, especially when conductor tension is absent</u>.

Generally speaking:

- Grounding wires must be properly utilized and placed
- Recommended sheave wheels should be employed (not too small)
- Mandrel axles should be properly matched to reel arbor holes
- Let-off brakes should be set to maintain proper back tension
- Good control of back tension and pulling speeds will mitigate conductor galloping
- Bull-wheels should be set back at a 3:1 distance from the 1st structure
- Sheaves wheels and bull wheels should be in good alignment
- Soft aluminum outer strands should not be scuffed during installation
- Sharp bending of conductor should be avoided, especially when tension is absent in the conductor.

6.2.   Field Experience & Conductor Maintenance

In January, 2011, a tornado downed a wood H-frame structure supporting an ACCC conductor in Arkansas. The core was not damaged, but the aluminum strands were. Approximately 150 feet of ACCC conductor was replaced on each phase on either side of the downed structures using two splices per phase. In an adjacent location, flying debris damaged the aluminum strands and the composite core. In this case a single full tension splice was installed.

As with ACSR or other conductor types, it is possible to use conventional methods to repair ACCC conductor strands. If the strands are damaged up to 15%, a line guard can be utilized. If the damaged strands are from 16% to 30%, a repair rod should be utilized. If the strands are damaged above 30% but the core is not damaged, a compression repair sleeve should be utilized. If the composite core is damaged in a localize area, a full-tension splice should be installed. If damage to the conductor is more widespread, a section of conductor should be removed and replaced. Generally, this type of damage is localized and the amount of conductor that needs to be replaced is minimal. For more information please refer to the "ACCC® Conductor Installation Guidelines[155]."

In January, 2012, a firestorm destroyed four wood H-frame structures supporting ACCC Linnet size conductor near Reno, Nevada. The ACCC conductor had been used to replace #2 copper. At the time the ACCC was installed, new metal cross arms were added. After the firestorm, the ACCC conductor and cross arms had dropped to the ground. No damage to the ACCC conductor was observed so the poles were replaced and the ACCC was pulled back into position and returned to service.[156]

---

[155] ACCC® Installation Guidelines Rev M 2011
[156] Jim Lehan, NV Energy

Figure 73 – ACCC Linnet conductor fallen to the ground after 4 wood H-frame structures burned in firestorm near Reno, Nevada. The conductor was undamaged. The H-frame structures and insulators were replaced, the conductors and metal cross arms were lifted back in place and the line re-energized.

In 2010, winds exceeding 100 miles per hour caused a number of non-guyed wood H-frame structures to be uprooted (wind force pulled poles from their soil embedment). The ACCC Linnet size conductors were not damaged.[157]

---

[157] Jim Lehan, NV Energy

Figure 74 – ACCC Linnet size conductor undamaged due to wind / pole deflection

6.3. ACCC Conductor Dead-Ends & Splices

The ACCC conductor requires specialized dead-ends and splices (Figure 75). While the outer aluminum sleeves are essentially the same types of compression sleeves or housings used in other conductor types (but slightly larger in diameter and mass to accommodate higher operating temperatures), the inner components of ACCC conductor dead-ends and splices utilize a collet assembly that grips the composite core to effectively transfer mechanical load to the adjacent component. The outer aluminum housings are compressed to the conductor using conventional 60 ton presses to effectively transfer electrical load through full tension splices or dead-end assemblies to jumper pads (Figure 76).
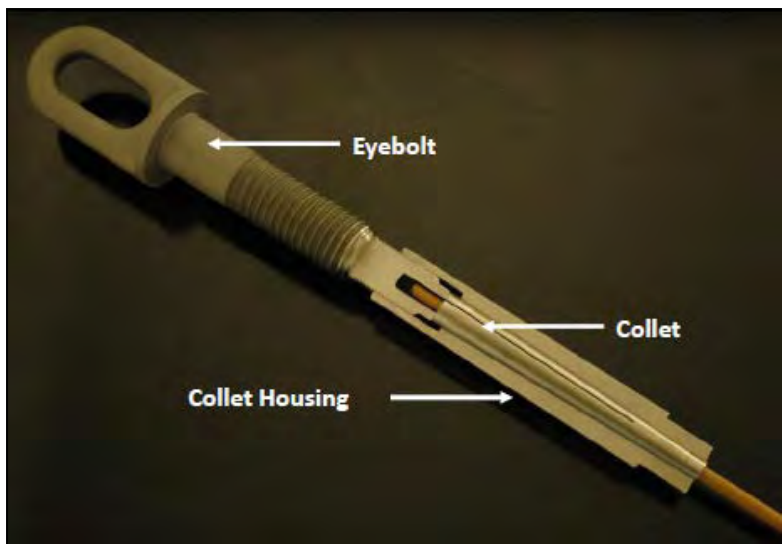
Figure 75 - Internal components of ACCC conductor dead-end assembly

Figure 76 - Conventional 60 ton compression press / die used to complete dead-end (or splice) assembly for ACCC conductor

6.4. ACCC Conductor Testing

ACCC conductor testing has followed numerous standardized protocols for testing bare overhead conductors. Additional test protocols, commonly used to assess non-metallic composite materials (common to the defense and aerospace industries), have also been utilized for a number of evaluations. Testing of the ACCC conductor began as a research and development (R&D) program in effort to reach performance and quality objectives. Accelerated aging and field trials were also performed to assess conductor performance and longevity. On-going testing is used for Quality Assurance and supply chain management purposes, such as when qualifying a new hardware supplier, to ensure high quality and high performance. The lists below reflect testing that began over 15 years ago.

Core Testing:

Tensile Testing
Flexural, Bending & Shear Tests
Sustained Load Tests
Tg Tests
CTE Measurements
Shear Testing
Impact and Crush Testing
Torsion Testing
Notched Degradation Testing
Moisture Resistance Testing
Long Term Thermal Testing
Sustained Load Thermal Testing
Cyclic Thermal Testing
Specific Heat Capacity Testing
High Temperature Short Duration
High Temperature Core Testing
Thermal Oxidation Testing
Brittle Fracture Testing
UV Testing
Salt Fog Exposure Tests
Creep Tests
Stress Strain Testing
Micrographic Analysis
Dye Penetrant Testing
High Temperature Shear Testing
Low Temperature Shear Testing

Mechanical Conductor Testing:

Stress Strain Testing
Creep Testing
Aeolian Vibration Testing
Galloping Tests
Self Damping Tests
Radial Impact and Crush Tests
Turning Angle Tests
Torsion Tests
High Temperature Sag Tests
High Temperature Sustained Load
High Temperature Cyclic Load Tests
Cyclic Ice Load Tests
Sheave Wheel Tests
Ultimate Strength Tests
Cyclic Thermo-Mechanical Testing
Combined Cyclic Load Testing
Conductor Comparison Testing

Systems & Hardware Testing:

Current Cycle Testing
Sustained Load Testing
Ultimate Assembly Strength Testing
Salt Fog Emersion Testing
Static Heat Tests
Suspension Clamp Testing
Thermo-Mechanical Testing
Cyclic Load Testing

Electrical Conductor Testing:

Resistivity Testing
Power Loss Comparison Testing
Ampacity
EMF Measurements
Impedance Comparison Testing
Corona Testing
Radio Noise Testing
Short Circuit Testing
Lightning Strike Testing
Ultra High Voltage AC & DC Testing

Field Evaluations & Monitoring:

Ambient Temperature
Tension, Sag, and Clearance
Conductor Temperature
Electric Current
Wind Speed and Direction
Solar Radiation
Rainfall
Ice Buildup
Splice Resistance
Infrared Measurements
Corona Observations
Electric and Magnetic Fields
Wind and Ice Load Measurements
Vibration Monitoring
Typhoon Test

In addition to numerous tests performed by CTC Global either in-house or in association with numerous labs, universities, or utilities worldwide[158], other entities such as EPRI have also performed various test protocols to address various concerns. In some cases, due in part to the severity or novelty of a new test protocol, modifications to initial test protocols have been made. For instance, EPRI, in association with EDF, developed a new thermo-mechanical test protocol wherein the ACCC conductor was held under a constant 25% RTS tension and thermally cycled from ambient lab temperature to 180°C 500 times. At the end of each 100 cycles, the conductor was then pulled to 70% RTS and held for 24 hours. During the first attempt at this test, the bolted electrical jumper and thermocouple became loose and overheated[159]. A new test was performed wherein a non-tensioned 'dummy' conductor was wired in series so

---

[158] *Note:* CTC has provided conductor & hardware samples to a number of entities that performed their testing independently (not funded by CTC)
[159] EPRI Report "Methodology for Aging Evaluation of a High-Temperature Low-Sag (HTLS) Conductor: Specifications for a Testing Procedure" (Product ID: 1015982) published 11/24/2008

233

thermocouple/jumper loosening would not occur again. This time the test was completed successfully (Table 47) and with excellent results[160].

Sample Number	Short Beam Shear Strength (6 x diameter)			Flexural Strength (16 x diameter)		Sample Number	Tensile Strength (1 Meter Lengths)		Percent RTS
	Maximum Short Beam Shear Strength Load (N)	Shear Strength (MPa)	Extension at Maximum Load (mm)	Maximum Flexural Load (N)	Extension at Maximum Flexural Load (mm)		Tensile Strength (lbs)	Tensile Strength (kgf)	
Sample A from "Tensioned & Heated" Section:
1	4,998.5	46.7	1.717	2,415.5	6.54	B	35,171	15,953	102%
2	4,933.5	46.1	1.685	2,248.6	6.20	C	35,736	16,210	104%
3	4,977.9	46.5	1.692	2,287.0	6.33	E	36,807	16,695	107%
Average:	4,970.0	46.5	1.691	2,317.0	6.36	Average:	35,905	16,286	104%
Sample I from "Heated Only" Section:
1	4,927.2	46.1	1.615	2,275.0	6.22	J	34,783	15,777	101%
2	4,969.9	46.5	1.625	2,436.6	6.80	K	36,223	16,430	105%
3	4,910.0	45.9	1.609	2,400.0	6.62	L (gap)	29,602	13,427	86%
Average:	4,935.7	46.1	1.616	2,370.5	6.55	Average:	35,503	16,104	103%
Unaged Samples:
1	4,795.9	45.1	1.592	2,364.6	6.42	1	37,216	16,881	108%
2	4,771.3	44.8	1.501	2,392.1	6.35	2	37,196	16,872	108%
3	4,969.1	46.7	1.515	2,293.0	6.18	3	37,049	16,805	107%
Average:	4,845.4	45.6	1.536	2,349.9	6.31	Average	37,154	16,853	108%

Post Testing Evaluation of Aged Core Samples from Thermo-Mechanical Testing at Kinectrics

Table 47 - Post testing evaluation of ACCC conductor core samples after EPRI/EDF 500 thermo-mechanical test at 180°C. No degradation in mechanical strength was observed (including matrix dominated SBS strength).

While a wealth of lab and field data has enabled the successful deployment of over 50,000 km of ACCC conductor at over 500 project sites in more than 45 countries, there has been some confusion from time to time regarding the ACCC conductor's performance characteristics due to the inclusion of prototype data in more recent documents. One such document published by PSERC in 2009[161] referred to the 1st R&D prototype core that was produced in 2003 (Figure 77). While the document itself offered an excellent discussion of new conductor technologies, the data it presented regarding the ACCC conductor's prototype core did not accurately reflect the characteristics of the product CTC Global developed and commercialized in 2005.

---

[160] EPRI Report "Specification for a Testing Procedure to Qualify Organic Matrix Core HTLS Conductors (Product ID: 1017785) published 11/17/2009
[161] Gorur, R; "Characterization of Composite Cores for High Temperature Low Sag (HTLS) Conductors" PSERC 2009
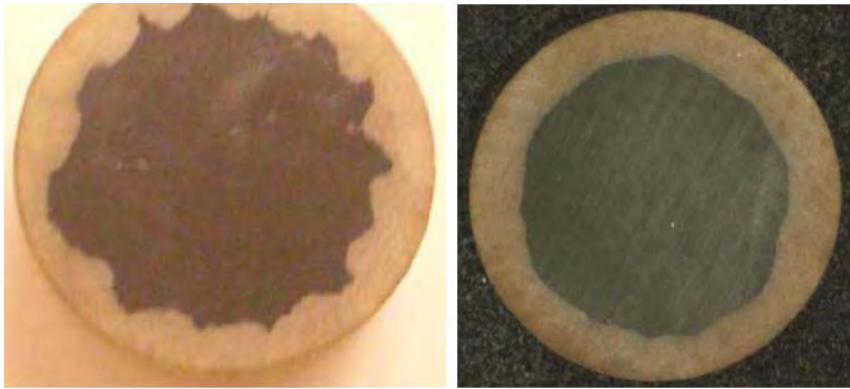
Figure 77 - Early 2003 prototype core (left) commercial 2005 core (right)

While the number of tests performed on the ACCC conductor by labs worldwide over the last ten years is substantial and have addressed a number of important concerns, one of the most important aspects relates to the conductor's upper thermal limits. In addition to the EPRI/EDF test described above wherein cyclic exposure to 180°C and high tensile loads confirmed the ACCC conductor's high-temperature performance, other sustained and cyclic load tests have also demonstrated the ACCC conductor's suitability for higher short-term emergency temperatures. One such test developed by National Grid UK included a test protocol, in Figure 78, where an ACCC conductor was held under high tension at a high angle of incidence through an AGS suspension clamp and cycled to 215°C (420°F) 40 times with 8-hour holds at 215°C to replicate an anticipated 'once-a-year' overload condition.[162] As with numerous other tests described in CTC's Summary Technical Report (and individual test report documents)[163], loss of mechanical strength was negligible.

---

[162] Zsolt Peter, Dmitry Ladin, Michael Kastelein, Greg Brown, Heat Cycling Test at Maximum Departure Angle on "LONDON" ACCC/TW Conductor Through A PLP AGS Suspension Assembly, Kinectrics North America Inc. Report No.: K-419205-RC-0002-R00 (Sept 2010)

[163] Please contact CTC Global for copies of any test reports and/or the 'Summary Technical Report' which discusses all ACCC conductor testing
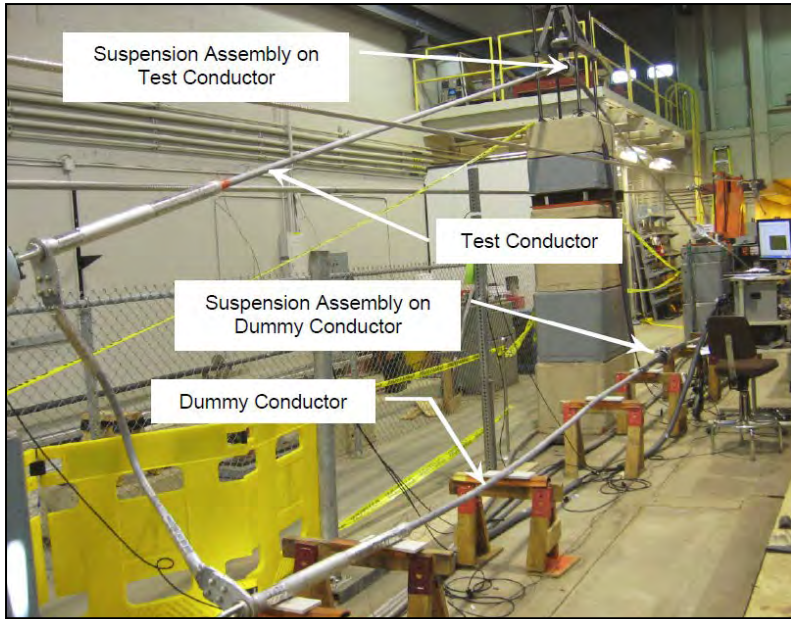
Figure 78 - National Grid UK thermal cycle test of ACCC conductor at 215°C to confirm emergency operating temperature suitability of conductor, dead-ends and AGS suspension clamps

Longer-term thermal aging tests have also been conducted by the University of Southern California's Material Science department. These tests have also shown the thermal stability of the ACCC conductor core at sustained high temperatures. After continuous exposure to temperatures of 180° and 200°C for 52 weeks, very little change in tensile strength was observed (Figure 79). It was also determined that surface (thermal) oxidation was limited to about 150 microns in depth - which created a dense oxidation layer retarding further oxidation as described in USC's paper[164].

---

[164] E. Barjasteh a, E.J. Bosze b, Y.I. Tsai a, S.R. Nutt a, "Thermal aging of fiberglass/carbon-fiber hybrid composites" Composites: Part A 40 (2009) 2038–2045
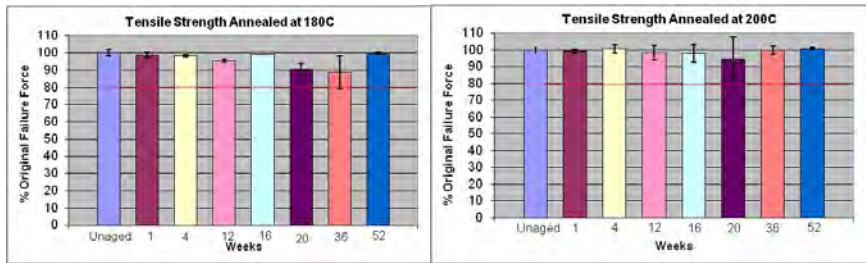
Figure 79 - Tensile strength of the hybrid composite rod exposed at (a) 180°C and (b) 200°C in air for 52 weeks.

While details of the substantial testing performed on the ACCC conductor is beyond the scope of this document, CTC Global asks that you contact them directly should you have any particular questions regarding ACCC conductor's performance, installation methods, or longevity, as there are a number of other documents and published technical papers that might address your concerns. A few frequently asked questions are addressed below:

6.5.   ACCC Frequently Asked Questions

What is ACCC conductor?

ACCC® conductor (Aluminum Conductor Composite Core) is a high capacity, low sag conductor which consists of a carbon fiber composite core encased in a protective fiberglass sheath that is helically wrapped with conductive aluminum strands. It was developed and patented by CTC Global. ACCC is a registered trademark of CTC. Though CTC produces all ACCC composite core at its manufacturing facility in Southern California, ACCC conductor is stranded by ~two dozen regional conductor manufacturers worldwide. Currently over 50,000 km of ACCC conductor has been installed at over 500 project sites.

What are the advantages of ACCC Conductor compared to conventional conductors?

Conventional conductors typically consist of aluminum strands wrapped around steel core wires. The steel core provides strength so supporting structures can be placed further apart. In some cases, steel core wires are not used, but an aluminum alloy is incorporated to improve the strength of the conductor. Special alloys increase electrical resistance which increases line losses. The ACCC conductor offers several advantages compared to conventional conductors with or without steel reinforcement:

- The high-strength composite core allows the incorporation of aluminum strands that provide the greatest conductivity (type 1350-O ≥ 63% IACS*). Various aluminum alloys can decrease conductivity to ≤ 53% IACS (*International Annealed Copper Standard).
- The composite core's lighter weight (compared to steel core wire) allows the incorporation of ~28% more aluminum without a weight or diameter penalty (using compact trapezoidal strands).
- The composite core's very low coefficient of thermal expansion enables the ACCC conductor to carry additional electrical current without causing excessive line sag that occurs when conventional conductors heat up under increased electrical load.

- *The ACCC conductor's additional aluminum content (and superior conductivity) substantially <u>reduces line losses</u> compared to any other conductor of the same diameter and weight.*
- *The ACCC conductor's non-metallic core also <u>eliminates magnetic hysteresis losses</u> that can be as high as 6% on 3 layer steel core conductor and 20% or more on single layer steel core conductor under high current conditions.*
- *The ACCC conductor's composite core is <u>non-corrosive</u> and will not cause a galvanic effect between the core and aluminum strands that can occur with conventional conductors.*
- *The ACCC conductor's composite core – in conjunction with the smooth surface of the trapezoidal shaped aluminum strands – <u>helps dissipate Aeolian vibration</u> more effectively.*
- *The dissipation of vibration allows the conductor to be installed at <u>higher initial tensions</u> often without the use of dampers (based on project specific analysis) which serves to extend the effective service life of the conductor.*
- *The high strength, light weight composite core enables installation over <u>long spans</u> which can <u>reduce overall project costs</u> by reducing the number (or height) of the required structures on new transmission or distribution projects.*
- *A reduction of structures can often <u>minimize environmental impact</u>, simplify the permitting process, and effectively <u>reduce construction time</u>.*
- *The ACCC conductor's ability to carry <u>up to twice the current</u> of a conventional conductor makes it ideally suited for increasing the capacity of existing transmission and distribution lines without the need to reinforce or replace existing structures.*
- *Higher capacity and reduced sag helps <u>improve the overall reliability</u> of the grid.*

Why were composite materials selected for this product?

Carbon & glass fiber hybrid composites offer superior strength to weight ratios (they are much stronger and lighter than steel). Hybrid composite materials do not exhibit the same fatigue failure as metals, nor do they rust, rot, or corrode. Unlike metal alloys, carbon fiber composite materials do not creep over time when subjected to cyclic or continuous high tensile load conditions. They also

do not yield (permanently deform) under extreme load conditions. Hybrid carbon and glass fiber composites exhibit elastic behavior and return to their original condition (length) when extreme loads dissipate.

Considering that the ACCC composite core is elastic, but the fully annealed aluminum strands yield under relatively low strain conditions, what happens to the aluminum strands when a heavy ice or wind load subsequently diminishes?

Following a heavy ice or wind load event (as can be observed in stress-strain testing), the aluminum strands relax around the core which allows the high strength core to carry the majority of the tensile load. While the relaxed strands re-engage under progressively higher tensile load conditions, the advantage of relaxed strands is that the conductor becomes more dimensionally stable under subsequent high current conditions, thereby reducing sag. A secondary advantage is a further improvement in vibration dissipation.

Non-ceramic insulators use a fiberglass composite core. Many of these products had problems with "brittle fracture." Is the ACCC composite core susceptible to brittle fracture?

Several non-ceramic insulator designs (when they were first introduced) utilized a relatively low grade glass fiber that contained boron to reduce manufacturing costs. These products also utilized a relatively low grade resin system that absorbed moisture as the outer silicon / rubber water sheds began to age. Once the sheds aged, moisture was able to wick into the ends of the fiberglass rods, which, when exposed to a highly charged electric field, became acidic. Nitric acid subsequently attacked the boron contained within the glass fibers which caused stress corrosion resulting in brittle fracture. The ACCC conductor's carbon and glass fiber core uses a hydrophobic epoxy that resists moisture absorption. Wicking does not occur as core ends are encapsulated very deep within sealed dead-ends and splices, and the glass fibers do NOT contain boron. Extensive testing has confirmed that the ACCC conductor core is not susceptible to stress corrosion or brittle fracture. Additionally, there is no electric potential to ground (as exists with insulators), so tracking, voltage puncture, and flashover cannot occur.

How do hybrid carbon fiber composites compare with metal matrix composites?

In the case of the ACCC core, the unidirectional carbon and glass fiber composite utilizes a high grade, high temperature, toughened epoxy matrix. The matrix binds the fibers together which effectively helps transfer and share mechanical loads between them. The generous layer of glass fibers (principally for preventing galvanic corrosion) provides excellent core flexibility and maximizes the structural properties of the high strength, low coefficient of thermal expansion fibers.

In the case of a metal matrix composite (as is utilized in 3M's ACCR conductor's core strands), metallic properties dominate and alumina fibers are added to the aluminum matrix to increase stiffness and strength. While metal matrix composites can be exposed to higher temperatures compared with epoxy (polymer) matrix composites (~300°C vs ~200°C), the overall composite still have a higher CTE than ACCC Core, and the vastly different CTE between the metal matrix and its reinforcing fibers limit the number of thermal cycles to which it can be exposed before micro-fractures propagate. The very limited tensile strain (<1% as compared to 2.2% in Carbon fibers and 4.5% in glass fibers) in Nextel fibers makes the ACCR core relatively brittle, requiring very large bending radius to avoid brittle fracture.

How is the ACCC core produced?

The ACCC composite core is produced via a pultrusion process where the carbon and glass fibers are impregnated with resin and pulled through a specially heated die to complete curing. The core is made in a continuous process and various lengths are then cut and placed on shipping reels after the entire length has been thoroughly tested.

What types of project applications are ACCC conductors normally selected for?

The ACCC conductor was initially developed as a "High Temperature Low Sag" conductor to mitigate thermal sag on transmission lines that were "capacity constrained" due to sag and clearance limitations that occurred when higher electrical currents caused the conductors to heat up and sag due to their high CTE. The ACCC conductor's low CTE composite core mitigated thermal sag. It therefore allowed existing transmission lines to be upgraded to carry

additional current and is considered to be ideally suited for reconductoring projects.

However, due to the ACCC conductor's increased aluminum content, greater strength, and excellent self-damping characteristics, the ACCC conductor is now also being utilized on new transmission and distribution lines as it offers increased electrical capacity, decreased line losses, and greater spans between fewer or lower structures. These attributes decrease permitting challenges, simplify tower placement, decrease upfront capital costs, and reduce lifecycle costs. The ACCC conductors improved efficiency and lower line losses can also decrease fuel consumption and associated GHG emissions as certified by SCS Global Services in November, 2016.

How does ACCC compare to conventional conductors?

The ACCC conductor's composite core is lighter and stronger than steel or special alloy core which allows the ACCC conductor to accommodate greater spans, with a lighter more compact design, and also allows approximately 28% more aluminum to be incorporated into any conductor design without a weight or diameter penalty. The added aluminum content decreases electrical resistance, line losses, fuel consumption (or generation requirement) and can help reduce associated emissions. While the ACCC conductor offers the least amount of thermal sag compared to any other high temperature low sag conductor, the ACCC conductor offers higher capacity with reduced losses compared to any other conductor available today.

What types of dead-ends and splices are used with ACCC?

The ACCC conductor requires specially designed dead-ends and splices. A dead-end assembly consists of a collet housing, collet, and threaded eyebolt. During installation, a lineman removes several inches of the outer aluminum strands to expose the composite core. The collet and collet housing are placed over the core and the threaded eyebolt is inserted into the collet housing (also threaded) and tightened with a pair of crescent wrenches. Tightening the eyebolt into the collet housing tightens the collet and allows it to grip the core. A conventional (though somewhat larger) aluminum sleeve is placed over the conductive aluminum strands and collet / eyebolt assembly and compressed with a conventional 60 ton press using a compression die sized for the particular conductor being installed. The compression sleeve has a jumper pad located

adjacent to the eyebolt which allows a jumper to be attached with a standard NEMA four bolt pattern, or other bolt pattern as specified by the customer. Dead-ends are back pressed to prevent conductor birdcaging.

Full tension splices contain two collet assemblies that are installed using the same procedure as is used with dead-ends. However, instead of tightening the collets down with the threaded eyebolt ends, a free rotating threaded coupler is used in this case. Once the collet assemblies have been attached and tightened down, a similar outer aluminum sleeve is placed over the collet assemblies and a 60 ton press is used to crimp the ends of the outer sleeve to the aluminum strands on either side of the inner collet assemblies. It is noteworthy that the added mass of dead-ends and splices allows them to operate at approximately one-half of the temperature of the conductor which helps ensure efficiency, performance, reliability, and longevity.

Can IMPLO technology be used to dead-end or splice ACCC?

Not at this time. However, the technology is currently being evaluated. CTC Global hopes to be able to offer this alternative in the coming months after testing is completed.

Can "back to back" reels of ACCC conductor be pulled in with splices preinstalled?

While it is quite easy to pull in back to back reels of ACCC conductor using back to back Kellum grips or "socks," CTC Global offers specially designed splice that can be pulled in through sheave wheels. Installation crews have successfully pulled in several 12,500 foot reels, in a single pull.

Can ACCC conductor be used to upgrade an existing line without de-energizing the circuit?

Quanta Services has successfully reconductored several transmission lines with ACCC conductor without shutting down the circuits. The most recent energized project – a 345 kV double-bundled reconductor project which won the EEI Edison Award in 2016, consisted of using over 1,440 miles of ACCC to replace 240 circuit miles of ACSR.

Does ACCC conductor require dampers?

ACCC conductor dissipates vibration energy more effectively than conventional round wire conductor designs, so in certain cases dampers may be unnecessary. However, the ACCC conductor's greater tensile strength is often utilized to increase spans under higher tensile loads. It is therefore recommended that designers contact CTC Global or a damper manufacturer to secure recommendations specific to their project. When dampers are recommended for a specific project the exact location of damper placement is specified. Dampers are generally mounted directly on armor rod.

What type of suspension clamps should be used with ACCC conductor?

CTC recommends that AGS Armor Grip® (Preformed Line Products) or similar suspension clamps be utilized. These suspension clamps employ high temperature rated rubber grommets and armor rod. When the angle of the line exceeds 30 degrees, CTC recommends that a double suspension clamp be used in conjunction with a yoke plate. Other suspension clamps may be utilized when span lengths, angles, anticipated ice load, and other factors are considered.

How is ACCC conductor installed? Are there any special requirements?

ACCC conductor is installed using conventional tools, techniques and equipment. While the installation of ACCC dead-ends and splices is slightly different than the installation of conventional ACSR, ACSS or AAAC fittings, the conductors are installed in a similar fashion. As with other types of conductors, it is important to follow IEEE 524 installation guidelines and select appropriately sized sheave wheels based on conductor diameter, pulling tension, and angle of the conductor's entry in / out of the sheave wheels. As with ACSS conductor, ACCC uses fully annealed aluminum strands that are slightly softer than non-annealed, hardened, or special alloy aluminum. Sheave wheels should be properly aligned so that scuffing of the aluminum strands does not occur and the conductor should not be dragged across the ground that could damage the aluminum strands and induce corona on an energized line. Additionally, as the ACCC conductor's composite core is essentially non-conductive, care must be exercised such that grounding clamps are placed directly on the aluminum strands.

Is there any advantage to pre-tensioning ACCC conductor during installation?

Pre-tensioning ACCC conductor can lower the conductor's thermal knee-point to further reduce thermal sag and quickly create an "after load" stable sag and tension condition. The thermal knee point is essentially the apex of the transition period when the aluminum strands thermally expand and relax to the point that they no longer carry any tensile load and all load is then carried by the very dimensionally stable and very strong composite core. While the conductive aluminum used for ACCC conductor yields under very little load, pre-tensioning can be done with very little effort in a very short period of time. Typically ACCC conductors are installed at 15 to 25% of their Rated Tensile Strength. Pre-tensioning the conductor by as little as 5 to 10% for a matter of 30 minutes can effectively relax the aluminum strands such that they no longer carry significant (or very little) tension under normal load conditions. However, should an extremely heavy ice or wind load condition occur in the future, the aluminum strands will reengage which increases the conductor's overall tensile strength and resistance to sag. Pre-tension also improves the conductor's self-damping as well as its fatigue resistance, and should be considered when permissible.

Have any installation issues or problems occurred during or after installation?

To date, over 500 projects have been successfully completed using ACCC conductor. During a few of these installations the following problems were encountered and resolved using the methods described below:

- *During the installation of dead-ends on earlier projects - where the grounding wires were clamped very closely to the entrance of the dead-ends - birdcaging of the conductor's strands occurred as a result the compression process where the aluminum strands began to extrude out of the nose of the dead-ends. This is a relatively normal occurrence, however, with the grounding wires clamped very closely to the dead-ends, the aluminum strands were not able to relax uniformly in such a small area. After the grounding wires were removed and the line was energized, the birdcaging dissipated.*

- *To prevent birdcaging in future installations, CTC Global developed a back pressing technique which has been successfully utilized on over 50,000 dead-ends and splices since the problem was first identified.*

- *During an early ACCC installation, the tension of the reel control brake was accidentally released which caused the conductor to jump over the side of the bullwheel which broke the conductor.*

o *CTC Global's installation support personnel provided feedback, added notes in their Installation Guideline Manual, and discuss the importance of proper reel control during preconstruction meetings and while they remain present during the installation.*

- *During a 100 circuit kilometer reconductor project (1st project in Poland) using ACCC Stockholm, the original ACSR conductor was used to pull in the new ACCC conductor. One segment worked by one of the sixteen crews (who ignored the guidance from CTC support personnel) 'rushed 5 km of conductors in a single afternoon' while encountering an extremely large number of repair sleeves and splices with undersized reel tension brake. As these splices and repair sleeves were pulled very quickly through each sheave wheel (stop and go motion), the tension of the conductors increased and dropped so dramatically that the conductor between the tensioner and the 1st sheave wheel galloped severely, creating a condition of sharp angle of entry for the conductor to the bull wheel around a very small 3" diameter alignment roller, as well as sharp bending angles in the conductor above the sheave wheel and guide wheel area. This resulted in damage to the conductor's core that did not become apparent until after the line had been installed, energized, and had fallen. All the three breaks were in the same segment installed by the screw.*

o *An assessment of the installation events, conditions, and failure mode confirmed the sequence of events that damaged the core. A decision was made to replace all ACCC conductor installed in the area by the specific crew where these events occurred. During the subsequent conductor replacement, larger hydraulic brakes were added to the reel holders (appropriate for heavier steel reels) and the conductor was directed around the undersized alignment pulley. The smaller ACCC conductors typically have the best flexibility due to its smaller core radius, but it is also more prone to experience larger stress. In addition to securing the support from the utility customer in obtaining commitment from installation crews for following installation best*

practice in the industry, CTC Global's installation support staff now offers additional recommendation/training on working with smaller ACCC conductors during preconstruction meetings and while on site during installation. A study sponsored by WAPA, performed by Denver University (M. Kumosa), is available for review[165]. To date, CTC Global has successfully completed over a dozen additional ACCC projects in Poland.

Is the ACCC composite core flexible?

The ACCC composite core is extremely flexible, but retains kinetic energy when bent, much like a fiberglass fishing pole. Like a fishing pole, the ACCC core exhibits a shape memory characteristic and prefers to be straight. While this characteristic makes it very easy to handle during installation, if the ACCC conductor is bent in a sharp angle (i.e., not around a radius), damage to the aluminum strands or core may occur. Care should be taken so this does not happen. To better understand the ACCC conductor's bending limitations AEP performed a simple bend test on a Drake size ACCC conductor as shown in Figure 80.[166] After being bent 10 times around a 6 inch (15 cm) radius conduit pipe bender, the only degradation noted to the 3/8 inch (9.5 mm) core was a 20 micron hole within the outer fiberglass shell as identified using fluorescent dye penetrant.

---

[165] M. Kumosa and B. Burks' "DU Report on in-service failures in Poland in 2008" Department of Mechanical and Materials Engineering University of Denver (DU) June 7, 2010

[166] Bryant, D; Engdahl, E; Pon, C. ACCC Conductor Combined Cyclic Load Test Report American Electric Power & CTC Global January 2009

Figure 80 - AEP Tight Radius Bending Test

A technical paper published in China discussed a phenomena they called "bamboo effect." What is bamboo effect?

The paper described thermal testing of the 'looped' ACCC conductor on a table (i.e., conductor is under no tension). At temperatures above 160°C, they observed compressive failure (buckling as in 'Bamboo' pattern) on the inner side of the core. Such test is not pertinent to the use of any overhead conductors, where they are always subjected to line tension significant enough to negate the compressive stress experienced in the 'bamboo' test. For the application of ACCC conductor as jumper cable, there is still a moderate amount of conductor tension due to its self-weight. The bend radius in the Chinese Bamboo test is significantly tighter than CTC recommended bending radius for ACCC jumper cable applications. When customers follow CTC engineering guidelines for jumper cable installation, there is no risk of any damage to the composite core conductor.

Can the ACCC conductor be used on long spans or on spans subjected to heavy ice loads?

CTC Global, in conjunction with their international stranding partners, offer a wide range of conductor sizes and designs to accommodate a wide range of applications. While extreme span conductor designs are highly specialized, heavy ice load designs fall within CTC's standard product line. CTC also

produces a high modulus, higher strength core known as ULS which can be used to combat extreme ice loads and extreme spans.

The ACCC conductor's core is made with carbon fiber surrounded by glass fiber. Why is the core not all carbon fiber?

The carbon fiber is surrounded with glass fiber to improve flexibility and toughness, and provide a durable protective layer to prevent galvanic coupling between the carbon fiber and aluminum strands. Galvanic coupling can happen if the aluminum strands are in "direct and substantial physical contact in the presence of an electrolyte within a certain pH range," so even if the outer glass layer was damaged or cracked, it would be difficult to create direct and substantial physical contact between the aluminum strands and central carbon fiber core.[167] Glass fibers as used in numerous aerospace applications for the same purpose due to their resistance to wear compared to other coatings.

What type of testing has been performed on the ACCC conductor?

During development several R&D tests were performed on the ACCC conductor's composite core to assess its suitability for this application. The core itself was tested for tensile strength under very high and low temperature conditions. It was also subjected to sustained and cyclic thermo-mechanical load tests, flexural fatigue tests, acid and moisture resistance tests, and dozens of other tests to assess its performance attributes, limitations, and longevity.

Additional tests were subsequently performed on numerous ACCC conductor samples in a wide range of sizes. These tests often included ancillary hardware components such as dead-ends, splices, dampers, spacers, and suspension clamps. In addition to numerous mechanical tests, other systems tests and electrical tests were performed. These tests included lightning strike tests, short circuit tests, corona tests, and other industry standard or specialized tests. In addition to lab tests, several utilities also installed and monitored the ACCC conductor on test spans. The data collected from these tests correlated very well with predicted values based on lab-scale empirical tests and computer modeling. The reports and results of all of these tests are available for customer

---

[167] D. A. Jones, "Principles and Prevention of Corrosion" Prentice Hall, Upper Saddle River, NJ 1996, p 61.

review. A Summary Technical Report is also available. Please contact CTC Global to gain access to these reports.

Considering ACCC is relatively new, what assurances does CTC Global offer relating to product Longevity?

While the ACCC conductor uses a hybrid carbon and glass fiber composite core that is relatively new to the electrical utility industry, especially as it relates to conductor, the reality is that carbon and glass fiber composites have evolved substantially over the last several decades and have been widely deployed in other demanding application where high strength, light weight, fatigue resistance, and longevity are extremely important. Carbon fiber composites, for instance, are now being used for primary aircraft structures not only for their high strength and light weight, but especially due to their resistance to cyclic thermo-mechanical fatigue. In the application of a conductor, the environmental challenges are numerous, combined, and very cyclic. The hybrid composite core developed and patented by CTC Global, and extensively tested by numerous laboratories and utilities internationally, is ideally suited for this demanding application. This technology allows the ACCC conductor to be operated at any voltage (including UHV) and from sub-zero conditions to a maximum continuous operating temperature of 180°C and up to 200°C for emergency operation. While operation at higher temperatures for relatively short periods of time is acceptable (in high voltage applications that may have thermal constraints - typically below 400kV), and will not void the product's warrantee (see warrantee discussion below), operation at higher temperatures for prolonged periods of time can reduce the ACCC conductor's effective service life.

In terms of line design, what guidelines exist?

Through substantial testing, field experience, and engineering interaction, CTC Global and other entities have well quantified the ACCC conductor's performance as it relates to tensile strength, flexural strength, vibration dissipation, ice load capacity, and electrical performance. The data compiled allows transmission line designers to take full advantage of the ACCC conductor's high electrical capacity, reduced line losses, high strength, and low sag. The data compiled allows transmission engineers (both electrical and mechanical) to accurately assess ACCC suitability for any project. Industry tools such as PLS CADD™ can be readily utilized to support the engineering

250

process. CTC Global's application engineers are also available to assist with analysis, comparisons, economic modeling and general support. Available at no charge, they can also provide life cycle cost analysis based on upfront capital costs, line losses / GHG emission reductions, increased capacity, improved longevity and other attributes of the ACCC conductor.

What Quality Assurance procedures does CTC utilize?

Quality is job #1 at CTC Global. CTC Global maintains ISO 9001-2008 certification and follows strict quality assurance procedures from the time it receives raw materials to the time when the finished conductor arrives at the project site. Each conductor core is carefully tested, documented, certified, and recorded. Finished conductor reels are also inspected. Core tests include tensile testing, bending tests (on the entire length of core), and thermal "glass transition" (Tg) tests. Production of the core is highly automated and designed to prevent / identify / remove any potential anomaly. CTC Global also offers one of the best warranties in the industry (up to 10 years).

Is ACCC conductor any more or less resistant to gunshot than other conductor types?

In 2010, WAPA (Western Area Power Administration) conducted testing on ACSR, ACSS, ACCR, AAC, and ACCC conductors[168]. With a five foot piece of each conductor tensioned to 6,000 pounds (2,720 kg), they shot at each conductor with a 12 gauge shotgun (3.5 magnum with #2 steel shot) from a distance of 25 feet (7.6 meters). Damage to each conductor was superficial. A second test was performed with a 30-06 hunting rifle using a 180 grain bullet with a ballistic tip. At a distance of 25 feet, direct hits to each of the conductor's cores caused failure of each conductor tested. No differences in resistance to gunshot were noted between any of the conductors tested. A copy of this report and video tape is available.

How can ACCC conductor be repaired if it is damaged by gunshot or other impact?

---

[168] Clark, R; "Ballistics test comparing HTLS vs conventional conductor designs" Western Area Power Administration (WAPA) IEEE WG meeting Minneapolis, MN July 2010

As with ACSR or other conductor types, it is possible to use conventional methods to repair ACCC conductor strands. If the strands are damaged up to 15%, a line guard can be utilized. If the damaged strands are from 16% to 30%, a repair rod should be utilized. If the strands are damaged above 30% but the core is not damaged, a compression repair sleeve should be utilized. If the composite core is damaged in a localize area, a full-tension splice should be installed. If damage to the conductor is more widespread, a section of conductor should be removed and replaced. Generally, this type of damage is localized and the amount of conductor that needs to be replaced is minimal.

Does ACCC conductor reduce EMF?

No.

Can CTC Global offer any recommendations regarding outside engineering, installation, or EPC firms?

CTC Global maintains a list of experienced engineering and installation firms. Please contact CTC Global for more information

Can CTC Global provide a list of customer contacts that have installed ACCC conductor?

CTC Global maintains a list of experienced engineering and installation firms. Please contact CTC Global for more information

Is ACCC conductor RUS Approved?

Yes

Is ACCC Conductor Guaranteed?

Yes. The ACCC conductor is delivered with a standard three year warrantee. Other conductor manufacturers typically offer a one year warrantee. For a nominal charge, this warrantee can be increased to up to ten years. Product warrantees may vary regionally, please contact CTC Global for more information

What is a typical production lead time for ACCC conductor and ancillary hardware?

Lead times can vary depending upon project size and current production backlog. A typical project lead time is 8 to 12 weeks. In the case of larger projects, CTC Global can often deliver finished conductor in phases to accommodate project requirements. CTC Global currently has nine international stranding partners who can support product delivery worldwide.

If I have additional questions about ACCC conductor who should I contact?

CTC Global
2026 McGaw Avenue
Irvine, CA 92614 USA

Telephone: +1 (949) 428-8500 Fax: +1 (949) 428-8515

Website: www.ctcglobal.com E-Mail: support@ctcglobal.com

Thank you for your interest in ACCC Conductor.
We look forward to answering any additional questions you might have.